Investigation of mammalian and viral Interleukin-10 family members during cytomegalovirus infection

Maria A Stacey

A thesis submitted to Cardiff University in candidature for the Degree of Doctor of Philosophy

Department of Infection and Immunity
School of Medicine
Cardiff University
Cardiff
Wales

2012

DECLARATION

This work has not been submitted in substance for any other degree or award at this or any other university or place of learning, nor is being submitted concurrently in candidature for any degree or other award.

Signed …… (candidate) Date ……

STATEMENT 1

This thesis is being submitted in partial fulfilment of the requirements for the degree of ……(insert MCh, MD, MPhil, PhD etc, as appropriate)
Signed …… (candidate) Date ……

STATEMENT 2

This thesis is the result of my own independent work/investigation, except where otherwise stated.
Other sources are acknowledged by explicit references. The views expressed are my own.
Signed …… (candidate) Date ……

STATEMENT 3

I hereby give consent for my thesis, if accepted, to be available for photocopying and for inter-library loan, and for the title and summary to be made available to outside organisations.
Signed …… (candidate) Date ……

STATEMENT 4: PREVIOUSLY APPROVED BAR ON ACCESS

I hereby give consent for my thesis, if accepted, to be available for photocopying and for inter-library loans **after expiry of a bar on access previously approved by the Academic Standards & Quality Committee.**
Signed …… (candidate) Date ……

Acknowledgements

I would like to offer my sincerest gratitude to a number of people. Firstly, I would like to thank my supervisor Dr Ian Humphreys for his constant support, encouragement and belief in me and I am extremely grateful for having had such fantastic supervision throughout my PhD. Secondly, I would like to thank Morgan Marsden who has provided me with the best technical help I could have wished for, and without whom, the early starts on experimental days would have been even earlier. Many thanks also to my secondary supervisor Prof. Gavin Wilkinson for his support and input as well as showing an interest in all the immunological aspects of my PhD despite being an avid virologist at heart. I would also like to thank the other students and post-docs who I have worked with over the years for their continuous help, advice and fun, and especially to my office colleagues who have put up with me and my endless renditions of jolly Christmas songs!

Beyond immunology, there are also many people I would like to give my thanks to. A massive thanks to Luke for being the most amazing light anyone could wish for at the end of the dark PhD tunnel. An enormous thank you to Jess for endless laughter, joy and loveliness as well as accompanying me in my journey to the inevitable madness that resulted from thesis writing (Pete also deserves a special mention for putting up with the pair of us)! Thanks also to Daniel for providing me with someone to celebrate and commiserate each minor scientific achievement and failure with. Unfortunately there are too many other people to name personally but a huge thank you to all my other wonderful friends who have given me amazing support and encouragement over the years, you know who you are.

Finally, I would like to offer my eternal thanks to my fantastic family, who despite not really having a clue about what I actually do, have provided me with continuous support, encouragement, love and hilarity all in their own very special ways.

Summary

Human cytomegalovirus (HCMV) infection in newborns and immunocompromised individuals with immature or deficient immune systems can cause life-threatening diseases. The clinical and subsequent economical burden of HCMV infection led the US Institute of Medicine designating a vaccine for HCMV as the highest level of priority. Complex virus-host interactions have developed over millions of years of co-evolution, making the understanding of the pathogenesis of HCMV disease particularly challenging. Consequently, a crucial factor in aiding the development of effective vaccinations and therapies to significantly reduce morbidity and mortality associated with HCMV infection is elucidating what immune mechanisms contribute to/impede protection against infection. For example, is the induction of immunomodulatory agents such as cytokines beneficial or harmful to the host during infection? Given the known immunosuppressive properties of one such cytokine, interleukin-10 (IL-10), in conjunction with the evolutionary acquisition by HCMV of its own IL-10 homologue, I hypothesised that mammalian- and viral-IL-10 suppress protective immunity during acute CMV infection. Utilising a mouse model of CMV infection, I revealed a surprising antiviral role for IL-10 during acute infection *in vivo*, which was achieved via limitation of activation-induced death of NK cells. The IL-10-related cytokine interleukin-22 (IL-22) provides critical protection against certain infectious agents and I therefore hypothesised that IL-22 provides protective immunity during acute CMV infection. Utilising the murine infection model once more, I discovered a tissue-specific antiviral role for IL-22 during acute infection *in vivo* and made the surprising finding that neutrophils play a protective role during infection. I also demonstrated that neutrophils can directly inhibit viral replication *in vitro*. Thus, novel insights into cytokine biology in the context of viral infections *in vivo* revealed by these studies highlighted important considerations for future research into herpesvirus infections, and has major implications for the treatment of this important infectious disease.

Table of Contents

Chapter 3 - Investigating the modulation of NK cells by IL-10 during acute murine cytomegalovirus infection

List of Figures

List of Tables

List of Abbreviations

AIDS - acquired immunodeficiency syndrome
APCs - Antigen presenting cells
APF – Aminophenyl fluorescein
BAC - Bacterial artificial chromosome
BTLA - B and T lymphocyte attenuator
cDNA – complementary DNA
DAF-FM diacetate – 4-amino-5-methylamino-2',7'-difluorofluorescein diacetate
DCs - Dendritic cells
ddH_2O – double distilled water
EBV - Epstein–Barr virus
ER - Endoplasmic reticulum
FCS – Fetal calf serum
FMO - Fluorescence minus one
gp – glycoprotein
MCMV gB – MCMV glycoprotein B
HAART - Highly Active Antiretroviral Therapy
HBV - Hepatitis B virus
HCMV - Human cytomegalovirus
HCV - Hepatitis C virus
HFFs – Human foreskin fibroblasts
HIV - Human immunodeficiency virus
HLA- Human leukocyte antigen
HSC – Haematopoietic stem cell
HSV - Herpes simplex virus
IBD - Inflammatory bowel disease
IE - Immediate early
IFNα – Interferon-alpha
IFNβ – Interferon-beta
IFNγ – Interferon-gamma
IL – Interleukin
IL-10R - Interleukin-10 receptor
IL-22BP - Interleukin-22 binding protein
IL-22R - Interleukin-22 receptor
ILCs - Innate lymphoid cells
IP - Intra-peritoneal
iNOS – Inducible nitric oxide synthase
iTregs - Inducible T regulatory cells
IV - Intravenous
KIRs - Killer-cell immunoglobulin-like receptors
LB media – Luria-Bertani media
LCMV - Lymphocytic choriomeningitis virus
LT – Lymphotoxin
LTB4 - Leukotriene B4
MCMV - Murine cytomegalovirus
MD-DCs - Monocyte-derived dendritic cells
MFI - Mean fluorescence intensity
MHC - Major histocompatibility complex
MMP – Matrix metalloproteinase
MOI - Multiplicity of infection
Muc - Mucin
NFkB - Nuclear factor kappa-light-chain-enhancer of activated B cells
NK cells - Natural killer cells
NO - Nitric oxide
nTregs - Natural T regulatory cells
ORF - Open reading frame
PAMPs - Pathogen-associated molecular pattern
PBMCs - Peripheral blood mononuclear cells
PFU - Plaque forming units
P.I – Post-infection
pp - Phosphoprotein
PRRs - Pattern recognition receptors
qPCR – real-time quantitative PCR
RhCMV - Rhesus cytomegalovirus
RA – Retinoic acid
ROS - Reactive oxygen species
RSV - Respiratory syncytial virus
RT - Room temperature
STAT - Signal transducer and activator of transcription
TCR - T cell receptor
T_{fh} cells - T follicular helper cells
TGF-β – Transforming growth factor-beta
T_H cells - T helper cells
TLRs - Toll-like receptors
TNFα - Tumour necrosis factor-alpha
Tregs - T regulatory cells
UL - Unique long
US - Unique short
VSV – Vesicular stromatitis virus
wt - wild-type

Chapter 1 – Introduction

1.1. Introduction to Thesis

Human cytomegalovirus (HCMV) is one of eight herpesviruses that commonly infects humans, and the public health impact of HCMV infection is arguably one of the most underappreciated of any infectious disease in the western world today (1). HCMV infections in healthy individuals are generally asymptomatic. However, in newborns and immunocompromised individuals with immature or deficient immune systems, infection can cause life-threatening disease affecting many organ systems. Due to millions of years of co-evolution, complex virus-host interactions have developed, making the understanding of the pathogenesis of HCMV disease particularly challenging (2). Therefore elucidating what immune mechanisms contribute to protection against infection will be crucial in aiding the development of effective vaccinations and therapies to significantly reduce morbidity and mortality associated with HCMV infection and disease, for example understanding if the induction of endogenous immunomodulatory agents such as cytokines is beneficial or harmful to the host during infection. In this thesis, I will describe the role that members of a particular family of cytokines known as the interleukin-10 family play in modulating the immune system during acute cytomegalovirus infection.

1.2. Cells of the innate immune system

The innate immune system represents the first line of host defence by providing an immediate response against invading pathogens. Cells of the innate immune system include natural killer (NK) cells, mast cells, granulocytes and phagocytic cells. Mast cells are found in the skin, at mucosal sites and in connective tissues. They play a central role in inflammatory responses and immediate allergic reaction. They release potent inflammatory mediators such as histamines (organic nitrogen compounds that increase the permeability of capillaries to allow greater influx of immune cells to infected tissues),

chemotactic factors (soluble molecules which attract and guide the movement of cells during an inflammatory response), and cytokines (small cell-signalling protein molecules used extensively in intercellular communications). Histamine is also released when mast cells detect injury, and these cells are therefore also important in wound healing (3).

Macrophages are large professional phagocytes capable of engulfing substantial numbers of microbes, including bacteria, as well as other cells. They are capable of moving across the capillary membrane into the area between cells in pursuit of pathogens. They act as immune sentinels within tissues and organs, regulating immune activation and inflammation as well as metabolism (4, 5). Organ-specific macrophages are differentiated from monocytes. Monocytes are also innate immune cells which move quickly to sites of infection in response to inflammatory signals and once in the tissue, divide and differentiate into macrophages and dendritic cells (DCs). DCs are also phagocytic cells and are found predominantly in the skin and mucosal linings of the respiratory and gastro-intestinal tracts. They are potent antigen-presenting cells (APCs) that capture antigens in the periphery, process them into peptides and present them to lymphocytes in the lymph nodes, thus are a key link between the innate and adaptive immune systems (6). There are several DC-subsets including myeloid-DCs which are most similar to monocytes and pick up antigen in the periphery before migrating to T cell areas to present antigen, plasmacytoid-DCs which are found in lymphoid organs and produce large amounts of the antiviral cytokines interferon-alpha (IFNα) and interferon-beta (IFNβ), and Langerhans cells which are DCs predominantly found in the skin and the mucosa. DCs are also involved in the induction of immunological tolerance in peripheral tissues under steady-state conditions (7) which is critical in preventing the immune system from mounting an immune response to self antigens or to harmless exogenous antigens.

Neutrophils are the most abundant type of phagocyte and are usually the first cells to arrive at the site of infection. They are known as granulocytes due to the presence of granules in their cytoplasm which release lytic enzymes and produce reactive oxygen intermediates with antimicrobial potential (8). These lytic enzymes include cathelicidin, defensins and cathepsins, all of which provide critical protection against bacteria, fungi and many enveloped and non-enveloped viruses. As well as providing defence against invading pathogens through phagocytosis and the release of soluble anti-microbial granules, neutrophils also generate neutrophil extracellular traps which bind, trap and kill microbes extracellularly (9). Other granulocytes of the innate immune system are basophils and eosinophils. Basophils release predominantly histamine from their granules and are important in defence against parasites but also have a role in allergic reactions such as asthma (10). Eosinophils on the other hand secrete a range of toxic proteins and free radicals which are highly effective in killing pathogens (10). NK cells are cytotoxic lymphocytes which survey host tissue for signs of infection, transformation and stress, and kill target cells that are detrimental or of no further use to the host (11). NK cells will be discussed in depth later in section 1.6.

1.3. Activation of the innate immune system

Inflammation is the first response of the immune system to harmful stimuli such as invading pathogens, damaged cells or irritants. Acute inflammation is initiated by cells already present in the injured or damaged tissue, including resident macrophages, DCs and mast cells. On the surface of these cells are receptors known as pattern recognition receptors (PRRs). These receptors are capable of identifying pathogen-associated molecular patterns (PAMPs) which are conserved molecules broadly expressed by microbial pathogens, but are clearly distinct from host proteins. A major subset of PRRs is the Toll-like receptors (TLRs). Extracellular infections are detected by a series of cell surface TLRs which become activated by microbial elements. Intracellular pathogens are recognised by endosomal TLRs. The engagement of TLRs with their cognate microbial

PAMPs stimulates intracellular reaction sequences, which leads to activation of transcription factors, primarily nuclear factor kappa-light-chain-enhancer of activated B cells (NF_KB), which is a protein complex that controls the transcription of DNA. These intracellular reactions not only trigger phagocytosis, but also the release of pro-inflammatory cytokines and chemokines (cytokines that induce directed chemotaxis in nearby responsive cells) to recruit and prime APCs for the initiation of the adaptive immune response.

1.4. Cells of the adaptive immune system

The adaptive immune system acts as a second line of host defence by providing an antigen-specific response which is retained after the elimination of the pathogen in the form of immunological memory, allowing for a faster and more efficient response during a subsequent encounter with the same pathogen or a slight variant of that pathogen. The adaptive immune system is predominantly mediated by two types of lymphocyte; B cells and T cells. T cells are primarily responsible for cell-mediated immunity and B cells are responsible for humoral immunity via production of antibodies, but they work together and in conjunction with cells of the innate immune system to mediate effective adaptive immunity (12).

B cell development begins in the fetal liver and continues in the fetal/adult bone marrow of most mammals. Subsequent functional maturation then occurs in the secondary lymphoid tissues (e.g. the lymph nodes and spleen), and their functional endpoint as mature B cells is antibody production by terminally differentiated plasma cells. B cells are characterised by the presence of a B cell receptor on their surface which is able to bind a specific antigen. Functions of B cells other than their principal role of making specific antibodies against these antigens include performing the role of APCs and eventually developing into long-lived memory B cells (13).

T cells originate from haematopoietic stem cells (HSCs) in the bone marrow which migrate to and populate the thymus by rapidly expanding to produce a large population of immature thymocytes. These early thymocytes lack both CD4 and CD8 co-receptors and are therefore referred to as double negative cells. As they develop, they become double positive thymocytes before segregating into separate immunocompetent populations of single positive $CD4^+$ and $CD8^+$ T cell precursors (14). $CD8^+$ T cells, or cytotoxic T cells, are a sub-group of T cells which induce the death of infected or damaged cells, or tumour cells. These cells recognise their target by binding to antigen associated with major histocompatibility complex (MHC) class I molecules. $CD4^+$ T cells, or T helper cells (T_H cells), assist other cells in various immunological processes, including the maturation of B cells and the activation of cytotoxic T cells and macrophages. $CD4^+$ T cells can also acquire cytotoxic activity and directly kill infected or transformed cells and are particularly associated with chronic viral infections including HCMV, hepatitis viruses and human immunodeficiency virus (HIV)-1 (reviewed in (15)). These cells only recognise antigen coupled to MHC class II molecules.

Naïve $CD4^+$ T cells can be differentiated into distinct effector and regulatory lineages. This differentiation is antigen-driven and is controlled by cytokine cues from innate and possibly adaptive immune cells upon sensing invading microbes (16). The first two major groups of distinct $CD4^+$ T cells to be discovered were designated as T_H1 and T_H2, and could be distinguished by the cytokines they produced as well as through the expression of cell surface molecules. T_H1 cells predominantly produce interferon-gamma (IFNγ) and also produce lymphotoxin (LT) and high amounts of interleukin (IL)-2. The signature cytokines of T_H2 cells are IL-4, lL-5 and IL-13 (reviewed in (17)). A third major effector population of $CD4^+$ T cells are the T_H17 cells and are characterised by the production of IL-17A, IL-17F and IL-22. As well as effector cells, a regulatory population of T cells (Tregs) can be induced to differentiate *in vitro* from naïve $CD4^+$ T cells, and are designated inducible Tregs (iTregs) in order to distinguish them from the naturally

occurring Tregs (nTregs) (reviewed in (17)). Additional subsets including T_H9 and T-follicular helper (T_{fh}) cells have also been described but remain less well characterised. The developmental pathways of distinct $CD4^+$ T cell subsets are summarised in Fig. 1.1 (adapted from (16)).

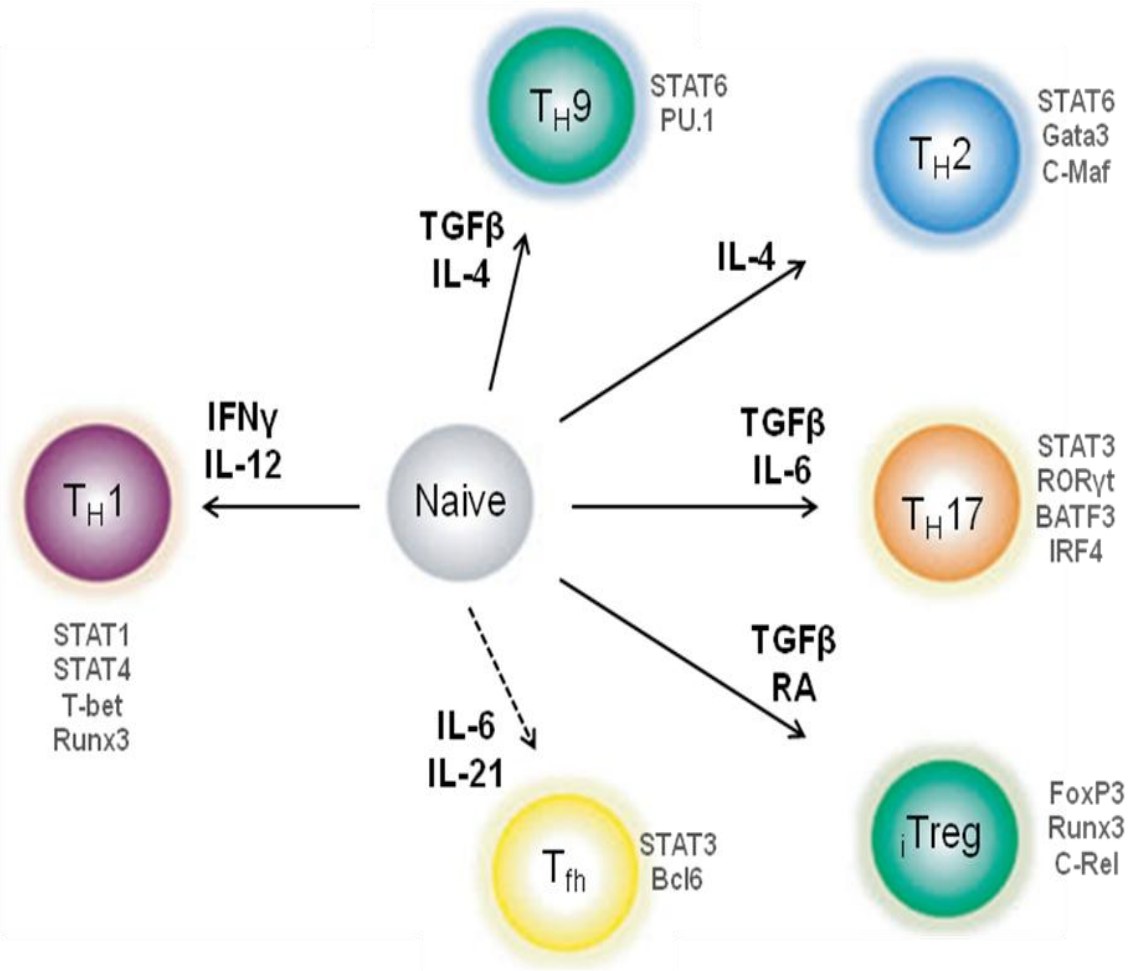

Figure 1.1. Developmental pathways of $CD4^+$ T cell subsets from naïve precursors Following exposure to foreign antigen, naïve $CD4^+$ T cells are directed towards distinct developmental programs by cytokines (shown in bold text) that differentially induce lineage specific transcription factors (shown in grey text). The broken line associated with the T_{fh} pathway represents the possibility that these cells may not develop directly from naïve precursors.

1.5. Activation of T cell mediated immunity

Efficient priming of adaptive immune responses requires not only the presentation of antigen in the context of MHC, but also the induction of accessory signals in the form of co-stimulation and cytokines from APCs (18). T cells are activated by the binding of the T cell receptor (TCR) to a short peptide presented by the MHC (MHC class I for $CD8^+$ T cells and MHC class II for $CD4^+$ T cells) on an APC (usually a DC in the case of a naïve response, but also B cells and macrophages). After this first antigen-specific signal, a second co-stimulatory signal is required for the T cell to become fully activated. The best characterised co-stimulatory molecule that T cells express is CD28, which interacts with CD80 and CD86 on the surface of APCs. This second signal licenses the T cell to respond to an antigen, as without it the T cell can become anergic (anergy is a state of immune unresponsiveness). Once activated, T cells undergo rapid clonal expansion. As described above, the T_H1 response is characterised by the release of IFNγ which activates macrophages and induces B cells to make opsonising antibodies that mediate phagocytosis, and in general is most effective against intracellular viruses and bacteria. The T_H2 response is characterised by the release of IL-4 which induces B cells to make neutralising antibodies; a response most effective against extracellular bacteria and parasites. $CD8^+$ T cells release perforin and granzymes which cause infected, damaged or dysfunctional target cells to lyse or undergo apoptosis. Upon the resolution of infection most effector cells will die. However a few cells will become long-lived memory cells that can rapidly expand to large numbers of effector cells upon re-exposure to their cognate antigen, thus providing immunological memory against re-infection.

1.6. NK cells: development and function

NK cells were discovered more than 30 years ago and were originally defined as effector lymphocytes of the innate immune system capable of cytolytic functions. However, a more advanced view of NK cells has emerged over the years due to the recognition that they express a repertoire of activating and inhibitory receptors which allow them to mount an

efficient assault against viral and bacterial infections, tumour development and invading pathogens, whilst ensuring self-tolerance. Recent studies have also revealed that NK cells can display a form of immunological memory, thus NK cells exhibit attributes of both innate and adaptive immunity (19).

NK cells have been shown to provide critical protection against a wide range of viral infections including arenaviruses (e.g. lymphocytic choriomeningitis virus (LCMV)), herpesviruses (e.g. CMV and herpes simplex virus (HSV)), orthomyxoviruses (e.g. influenza virus) and picornaviruses (e.g. coxsackie virus) (reviewed in (20)). The importance of NK cells in early defence can clearly be seen in studies using mice with NK cell deficiencies or using NK cell depletion techniques (21-27). Defects in NK cells in humans are rare, signifying the essential role for NK cells in host defence, but interestingly, patients with NK cell defects are usually extremely susceptible to herpesvirus infections (28). NK cells have also been shown to have a role in tumour-surveillance as numerous studies in mice support the notion that NK cells are associated with the eradication of tumour cells, where as in humans, most evidence is derived from correlative studies (reviewed in (29)).

NK cells develop primarily in the bone marrow and do not require the thymus for their development (11). Production of NK cells from bone marrow precursor cells requires the stromal cell-derived cytokine IL-15. Furthermore, a study with IL-$15^{-/-}$ mice showed that not only is IL-15 required for development, but is also essential for mature NK cell survival *in vivo* (30). NK cells possess an elaborate array of receptors that regulate their functions upon interaction with MHC class I proteins on target cells. In humans, these receptors are known as killer cell immunoglobulin-like receptors (KIRs), and in the mouse, they are known as Ly49 receptors (31). These receptor families include both inhibitory and activating receptors. Immature human and mouse NK cells express inhibitory KIRs and Ly49 receptors respectively during their development which is essential for establishing

efficient ‘missing self’ recognition. The missing self hypothesis was based on the observation that upon encounter with a normal autologous cell expressing MHC class I, NK inhibitory receptors are engaged. Loss of MHC class I expression (‘missing self’), in combination with the expression of one or more ligands for activating NK receptors, leads to the activation of the NK cell which then provokes NK cell-mediated attack on the target cell. Engagement of these inhibitory receptors during development results in the generation of functional NK cells in the periphery. In addition, the number of inhibitory receptors for autologous MHC class I molecules that NK cells express leads to varying responsiveness; with each additional self-MHC-specific inhibitory receptor, responsiveness increases quantitatively (reviewed in (11)).

Two of the major effector functions of NK cells are 1) to mediate significant levels of cytotoxic activity and 2) to produce high amounts of certain cytokines and chemokines. Virus-induced IFNα and IFNβ are potent inducers of NK cell-mediated killing but in addition to these type I interferons, many other innate cytokines are also important in regulating NK cell cytotoxicity, proliferation and IFNγ production. These include IL-12, tumour necrosis factor (TNF)-α, IL-1α/β, IL-6, IL-10, transforming growth factor (TGF)-β, IL-15 and IL-18 (reviewed in (20)). There are two major mechanisms by which NK cells kill target cells, both of which require direct effector/target cell contact. The first involves the secretion of cytoplasmic granule toxins, predominately perforin, which disrupts the membranes of target cells, and granzymes, which are a family of structurally related serine proteases. Together, these induce apoptosis of the target cell. NK cell-derived perforin is not only important for the killing of virally infected cells but has also been shown to be the predominant NK cell antifungal mechanism against cryptococcal infection (32). The second mechanism involves the engagement of death receptors on the target cells (e.g. Fas) by their cognate ligands (e.g. FasL) on NK cells which results in classical caspase-dependent apoptosis (review in (33)). Caspases are highly conserved proteins that play a central role in the transduction of death-receptor apoptotic signals. Initiator

caspases first become activated which in turn activate effector caspases, leading to programmed cell death initiated by degradation of a host of intracellular proteins.

As well as eradicating infected cells or tumour cells via their ability to mediate spontaneous cytotoxicity, NK cells also play an important role in restricting infections and stimulating the adaptive immune response via their production of cytokines. It is now well established that cytokines such IFNγ and TNFα produced by NK cells contribute to the control of multiple murine and human viral (34) and bacterial infections (35, 36). As well as having direct antiviral activity, IFNγ has multiple effects in the activation of innate and adaptive immunity (reviewed in (37)) and include stimulation of bactericidal activity of phagocytes, stimulation of antigen presentation through MHC class I and class II molecules, orchestration of leukocyte-endothelium interactions, effects on cellular proliferation and apoptosis, as well as being involved in the regulation of over 200 known IFN-stimulated genes. Therefore, cytokines secreted by NK cells, in particular IFNγ, are important effector molecules that contribute to direct pathogen control (34).

Finally, immunological memory was until recently thought to be a property strictly limited to adaptive immunity. However, recent studies have suggested that NK cells have the capacity to alter their behaviour based on prior activation (reviewed in (38)). NK cells have been shown to mediate antigen-specific recall responses in several different model systems. In the absence of T and B cells, NK cells can mediate a hapten-specific contact hypersensitivity response to haptens which the mice were previously sensitised to (39). In addition, cytokine-activated NK cells transferred into naïve hosts produce significantly more IFNγ when restimulated as compared to naïve NK cells (40). Furthermore, NK cells have been shown to exhibit immunological memory against viral infections, as virus-sensitised NK cells adoptively transferred into naïve recipients results in a robust secondary expansion, protective immunity and enhanced survival when rechallenged with mouse cytomegalovirus (MCMV) (41), influenza or vesicular stomatitis virus (VSV) (42).

Although NK cells do not rearrange the genes encoding their activating receptors, NK cells can generate long-lived memory cells which mediate a more efficient secondary response against previously encountered pathogens (43). Thus NK cells can be described as exhibiting attributes of both innate and adaptive immunity. The multiple roles of NK cells are summarised in Fig. 1.2.

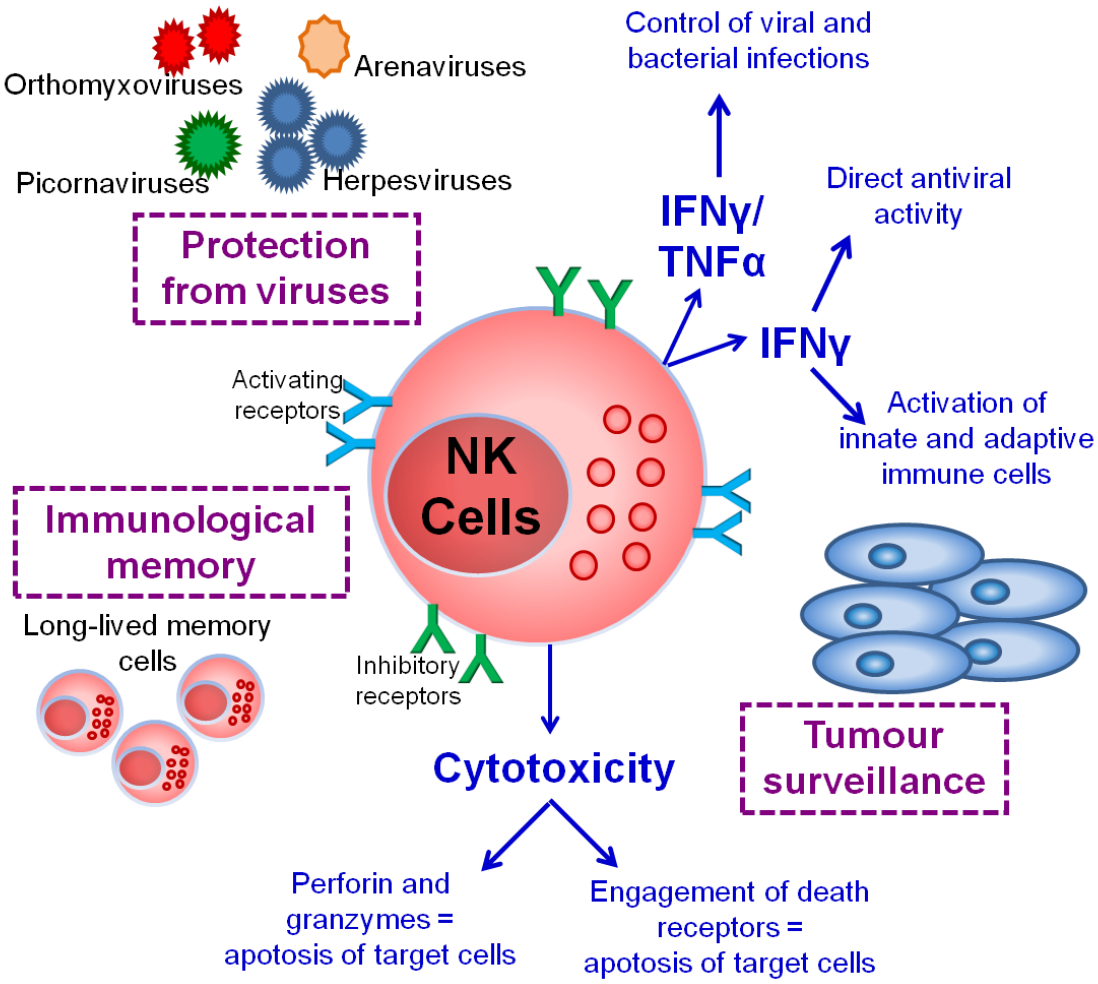

Figure 1.2. The multiple roles of NK cells
NK cells express a repertoire of activating and inhibitory receptors which allow them to mount an efficient assault against viral and bacterial infections as well as tumour development. This is achieved via the production of cytokines such as IFNγ and TNFα and through cytotoxic mechanisms. NK cells can also display a form of immunological memory where-in long-lived memory NK cells develop.

1.7. Human cytomegalovirus (HCMV)

1.7.1. Clinical implications of HCMV infection

HCMV is a member of the *Herpesviridae* family of viruses. It is a β-herpesvirus, and like all viruses in this subfamily, exhibits species specificity and infects only particular types of differentiated cells within that species. During natural infection, HCMV is thought to replicate productively in fibroblasts; epithelial, endothelial, smooth muscle and neuronal cells; hepatocytes; granulocytes; and monocyte-derived macrophages; and is capable of infecting $CD34^+$ haematopoietic cells in the bone marrow (44). The entry of herpesviruses into cells is a complex process initiated by adsorption and receptor binding followed by fusion of the virus envelope with a cell membrane (45). The method of HCMV entry is cell-dependent. It is known that HCMV fuses with the membranes of fibroblasts, but enters endothelial and epithelial cells via endocytosis (45). HCMV can be transmitted via saliva, sexual contact, placental transfer, breastfeeding, blood transfusions and solid-organ or haematopoietic stem cell transplantation. Seroprevalence of HCMV in the worldwide population ranges between 45-100%. The highest prevalence is in South America, Africa and Asia and the lowest is in Western Europe and the United States (46).

One of the most important clinical manifestations of primary HCMV infection is seen in newborn babies infected during pregnancy. The majority of congenitally infected babies are asymptomatic at birth, however 10-17% of these subsequently develop hearing defects or neurodevelopmental sequelae (47, 48). Approximately 10-15% of congenitally infected babies are symptomatic at birth, exhibiting irreversible central nervous system damage including microcephaly, encephalitis, seizures and deafness, as well as jaundice, hepatitis, pneumonitis, hepatosplenomegaly and thrombocytopenia (47, 48).

Primary infection in an immunocompetent host is usually asymptomatic and rarely causes illness. In a few cases, infection can result in mononucleosis syndrome which manifests symptoms almost indistinguishable from those of Epstein-Barr virus (EBV)-induced

mononucleosis, including fever, sore throat and fatigue. After primary infection, HCMV establishes lifelong latency infection within the host. Therefore, in immunocompromised individuals, HCMV primary infection as well as reactivation from latency can lead to severe complications. HCMV is still regarded as being the most significant infectious pathogen in recipients of solid-organ transplants as, despite improved surveillance and treatment, it continues to cause morbidity and mortality after transplantation. For example, in the absence of preventative measures, 40-100% of all kidney transplantation recipients develop HCMV infection and up to 67% develop HCMV disease (49). Cytomegalovirus-associated disease initially localises in the transplanted organ, but can subsequently spread systemically causing pneumonitis, hepatitis, nephritis, pancreatitis, myocarditis and retinitis among others (48). Reactivation of latent virus causes a significant risk for HSC transplantation recipients due to prolonged periods of immunodeficiency. In approximately 80% of cases, reactivation occurs in patients that were seropositive before transplantation, and again can lead to HCMV disease such as pneumonitis, entercolitis and gastritis (47).

Prior to the introduction of highly active antiretroviral therapy (HAART), HCMV disease caused a significant problem for HIV-infected patients due to an impaired adaptive immune response, with approximately 40% of patients suffering from HCMV disease (47). Despite the decline in HCMV incidence in patients with acquired immune deficiency syndrome (AIDS) since the availability of HAART, HCMV infection can still be problematic for HIV patients. The most common manifestation of HCMV disease in HIV patients is retinitis, which leads to progressive loss of vision and blindness, and incidence of retinitis is between 10-40% in AIDS patients with low $CD4^+$ cell counts (<100/µl) (50).

Finally, it is interesting to note that the total HCMV-specific T cell response in HCMV seropositive subjects has been measured and is extremely large, with on average ~10% of the $CD4^+$ and $CD8^+$ T cell population being specific for HCMV peptides (51). This

‘memory inflation’ may have consequences for elderly individuals as the expansion of HCMV-specific memory cells may result in loss of naïve and non-HCMV-specific memory cells which could potentially lead to dysregulated immune responses to other pathogens (51). HCMV-associated changes in the immune system are highly predictive of early mortality among older persons (52) whilst HCMV reactivation in critically ill older patients also predicts early mortality (53).

Due to the heavy burden that HCMV exacts when it infects children and immunocompromised individuals, a vaccine for HCMV was assigned the highest priority by the US Institute of Medicine in 1999. This was based on the financial cost and human suffering that would be alleviated by reducing the disease burden of congenital HCMV infections (54).

1.7.2. HCMV genome structure and viral strains

HCMV has the largest genome of any human virus (~235kb) and is estimated to encode a minimum of 166 protein-coding genes. HCMV has a linear DNA genome with a unique long (U_L) region and a unique short (U_S) region, flanked by two sets of inverted repeats. HCMV research has historically relied on laboratory strains that have been heavily passaged on human foreskin fibroblasts (HFFs) *in vitro*; in particular strains AD169 and Towne (55). Propagation for even limited passages, such as the low-passage Toledo strain, introduces mutations in the genome (55). The broad tissue tropism exhibited by HCMV *in vivo* is lost in cell culture due to the adaptation of the virus to fibroblasts, which is strongly associated with mutations in the genes UL128, UL130 and UL131A (56). These genes are known to be essential for growth of HCMV in endothelial cells, epithelial cells and DCs (57). Mutations in these genes along with mutations in other regions of the genome that occur when HCMV is passaged *in vitro* consequently results in the laboratory virus strains used for research fundamentally differing from wild-type (wt) HCMV. The HCMV strain Merlin was originally isolated from the urine of a congenitally

infected infant and was sequenced after only 3 passages in HFFs. Of the lab strains sequenced to date, Merlin is considered to most accurately reflect the wt complement of genes as it contains no obvious mutations other than a frameshift in the RL13 gene and a single nucleotide substitution that truncates the UL128 gene (55, 58).

1.7.3. HCMV and immune evasion

Binding and entry of HCMV into target cells initiates a number of pathways that ultimately leads to the production of type I IFNs and other inflammatory cytokines that activate APCs and recruit NK cells which subsequently drives the development of adaptive immunity. Over millions of years of co-evolution of virus and host, HCMV has evolved multiple mechanisms to modulate and evade the host immune response. HCMV contains many genes that for example, regulate expression of MHC class I molecules, intracellular and extracellular receptors, cytokines and chemokines, some of which are homologues acquired from host genes (59). A viral homologue of the anti-inflammatory cytokine IL-10 is encoded by the UL111A gene and has some of the immunosuppressive properties of cellular IL-10 (discussed in depth in section 4.1.1), and a viral homologue of CXCL1 encoded by the UL146 gene acts as an agonist for CXCR2 and induces neutrophil chemotaxis, which has been hypothesised to aid viral dissemination (60). The US28 gene encodes a viral chemokine receptor which can sequester CC-chemokines and deplete them from the medium, thus altering the chemokine environment of infected cells (60). A viral homologue of the TNF-receptor encoded by the UL144 gene has also been identified and is a potent activator of NF_kB and CCL22 which attracts T_H2 cells and Treg cells (61). The glycoprotein (gp) UL144 also binds to the inhibitory receptor B and T lymphocyte attenuator (BTLA) and inhibits T cell proliferation. BTLA expression is induced during activation of T cells and remains expressed on T_H1 cells, and binding of UL144 to this inhibitory receptor consequently inhibits T cell proliferation (62).

Another major evasion mechanism relies on the inhibition of MHC class I-restricted antigen presentation and consequently impedes cytotoxic $CD8^+$ T cell immunosurveillance. HCMV achieves this by several methods; US3 encodes a protein that binds MHC class I molecules and retains them in the endoplasmic reticulum (ER), gpUS2 and gpUS11 rapidly degrade MHC class I molecules, US6 encodes another glycoprotein that down-regulates MHC class I expression and finally, gpUS10 slows MHC class I maturation and egress from the ER (59, 63). HCMV also interferes with the presentation of MHC class II on professional APCs and subsequently impedes signalling to $CD4^+$ T cells. Genes involved in impeding this signalling are US2 and US3 which encode proteins that bind and downregulate MHC class II expression (63).

Cell death by apoptosis is a primitive mechanism of protection against viral infections. Four HCMV gene products, encoded by the immediate early (IE)1, IE2, UL36 and UL37 genes, have been implicated in blocking apoptosis (reviewed in (64)) which may aid in viral propagation as well as avoiding immune clearance by cytotoxic T cells or NK cells. Furthermore, protection from mitochondria-induced cell death is mediated by a virally encoded RNA, β2.7, which interacts with complex I (the first enzyme in the mitochondrial respiratory pathway) which stabilises the mitochondrial membrane, thus aiding successful completion of the HCMV life cycle (65).

Two HCMV Fcγ receptor homologues have also been identified, gp34 and gp68 (66). It was initially assumed that they would function like the viral Fcγ receptor from HSV-1, which protects against antibody-dependent cell-mediated cytotoxicity and complement activation, but the proteins have different pH requirements for binding which probably relates to different mechanisms following IgG engagement and therefore their function is still to be properly determined (63).

Other immune evasion genes include those for the production of proteins encoded by IE1 and IE2 that interfere with IFN signalling (63), and a vast array of mechanisms to evade NK cell killing, discussed in detail below.

1.7.4. HCMV and NK cells

There is limited but compelling clinical evidence for the role of NK cells in immunity to HCMV infection. Individuals with rare NK cell defects often exhibit enhanced susceptibility to herpesvirus infections and can have serious recurrent episodes of HCMV disease (67, 68). In renal transplant patients, enhanced NK cell activity was implicated in recovery from HCMV infection (69). Recovery of NK cell cytotoxicity following bone marrow transplantation also correlated with survival from HCMV related disease (70).

Indirect evidence for the importance of NK cells in response to HCMV infection is suggested by the extensive mechanisms HCMV employs to evade or modulate NK cell function (71). As described in section 1.7.3, the HCMV genome encodes several proteins which contribute to the downregulation of MHC molecules on the cell surface. In theory, this should make HCMV-infected cells with downregulated expression of MHC molecules vulnerable to NK-mediated lysis. However, the UL18 gene encodes an MHC class I homologue (72) that acts as a decoy protein and is expressed on the cell surface and binds to the NK cell inhibitory receptor LIR1 (reviewed in (73)). Furthermore, a glycoprotein encoded by UL40 contains a sequence homology to a human leukocyte antigen (HLA)-E binding peptide which can substitute and up-regulate cell-surface expression of HLA-E on infected cells (74). HLA-E is a non-classical MHC class I molecule which binds to the NK inhibitory receptor complex CD94/NKG2A and therefore suppresses NK cell recognition of infected cells. NKG2D is a potent NK activating receptor and can recognise an array of ligands. Expression of these ligands is activated in response to viral infections. Glycoproteins encoded by UL16 and UL142 prevent cell surface expression of these NKG2D ligands, as does the non-coding microRNA

miRUL112 (reviewed in (73)) thus impeding NK recognition of infected cells. Other mechanisms to evade NK cell killing include production of a tegument phosphoprotein, pp65, which inhibits signalling mediated through the activating receptor NKp30 (75), and production of gpUL141 which prevents surface expression of CD155, a ligand for the activating receptor CD226 (76). The multiple evasion mechanism employed by HCMV, including those for NK cell evasion, are depicted in Fig1.3.

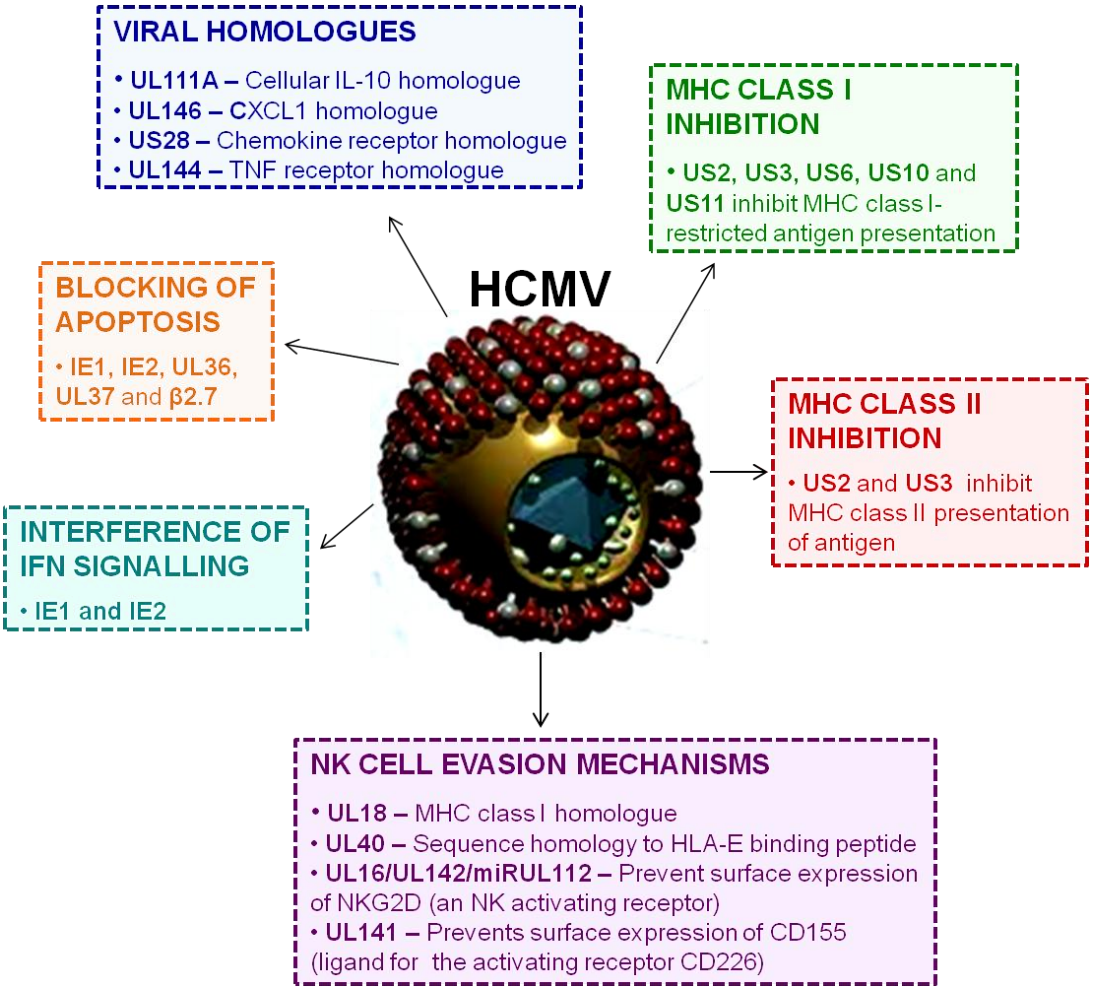

Figure 1.3. Immune evasion mechanisms of HCMV
Millions of years of co-evolution of virus and host has led to HCMV evolving multiple mechanisms to modulate and evade the host immune response. HCMV contains many genes for this immune evasion and are shown in bold text.

Despite the multiple evasion strategies evolved by the virus, NK cells have evolved further mechanisms to aid in their control of HCMV infection. To date the vast majority of *in vitro* studies examining the effector mechanisms used by NK cells to control HCMV infection have focused on their ability to recognise target cells and subsequently eliminate them via perforin-dependent cytolysis. However, NK cells have also been shown to inhibit HCMV replication through a non-cytolytic mechanism. Activated NK cells express LTαβ, and also secrete LTα and TNFα, which contributes to the release of IFNβ from the infected cell. The potent combination of IFNβ along with NK cell derived-IFNγ, inhibits virus replication (77). Finally, a recent study showed preferential expansion of a unique NK cell subset that co-express the activating receptor CD94/NKG2C and CD57 in $HCMV^{+}$ donors. These cells preferentially lack expression of inhibitory receptors NKG2A and KIR3DL1 and the percentage of these cells rapidly increases in solid-organ transplant recipients with active HCMV infection (78). The authors of this study propose that this subset of NK cells may even act as 'memory' NK cells that have expanded in response to HCMV infection (78).

1.8. Murine cytomegalovirus (MCMV)

1.8.1. MCMV as a model for HCMV infection

MCMV is a β-herpesvirus and like other cytomegaloviruses, is a member of the *Herpesviridae* family of viruses. It has a double stranded DNA genome encoding 170 open reading frames (ORFs) (79). Like HCMV, MCMV demonstrates species specificity and establishes life-long persistence after the resolution of acute infection. It has a prevalence of between 60-90% in the wild mouse population. The route(s) of horizontal transmission are not yet clearly determined. However, infectious virus can be detected in saliva of chronically infected mice and productive infection is confined to glandular epithelial cells of the salivary glands for prolonged periods of time, even in an immunocompetent host, thus, saliva is likely to be a major source of virus for horizontal distribution (80). Sexual transmission may also be an important means of horizontal spread. The main entry route for MCMV is the epithelium of the gastrointestinal, upper

respiratory and genitourinary tracts (80). After entry into the host, the virus then spreads to various organs and infects many cell types including endothelial and epithelial cells, myocytes, fibrocytes, macrophages and bone marrow stromal cells (80). The entry route of MCMV and the earliest events of its transport into the nucleus are still poorly understood, but do include attachment of the virion to the cell surface, penetration through the cell membrane and transport of viral genes to a site where viral DNA replication can occur (81). MCMV infection is characterised by 3 stages: 1) the acute-phase wherein the visceral organs such as the liver, lungs and spleen are the main sites of infection with titres peaking between days 3 and 5 post-infection (p.i) and the $CD8^+$ T cell response peaking at day 7 p.i; 2) the persistent phase where by infection in the visceral organs is under control but virus titres now peak in the salivary glands and $CD4^+$ T cells are the main cell subset responsible for controlling infection; 3) latent infection when infectious virus can only be sporadically detected (82). The time course of MCMV infection is depicted in Fig. 1.4.

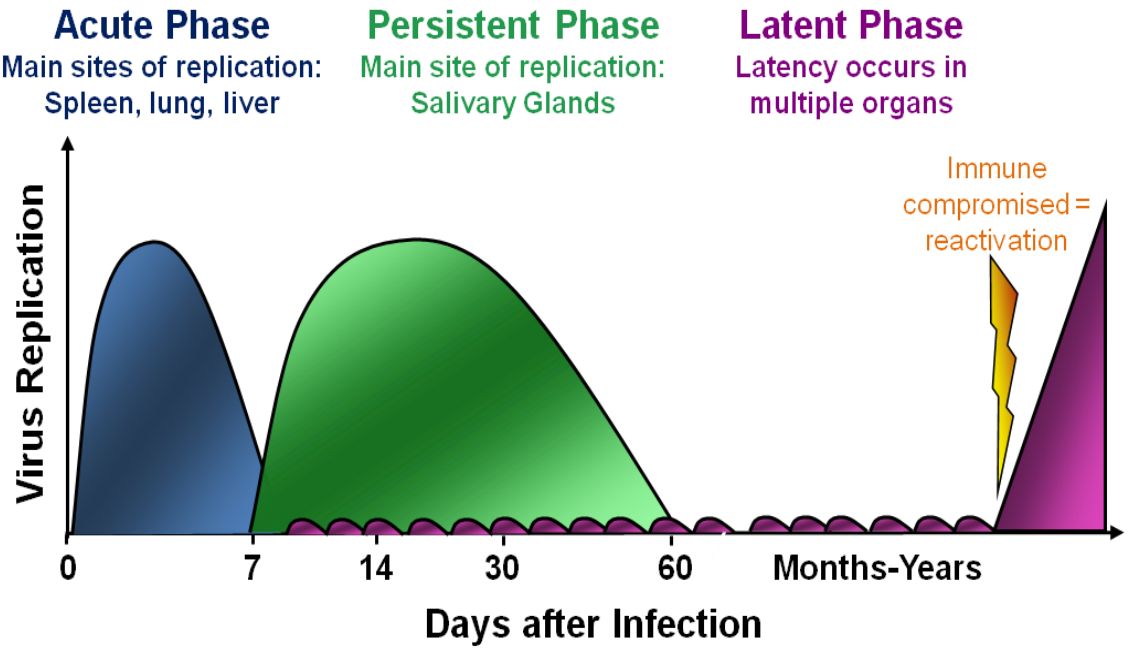

Figure 1.4. Time course of MCMV infection
MCMV infection is characterised by 3 distinct stages known as the acute phase, the persistent phase and the latent phase. Once latency is established, low levels of replicating virus can only be detected sporadically whilst the host remains immune competent. If the host becomes immune compromised, the virus can reactivate and high levels of replicating virus can once again be detected.

The experimental mouse models of MCMV infection have been extensively used for over 40 years to study the individual components of the host response that mediate resistance to acute, chronic and recurrent infections. The Smith and the K181 laboratory strains of MCMV are the most widely used in MCMV infection models. The Smith strain was derived from the original isolate of MCMV and is the most commonly used. MCMV infection of experimental mice mimics virus-induced disease in humans, for example, high viral titres in target organs are associated with pneumonitis, hepatitis and retinitis, and there are even models of congenital viral infection by MCMV (83). Importantly, different strains of inbred mice exhibit striking differences in their levels of susceptibility to MCMV infection due to genetic differences and is explained in detail in section 1.8.3. These differences make the mouse an excellent model to examine the heterogeneous response seen in humans and the identification of these genetic determinants may aid the identification of key components of the host immune response that are required for effective control of viral infections in humans (83).

1.8.2. MCMV and immune evasion

Similarly to HCMV, MCMV encodes a number of proteins that function to evade the host immune system. For example, MCMV encodes 3 products that alter MHC class I function – encoded by *m*152, *m*4 and *m*6 - consequently interfering with the ability of infected cells to present antigen to $CD8^+$ T cells (79, 82). MCMV also encodes three proteins that downregulate ligands of the activating receptor NKG2D – encoded by *m*145, *m*155 and *m*152 – thus inhibiting NK cell-mediated clearance (63). In conjunction with this, the MCMV gene *m*144 encodes a homologue for MHC class I. It has been suggested that this acts as a decoy for NK cells by engaging inhibitory NK receptors and protecting infected cells from cytolytic activity (80). MCMV also encodes a CC-chemokine homologue, MCK-2 which recruits leukocytes and aids dissemination of the virus to the salivary glands (84, 85). Furthermore, the protein encoded by *m*45 has been shown to protect infected

endothelial cells from premature cell death, thus allowing the completion of viral replication to occur within these cells (86).

1.8.3. MCMV and NK cells

The importance of NK cells in the defence against MCMV infection has been well characterised. The NK cell response does not develop to maturity in suckling mice until the third week of life, and until this stage, mice are extremely susceptible to MCMV infection. Adoptive transfer experiments using purified culture-derived NK cells from adult splenocytes showed that NK cells protected suckling mice (and also irradiated adult mice) from MCMV (87). Mice with genetic deficiencies in NK cell function are also highly sensitive to MCMV infection (88). Furthermore, *in vivo* depletion of NK cells results in substantially elevated titres of MCMV during early infection (89-91). During acute MCMV infection, NK cells execute their antiviral functions through the secretion of IFNγ and cytotoxic action, which are promoted by the production of pro-inflammatory cytokines IL-12 and IFNαβ respectively (20, 92).

Certain mouse strains are more resistant to MCMV infection than others. The mechanism that controls resistance was identified through genetic mapping which indicated a non-MHC linked resistance gene, designated *Cmv-1*, which encodes an NK activation receptor Ly49H. The Ly49 family of receptors, which are analogous to the human KIRs, are cell surface receptors expressed primarily on NK cells. They interact either with host classical MHC class I molecules or virus-encoded ligands (93). Their ectodomain is responsible for their specificity but it is the intracellular portion of the receptor which defines them as inhibitory (such as Ly49A and Ly49C) or activating (such as Ly49H and Ly49P) (94). In MCMV-resistant C57BL/6 mice, approximately 50% of NK cells express the Ly49H receptor under normal homeostatic conditions. Susceptible strains such as BALB/c, do not express this receptor. The Ly49H receptor in resistant mice binds directly to m157, a MCMV-encoded glycoprotein with structural homology to murine MHC class I.

Ly49H-m157 interactions during acute MCMV infection initiate an activating signalling cascade which results in rapid clonal proliferation of Ly49H$^+$ NK cells, killing of infected cells and secretion of pro-inflammatory cytokines, consequently reducing virus load (95). In resistant mice, infection with an *m*157-deleted virus renders them susceptible to MCMV as does the deletion of the host Ly49H gene. Conversely, transgenesis of Ly49H into susceptible strains was found to afford resistance to MCMV (reviewed in (95)), demonstrating the importance of this receptor-ligand pairing in the control of MCMV.

The retention of a viral protein that specifically activates an immune response appears paradoxical to survival of the virus. A possible explanation for this is that m157 is an MHC class I homologue and may have evolved to engage inhibitory NK cell receptors. In certain strains of mice, m157 binds the inhibitory receptor Ly49I. The *Ly49I* gene is evolutionary older than the *Ly49H* gene and since the Ly49 locus evolves rapidly, the inhibitory receptor could have been converted to an activating one whilst retaining the ability to bind m157 (96).

1.9. Interleukin-10 and the Interleukin-10 receptor

Activated haematopoietic cells secrete cytokines that play important roles in the regulation of immune responses by controlling cellular proliferation, differentiation and effector functions. IL-10 was first described as cytokine synthesis inhibitory factor and was identified as a product of T_H2 cells (97). It is an α-helical cytokine that belongs to the same family as type I IFNs and IFNγ. Mouse IL-10 and human IL-10 cDNAs encode very similar ORFs of 178 amino acids, sharing 73% amino acid homology (98). Human IL-10 is produced predominantly by macrophages, DCs, B cells and Tregs (99), although it can be produced by virtually all T cell subsets (100). Expression of IL-10 is regulated by several different mechanisms including the enhancing or silencing of *IL10* transcription which is under the control of specific transcription factors, as well as regulation at the post-transcriptional level (101). The control of IL-10 mRNA stability at a

post-transcriptional level may facilitate more rapid control of IL-10 expression under certain circumstances than could be achieved by activation of transcription alone (98).

The IL-10 receptor (IL-10R), like all receptors of α-helical cytokines, is composed of an extracellular binding module and an intracellular domain, and two subunits are required to generate a functional receptor complex (99). The IL-10R1 (IL-10Rα) is the ligand-binding subunit and is expressed by most haematopoietic cells, although generally at levels of only a few hundred molecules per cell. The IL-10R2 (IL-10Rβ) is the accessory subunit for signalling and is constitutively expressed in most cells and tissues. As there is no evidence for significant up-regulation of IL-10R2 in response to activation, any stimulus capable of activating IL-10R1 should therefore render most cells responsive to IL-10 (98). The interaction of IL-10 with its receptor engages the Jak family of tyrosine kinases Jak1 and Tyk2, which are constitutively associated with IL-10R1 and IL-10R2 respectively. This leads to tyrosine phosphorylation and activation of STAT (signal transducer and activator of transcription) proteins, predominantly STAT3 and to a lesser extent STAT1 and STAT5. STAT3 is the common transcription factor downstream of IL-10-IL-10R that mediates most inhibitory actions of IL-10 upon innate and adaptive responses (98, 99).

1.9.1. IL-10 modulation of immune cell function

The majority of the literature to date demonstrates that IL-10 is a suppressive cytokine. It potently inhibits the production of a number of cytokines by activated monocytes and macrophages, including TNFα and IL-1αβ which often have synergistic activities on pro-inflammatory pathways. IL-10 also inhibits monocyte production of chemokines that are involved in inflammation by recruiting monocytes, DCs, neutrophils and T cells (102). In addition to reducing pro-inflammatory mediators, IL-10 also enhances expression of their natural antagonists and anti-inflammatory molecules, for example IL-1R antagonist, whilst also inhibiting expression of IL-1R1 and IL-1R2 on monocytes (102).

Another important function of IL-10 is the inhibition of expression of MHC class II and co-stimulatory molecules, such as CD80 and CD86, on monocytes which consequently affects the ability of these cells to present antigen to and activate T cells. Interestingly, it is not the transcription or synthesis of MHC class II which is inhibited by IL-10, rather the prevention of the newly synthesised molecules reaching the plasma membrane, resulting in the accumulation of internalised MHC class II complexes in intracellular vesicles (103). Inhibited expression of co-stimulatory molecules by IL-10 is also observed on DCs, again impeding T cell responses. IL-10 also inhibits the generation and maturation of monocyte-derived-DCs (MD-DCs) with reduced levels of co-stimulatory and MHC class II molecules (102). IL-10 not only modulates cytokine production by monocytes, macrophages and DCs, but also by neutrophils. Furthermore, local and systemic inflammation driven by early influx of neutrophils is also reduced by IL-10, either indirectly through inhibition of neutrophil chemo-attractant production by macrophages, or directly via increased neutrophil apoptosis (reviewed in (104)).

In addition to the indirect inhibition of T cell activation and proliferation due to the downregulation of MHC molecules, co-stimulatory molecules and pro-inflammatory mediators by APCs, IL-10 also has direct effects on T cells by inhibiting cytokine production and chemokine receptor expression by $CD4^+$ T cells. Interestingly, activation of T cells in the presence of IL-10 can induce anergy, which can be associated with the induction of a population of Tregs that produce high levels of IL-10, consequently suppressing antigen-specific responses (102). IL-10 has differential effects on $CD8^+$ T cells depending on their activation state. As discussed above, in the presence of professional APCs, IL-10 indirectly suppresses proliferative responses and induces anergy, however if $CD8^+$ T cells are activated via their TCR in the absence of APCs, IL-10 in combination with low-dose IL-2 directly initiates growth-promoting activity of $CD8^+$ T cells (105).

Paradoxically, IL-10 has been shown to enhance survival of normal human B cells, although this does depend on activation state as discussed in (106), is a potent cofactor for B cell proliferation, and induces Ig production, isotype class switching and the differentiation of plasma cells into memory B cells (102). IL-10 also affects NK cell function in terms of cytotoxicity and IFNγ production which will be discussed in depth in section 3.1.1. The pleiotropic effects of IL-10 are summarised below in Fig. 1.5.

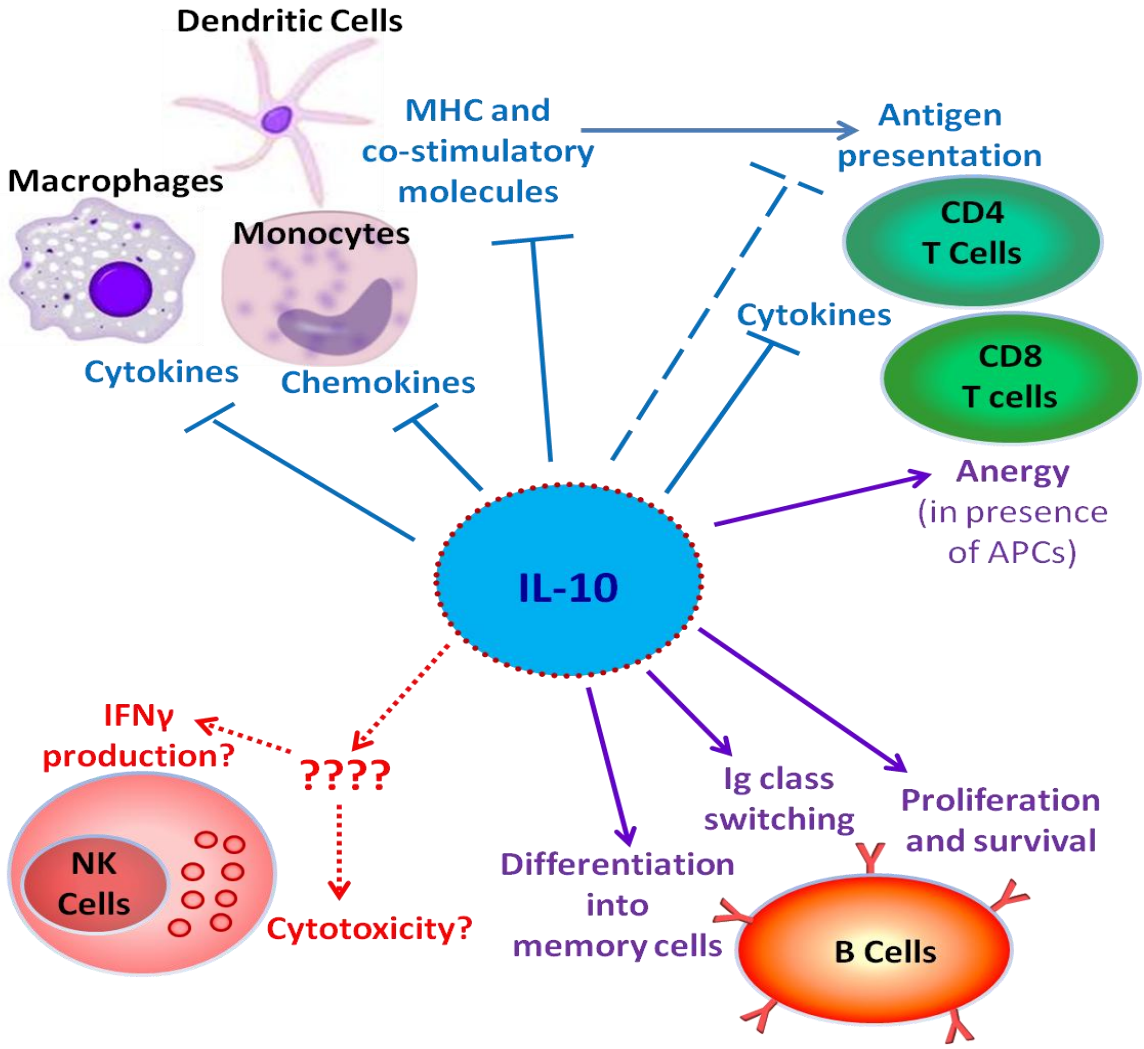

Figure 1.5. The pleiotropic effects of IL-10
IL-10 has direct immune suppressive effects on antigen presenting cells and both direct and indirect suppressive effects on T cells. Conversely, IL-10 has immune stimulatory effects on B cells. The effects of IL-10 on NK cell cytotoxicity and IFNγ production are variable between *in vitro* and *in vivo* experiments and are to be discussed in depth in section 3.1.1. Blue solid lines = direct inhibition by IL-10, blue dashed line = indirect inhibition by IL-10, purple solid arrows = functions enhanced by IL-10 and red dashed arrows = unknown effects (still to be discussed in section 3.1.1).

1.9.2. The role of IL-10 in infections

IL-10 has emerged as a key regulator of immune responses induced by viral, bacterial, fungal and protozoal infections. Typically, IL-10 functions to dampen over-exuberant responses elicited by the pathogens and subsequently, the absence of endogenous IL-10 or blocking of the IL-10 signalling pathway during these infections results in the onset of severe or often fatal infection-induced immune pathologies (107). For example, IL-10 deficient mice succumb to *Toxoplasma gondii* infection within 2 weeks of infection where as wt littermates exhibit 100% survival (108). Enhanced mortality is associated with increased levels of the T_H1 cytokines INFγ and IL-12 (108). In addition, IL-10 deficient mice also suffer from more severe disease and exhibit higher mortality rates than wt controls when infected with *Plasmodium chabaudi*, and enhanced pathology is associated with elevated levels of the T_H1 cytokine TNFα (109). T_H2 responses that lead to overproduction of IL-4, IL-5 and IL-13 can cause severe fibrosis in certain infections and are also regulated by IL-10 (107). Mice treated with IL-10 developed less liver, lung and pancreatic fibrosis when challenged with carbon tetrachloride, bleomycin and cerulean respectively (110-112). IL-10 treatment also reduced the severity of liver fibrosis in patients with chronic hepatitis C (HCV) infection (113).

During acute viral infections, IL-10 appears to have contrasting functions. For example, IL-10 can limit infection-induced immunopathology induced by respiratory syncytical virus (RSV) (114), and influenza (115). However, following high dose influenza infection, IL-10-deficient mice exhibit accelerated clearance of virus which is associated with the induction of antiviral T_H17 cells (116), suggesting that the biological outcome of IL-10R signalling during acute infection may vary depending on the virus pathogen and the infectious dose. Conversely, during chronic virus infection, there is no evidence to suggest IL-10R signalling affords benefit to the host, as demonstrated in the LCMV model where IL-10 actually antagonizes antiviral immunity and promotes virus chronicity (117, 118).

Interestingly, in certain persistent human viral infections including HCV, HIV and EBV, an increase in systemic IL-10 production can be observed, supporting the hypothesis that IL-10 may play a role in maintaining chronicity and pathogenicity in chronic infections; however, absolute proof of concept in humans is yet to be achieved (119).

The role that IL-10 plays in regulating anti-herpesvirus immunity *in vivo* has been elucidated in murine systems, particularly the MCMV model of infection, and will be discussed in detail in section 3.1.2.

1.9.3. Viral homologues of IL-10

Multiple members of the *Herpesviridae* and *Poxviridae* family of viruses have IL-10-like ORFs which have been identified by sequence homology. The *Poxviridae* viruses that encode an IL-10 homologue all infect ruminants and include orfpox virus, sheeppox virus, goatpox virus and lumpy skin disease virus, although the biological properties of most of these remain to be determined (120-122). All of the herpesviruses determined to date as encoding IL-10 homologues are found in the beta- and gamma-herpesvirinae subfamilies and include rhesus CMV, African green monkey CMV, baboon CMV, rhesus LCV, equine HV 2, ovine HV 2 and the human herpesviruses HCMV and EBV (summarised in (120)). These viral IL-10 homologues range in size from 139-191 amino acids, comparable in size to mammalian IL-10 proteins (176-180 amino acids) (120).

The EBV-encoded protein BCRF1 was the first herpesvirus-encoded protein identified to contain sequence homology (90% at amino acid level) with human IL-10 (123). BCRF1 is expressed during lytic infection (124) and inhibits monocyte stimulation of T cells and antagonizes expression of MHC class II (125) as well as co-stimulatory ligands (126) on the surface of macrophages and monocytes, suggesting BCRF1 functions to inhibit the activation of virus-specific $CD4^+$ T cells. Furthermore, during active replication in B cells, BCRF1 may contribute to evasion of direct recognition by $CD8^+$ T cells by interfering with B cell translocation of antigenic peptides to the ER for loading onto MHC class I (127).

BCRF1 may also exert more broad suppressive effects on the antiviral immune response via inhibition of cytokine production by T cells (123) and monocytes (125). Conversely, BCRF1 also promotes B cell survival (128) and proliferation (129) in a comparable manner to cellular IL-10, thus implying that BCRF1 may promote carriage of latent virus in B cells.

The IL-10 homologue encoded by HCMV is termed cmvIL-10. Unlike the high sequence homology of BCRF1, cmvIL-10 only exhibits 27% homology to human IL-10, but despite this, it can bind to IL-10R1 with essentially the same affinity as IL-10 and initiate IL-10R signalling (130). A latency-associated cmvIL-10 transcript (LAcmvIL-10) was also identified from the alternate splicing of the cmvIL-10 transcript (131). The functions of both cmvIL-10 and LAcmvIL-10 will be discussed in depth in section 4.1.1.

1.10. Interleukin-22 and the Interleukin-22 receptor

The IL-10 family of cytokines consist of 9 members which are divided into three subgroups. The first subgroup contains only IL-10 itself. The second subgroup is the IL-20 subfamily of cytokines composed of IL-19, IL-20, IL-22, IL-24 and IL-26. Broadly, their major functions are to protect against extracellular pathogens as well as to drive tissue remodelling and wound healing. Type III IFNs made up of the closely related cytokines IL-28A, IL-28B and IL-29 make up the third subgroup (100). This section will focus on one member of the IL-20 subgroup, IL-22.

IL-22 was initially known as IL-10 related T cell-derived inducible factor when it was first characterised by Dumoutier *et al* as it was a cytokine induced in mouse $CD4^+$ T cells after stimulation with IL-9, and was found to share 22.8% homology with IL-10 (132). It was renamed IL-22 after the human protein was discovered along with other structurally related cytokines mentioned above (133). Murine IL-22 has 80.8% homology to human IL-22, and like all other IL-10 family members has an α-helical structure (134).

The IL-22 receptor (IL-22R) is a heterodimer composed of IL-22R1 (IL-22Rα) and IL-10R2. As discussed in section 1.9, IL-10R2 is constitutively expressed on most cell types, whereas IL-22R1 expression is limited to non-haematopoietic cells of the skin, lung, small intestine, liver, colon, kidney and pancreas (133). IL-22 binds first to IL-22R1 and then the IL-22-IL-22R1 complex binds to IL-10R2, which propagates downstream signalling similar to that of the other IL-10 family members (135), primarily resulting in activation of STAT3 (136).

Unlike IL-22R1 expression which is restricted to non-hematopoietic cells, IL-22 can be expressed by a number of innate and adaptive immune cells. T_H17 cells are a major source of IL-22 production, along with activated NKT cells and γδ T cells, and $CD8^+$ T cells can express IL-22 *in vitro* when cultured with the same cytokines that induce IL-22 in $CD4^+$ T cells (136). Activated NK cells also express high levels of IL-22 (136), as do a heterogeneous population of innate lymphoid cells (ILCs) which largely lack expression of most lineage markers; the best characterised populations of ILCs being the $NKp46^+$ILCs and the $CD4^+$ILCs (135). A soluble secreted receptor of IL-22 also exists and is known as IL-22-binding protein (IL-22BP) (137). IL-22BP has been shown to counteract IL-22-IL-22R binding *in vitro* and may in fact have a higher binding affinity to IL-22 than that of IL-22 to IL-22R. However the pathways that regulate the expression of this receptor and its functions *in vivo* are yet to be characterised (135).

1.10.1. Functions of IL-22

To date, IL-22 has been shown to have multiple functions in tissue inflammation, immunosurveillance and homeostasis, particularly at barrier sites such as the skin and mucosal surfaces. Initial studies characterising the functions of this cytokine showed that keratinocytes stimulated with IL-22 caused marked induction of genes involved in antimicrobial defence (138). Subsequent studies showed that production of antimicrobial proteins by epithelial cells in the lung and the gut were also induced by IL-22 (reviewed in (139)). Antimicrobial proteins constitute an ancient form of innate immunity against extracellular microbial infection that encompasses pathogen recognition, inflammation, pathogen-clearance and resolution of inflammation, and therefore provide excellent protection at skin and mucosal surfaces. Thus, the induction of these proteins by IL-22 is important for the maintenance of mucosal immunity (140, 141). IL-22 can also up-regulate expression of acute-phase proteins such as serum amyloid A, which recruits immune cells to the sites of inflammation, especially in the liver, and sustained IL-22 exposure induces a systemic acute-phase response (142). The acute-phase proteins serve a range of physiological functions such as inhibiting the growth of microbes, trapping pathogens via increased coagulation, and increasing vascular permeability to enhance cellular recruitment to the sites of inflammation. These studies suggested that IL-22 is an important immune mediator acting on mucosal tissues to regulate host responses (143). The multiple functions of IL-22 at different sites are summarised in Fig. 1.6.

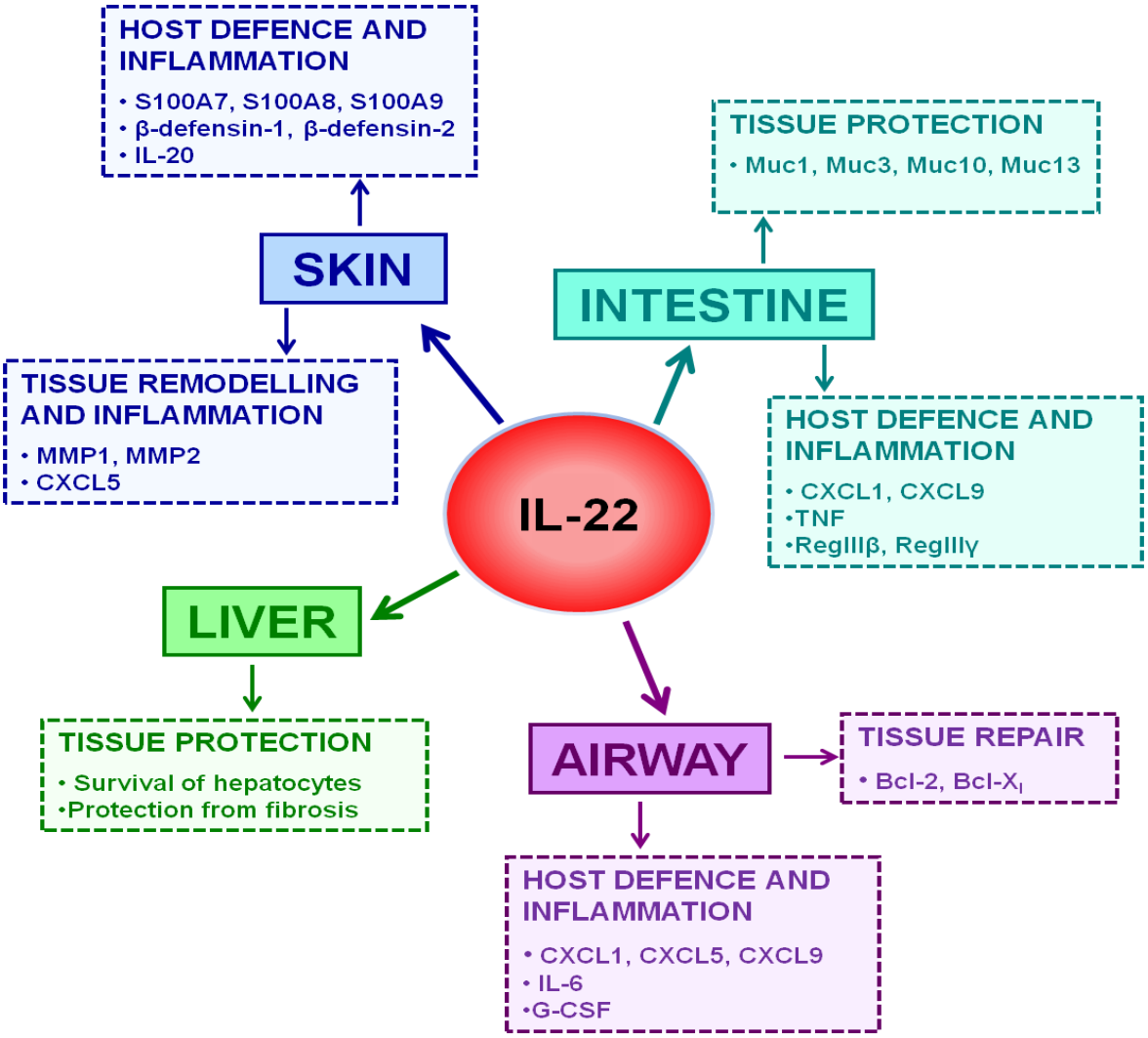

Figure 1.6. The multiple functions of IL-22
IL-22 has important functions in tissue inflammation, immunosurveillance and homeostasis, particularly at barrier sites, mucosal surfaces and the liver. IL-22 regulates the expression of genes encoding molecules associated with inflammation, repair, chemotaxis and the expression of antimicrobial peptides.

In addition to regulating the expression of antimicrobial peptides and acute-phase proteins, IL-22 has been shown to have other important functions which are somewhat context dependent, as IL-22 can both promote pathological inflammation and also prevent tissue destruction. For example, IL-22 is necessary for the induction of dermal inflammation in a mouse model of psoriasis-like skin inflammation by inducing IL-1, IL-6 and TNFα gene expression, as well as inducing gene expression of the antimicrobial

peptides S100A8, S100A9, defensin β1 and cathelicidins, which recruit and activate $CD4^+$ T cells, neutrophils, macrophages and DCs (144). In the intestine, up-regulation of IL-22 during infection with *Toxoplasma gondii* was essential for the development of ileitis in mice, and was associated with the upregulation of matrix metalloprotease 2, which drives immunopathology (145). Furthermore, in a collagen-induced arthritis model (a mouse model for rheumatoid arthritis), IL-22 was found to promote arthritic inflammation in the joints (146).

In contrast, IL-22 has also been shown to have protective roles in the lung. Not only was it demonstrated that IL-22 attenuated antigen-induced airway inflammation, possibly by the inhibition of eosinophil recruitment into the airways via expression of IL-25, (147), but also γδ T cell-derived IL-22 protects against lung fibrosis via inhibition of collagen deposition in a mouse model of hypersensitivity pneumonitis, possibly involving IL-22 diminished recruitment of αβ T cells (148).

Several groups have shown that in the liver, IL-22 is tissue protective during inflammation in mouse models of hepatitis. During hepatitis, hepatocytes are damaged leading to reduced liver function. However, IL-22 is a survival factor for hepatocytes and thus plays a protective role in preventing tissue injury (149, 150). Furthermore, during inflammatory bowel disease (IBD) where the epithelium of the gastrointestinal tract is destroyed, IL-22 actually protects mice from IBD, in particular $CD4^+$ T cell-mediated colitis as well as colitis mediated by the innate immune system (151). Conversely, in a colitis model induced by memory/effector $CD4^+$ T cells rather than naïve cells, T cell-derived IL-22 is actually pathogenic, highlighting the different ways IL-22 impacts IBD (152).

IL-22 also has a role in the host response to infectious diseases. IL-22 is highly expressed during certain infections, especially in response to extracellular pathogens. In the lung, IL-22 is important for controlling *Klebsiella pneumonia* infection in mice (143). It plays an

equally important role in protection from *Citrobacter rodentium* infection, as IL-22$^{-/-}$ mice have increased intestinal epithelium damage, greater bacterial loads and increased mortality (153). The critical role IL-22 plays in limiting bacterial replication and dissemination in these models is probably in part due to IL-22 inducing the expression of antimicrobial peptides from epithelial cells at these barrier surfaces (135). Interestingly an *in vitro* study using human NK cells demonstrated that NK cell-derived IL-22 contributed to defences against *Mycobacterium tuberculosis* by inhibiting its growth in macrophages via enhancing phagolysosomal fusion (154).

1.11. Thesis aims

Understanding how antiviral immune responses are suppressed during HCMV infection and identifying what immune mechanisms contribute to protection will assist in the design of effective vaccination and immune therapeutic strategies. Given the immunosuppressive functions of IL-10 and the evolutionary acquisition by HCMV of its own IL-10 homologue, elucidating the *in vivo* role of mammalian- and viral-IL-10 during acute infection is likely to aid in vaccine/therapy design. Moreover, IL-22 has been shown to provide critical protection against certain infectious agents, particularly bacterial infections. However, the role that IL-22 plays in antiviral immunity is not clear. Therefore, understanding how IL-22 acts during *in vivo* MCMV infection may also profoundly influence the development of novel therapies to counter HCMV.

The overall aims of this thesis are:

1) Utilise the MCMV model of infection to elucidate the *in vivo* role of mammalian IL-10 during acute cytomegalovirus infection
2) Ascertain the *in vitro* role of viral-IL-10 during HCMV infection
3) Determine the function of IL-22 during acute MCMV infection

The specific hypotheses I will be testing experimentally will be discussed in finer detail in each individual results section (chapters 3-5).

Chapter 2 - Materials and Methods

2.0. Treatment of animals

Wild-type (wt) C57BL/6 experimental mice were obtained from the external suppliers Harlan UK (Blackthorn, UK). Animals were kept under a Home office licence issued to Dr Ian Humphreys (PPL 30/2442) and were treated according to home office regulations. All mice were kept in specified pathogen free Scantainer housing at the home office designated facility at Heath Park Cardiff University. $Rag^{-/-}$ mice and IL-$10^{-/-}$ mice (both on a C57BL/6 background) were obtained from breeding colonies within the facility and were kept in filter top cages. Health status of animals within the facility was determined by sentinel screening every three months. Mice were culled by an approved schedule one method of euthanasia.

2.1. MCMV virus generation

Three to four week old, female BALB/c mice were obtained from Harlan and were infected with 1×10^4 plaque forming units (PFU) of low passage Smith strain (American Type Culture Collection, Manassas, VA) MCMV by intra-peritoneal (IP) injection. At day 13 p.i, salivary glands were harvested, and homogenised using an IKA T10 basic electric tissue homogeniser (Thermo Fisher Scientific, East Sussex, UK). The resulting homogenate was centrifuged (2000rpm, 10 minutes, 4^oC) to pellet cellular debris. The virus-containing supernatant was overlaid onto a sorbitol cushion (section 2.23) and centrifuged at high speed (18100rpm, 75 minutes, 4^oC). The virus pellet was then resuspended in endotoxin low 1 x PBS and sonicated for 5 minutes on ice. The sample was centrifuged (2000rpm, 10 minutes, 4^oC) and the supernatant was taken and aliquoted and stored under -80^oC freezing conditions. Virus stocks were titred by plaque assay (section 2.7) on two-three separate occasions and an average taken.

2.2. Viral infections and treatments

Mice were infected by IP injection with 5 x 10^4 PFU or 3 x 10^4 PFU MCMV. In some experiments, mice were also administered by IP injection on the day of infection 250µg of either rat IgG (Chemicon International, Temecula, CA) or anti-IL-10R (clone 1B1.3A, BioXCell, West Lebanon, NH). For the NK cell depletion experiments, mice were administered 200µg of anti-NK1.1 antibody (clone PK136, BioXCell) on days -2, 0 and +2 of infection by IP injection. In other experiments, mice were administered 50µg of either goat IgG (Chemicon) or anti-IL-22 (R&D Systems, Minneapolis, MN) by intravenous (IV) injection on days 0 and +2 of infection. For the neutrophil depletion experiments, mice were injected by IP with 100µg anti-Ly6G (clone 1A8, BioXCell) on days 0 and +2 of infection.

2.3. Leukocyte isolation

To isolate pulmonary leukocytes, mice were perfused with 10ml sterile PBS and lungs surgically excised, cut into small pieces and incubated in collagenase-containing buffer (section 2.23) at 37^{o}C with mild agitation for 45 minutes. Cells were then passed through a 70µm nylon cell strainer, washed in PBS and resuspended in red blood cell lysis buffer (section 2.23) for 5 minutes at room temperature (RT). Samples were then washed in PBS and resuspended in a specific volume of R10 media (section 2.23). Spleens were excised and cells isolated by passage through a 70µm nylon cell strainer prior to washing with PBS, red blood cell lysis and resuspension in R10. Livers were also excised and passed through a 70µm and washed in PBS. Cells were resuspended in 37.5% percoll (diluted in PBS) and centrifuged at 2000rpm for 6 minutes before red blood cell lysis and resuspension in R10. Viable lymphocytes were quantified using trypan blue exclusion.

2.4. FACS staining

Leukocytes (1 x 10^5 cells/200µl well) were incubated with Fc receptor blocking reagent (eBioscience, San Diego, CA) in facs buffer (section 2.23) and stained with various antibody panels to identify surface markers (see Table 1 for antibodies used). All antibodies for surface staining were diluted in facs buffer and incubated in 25µl volumes unless otherwise stated. Cells were then fixed with 3% paraformaldehyde (Thermo Fisher Scientific). In some instances, cells were permeabilised with saponin buffer (section 2.23) and stained with intracellular antibodies (see Table 2 for antibodies used).

2.4.1. FACS staining to assess proliferation

Isolated leukocytes were surface stained with anti-NK1.1-APC and anti-CD3-PE-Cy5, cells were fixed and permeabilised and stained with anti-Ki67-FITC.

2.4.2. FACS staining to assess early NK cell apoptosis

Isolated leukocytes were incubated with Live/Dead Fixable Aqua (Invitrogen, Carlsbad, CA), then stained with anti-CD3-Percp-Cy5.5, anti-NK1.1-APC and either Annexin-V FITC (BD Pharmingen, Franklin Lakes, NJ), or anti-caspase-3-PE (active form), according to manufacturer's instructions. Briefly, for caspase-3 staining, after surface staining, cells were resuspended in BD Cytofix/Cytoperm solution and incubated for 20 minutes on ice in the dark. Cells were washed with BD Perm/Wash buffer and resuspended in Perm/Wash buffer containing the anti-caspase-3 antibody and incubated for 30 minutes at RT in the dark. Cells were again washed and resuspended in Perm/Wash buffer. For Annexin-V staining, after surface staining, cells were resuspended in 1 x BD Binding Buffer containing the Annexin V-FITC probe (1:50 dilution) and incubated for 15 minutes at RT in the dark. Cells were washed and resuspended in BD binding buffer and analyzed by flow cytometry within 1 hour.

2.4.3. FACS staining to assess *ex vivo* cytokine production

Leukocytes were incubated at 1 x 10^5 cells/ml for 4 hours at 37°C in the presence of 2µg/ml brefeldin A (Sigma-Aldrich, UK). Cells were then washed and incubated with Fc block and surface stained with appropriate antibodies prior to fixation with 3% formaldehyde (Thermo Fisher Scientific). Cells were then permeabilised with saponin buffer and stained with anti-IFNγ-FITC or anti-IFNγ-PE-Cy7. To assess IL-10 expression, splenocytes and lung leukocytes were stimulated for 5 hours at 37°C with either 50ng/ml PMA and 500ng/ml ionomycin (for expression by T cells and NK cells), 10µg/ml LPS, 50ng/ml PMA and 500ng/ml ionomycin (for expression by B cells) or 10µg/ml LPS (for expression by APCs) (all reagents from Sigma-Aldrich). Cells were then incubated with Fc block and surface stained with anti-CD4-PB, anti-CD8-APC-H7, anti-CD3-PerCP-Cy5.5, anti-NK1.1-APC, anti-gamma delta TCR-FITC, anti-CD11b-PE-Cy7, or anti-B220-PE-Cy7 prior to fixation, permeabilisation and intracellular staining with anti-IL-10-APC. To assess IL-22 expression, splenocytes and lung and liver leukocytes were stimulated for 4 hours at 37°C with 50ng/ml PMA, 500ng/ml ionomycin and 50ng/ml IL-23 (R&D systems) in the presence of 2µg/ml brefeldin A. Cells were then incubated with Fc block and surface stained with anti-CD3-APC-Cy7, anti-NK1.1-APC, anti-gamma delta TCR-FITC, anti-CD4-PB and anti-CD8-PerCP prior to fixation, permeabilisation and intracellular staining with anti-IL-22-PE.

2.4.4. FACS staining to assess NK cell cytotoxicity

Leukocytes were incubated for 1 hour with anti-CD107a-FITC (2µl/well = 5µg/ml) and then 0.7µg/ml monensin (BD Pharmingen) was added for a further 4 hours at 37°C. Cells were then surface stained with anti-CD3 and anti-NK1.1.

Table 1. Details of antibodies used for flow cytometric detection of cell surface-expressed proteins

Antibody	Conjugate	Clone	Company	Dilution
α-Gamma Delta-TCR	FITC	GL3	BD Pharmingen	1:75
α-CD107a	FITC	1D4B	BD Pharmingen	2µl/well = 5µg/ml
α-CD122	FITC	TM-b1	eBioscience	1:100
α-CD19	FITC	eBIO13D	BD Pharmingen	1:100
α-CD69	FITC	H1.2F3	BD Pharmingen	1:100
α-Gr-1	FITC	RB6-8C5	Biolegend	1:100
α-KLRG1	FITC	2F1	Southern Biotech	1:100
α-Ly49H	FITC	3D10	BD Pharmingen	1:200
α-Ly6B	FITC	7/4	AbD Serotech	1:100
α-NKp46	FITC	29A1.4	eBioscience	1:100
α-CD122	PE	TM-b1	eBioscience	1:100
α-CD210 (IL-10R)	PE	1B1.39	BD Pharmingen	1:100
α-CD25	PE	PC61-5	eBioscience	1:100
α-CD27	PE	LG.7F9	eBioscience	1:100
α-Ly6G	PE	1A8	BD Pharmingen	1:100
α-Ly6B	PE	7/4	AbD Serotech	1:20
α-NK1.1	PE	PK136	eBioscience	1:100
α-TCRβ	PE-Cy5.5	H57-597	eBioscience	1:50
α-CD8α	PerCP	53-6.7	BD Pharmingen	1:100
α-CD3	PerCP-Cy5.5	145-2C11	BD Pharmingen	1:50
α-I-A/I-E (MHC II)	PerCP-Cy5.5	M5/114.15.2	Biolegend	1:200
α-B220	PE-Cy7	RA3-6B2	Biolegend	1:100
α-CD11b	PE-Cy7	M1/70	eBioscience	1:100
α-CD11c	PE-Cy7	N418	BD Pharmingen	1:100
α-CD69	PE-Cy7	H1.2F3	eBioscience	1:50
α-CD95	PE-Cy7	Jo2	BD Pharmingen	1:100
α-KLRG1	PE-Cy7	2F1	eBioscience	1:50
α-F4/80	APC	BM8	eBioscience	1:100
α-NK1.1	APC	PK136	BD Pharmingen	1:100
α-CD11b	APC-Cy7	M1/70	BD Pharmingen	1:75
α-CD3	APC-Cy7	145-2C11	Biolegend	1:75
α-CD8α	APC-H7	53-6.7	BD Pharmingen	1:100
α-CD127 (IL-7Rα)	PB	A7R34	eBioscience	1:100
α-CD4	PB	RM4-5	BD Pharmingen	1:100

Table 2. Details of antibodies used for flow cytometric detection of intracellular proteins

Antibody	Conjugate	Clone	Company	Dilution
α-Granzyme B	FITC	GB11	Biolegend	1:100
α-IFNγ	FITC	XMG1.2	eBioscience	1:100
α-Ki67	FITC	B56	BD Pharmingen	1:25
α-Caspase-3 (active form)	PE	C92-605	BD Pharmingen	1:6
α-IL-22	PE	IC582P	R&D systems	1:50
α-IFNγ	PE-Cy7	XMG1.2	BD Pharmingen	1:75
α-IL-10	APC	JES5-16E3	eBioscience	1:100

FITC = Fluoresceine-isothiocyanate
PE = Phycoerythin
PE-Cy5.5 = Phycoerythin-Cyanine 5.5
PE-Cy7 = Phycoerythin-Cyanine 7
PerCP = Peridinin chlorophyll
PerCP-Cy7 = Peridinin chlorophyll-Cyanine 7
APC = Allophycocyanin
APC-Cy7 = Allophycocyanin-Cyanine 7
PB = Pacific Blue

2.4.5. FACS staining to assess MCMV specific $CD4^+$ T cells

Examination of MCMV specific $CD4^+$ T cell responses was carried out by peptide stimulation with MHC class II restricted peptides. Splenocytes and lung leukocytes were incubated for 5 hours at 37°C in the presence of 2µg/ml brefeldin A and 3µg/ml MCMV-derived peptides (Genscript, Piscataway, NJ). A medium alone control without peptides was run alongside the stimulations. The sequences of the peptides used were:

M25: NHLYETPISATAMVI

m139: TRPYRYPRVCDASLS

m142: RSRYLTAAAVTAVLQ

Cells were then stained with anti-CD4-PB and anti-CD3-PE-Cy5 before fixation, permeabilisation and intracellular staining with anti-IFNγ-FITC.

2.4.6. Acquisition and analysis

All data were acquired on a BD FACS Canto II. Electronic compensation was performed with antibody-capture beads (BD Pharmingen) stained with individual monoclonal antibodies used in the experimental panel. A minimum of 30,000 events were acquired in each case and data were analyzed using FlowJo software version 8.5.3 (TreeStar Inc, Ashland, OR). Total numbers of different cell populations were calculated by multiplying the total number of viable leukocytes (assessed by trypan blue exclusion) by percent positive cells, as detected by flow cytometry.

2.5. Cytometric Bead Array

Excised lungs, livers and spleens (~50mgs) were weighed and washed once in PBS and then homogenised in 1ml DMEM (Invitrogen) prior to centrifugation at 2000rpm for 10 minutes. Undiluted supernatants were then assayed for cytokines by cytometric bead array (Bender MedSystems, Vienna, Austria) according to manufacturer's instructions. Briefly, standard curves were generated in duplicate by serial dilution and samples were also measured in duplicate. Standards and samples were incubated with bead mix and biotin-conjugate mix for 2 hours at RT on a plate shaker at 500rpm. After two washes, standards and samples were then incubated with streptavidin-PE mix for 1 hour at RT on a plate shaker at 500rpm. After two washes, standards and samples were resuspended and acquired using a FACS canto II. Data was analysed using FlowCytomix Pro 2.3 software. Results were then calculated as pg cytokine/g tissue.

2.6. ELISAs

Excised lungs, livers and spleens (~50mgs) were weighed and then homogenised in 1ml DMEM prior to centrifugation at 2000rpm for 10 minutes. Undiluted supernatants were then assayed for IL-12, IL-22 and CXCL1 by ELISA.

2.6.1. IL-12: IL-12 was detected using a Peprotech (Rocky Hills, NJ) ELISA kit as per manufacturer's instructions. Briefly, capture antibody (diluted as instructed on Certificate of Analysis) was added to an ELISA plate (Nunc, Roskilde, Denmark) and incubated over night at RT (all further incubations were also carried out at RT). The next day, wells were washed 5 times with ELISA wash buffer (section 2.23) and incubated with block buffer (1% BSA (Sigma-Aldrich) in PBS) for 1 hour. Wells were washed again before standards and tissue homogenate samples were added in duplicate to the plate and incubated for two hours. After washing, detection antibody (diluted as instructed) was added and incubated for 2 hours. After the wells were washed again, streptavidin-HRP was added for 30 minutes. After the final washes, ABTS substrate (Sigma-Aldrich) was added. Colour development was monitored with a FLUOstar OPTIMA plate reader at 450nm wavelength with values subtracted at 570nm and optical density readings taken every 5 minutes over a 35 minute period.

2.6.2. IL-22: IL-22 was detected using an eBioscience ELISA kit as per manufacturer's instructions. Briefly, capture antibody (diluted as instructed on Certificate of Analysis) was added to an ELISA plate provided and incubated overnight at 4°C. The next day, wells were washed 5 times with wash buffer and the plate was blocked with 1 x assay diluent provided and incubated for 1 hour at RT (all further incubations were carried out at RT). Wells were washed again before the standards and tissue homogenate samples were added in duplicate to the plate and incubated for 2 hours. After washing, detection antibody (diluted as instructed) was added and incubated for 1 hour. After washing, working dilution of streptavidin-HRP was added and incubated for 30 minutes. The wells were then washed 7 times and incubated with substrate solution provided. After 15 minutes, 50µl of stop solution (1M H_3PO_4) was added. Absorption was measured with a FLUOstar OPTIMA plate reader at 450nm wavelength with values subtracted at 570nm.

2.6.3. CXCL1: CXCL1 was detected using an R&D systems ELISA kit as per manufacturer's instructions. Briefly, capture antibody (diluted as instructed) was added to an ELISA plate and incubated overnight at RT (all further incubations were also carried out at RT). The next day, wells were washed 5 times with wash buffer and blocked with reagent diluent (1% BSA in PBS) and incubated for 1 hour. Wells were washed again before standards and tissue homogenate samples were added in duplicate to the plate and incubated for 2 hours. After washing, detection antibody (diluted as instructed) was added and incubated for 1 hour. After washing, streptavidin-HRP was added and incubated for 20 minutes. The wells were then washed again and incubated with substrate solution for 20 minutes before stop solution was added. Absorption was measured with a FLUOstar OPTIMA plate reader at 450nm wavelength with values subtracted at 570nm).

Standard curves for each ELISA were generated in Graphpad Prism (version 5.0) by logarithmic transformation and unknown values generated for each sample. Values were then calculated as either pg/ml or as pg/g of tissue.

2.7. Plaque assay

Replicating virus in organs of MCMV-infected mice was detected by plaque assay. Tissue samples taken were snap-frozen in liquid nitrogen and then stored at -80°. Tissue samples were weighed prior to use. The embryonic fibroblast cell line NIH-3T3 was obtained from the internal Cardiff University cell bank and cultured in a humidified cell culture incubator (37^{o}C, 5% carbon dioxide) in D10 media (section 2.23). These cells were seeded onto Corning flat bottom 24 well cellbind plates (Appleton Woods, Birmingham, UK) at a concentration of 1.5×10^{5} cells per well in 1ml of D10 and incubated overnight. Cells were checked the next day to ensure they had formed a monolayer of approximately 80-90% confluency. The snap-frozen samples were mechanically broken down in DMEM using an IKA T10 electric tissue homogeniser in

polypropylene snap-cap tubes (BD Pharmingen). Samples were serially diluted in DMEM. The D10 media from the plates containing the confluent cells was then removed by gently pouring into bleach, and 200µl of each serial dilution from the homogenised samples was added to duplicate wells. For high sensitivity plaque assays, plates were centrifuged at 1200g for 30 minutes at RT and for standard plaque assays, plates were incubated at 37°C for 1 hour. The serially diluted samples were then aspirated off into bleach and warm CMC media (section 2.23) was added to each well. Cells were incubated for 6 days at 37°C to allow plaques to develop. After 6 days, the CMC media was removed by gently pouring into bleach and the cells were fixed with 10% paraformaldehyde in PBS for 2-3 hours or overnight, and stained with crystal violet solution (section 2.23) for 10 minutes. Plates were then gently washed under running water and left to air-dry. Plaques were counted and replicating virus calculated using the formula:

PFU MCMV/ml = average number of plaques x dilution factor x 5 (200µl of virus-containing media was used/well)

To calculate PFU/gram tissue, the following formula is used:
PFU/gram tissue = 1/sample weight x PFU/ml (as calculated above).

2.8. DNA extraction from tissues

Genomic DNA was isolated from spleen, lung and liver tissue using a DNeasy tissue kit (Qiagen, Valencia, CA), using a modified protocol. Tissue samples taken for DNA extractions were snap-frozen in liquid nitrogen and stored at -80°C. All DNA extraction work was done in an area that had been cleaned thoroughly with ethanol. All plastic-ware used was certified DNase and RNase free. Samples were incubated with 360µl of buffer ATL and 40µl of proteinase K at 56°C overnight in a shaking incubator. Samples were then forced through a G27 gavage needle (0.4 mm x 13 mm) until fully viscous. 400µl of buffer AL and 400µl of ethanol (96-100%) were added and samples vortexed. The mixture was then added to mini spin columns and centrifuged for 1 minute at 8000rpm. The flow

through was discarded and the spin column was placed into a new collection tube. The columns were then washed twice with 500µl of buffer AW1 (1 minute at 8000rpm) and washed once with 500µl of buffer AW2 (3 minutes at 13000rpm to ensure the spin column membrane was dry). DNA was eluted by adding 150µl of buffer AE and centrifuged for 1 minute at 8000rpm. Sample DNA concentration and purity (260/280 ratio >1.8) was determined using a ND-1000 NanoDrop^{TM} spectrophotometer from Thermo Fisher Scientific. Samples were kept at -80^{o}C for long term storage.

2.9. Viral genome detection

MCMV glycoprotein B (gB) was assayed by real-time quantitative PCR (qPCR) using Platinum SYBR green mastermix reagent (Invitrogen) and a Mini Opticon (Biorad Laboratories, Hercules, CA). For each 20µl reaction, the following components were added; 1.6µl DNA (as extracted using protocol in section 2.8), 10µl SYBR green, 0.4µl forward primer, 0.4µl reverse primer and 7.6µl DNase/RNase free water (Invitrogen). MCMV gB was measured relative to the amount of housekeeping gene β-actin. The primer sequences used for detection of the β-actin were forward: GATGTCACGCACGATTTCC and reverse: GGGCTATGCTCTCCCTCAC; primers used for detection of gB were forward: GAAGATCCGCATGTCCTTCAG and reverse: AATCCGTCCAACATCTTGTCG. 100ng aliquots of DNA were used as templates for each reaction, and diluted in DNase/RNase free water. Samples were run in triplicate and an average taken. Cycling parameters were as follows:

1. Incubate at 95°C for 15 minutes
2. Incubate at 95°C for 15 seconds
3. Incubate at 60°C for 1 minute 30 seconds
4. Plate read
5. Go to line 2 for 40 more times
6. Melting curve from 70°C to 90°C, read every 0.3°C, hold for 15 seconds
7. End

Relative amounts of viral genome were calculated using the following formula:

$$\text{Ratio gB:β-actin} = \frac{1}{2^{\wedge}(\text{Average reading for β-actin} - \text{Average reading for gB})}$$

Relative levels of viral genome were converted to genome copy numbers by extrapolating from a titration curve produced using the pARK25 MCMV plasmid (a gift from A. Redwood, University of Western Australia, Perth, Western Australia, Australia) by using Graphpad Prism software. The limit of detection was 10 genome copies/100ng DNA.

2.10. RNA extraction

RNA was isolated from liver, spleen and lung tissue or from populations of cells following MACS separation (section 2.13) using an RNeasy mini kit (Qiagen). Tissue samples taken for RNA extractions were frozen on dry ice in RNA later stabilisation reagent and then stored at -80°C. All RNA extraction work was done in an area that had been cleaned thoroughly with ethanol and then with RNase ZAP reagent (Invitrogen). All plastic-ware used was certified DNase and RNase free. Tissue samples were removed from the stabilisation buffer and transferred to 12ml screw cap tubes (Greiner Bio-one, Austria) containing buffer RLT and β-mercaptoethanol and mechanically broken down using an IKA T10 electric tissue homogeniser. Samples were centrifuged at full speed (13000rpm) for 5 minutes to pellet cellular debris. To remove the genomic DNA, the sample supernatant was added to a gDNA eliminator spin column and centrifuged at 8000rpm for 30 seconds. 70% ethanol (50% for liver samples) was added to the flow through. The mixture was then transferred to an RNeasy spin column provided and centrifuged at 8000rpm for 15 seconds. The RNeasy spin column was washed with buffer RW1, then twice with buffer RPE. The spin column was placed in a new collection tube and centrifuged at full speed for 1 minute to completely dry the membrane. The column was

then placed in a new collection tube and RNase free water was added. Tubes were centrifuged at 8000rpm for 1 minute to elute the RNA.

RNA concentration and purity (260/280 ratio <1.6) was determined using a ND-1000 NanoDrop^{TM} spectrophotometer. Samples were kept at -80^{o}C for long-term storage. Stable complementary DNA (cDNA) was made from the RNA (refer to section 2.11).

2.11. cDNA synthesis

RNA was converted into cDNA using a reverse transcription kit (Applied Biosystems, UK). All work was done in an area that had been cleaned thoroughly with ethanol and then with RNase ZAP reagent. All plastic-ware used was certified DNase and RNase free. A master mix of reaction components was prepared and added to each RNA sample. For each 10µl reaction, the following components were added: 3.85µl RNA, 1.0µl 10 x Taqman RT buffer, 2.2µl $MgCl_2$ (25mM), 2.0µl deoxyNTPs (2.5mM), 0.5µl random hexamers (50µM), 0.2µl RNase inhibitors (20U/L) and 0.25µl of multiscribe reverse transcriptase (500U/L).

Samples were then synthesised using a DNA Engine DYAD Peltier Thermal Cycler (Biorad Laboratories) using the following cycling parameters:

1. Incubate at 25^{o}C for 10 minutes
2. Incubate at 48^{o}C for 45 minutes
3. Incubate at 95^{o}C for 5 minutes
4. Incubate at 4^{o}C for ever

Samples were kept at -80^{o}C for long term storage.

2.12. qPCR reactions for gene expression

Levels of gene expression were measured by qPCR using the SYBR green master mix reagent as in section 2.9. For each 20µl reaction, the following components were added; 1.6µl cDNA (section 2.11), 10µl SYBR green, 0.4µl forward primer, 0.4µl reverse primer and 7.6µl DNase/RNase water. Amount of each gene of interest was measured relative to the house keeping gene β-actin. The primer sequences for each gene are listed in Table 3. Samples were run in duplicate and an average taken. The cycling parameters were the same as in section 2.9. Relative amounts of each gene were calculated using the following formula:

$$\text{Ratio of gene of interest:β-actin} = \frac{1}{2^{\wedge(\text{Average reading for β-actin - Average reading for gene of interest})}}$$

Table 3. Primer sequences for qPCR reactions to analyse gene expression

Gene of interest	Forward primer	Reverse primer
β-actin	GGGCTATGCTCTCCCTCAC	GATGTCACGCACGATTTCC
Cathepsin C	CCGGGCATTTTACCCTCAT	TTGAAAAACGCAAACCATTTGT
CXCL1	CTCAAGAATGGTCGCGAGGCT	GCACAGTGGTTGACACTTAGTGGTCTC
CXCL2	CTCAAGAATGGTCGCGAGGCT	TACGATCCAGGCTTCCCGGGT
CXCL5	CTCAGTCATAGCCGCAACCGAGC	CGCTTCTTTCCACTGCGAGTGC
CXCL15	GGTGATATTCGAGACCATTTACTG	GCCAACAGTAGCCTTCACCCAT
IFNα	GTCAGTGTCAGAAGCTCCTGTGGC	CTATGGTCCAGGCACAGTGACTG
IFNβ	GAATCTCTCCTTTCTCCTG	CTGACAACCTCCCAGGCAC
IFNγ	GCCGTGGCAGTAACAGCC	AACGCTACACACTGCATCTGGG
iNOS	GGCAGCCTGTGAGACCTTTG	GCATTGGAAGTGAAGCGTTTC
LTα	AACCCAAGAATTGGATTCCAGG	TGTGACCCTTGAAACAACGGT
LTβ	TGTCTCCAGCTGCGGATTCTA	TTTGGCAGCTGTTGAACCC
Mx1	TCTGAGGAGAGCCAGACGAT	ACTCTGGTCCCCCAATGACAG
TNFα	CATCTTCTCAAAATTCGAGTGACAA	TGGGAGTAGACAAGGTACACCCC
Viperin	CTTCAACGTGGACGAAGACA	GACGCTCCAAGAATGTTTCA

2.13. Cell separation

2.13.1. Positive selection

Leukocytes were isolated from the livers of MCMV-infected wt mice and separated by MACS separation according to manufacturer's instructions. Briefly, cells were stained with anti-Ly6G at 4°C, then washed with MACS buffer (section 2.23) and incubated with anti-PE beads (Miltenyi Biotec, Germany) also at 4°C. Cells were washed, resuspended in MACS buffer and run down an LS column (Miltenyi Biotec) attached to a magnet. The flow through was the negative fraction. The column was then removed from the magnet and magnetically labelled $Ly6G^+$ cells were flushed out with MACS buffer; this flow through was the positive fraction. The purity of the separated cell fractions were analysed by flow cytometry. For RNA analysis of the $Ly6G^+$ population, a purity of >80% was used and for the $Ly6G^-$ population, <2% of cells were $Ly6G^+$.

2.13.2. Sequential negative and positive selection

Splenic neutrophils from $Rag^{-/-}$ mice were isolated and sorted by using a negative selection kit (Stemcell technologies, France) and a positive selection kit (Miltenyi Biotec) according to manufacturer's instructions. Briefly, for negative selection, cells were incubated with EasySep mouse neutrophil enrichment cocktail, washed and then incubated with EasySep biotin selection cocktail. The cells were then incubated with EasySep magnetic particles and then run through an LS column. The flow through was the negative fraction which was then subjected to the positive selection process as described in 2.13.1. The purity of the separated cell fractions were analysed by flow cytometry and cells were used at a purity of >90%.

2.14. Nitric oxide and reactive oxygen species analysis

Purified neutrophils (section 2.13.2) from wt and $Rag^{-/-}$ mice were plated out at a concentration of 1×10^4/200µl well and incubated at 37°C with APF (Aminophenyl fluorescein), which is an indicator for reactive oxygen species, or DAF-FM Diacetate (4-

amino-5-methylamino-2',7'-difluorofluorescein diacetate), which detects low concentrations of nitric oxide (both from Invitrogen). After 1 hour, cells were centrifuged (1500rpm, 5 minutes) and supernatants containing unbound reagents were discarded. Cells were then incubated with 1×10^4 PFU MCMV overnight. Neutrophils were then washed and stained with anti-Ly6G-PE and anti-CD11b-APC-Cy7 before being analysed on the BD Canto II.

2.15. Neutrophil *in vitro* killing assay

3T3 cells were plated out at a concentration of 5×10^4 in a 48 well plate (Nunc) and incubated overnight at 37°C in D10 media. The next day, media was removed and cells were infected with MCMV at a multiplicity of infection (MOI) of 0.02 in 200µl volumes by centrifugation at 1200g for 30 minutes followed by 30 minutes incubation at 37°C. Supernatant was then flicked off and purified neutrophils (section 2.13.2) were added to the 3T3s at varying effector to target ratios (neutrophils:3T3s), with 0:1 being the lowest, and 1:1 the highest. Freeze-thawed neutrophils were used as a negative control. Plates were then incubated for 7 days at 37°C. Supernatants were then removed and analysed for levels of replicating virus in a standard plaque assay (section 2.7).

2.16. Recombineering

A bacterial artificial chromosome (BAC) containing almost the full length genome of the low passage HCMV strain Merlin was kindly made available by Dr Richard Stanton (58). This BAC is a self-exercising Merlin BAC containing a gene encoding Cre recombinase which upon transfection into mammalian cells, mediates removal of the BAC vector by recombination between *loxP* sites. The *E. coli* plasmid cloning vector used for the construction of this BAC is pBeloBAC11 (see Fig. 2.1). The technique of recombineering (as described in (155, 156)) was then used to modify the Merlin BAC, described in detail in sections 2.16.1 and 2.16.2.

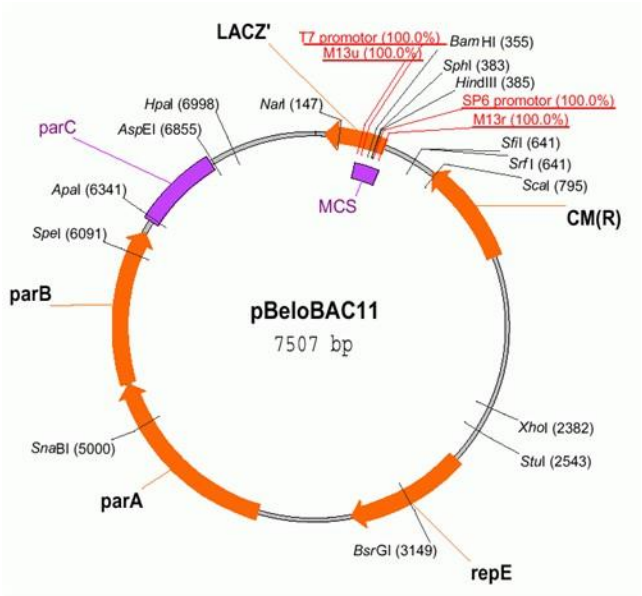

Fig 2.1. pBeloBAC11 vector diagram
The pBeloBAC11 vector was used in the construction of the Merlin BAC kindly made available by Dr Richard Stanton (58)

2.16.1. Generation of selectable cassette for first round of recombineering

A selectable cassette encoding lacZ, ampicillin resistance and sacB was inserted into the BAC during the first round of recombineering. The *sacB* gene encodes the secreted enzyme levansucrase which catalyzes the hydrolysis of sucrose and synthesis of levans and expression of this gene in *E. coli* in the presence of sucrose is lethal. The cassette was amplified by PCR using primers with overlapping homology of ~20bp to the cassette and ~80bp to the target insertion site in the BAC. The primer sequences are listed in Table 4. PCR products were amplified using the Roche (UK) Expand Hi-Fi kit. For each 50µl reaction, the following components were added; 42µl double-distilled water (ddH_2O), 5µl 10 x buffer 2 (containing $MgCl_2$), 1µl dNTPs, 1µl forward primer, 1µl reverse primer, 0.5µl template DNA and 0.5µl enzyme. Samples were synthesised using a T3 Thermocycler (Biometra, Germany) using the following parameters:

1. Incubate at 95°C for 2 minutes
2. Incubate at 95°C for 30 seconds
3. Incubate at 55°C for 30 seconds
4. Incubate at 68°C for 4 minutes and 30 seconds
5. Go to line 2 for 9 more cycles
6. Incubate at 95°C for 30 seconds
7. Incubate at 55°C for 30 seconds
8. Incubate 68°C for 4 minutes and 30 seconds plus 20 seconds/cycle
9. Go to line 6 for 24 more cycles
10. Incubate at 68°C for 15 minutes

The PCR product was then run on a 0.7-0.8% agarose gel (section 2.23) and gel purified using GE Healthcare (Waukesha, WI) GFX columns following manufacturer's instructions.

2.16.2. First round of recombineering

SW102 bacteria containing the full length Merlin genome were incubated overnight in 5ml Luria-Bertani (LB) (Melford Laboratories, UK) media (section 2.23) containing 12.5µg/ml chloramphenicol (Sigma-Aldrich) in a shaking incubator at 32°C. 0.5ml of overnight culture was then cultured in 25ml of LB media containing chloramphenicol in a shaking incubator at 32°C until an optical density$_{600}$ of ~0.6 was reached. Optical density was measured on an Ultraspec 3000 (Pharmacia Biotech, Golden Valley, MN). To make the bacteria competent and activate the lambda red genes, the culture was then transferred to a 50ml falcon tube and incubated in a water bath at 42°C for 15 minutes and then chilled on ice for 20 minutes before begin centrifuged for 5 minutes at 4000rpm at 0°. The pellet was then washed twice with 25ml ice-cold ddH_2O and resuspended in ~400µl ddH_2O. 25µl was added to an eppendorf along with 4µl purified PCR product and transferred to a pre-cooled 0.2cm cuvette (Biorad Laboratories), left to rest on ice for 5 minutes and then electroporated at 2.5kV using a Biorad Micropulser. Bacteria were then

recovered in 1ml of LB media for 1 hour at 32°C. Bacteria were then spun down and the pellet resuspended in ~150µl LB media and spread onto an LB plate containing ampicillin (section 2.23) and incubated at 32°C until blue colonies appear. To check for sacB functionality, 4 different blue colonies were picked and streaked onto both LB plates containing ampicillin and LB plates containing sucrose but no salt (section 2.23), and also inoculated into 5mls of LB media and incubated overnight at 32°C.

Table 4. Primer sequences used in recombineering

Amplifying sacB cassette	**Forward primer:** ACGGCACGCGGAAAGGTCTCAGCGAGTTGGACACGTTGTTTAGCCGTCTC GAAGAGTATCTGCACTCGAGAAAGTAGCCTGGTACGGAAGATCACTTCG **Reverse primer:** CACGACGCAACGTGGTTAAACAGTACGTTTATTAAAGTAACTGGGTGAACG ACATCGGAGCGGACTGCAAATCGCAACGCTGAGGTTCTTATGGCTCTTG
Sequencing sacB cassette	**Primer 1:** ACGGAAATGTTGAATACTCATACTCT **Primer 2:** TTGAAAAACGCAAACCATTTGT
Amplifying GFP for insertion after UL111A	**Primer 1:** CGGATAACGGCACGCGGAAAGGTCTCAGCGAGTTGGACACGTTGTTTAGC CGTCTCGAAGAGTATCTGCACTCGAGAAAGGGTAGCGCTGGATCAGCAGG **Primer 2:** CGACGCAACGTGGTTAAACAGTACGTTTATTAAAGTAACTGGGTGAACGAC ATCGGAGCGGACTGCAAATCGCAACGTTACTTGTACAGCTCGTCCATGC
Amplifying GFP to replace UL111A	**Primer 1:** TGACAAAAACATCATAACATAAAGGACCACCTACCTGGGACGCGCAGTTGG GCGGCGGATTGGGGCGGCATGCTGCGGCGATGGTGAGCAAGGGCGAGGA **Primer 2:** CGACGCAACGTGGTTAAACAGTACGTTTATTAAAGTAACTGGGTGAACGAC ATCGGAGCGGACTGCAAATCGCAACGTTACTTGTACAGCTCGTCCATGC
Oligo. to delete UL111A	CTACCTGGGACGCGCAGTTGGGCGGCGGATTGGGGCGGCATGCTGCGGC GCGTTGCGATTTGCAGTCCGCTCCGATGTCGTTCACCCAGTTACTTTAATA
Sequencing deleted UL111A	GCCGGAGACAACGGCGGCGG
Sequencing inserted GFP	**From start of GFP running towards end:** GCAAGGGCGAGGAGCTGT **From after ATG running backwards:** CAGGGTCAGCTTGCCGTAGGT **From middle of GFP out past TAG:** CCAGCAGAACACCCCCATCG

2.16.3. Minipreps, restriction digest and sequencing

Miniprep kits (Qiagen) were used to isolate DNA from colonies showing a functional sacB gene following manufacturer's instructions. Briefly, the 5ml overnight cultures (section 2.16.2) were centrifuged at 4000rpm for 5 minutes and resuspended in 250µl buffer P1. 250µl buffer P2 was then added and incubated for 5 minutes at RT before 250µl buffer N3 was added, and then centrifuged at 13000rpm for 10 minutes. To precipitate DNA, 250µl isopropanol was added and centrifuged at 13000rpm for 10 minutes at 4°C. Supernatant was removed and 500µl 70% ethanol was added and then centrifuged at 13000rpm for 10 minutes. Supernatant was discarded and pellet left to air dry before being re-dissolved in 30µl Tris. Restriction digest was performed using the restriction endonucleases *Bam*HI or *Hind*-III (New England Biolabs, Ipswich, MA), by combining 8µl DNA, 1µl enzyme and 1µl buffer, incubated for 1 hour at 37°C, and then loaded and run on a 1% agarose gel.

For sequencing, 2 primers were used which read out of the sacB cassette, the sequences of which are in Table 4. For each 10µl reaction, the following components were used; 5µl DNA, 1µl primer and 4µl BigDye Mix (ABI, Applied Biosystems) and run using the following cycling parameters;

1. Incubate at 95°C for 5 minutes
2. Incubate at 95°C for 30 seconds
3. Incubate at 55°C for 10 seconds
4. Incubate at 60°C for 4 minutes
5. Go to line 2 for 99 more times

The reactions were cleaned up by running on a Performa DTR column (Edge Biosystems, Gaithersburg, MD). The cleaned up products were then run on an ABI Prism 3130xl genetic analyzer (Applied Biosystems) for sequence analysis.

2.16.4. Second round of recombineering (negative selection)

SW102 bacteria containing the sacB cassette generated above were prepared and made competent following the protocol described in section 2.16.2. PCR products were also prepared following protocol described in section 2.16.1 and the primer sets used are listed in Table 4.

The competent SW102 bacteria and the PCR products were then combined and electroporated as described in section 2.16.2. To delete UL111A, 1µl of an oligonucleotide with ~40bp of homology to the left and to the right of UL111A was electroporated into the competent SW102 bacteria instead of a PCR product. The sequence of the oligonucleotide is listed in Table 4.

After electroporation, the bacteria were recovered for 4 hours at 32°C before being spread onto LB plates containing sucrose but no salt. After 48-36 hours, 4 white colonies were picked and minipreps, restriction digest and sequencing were performed as described in section 2.16.3. The primer for sequencing of the UL111A deletion and the primers for sequencing GFP are listed in Table 4.

2.17. Isolation and transfection of BAC DNA

500mls of recombineered bacteria was cultured overnight in a shaking incubator at 32°C and BAC DNA was isolated by maxiprep using a NucleoBond BAC100 kit (Machery Nagel, Germany) according to manufacturer's instructions. Briefly, cultures were centrifuged at 6000g for 15 minutes, the pellet was resuspended in 24mls of buffer S1 and then 24mls of buffer S2 was added and inverted 6-8 times to mix and rested at RT for 4 minutes. 24mls of buffer S3 was immediately added, mixed by inversion and then chilled at 4°C for 5 minutes. The mixture was then centrifuged at 6000g for 15 minutes, filtered through filter paper and poured onto a column provided. The column was washed twice with buffer N3 and then eluted with 15mls of buffer N5. DNA was precipitated by adding 11mls of isopropanol and centrifuged at 15000g for 30mins at 4°C. After discarding supernatant, 5mls 70% ethanol was added and centrifuged at 15000g for 10

minutes at RT. Ethanol was removed and the pellet was air-dried for 20 minutes and then resuspended in ~200µl Tris-HCl (10nM, pH8). Concentration of DNA was measured on an ND-1000 NanoDrop^{TM} spectrophotometer.

BAC DNA was transfected into the human retinal pigment epithelial cell line ARPE-19 obtained from the internal Cardiff University cell bank, using an effectene transfection kit (Qiagen) according to manufacturer's instructions. Briefly, 1 x 10^6 cells were plated out into a 25cm^3 flask and grown overnight in D10 medium (section 2.23). The next day, 1µg DNA was diluted into buffer EC to a total of 150µl and to this, 8µl enhancer was added, mixed by vortexing and incubated for 5 minutes. 25µl of effectene transfection reagent was added, mixed by pipetting and incubated for 5-10 minutes. 1ml of D10 media was then added to the DNA mixture which was then added dropwise to the cells. Cells were then incubated at 37°C to allow the virus to grow.

2.18. Generation of modified viruses

Supernatants from ARPE-19 infected cells were used to infect HFF cells. Once plaques were visible and HFF cells started to round up, supernatants were collected every 2-3 days and stored at -80°C until infection destroyed all the cells. Supernatants were then centrifuged at 12000rpm for 2 hours at RT. Pellets were resuspended in 1ml D10 media by pipetting up and down and then forced through a G27 gavage needle (0.4 mm x 13 mm) until fully viscous and aliquoted into ~300µl samples and stored at -80°C until use.

2.19. Titration of viruses

Purified viruses (section 2.18) were titrated by plaque assay by adding serial dilutions of virus in duplicate to confluent HFF cells in a 6 well plate (plated out at 6 x 10^5 cells per well the previous day) and incubated on a rocking platform for 2 hours at 37°C. Media containing the virus was then removed and 10mls of 1% avicel (FMC Biopolymer, Philadelphia, PA) overlay (section 2.23) was added and the cells cultured for 14 days at

37°C. Avicel overlay was then removed and plates were washed with PBS. Visible plaques were then counted and virus titre calculated as PFU/ml.

2.20. Western Blots

HFFs were infected with modified viruses at an MOI of 3 for 24, 72 and 144 hours. The media was collected and ~40µl of diluted (1:3) NuPAGE LDS sample buffer (Invitrogen) was added to the cells which were then gently scraped off and collected. DTT (~3µl) (Sigma-Aldrich) was then added to cell lysates and samples were heated at 99°C for 10 minutes and then cooled to 37°C. Samples were then vortexed and centrifuged at 13000rpm for 5 minutes. Samples were then loaded onto pre-cast NuPAGE 4-12% Bis-Tris gels (1mm x 10 well, Invitrogen) and run at 200V for 50 minutes. Gels were then transferred onto Hybond ECL nitrocellulose membranes (GE Healthcare) at 13V for 2 hours before being incubated for 10 minutes on a rocking platform with antibody extender solution (Thermo Fisher Scientific) and then washed with ddH_2O. Membranes were then blocked by incubating overnight with TBST (section 2.23) containing 5% powdered milk (Marvel, UK), washed with TBST and then incubated overnight with primary antibody (see Table 5 for antibodies used) in TBST containing 5% milk on a rocking platform at 4°C. The next day, membranes were thoroughly washed with TBST containing 5% milk before being incubated with secondary antibody (see Table 5 for antibodies used) for 1 hour at RT and then washed thoroughly in TBST. Membranes were then incubated for 5 minutes in SuperSignal West Pico chemiluminescent substrate (Thermo Fisher Scientific) and exposed to film. To re-probe the membranes, they were washed in TBST and incubated with stripping buffer (Thermo Fisher Scientific) for 1 hour, washed, and re-probed as above.

Table 5. Primary and secondary antibodies for western blotting

Primary antibody	Host	Concentration	Company
α-actin	Rabbit	1:10000	Sigma-Aldrich
α-GFP	Rabbit	1:200	Santa Cruz Biotechnology
α-viral-IL-10	Mouse	1:1000	In-house, ascites
Normal IgG	Mouse	1:1000	Santa Cruz Biotechnology
Secondary antibody	**Host**	**Concentration**	**Company**
α-mouse-HRP	Goat	1:2000	Biorad Laboratories
α-rabbit-HRP	Goat	1:10000	Biorad Laboratories

2.21. Generation of monocyte-derived DCs

Peripheral blood mononuclear cells (PBMCs) were isolated from blood using the standard ficol separation method and separated by MACS separation according to manufacturer's instructions. Briefly, cells were stained with anti-CD14-PE (BD Parmingen) at 4°C, then washed with MACS buffer (section 2.23) and incubated with anti-PE beads (Miltenyi Biotec) also at 4°C. Cells were washed, resuspended in MACS buffer and run down an MS column (Miltenyi Biotec) attached to a magnet. The flow through was the negative fraction. The column was then removed from the magnet and magnetically labelled $CD14^+$ cells were flushed out with MACS buffer; this flow through was the positive fraction. The purity of the separated cell fractions were analysed by flow cytometry. The purified monocytes were then cultured for 5-7 days at 1 x 10^6/ml in monocyte-derived DC growth media (section 2.23). Culture was replenished every 2 days by removing 50% of spent media and adding back fresh growth media.

2.22. Statistics

Statistical significance was determined using the two-tailed Student's *t* test (flow cytometry data), the Mann-Whitney *U* test (viral load analysis comparing two groups) or one-way ANOVA following logarithmic transformation (viral load analysis comparing more than two groups). * = $p<0.05$, ** = $p<0.01$, *** = $p<0.005$.

2.23. Buffers, media, gels and agarose plate preparations

Sorbitol cushion: 20% (w/v) sorbitol (Thermo Fisher Scientific) in ddH_2O and then sterile filtered.

Collagenase-containing buffer: RPMI (Invitrogen), 5% heat inactivated fetal calf serum (FCS), 1mg/ml collagenase D (Roche), 5mM sterile $CaCl_2$, 50µg/ml DNase 1 (Sigma-Aldrich).

Lysis buffer: 500ml ddH_2O, 4.145g NH_4Cl, 0.5g $KHCO_3$, 18.6mg EDTA (all Thermo Fisher Scientific).

R10 media: RPMI, 10% heat inactivated FCS, 250units Penicillin/Streptomycin, 0.26mg/ml L-Glutamine, 97mg/ml Sodium pyruvate (all from Gibco, UK).

Facs buffer: PBS, 2% heat inactivated FCS, 0.05% sodium azide (Sigma-Aldrich).

Saponin buffer: PBS, 2% heat inactivated FCS, 0.05% sodium azide (Thermo Fisher Scientific) and 0.5% saponin (Sigma-Aldrich).

ELISA wash buffer: 0.05% Tween-20 (Thermo Fisher scientific) in PBS.

D10 media for mouse cells: DMEM (Invitrogen), 10% heat inactivated foetal calf serum, 250units Penicllin/Streptomycin, 0.26mg/ml L-Glutamine, 97mg/ml Sodium pyruvate.

CMC media: DMEM, 10% FCS, 250units Penicllin/Streptomycin, 0.26mg/ml L-Glutamine, 97mg/ml Sodium pyruvate, 4g carboxy methyl cellulose (Thermo Fisher Scientific DMEM, 10% heat inactivated FCS, 250units Penicllin/Streptomycin.).

Crystal violet solution: 0.1% (w/v) crystal violet (Sigma-Aldrich) in ddH_2O.

MACS buffer: 2mM EDTA and 0.5% BSA in PBS.

Agarose gel (1%): 1% agarose powder (AGTC Bioproducts, UK) in 1 x TAE buffer (National Diagnostics, Atlanta, GA). Adjust amount of agarose accordingly as required.

LB media: 20g/L of LB low salt broth (Melford Laboratories) in ddH_2O.

LB plates containing ampicillin: LB low salt media, 1.5% agar, 1:1000 chloramphenicol, 1:1000 ampicillin, 1:500 IPTG and 1:500 X-GAL (all from Sigma-Aldrich).

LB plates containing sucrose: 10g/L tryptone (Thermo Fisher Scientific), 5g/L yeast extract (Sigma-Aldrich), 5% sucrose (Thermo Fisher Scientific), 1.5% agar, 1:1000

chloramphenicol, 1:500 IPTG and 1:500 X-GAL.

D10 media for human cells: DMEM (Invitrogen), 10% heat inactivated foetal calf serum, 250units Penicllin/Streptomycin.

1% Avicel overlay: 250mls 2% avicel, 125mls ddH_2O, 50mls 10 x MEM (Gibco), 50mls FCS, 15mls sodium bicarbonate (Gibco), 10mls Penicllin/Streptomycin, 5mls glutamine.

TBST: 20mM Tris pH7.5-8, 500mM NaCl, 0.05% Tween-20, 0.05% TritonX-100 (Thermo Fisher Scientific) in ddH_2O.

Monocyte-derived DC growth media: RPMI, 50ng/ml GM-CSF, 20ng/ml IL-4 (both Peprotech).

Chapter 3 - Investigating the modulation of NK cells by IL-10 during acute murine cytomegalovirus infection

3.1. Introduction

3.1.1. IL-10 regulation of NK cell responses

The regulation of T cell responses by IL-10, both directly and indirectly via regulation of APCs, has been discussed in depth in section 1.9.1. However, the role that IL-10 plays in regulating NK cell responses requires more research investigation.

Human NK cells express the IL-10R transcript *in vitro* (157) and binding studies revealed that the IL-10R protein is constitutively expressed on resting NK cells with approximately 90 IL-10R molecules per cell (158), implying that NK cells can directly respond to IL-10. Therefore, the functional consequences of IL-10 binding directly to human NK cells were investigated. *In vitro* studies showed that IL-2-induced proliferation of human NK cells is enhanced with addition of IL-10 (158), and IL-2 activated murine NK cells exhibit increased proliferation when incubated with IL-10 alone. Moreover, when stimulated with IL-18 in conjunction with IL-10, NK cell proliferation is further enhanced (159).

Interestingly, the combination of IL-10 and IL-18 also significantly increases NK cell cytotoxicity, as assessed by NK cell killing of MHC-deficient target (YAC-1) cells *in vitro* (159). The ability of IL-10 to enhance NK cell killing was further supported by an *in vitro* study showing that IL-10 production by regulatory DCs could activate NK cells and enhance their ability to kill YAC-1 cells (160); a finding corroborated by experiments demonstrating that incubation of human NK cells with IL-10 increased *in vitro* cytotoxicity (161).

In addition to increased proliferation and cytotoxicity, several *in vitro* studies have also demonstrated that IL-10 augments IFNγ production by NK cells in conjunction with other cytokines. IFNγ levels were significantly enhanced when NK cells were simultaneously stimulated with IL-10 and IL-18 with (162) or without (159) IL-12. Paradoxically however, *in vivo* experiments revealed that IL-10 suppresses NK activation and IFNγ production. In a mouse model of polymicrobial peritonitis, treatment with anti-IL-10 led to a considerable increase in NK cell activation as measured by CD69 expression, as well as a significant increase in IFNγ production (163). Furthermore, blockade of IL-10 signalling mobilises IFNγ producing NK cells in LPS-challenged lungs of aged mice (164).

3.1.2. The role of IL-10 in MCMV infection

Induction of pro-inflammatory cytokines is a critical part of the host response to viral infections and is necessary for control and clearance of viruses. As previously discussed (section 1.9.2), IL-10 plays an important role in limiting the detrimental effects to the host that could arise from an excessive pro-inflammatory response elicited by infection. Several studies have utilised the MCMV infection model in an attempt to understand more clearly the role that IL-10 plays in the host response to herpesvirus infection. IL-10 deficient mice have been shown to suffer from more severe MCMV-induced disease than wt background strain, including increased weight loss thought to be driven by over-exuberant T cell responses (165). Furthermore, MCMV infection of the brain causes lethal disease in IL-10 knockout mice as compared to wt animals that could control the virus (166). Importantly, increased mortality seen in the knockout mice is not due to a failure in controlling viral replication, as levels of replicating virus were comparable to wt mice. These studies suggest that IL-10 is important in protecting the host during acute infection. However, during the persistent and chronic phases of infection, the absence of IL-10 appears to be advantageous to the host. Memory T cell inflation in IL-10 deficient mice is dramatically amplified during infection, with T cells being oligoclonal and exhibiting a highly activated phenotype, leading to a reduction in latent virus load (167). Importantly,

these results were recapitulated when IL-10R blockade in wt mice was utilised (167). In addition, blockade of IL-10R in wt mice markedly reduced virus load in the salivary glands during persistent infection, with some mice clearing the virus from this organ completely (168). Collectively, these data demonstrate that IL-10 limits virus-induced pathology during acute infection yet, paradoxically, impairs antiviral immunity during virus chronicity. The role that IL-10 plays in regulating protective immunity to acute infection, however, is unclear.

3.1.3. Hypothesis

The impact that IL-10 has in regulating NK cell responses, particularly *in vivo*, remains poorly understood. Furthermore, nothing is known regarding the role of this cytokine in modulating antiviral NK cell responses. NK cells are critical in controlling early MCMV infection. Utilising an antagonistic, non-depleting anti-IL-10R antibody in this model, I tested the following hypothesis:

"Virus induced IL-10 suppresses NK cell-mediated protective immunity during acute virus infection".

3.2. Results

3.2.1. IL-10 expression is induced in the lung and spleen during acute MCMV infection

During acute MCMV infection in C57BL/6 (wt) mice, the visceral organs including the lung and the spleen are two major sites targeted by the virus. Lung and spleen homogenates were taken 4 days p.i, analysed for IL-10 protein expression and compared to levels found in homogenates from naïve control mice. IL-10 protein expression was significantly up-regulated upon MCMV infection in both organs (Fig. 3.1A). Infected lungs and spleens showed on average a 3-fold and 6-fold increase in expression compared to uninfected organs respectively.

In order to identify the source of IL-10 during MCMV infection, pulmonary and splenic lymphocytes from day 4 infected mice and naïve controls were polyclonally stimulated *ex vivo* and IL-10 production by different cell types was examined. B cells ($CD19^{+}CD3^{-}$) derived from the lung (Fig. 3.1B) and spleen (Fig. 3.1C) were one of the predominant cell types capable of expressing IL-10 after 4 days of infection. Inflammatory macrophages ($7/4^{hi}F4/80^{int}Ly6G^{-}CD11c^{low/int}CD11b^{hi/int}$) and splenic dendritic cells ($CD11c^{hi}$MHC II^{hi}) also represented significant populations of IL-10 expressing cells after *ex vivo* stimulation. To assess the specificity of the anti-IL-10 antibody, splenic B cells from MCMV-infected wt mice (Fig. 3.2A) and IL-$10^{-/-}$ mice (Fig. 3.2B) were stained for intracellular IL-10 production. As a further control, a fluorescence minus one (FMO) negative staining control was also included (Fig. 3.2C). Both the IL-$10^{-/-}$ and the FMO control showed no positive staining for IL-10.

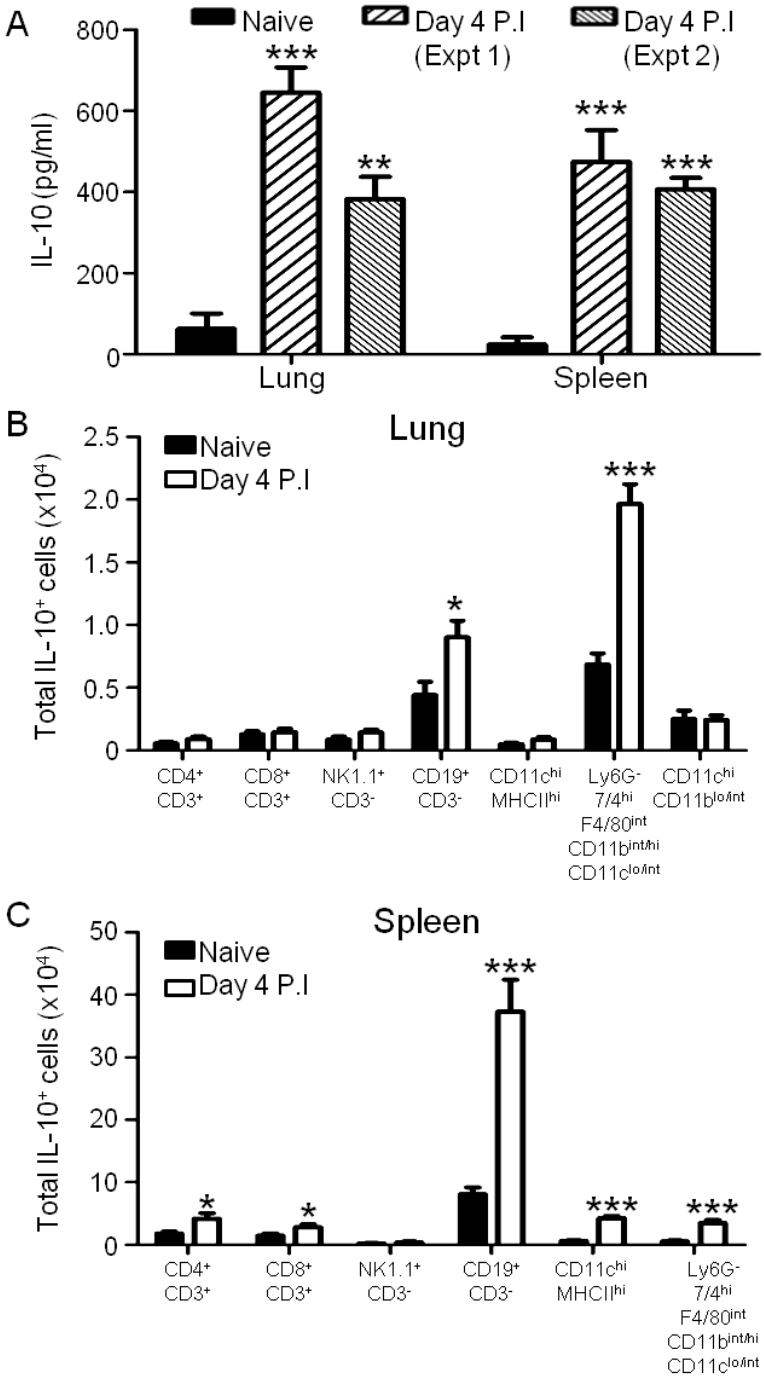

Figure 3.1. IL-10 expression in the lung and spleen of naïve and MCMV-infected mice 4 days post-infection

(A) IL-10 protein concentrations in lung and spleen homogenates from naïve wt mice (closed bars) and MCMV-infected wt mice 4 days p.i (cross hatched bars). Results represent the mean ± SEM of 4-6 mice per group. (B and C) IL-10 expression by pulmonary (B) and splenic (C) lymphocytes following *ex vivo* stimulation (see section 2.4.3) in naïve mice (closed bars) and mice infected for 4 days with MCMV (open bars). Results show the mean ± SEM of 7 mice per group and represent 3 independent experiments. *p<0.05, **p<0.01, ***p<0.001

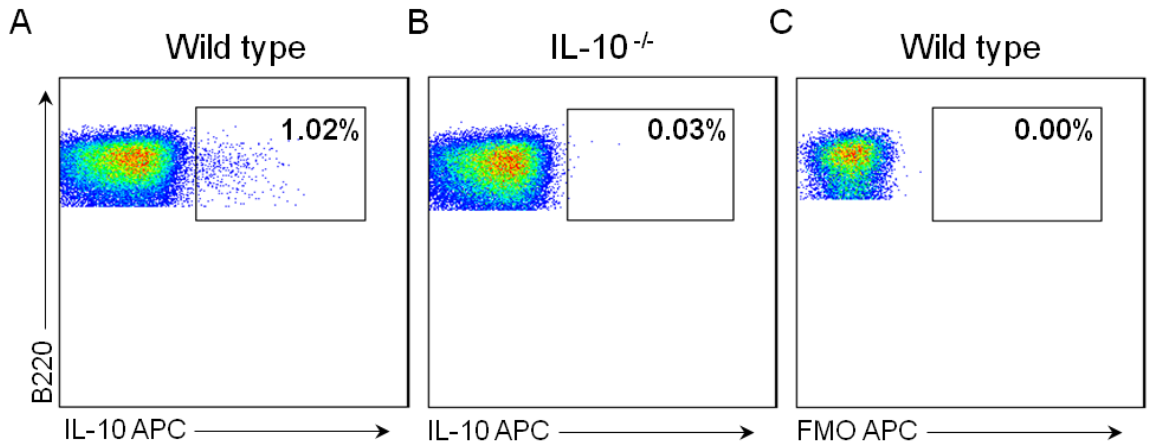

Figure 3.2. Analysis of intracellular IL-10 antibody staining by flow cytometry
(A and B) Representative bivariate flow cytometry plots showing IL-10 expression by splenic B cells from MCMV-infected wt mice (A) and IL-10$^{-/-}$ mice (B) 4 days p.i. Cells were incubated for 4 hours with PMA/Ionomycin and LPS. Following surface staining, cells were then stained for intracellular IL-10 production with anti-IL-10-APC (A and B) or without anti-IL-10-APC (C) as an FMO staining control.

3.2.2. IL-10R blockade exacerbates weight loss during acute MCMV infection

I hypothesised that virus-induced IL-10 suppressed protective immunity during acute infection. To test this, MCMV-infected mice were administered an antagonist non-depleting anti-IL-10R antibody on the day of infection (in all experiments described in this chapter). As previously reported in experiments utilising IL-10 deficient mice (165), impaired IL-10R signalling with anti-IL-10R antibody prolonged and exacerbated virus-induced weight loss as compared to IgG controls (Fig. 3.3A and B) over the first 7 days of MCMV infection, suggesting that IL-10R blockade enhanced the clinical signs of disease.

3.2.3. Inhibition of IL-10R signalling increases virus load during acute MCMV infection

Virus load was then assessed at days 2, 4 and 7 p.i by measuring MCMV DNA in the lungs and spleens of mice treated with anti-IL-10R or IgG control, as detected using MCMV gB-specific primers. Contrary to my initial hypothesis, viral DNA loads at day 2 p.i in the lungs (Fig. 3.4A) and spleen (Fig. 3.4B) were not influenced by anti-IL-10R treatment. Interestingly, virus genome content by day 4 p.i in the lungs and spleen was actually significantly increased following IL-10R blockade. However, anti-IL-10R treatment did not significantly influence the low levels of replicating virus detectable in the lungs (IgG: $2.1x10^3$ pfu/g versus αIL-10R: $3.4x10^3$ pfu/g; Fig. 3.4C) and spleens (IgG: $1.4x10^4$ pfu/g versus αIL-10R: $1.9x10^4$ pfu/g; Fig. 3.4D). This suggests that in the absence of IL-10R signalling, MCMV genome load is moderately enhanced.

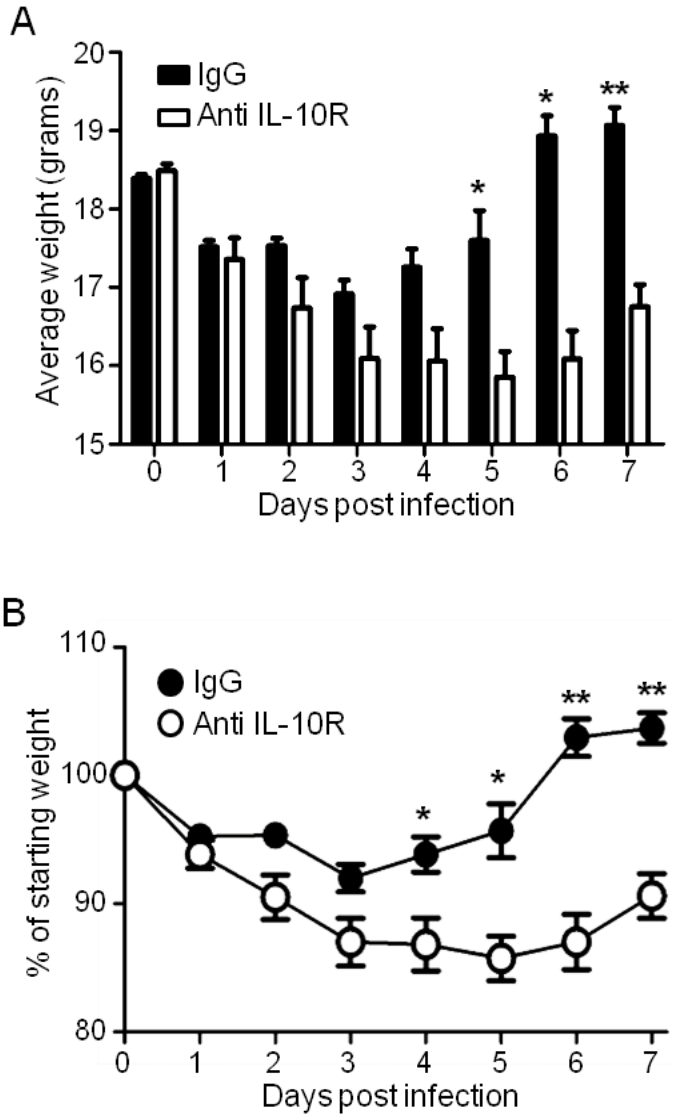

Figure 3.3. IL-10R blockade exacerbates weight loss during acute MCMV infection
Mice were infected with MCMV and treated with IgG (closed bars/circles) or anti-IL-10R (open bars/circles). (A) Average daily weight shown in grams. (B) Weight loss shown as percent of starting weight. Results are expressed as mean ± SEM of 4 mice per group and represent 2 independent experiments. *p<0.05, **p<0.01

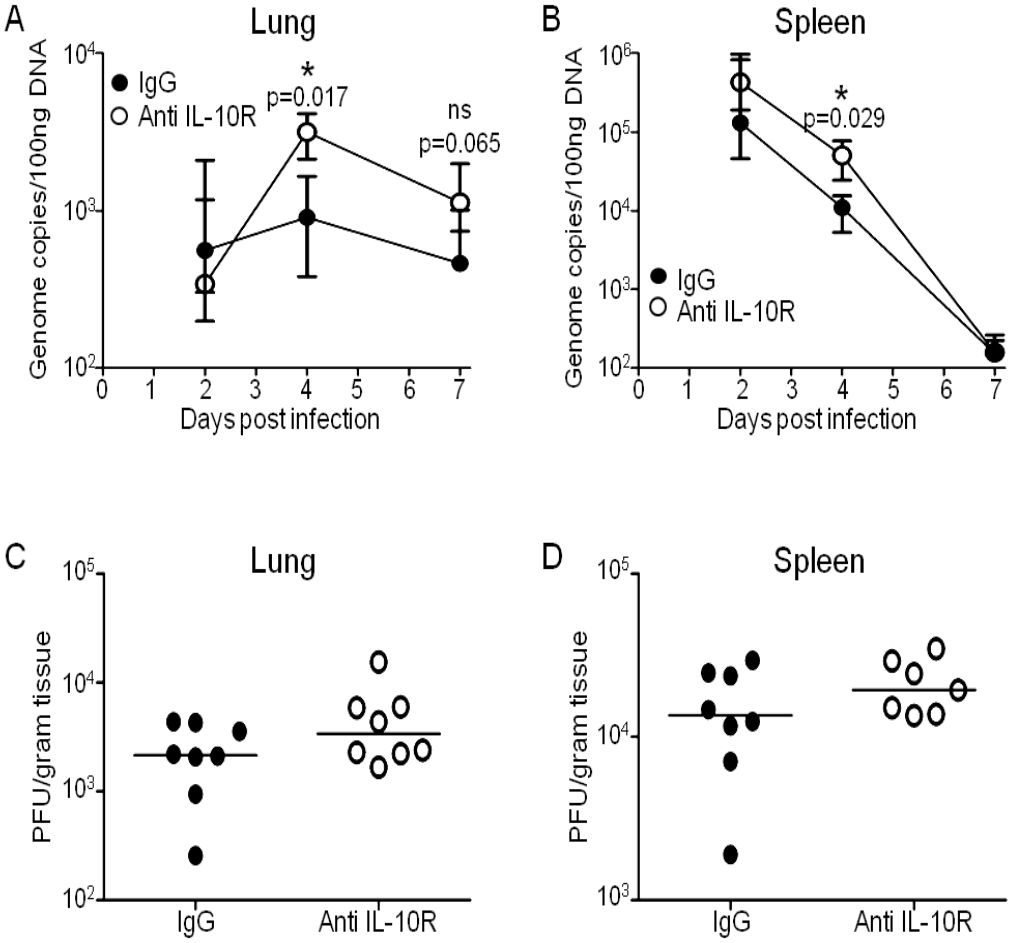

Figure 3.4. IL-10R blockade transiently increases viral genome load during acute MCMV infection

Mice were infected with MCMV and treated with IgG (closed circles) or anti-IL-10R (open circles). (A and B) Genomic DNA was isolated from the lungs (A) and spleens (B) 2, 4 and 7 days p.i and MCMV gB was detected by qPCR. Data was normalized to β-actin and is expressed as genome copy number per 100ng genomic DNA. Median of 4-6 mice/group ±_interquartile range is shown. (C and D) Homogenates from the lungs (C) and spleens (D) of mice infected for 4 days were prepared for high sensitivity plaque assays to detect replicating virus. Data is expressed as PFU per gram of tissue. Horizontal bars show median values. Data represent 2-5 independent experiments. *p<0.05, ns=not significant.

3.2.4. Anti-IL-10R treatment impedes the accumulation of NK cells during acute MCMV infection

NK cells have been shown to play a critical role in controlling early MCMV infection (87, 169, 170). To determine whether elevated viral DNA load after IL-10R blockade was associated with an NK cell defect, NK cell accumulation was examined. During infection, a significant population of $NK1.1^{+}CD3^{-}$ cells was present in the lung (Fig. 3.5A) and spleen (Fig. 3.5B). When tracked over the course of acute infection, $NK1.1^{+}CD3^{-}$ cell numbers routinely contracted by 2 days p.i compared to numbers observed in uninfected controls, before recovering and expanding. This transient reduction in NK cell numbers has been previously observed (171-173). Interestingly, IL-10R blockade prolonged this contraction of pulmonary (Fig. 3.5A and C) and splenic (Fig. 3.5B and D) NK cells and impeded their expansion from 4 days p.i and beyond.

3.2.5. NK cells are critical for early control of MCMV infection

To assess the potential importance of IL-10 regulation of NK cells in this infection model, mice were infected with MCMV, treated with or without depleting anti-NK1.1 antibodies, and administered IgG or anti-IL-10R. To demonstrate that NK cells were depleted to a sufficient level, lung leukocytes from mice treated with or without depleting anti-NK1.1 were stained for NKp46 at 4 days p.i, demonstrating efficient (<0.05% of remaining cells) NK cell depletion (Fig. 3.6A). Virus load in the lung (Fig. 3.6B) increased from approximately 10^3 genome copies/100ng DNA in control mice to 10^5 genome copies in NK depleted mice, and in the spleen (Fig. 3.6C) from 10^4 to 10^7 genome copies/100ng of DNA, demonstrating the importance of NK cells in controlling early MCMV infection. Interestingly, IL-10R blockade in NK depleted mice did not further elevate viral genome copies (Fig. 3.6B and C); implying that defective control of virus load following IL-10R blockade was intrinsically linked to NK cell responses.

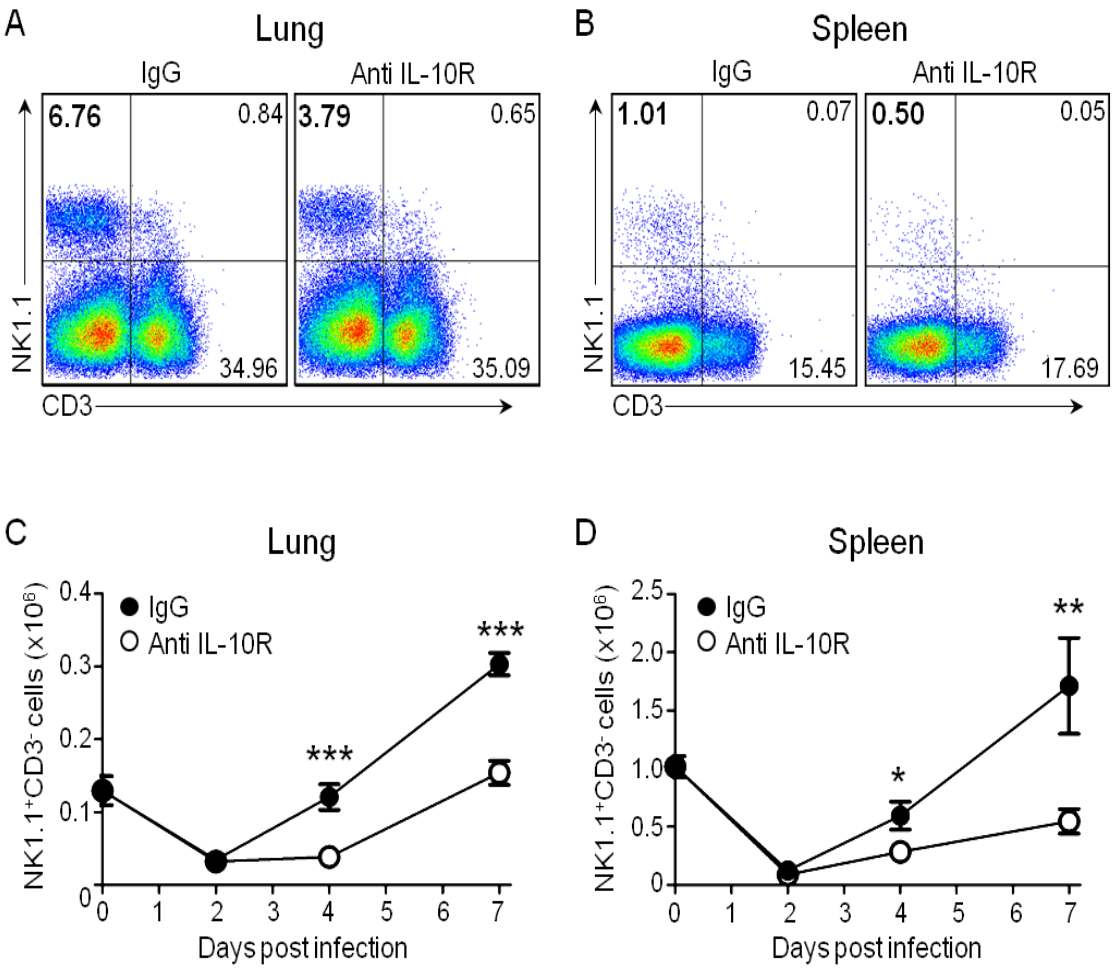

Figure 3.5. IL-10R blockade impedes the accumulation of NK cells during acute MCMV infection

MCMV-infected mice were treated with IgG or anti-IL-10R on day 0 and cellular accumulation assessed 2, 4 and 7 days later. (A and B) Representative bivariate flow cytometry plots showing $NK1.1^{+}CD3^{-}$ cell accumulation in lungs (A) and spleens (B) of IgG (left panel) and anti-IL-10R (right panel) treated mice, 4 days p.i. (C and D) Numbers of $NK1.1^{+}CD3^{-}$ cells in the lungs (C) and spleens (D) of IgG (closed circles) and anti-IL-10R (open circles) treated mice analyzed over 7 days. Results are expressed as the mean ± SEM of 3-6 mice per group and represent 5 independent experiments. *p<0.05, **p<0.01, ***p<0.001

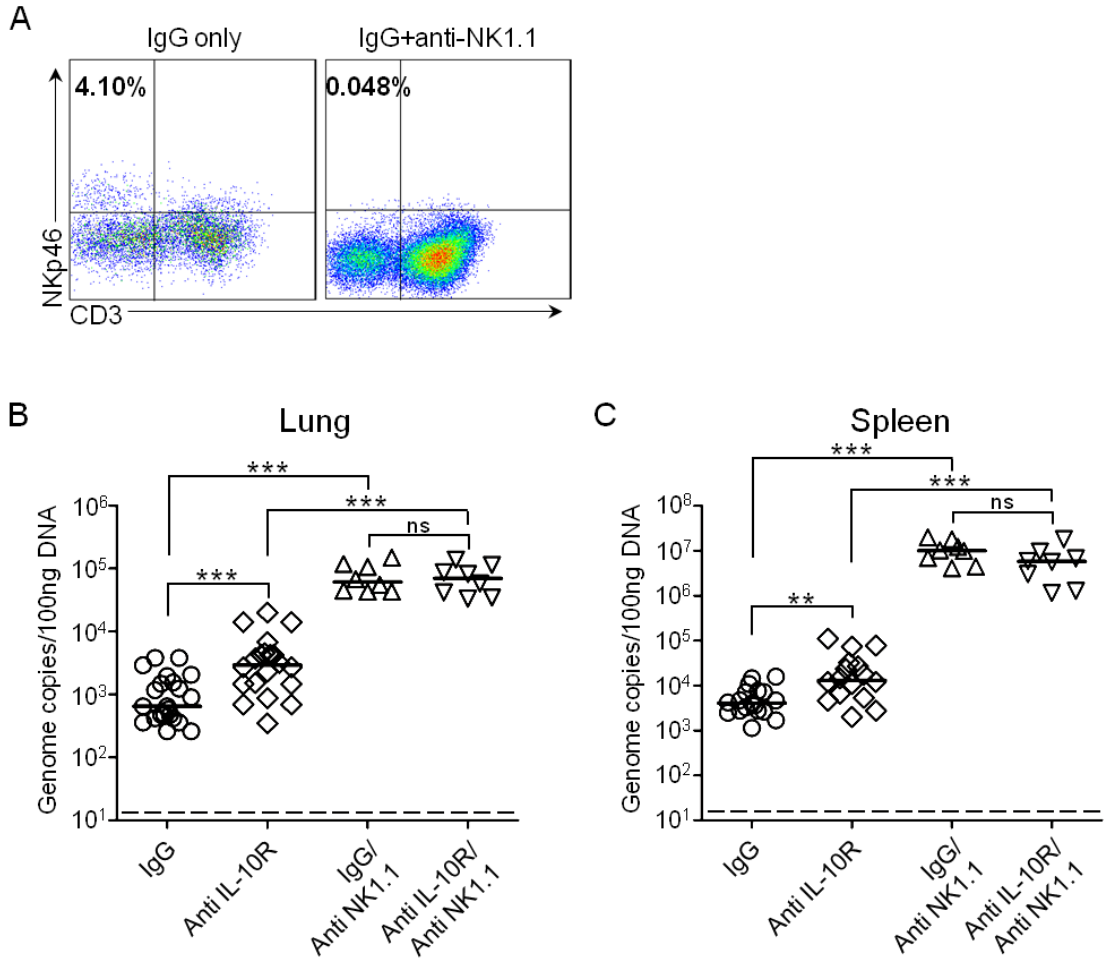

Figure 3.6. NK cells are critical for early control of MCMV infection
MCMV-infected mice were treated with IgG or anti-IL-10R, ± depleting anti-NK1.1 antibody. (A) Representative bivariate flow cytometry plots showing lung leukocytes with (right panel) and without (left panel) anti-NK1.1 administration at 4 days p.i. (B and C) After 4 days of infection, genomic DNA was isolated from the lungs (B) and spleens (C) and MCMV gB-encoding DNA was detected by qPCR. Data was normalized to β-actin and is expressed as genome copy number per 100ng genomic DNA. Horizontal solid bars show median values and horizontal dashed lines depict the lower limit of detection. Data from 2-3 independent experiments are shown. **p<0.01, ***p<0.001, ns=not significant.

3.2.6. IL-10R blockade does not influence accumulation of hepatic NK cells during acute MCMV infection or influence virus load

The influence of IL-10R signalling on expansion of NK cells at another important site of acute MCMV replication, the liver, was examined. Interestingly, anti-IL-10R treatment did not reduce the proportion (Fig. 3.7A) or total numbers (Fig. 3.7B) of hepatic NK cells at day 4 p.i as compared to IgG treated controls. In accordance with the observation that NK cell numbers were not affected, IL-10R blockade did not influence hepatic virus load, as determined by detection of MCMV gB (Fig. 3.7C) or replicating virus (Fig. 3.7D). These data imply that hepatic NK cells are differentially responsive to IL-10, and highlight the association between NK cell accumulation in infected tissue and subsequent control of MCMV replication.

3.2.7. Anti-IL-10R treatment enhances accumulation of virus-specific $CD4^+$ T cells

Reduced NK cell accumulation 7 days after IL-10R blockade was not associated with increased viral burden at this time (Fig. 3.4A and B). Strikingly, IL-10R blockade led to a large increase in accumulation of virus-specific $CD4^+$ T cells at day 7 p.i (Fig. 3.8A and B), suggesting that increased accumulation of antiviral T cells may compensate for reduced NK cell responsiveness at later times during acute infection.

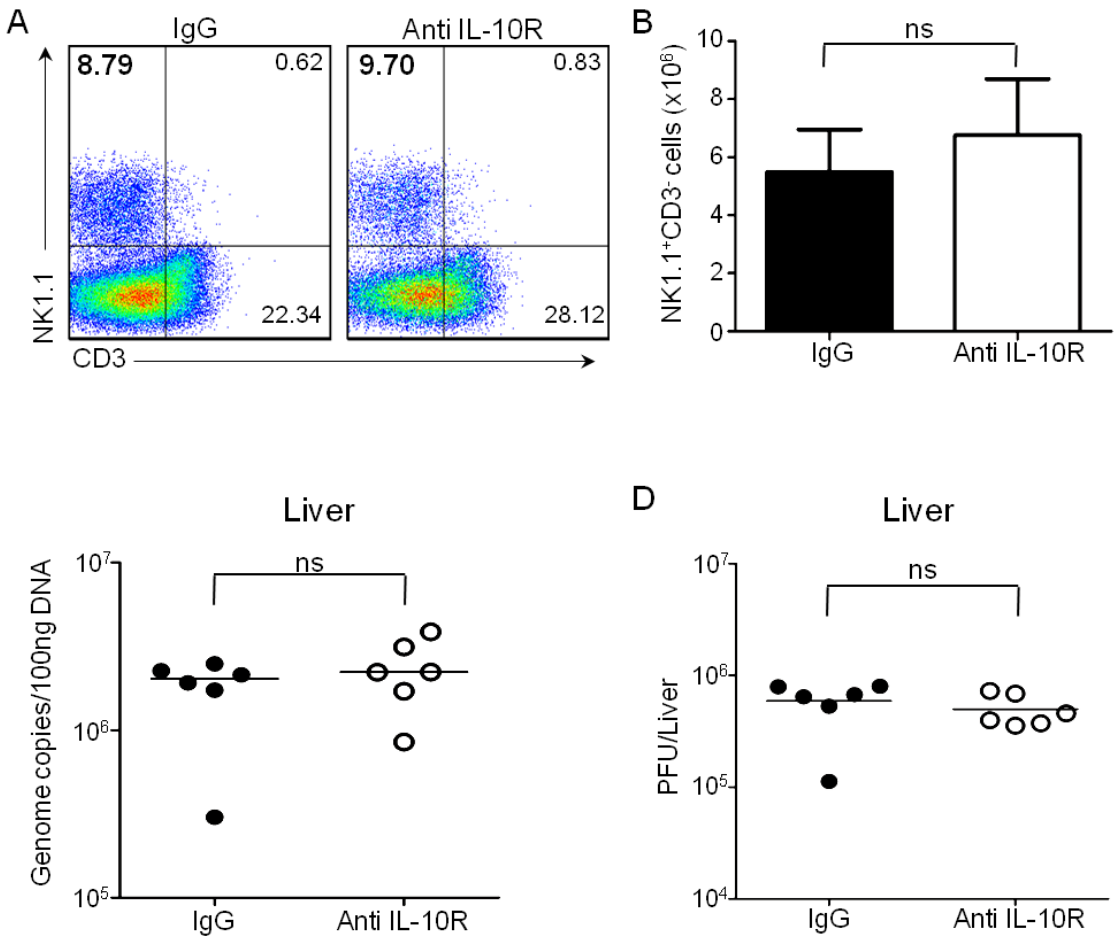

Figure 3.7. Anti-IL-10R blockade does not influence accumulation of hepatic NK cells during acute MCMV infection or influence virus load

MCMV-infected mice were treated with IgG or anti-IL-10R on day 0 and NK^+CD3^- cell accumulation assessed 4 days later. (A) Representative bivariate flow cytometry plots showing $NK1.1^+CD3^-$ cell accumulation in the liver of IgG (left panel) and anti-IL-10R (right panel) treated mice. (B) Numbers of NK^+CD3^- cells in the liver of IgG (closed bars) and anti-IL-10R (open bars) treated mice 4 days p.i. Results are expressed as the mean ± SEM of 5 mice per group. (C and D) Virus load in the liver was assessed at 4 days p.i. (C) Genomic DNA was isolated from the livers and MCMV gB-encoding DNA was detected by qPCR. Data was normalized to β-actin and is expressed as genome copy number per 100ng genomic DNA. (D) Replicating virus in the livers was detected by plaque assay. Data is expressed as PFU per liver; horizontal bars represent median values. ns=not significant.

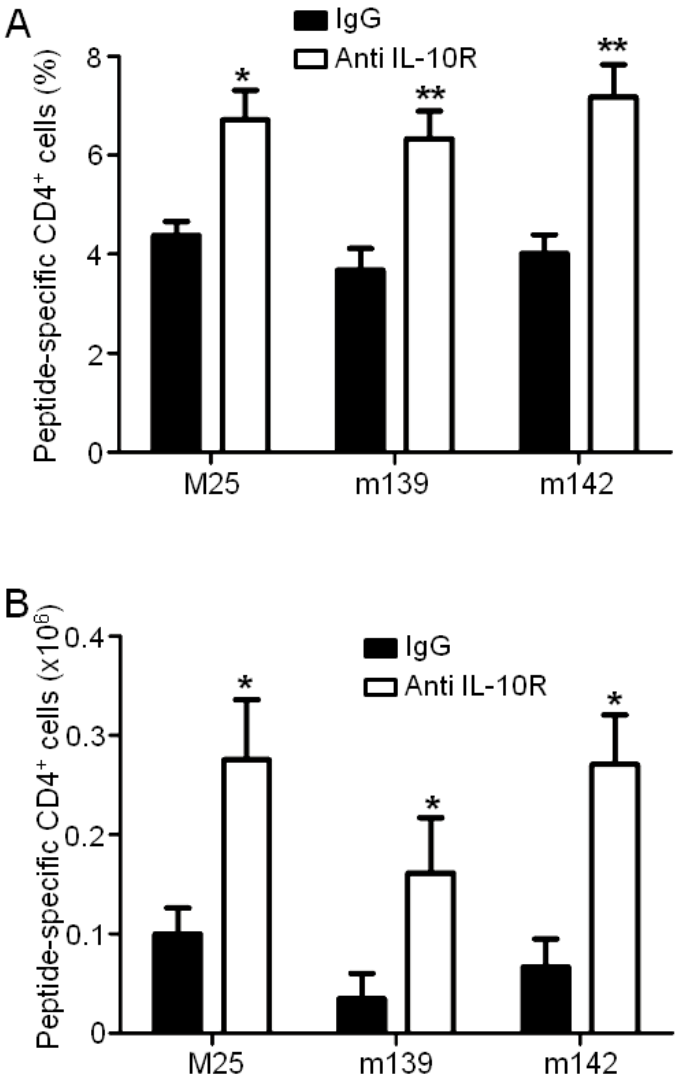

Figure 3.8. Anti-IL-10R treatment enhances accumulation of virus-specific CD4$^+$ T cells

Proportion (A) and total numbers (B) of virus-specific splenic CD4$^+$ T cells of IgG (closed bars) and anti-IL-10R (open bars) treated mice, 7 days p.i, following *ex vivo* stimulation with MHC class II specific MCMV peptides. Results are expressed as mean ± SEM of 4 mice per group and represent 2 independent experiments. *p<0.05, **p<0.01

3.2.8. IL-10R blockade does not preferentially inhibit Ly49H$^+$ NK cell accumulation during infection

C57BL/6 mice are capable of mounting a large NK cell response against MCMV due to the presence of the NK cell activating receptor Ly49H, which recognises the MCMV-encoded MHC-like protein m157 (see section 1.8.2). After the initial contraction of NK cells following MCMV infection, NK cell numbers expand between 2 and 7 days p.i, which is thought to be largely a consequence of Ly49H-dependent activation (95, 171). The proportion (Fig. 3.9A and B) and total numbers (Fig. 3.9C and D) of Ly49H$^+$ and Ly49H$^-$ NK cells were examined at days 2, 4 and 7 p.i in both the lung and spleen (Fig. 3.9A and C and Fig. 3.9B and D, respectively) of wt mice. In both organs, a preferential expansion of the Ly49H$^+$ NK cells was observed from 4 to 7 days p.i.

To elucidate whether the absence of IL-10R signalling preferentially inhibited the Ly49H$^+$ NK cell response in the lung and spleen, accumulation of Ly49H$^+$ and Ly49H$^-$ NK cells was examined. Comparable ratios of Ly49H$^+$ and Ly49H$^-$ NK cells in the lung (Fig. 3.9E) and spleen (Fig. 3.9F) were observed over time in IgG and anti-IL-10R treated mice. A comparable enrichment of the Ly49H$^+$ compartment was observed in both groups, from 50-56% of all NK1.1$^+$CD3$^-$ cells at day 0, to 75-85% by day 7 p.i. These data suggests that IL-10R blockade did not preferentially inhibit Ly49H$^+$ NK cell accumulation during MCMV infection.

3.2.9. Impaired cellular accumulation following anti-IL-10R treatment during MCMV infection is restricted to NK1.1$^+$CD3$^-$ cells

To assess whether the impairment in cellular accumulation observed following IL-10R blockade was restricted to the NK1.1$^+$CD3$^-$ cell compartment, the influence of IL-10R blockade on numbers of T cells, neutrophils and APCs present in MCMV-infected tissues were assessed. Populations of pulmonary (Fig. 3.10A) and splenic (Fig. 3.10B) neutrophils (Ly6G^{hi}7/4$^{lo/int}$F4/80^{lo}CD11b^{hi}CD11c$^{lo/int}$) and APCs including DCs

(CD11c^{hi}MHCII^{hi}), inflammatory macrophages (Ly6G^{lo}7/4^{hi}F4/80^{int}CD11b$^{int/hi}$CD11c$^{lo/int}$) and alveolar macrophages (CD11c^{hi}CD11b$^{lo/int}$; lung only) were unaffected following anti-IL-10R treatment of MCMV-infected mice. Total numbers of T cells (CD3^{+}NK1.1^{-}) were also comparable in mice treated with either anti-IL-10R or IgG in both organs (Fig. 3.10A and B). Collectively, these data show that blockade of IL-10R signalling exclusively reduced NK cell accumulation during acute MCMV infection.

3.2.10. Inhibition of IL-10R signalling inhibits the accumulation of cytotoxic NK cells during acute MCMV infection

Having established that NK cell accumulation is inhibited during acute infection in the absence of IL-10R signalling, it was important to then evaluate whether IL-10R blockade influenced NK cell function. Recent degranulation was first quantified using a flow cytometry based assay for detecting CD107a mobilisation (for antibody specificity and staining controls, refer to Fig. 3.11A-C). The percentage of NK cells that were degranulating directly *ex vivo* without any further stimulation (CD107a^{+}) in the lung (Fig. 3.12A) and the spleen (Fig. 3.12B) were comparable in IgG (left hand panels) and anti-IL-10R (right hand panels) treated mice at 4 days p.i. However, when total numbers of CD107a^{+} NK cells were calculated, reduced numbers of degranulating NK cells were observed in the lung (Fig. 3.12C) and spleen (Fig. 3.12D) of anti-IL-10R treated mice. In addition, granzyme B expression by NK cells was assessed (for staining controls, refer to Fig. 3.11D-E), and was also comparable between both groups of mice in the lungs (Fig. 3.13A) and spleen (Fig. 3.13B) at day 4 p.i. However, when calculated back to total numbers, there were less granzyme B^{+} NK cells in mice treated with anti-IL-10R (Fig. 3.13C and D). Therefore, these data suggest that the loss of cytotoxic NK cells following anti-IL-10R treatment reflected the overall reduction in NK cells rather than a specific IL-10-dependent regulation of cytotoxicity.

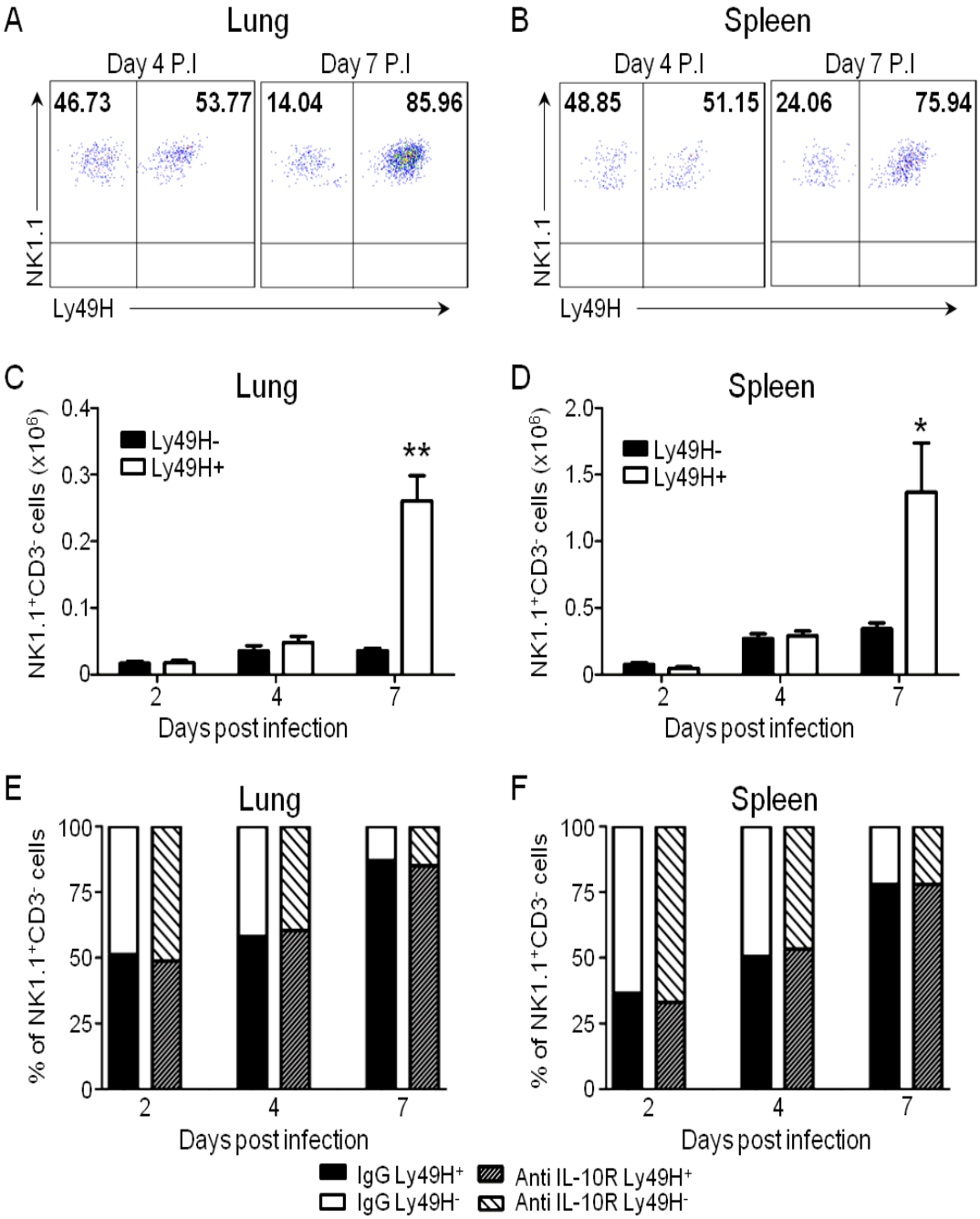

Figure 3.9. Ly49H$^+$ NK cells preferentially expand between day 4 and 7 post-infection

NK cells of MCMV-infected mice were examined for expression of Ly49H over 7 days. (A and B) Representative bivariate flow cytometry plots showing Ly49H$^-$ and Ly49H$^+$ NK cells in lungs (A) and spleens (B) at 4 (left panel) and 7 (right panel) days p.i. (C and D) Total numbers of Ly49H$^-$ (closed bars) and Ly49H$^+$ (open bars) NK cells in the lungs (C) and spleens (D) over 7 days. Results are expressed as the mean ± SEM of 6 mice per group. (E and F) Ly49H$^-$ and Ly49H$^+$ NK cells expressed as a percentage of the total NK$^+$CD3$^-$ population in the lungs (A) and spleens (B) of IgG (left-hand bars) and anti-IL-10R (right-hand bars) treated mice. Results are expressed as the mean of 4-6 mice per group. Data represent 3 independent experiments. *p<0.05, **p<0.01

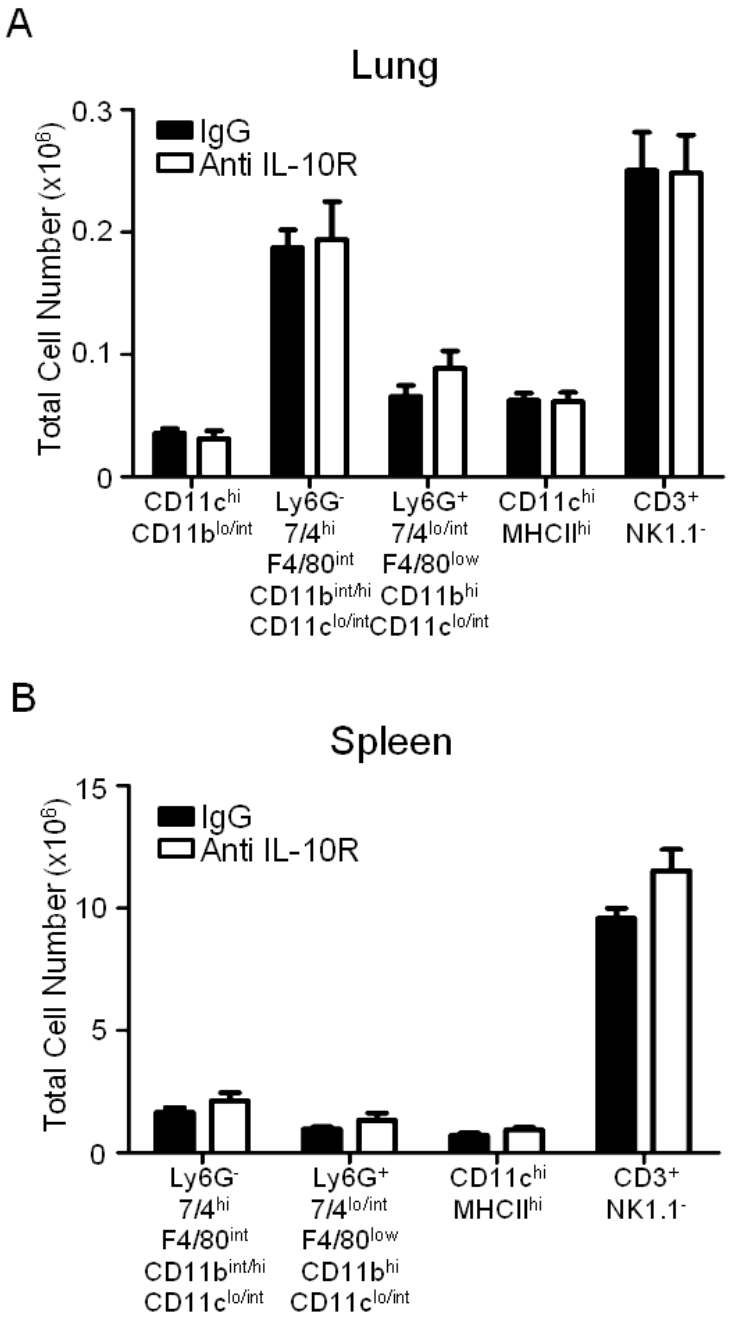

Figure 3.10. Impairment of cellular accumulation by IL-10R blockade during MCMV infection is restricted to the NK1.1$^+$CD3$^-$ compartment
Numbers of antigen presenting cells and CD3$^+$ T cells in the lungs (A) and spleens (B) of IgG (closed bars) and anti-IL-10R (open bars) treated mice, 4 days p.i. Results are expressed as mean ± SEM of 6 mice per group and represent 2 independent experiments.

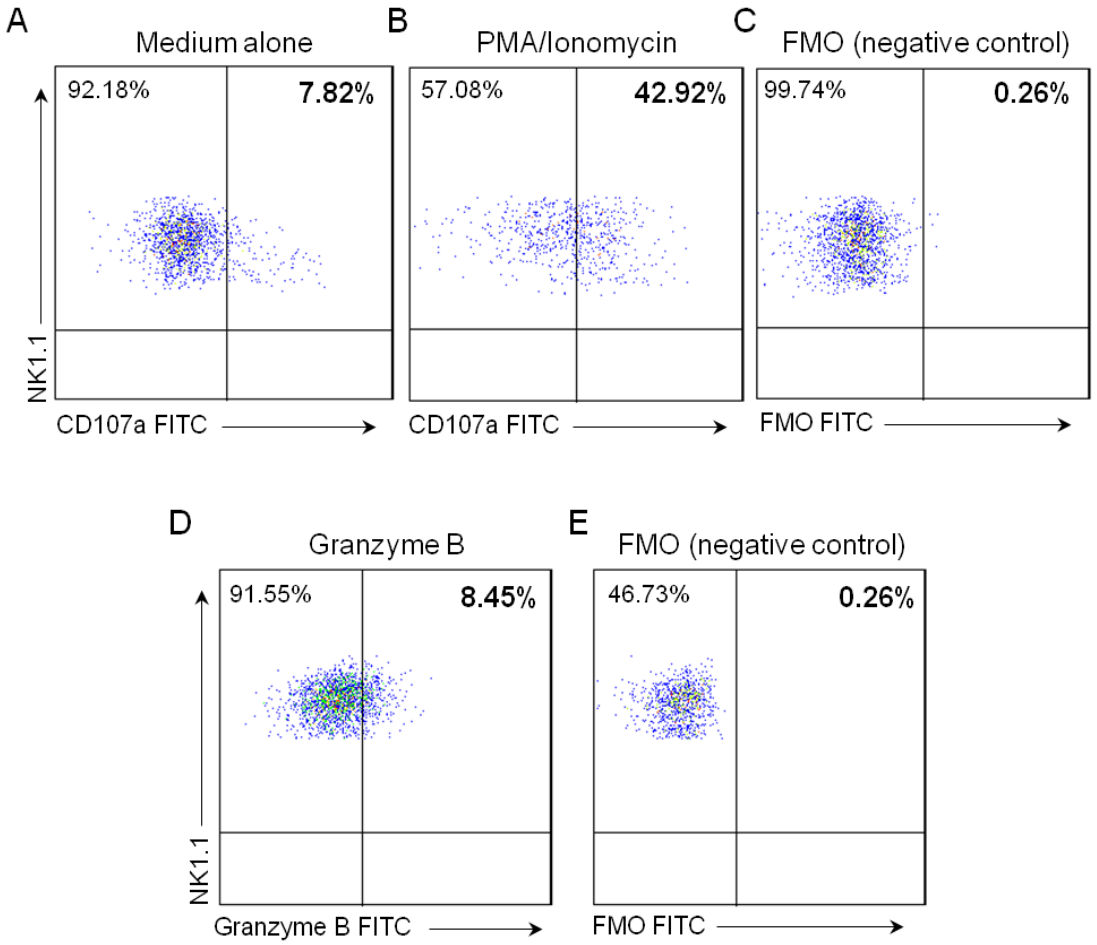

Figure 3.11. Analysis of CD107a and intracellular granzyme B antibody staining by flow cytometry

(A-C) Representative bivariate flow cytometry plots showing CD107a expression by pulmonary NK cells from MCMV-infected mice at 4 days p.i. Expression was analysed after 5 hours incubation with monensin and medium alone (A) or with monesin and PMA/Ionomycin (B). (C) FMO staining control following incubation with monensin and PMA/Ionomycin. (D-E) Representative bivariate flow cytometry plots showing intracellular granzyme B production by pulmonary NK cells from MCMV-infected mice 4 days p.i. Following surface staining, cells were stained with (D) or without (FMO) (E) intracellular granzyme B-FITC.

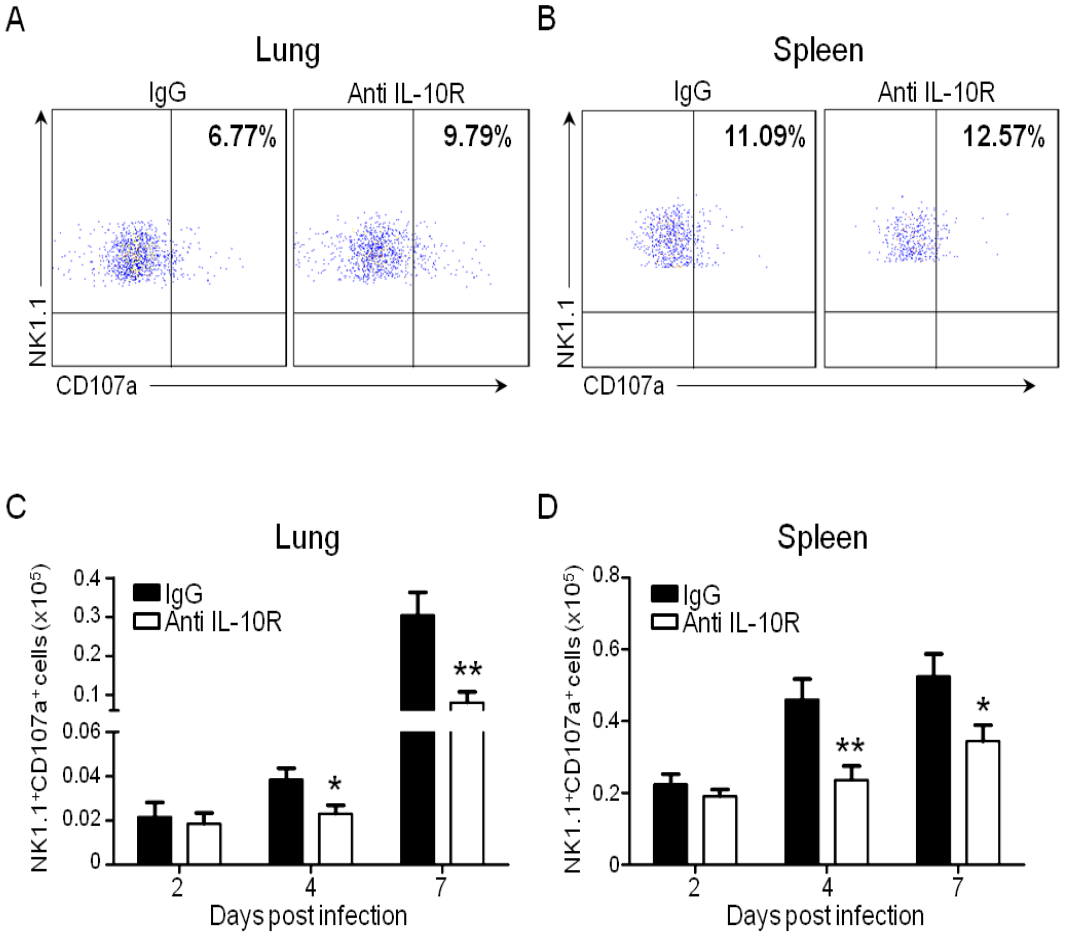

Figure 3.12. IL-10R blockade inhibits the accumulation of cytotoxic NK cells during acute MCMV infection

MCMV-infected mice were treated with IgG or anti-IL-10R on day 0 and cytotoxicity assessed by surface CD107a at days 2, 4 and 7 p.i. (A and B) Representative bivariate flow cytometry plots showing surface CD107a expression by NK cells following incubation with monensin. NK cells were derived from the lungs (A) and spleens (B) of IgG (left panel) and anti-IL-10R (right panel) treated mice, 4 days p.i. (C and D) Numbers of $CD107a^+$ NK cells in the lungs (C) and spleens (D) of IgG (closed bars) and anti-IL-10R (open bars) treated mice, after *ex vivo* incubation with monensin. Results are expressed as the mean ± SEM of 5-6 mice per group and represent 3 independent experiments. *p<0.05, **p<0.01

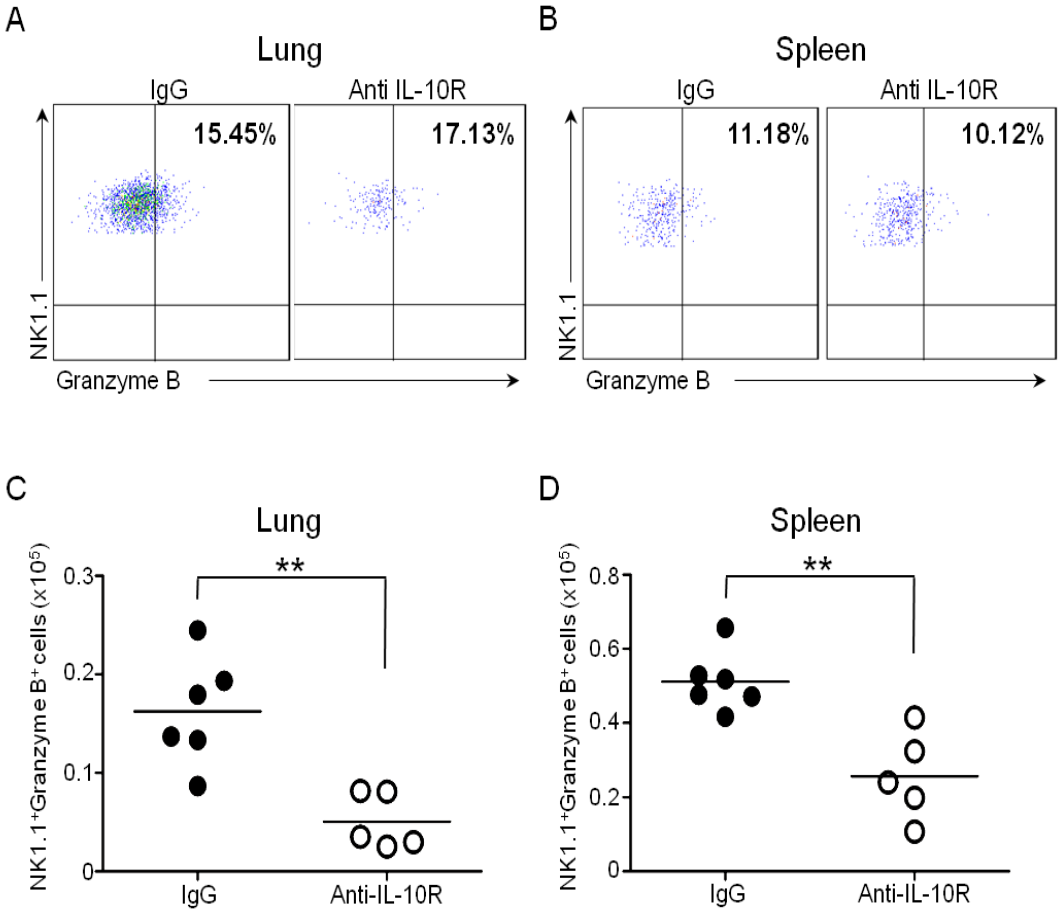

Figure 3.13. IL-10R blockade inhibits the accumulation of granzyme B expressing NK cells during acute MCMV infection

MCMV-infected mice were treated with IgG or anti-IL-10R on day 0 and granzyme B production assessed 4 days p.i. (A and B) Representative bivariate flow cytometry plots showing intracellular granzyme B expression directly *ex vivo* by NK cells from the lungs (A) and spleens (B) of IgG (left panel) and anti-IL-10R (right panel) treated mice. (C and D) Numbers of granzyme B^+ NK cells in the lungs (C) and spleens (D) of IgG (closed circles) and anti-IL-10R (open circles) treated mice, directly *ex vivo*. Data represent 2 independent experiments. **p<0.01

3.2.11. Anti-IL-10R treatment increases IFNγ expression by NK cells but does not influence overall accumulation of IFNγ producing NK cells

In addition to controlling acute infection by direct killing, IFNγ production is also an important antiviral effector function of NK cells. The effect of IL-10R blockade on spontaneous *ex vivo* IFNγ production was therefore evaluated by flow cytometry (for antibody specificity and staining controls, refer to Fig. 3.14A-C). At 4 days p.i, blockade of IL-10R signalling led to an increase in the percentage of NK cells in both the lung (Fig. 3.15A) and the spleen (Fig. 3.15B) that were producing IFNγ directly *ex vivo*. NK cells from anti-IL-10R treated mice also expressed more IFNγ on a per cell basis (as indicated by mean fluorescent intensity (MFI); Fig. 3.15A and B). However, when total IFNγ producing NK cells were calculated over a 7 day time course, a trend towards decreased numbers following IL-10R blockade was observed, although this did not reach statistical significance (Fig. 3.15C-D). Thus, in the absence of IL-10R signalling MCMV-induced accumulation of cytotoxic but not IFNγ expressing NK cells is impaired.

3.2.12. IL-10R blockade increases pro-inflammatory cytokine production in the lung and spleen of MCMV-infected mice

Pro-inflammatory cytokines have been shown to be critical for the accumulation of NK cells during viral infection (24, 92, 174). I hypothesised that a possible mechanism for impaired accumulation of NK cells following IL-10R blockade was reduced levels of pro-inflammatory cytokines. However, in the absence of IL-10R signalling, a significant increase in IL-6, IFNγ and IL-12 protein was observed in homogenates from the lung (Fig. 3.16A) and spleen (Fig. 3.16B), as well as a significant increase in IL-1α and TNFα (lung only) at 4 days p.i. Therefore, reduced pro-inflammatory cytokine production in anti-IL-10R treated mice was not responsible for defective NK cell responsiveness observed.

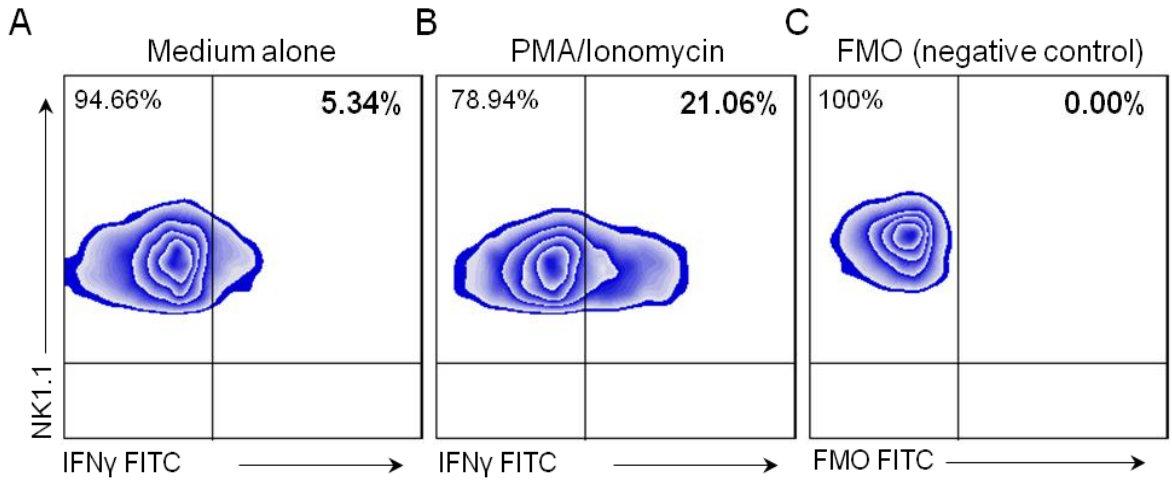

Figure 3.14. Analysis of intracellular IFNγ antibody staining by flow cytometry
Representative bivariate flow cytometry plots showing intracellular IFNγ production by pulmonary NK cells from MCMV-infected mice at 4 days p.i. Cells were incubated for 4 hours with 2µg/ml brefeldin A and medium alone (A and C) or with 2µg/ml brefeldin A and PMA/Ionomycin (B). Following surface staining, cells were stained with (A and B) or without (FMO) (C) intracellular IFNγ-FITC.

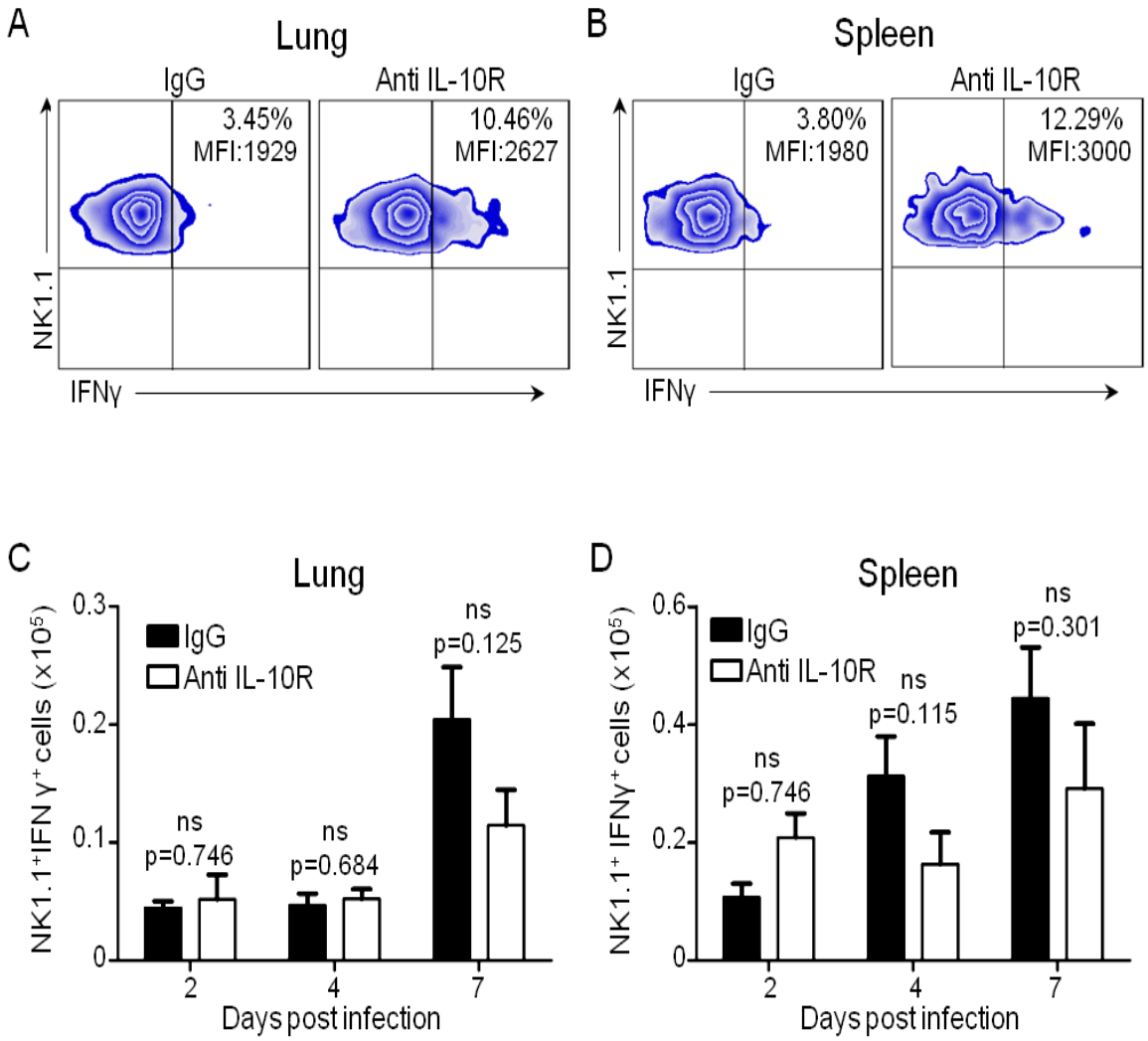

Figure 3.15. Anti-IL-10R treatment increases spontaneous IFNγ expression on a per cell basis but does not affect overall accumulation of IFNγ producing NK cells
MCMV-infected mice were treated with IgG or anti-IL-10R on day 0 and *ex vivo* IFNγ production by NK cells was assessed over 7 days. (A and B) Representative zebra flow cytometry plots showing direct *ex vivo* IFNγ production by NK^+CD3^- cells in lungs (A) and spleens (B) of IgG (left panel) and anti-IL-10R (right panel) treated mice, 4 days p.i. Percentage and MFI are shown and are representative of over 18 mice per group. (C and D) Proportion of IFNγ producing NK^+CD3^- cells in the lungs (C) and spleens (D) of IgG (closed bars) and anti-IL-10R (open bars) treated mice analysed over 7 days. (E and F) Total numbers of IFNγ producing NK^+CD3^- cells in the lungs (A) and spleens (B) of IgG (closed bars) and anti-IL-10R (open bars) treated mice analysed over 7 days. Results are expressed as the mean ± SEM of 6 mice per group and represent 3 independent experiments. ns=not significant.

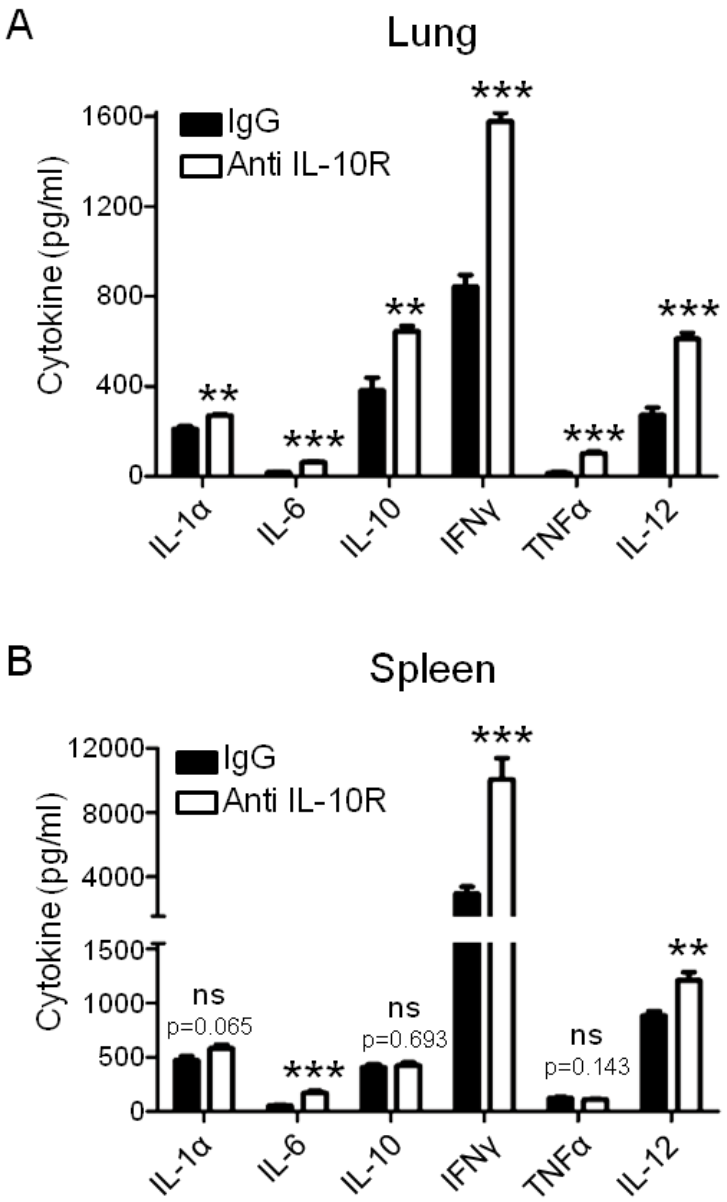

Figure 3.16. Anti-IL-10R treatment increases pro-inflammatory cytokine production in the lung and spleen of MCMV-infected mice

Mice were infected with MCMV and treated with IgG (closed bars) or anti-IL-10R (open bars). Levels of cytokines were assessed at 4 days p.i. Cytokine protein concentrations in lung (A) and spleen (B) homogenates were measured by either cytometric beads (IL-1α, IL-6, IL-10, IFNγ and TNFα) or ELISA (IL-12). Results represent the mean ± SEM of 6 mice per group. **p<0.01, ***p<0.001, ns=not significant.

3.2.13. Anti-IL-10R treatment does not influence NK cell proliferation

To further investigate how IL-10R blockade was inhibiting NK cell accumulation, NK cell proliferation was examined by monitoring intracellular Ki67 expression, a protein expressed during all active phases of the cell cycle. In accordance with the kinetics of NK cell expansion (Fig. 3.5A and B) and previously published data (171), proliferation in the lungs and spleens was highest between 4 and 7 days p.i (Fig. 3.17A and B). However, anti-IL-10R treatment did not influence Ki67 expression by either pulmonary (Fig. 3.17A and C) or splenic (Fig. 3.17B and D) NK cells at any time point during acute infection, therefore demonstrating that reduced proliferation was not the mechanism for reduced NK cell numbers following IL-10R blockade.

3.2.14. Inhibition of IL-10R signalling enhances NK cell apoptosis during acute MCMV infection

Next, I measured NK cell apoptosis over a time course to investigate whether IL-10R blockade was triggering cell death. Interestingly, a high proportion of apoptotic NK cells, as measured by Annexin V binding, in the lungs (Fig. 3.18A and C) and spleens (Fig. 3.18B and D) was observed during the first 4 days of infection, demonstrating that the contraction of NK cell numbers during this period, as shown in Fig. 3.5C and D, was a consequence of apoptosis. The percentage of apoptotic NK cells at 2 days p.i was comparable between anti-IL-10R and control treated mice (Fig. 3.18C and D). Importantly however, the frequency of apoptotic NK cells further increased in mice treated with anti-IL-10R at 4 days p.i in the lung (Fig. 3.18A and C) and spleen (Fig. 3.18B and D) as compared to IgG controls.

The engagement of the TNF family member Fas upon encounter with cells expressing Fas-ligand is one mechanism that triggers cellular apoptosis (175). Therefore Fas expression on NK cells 4 days p.i was examined. The proportion of NK cells that expressed Fas in the lungs (Fig. 3.19A and C) and spleens (Fig. 3.19B and C) was significantly higher in mice treated with anti-IL-10R as compared to IgG treated mice. NK cells from anti-IL-10R treated mice also expressed more Fas on a per cell basis (as indicated by MFI; Fig. 3.19D). This increase in Fas expression is in accordance with the time point where the highest levels of apoptosis are observed in the anti-IL-10R treated mice (Fig. 3.19C and D). Furthermore, Fas-ligand mediated apoptosis is caspase-dependent, and caspase-3 is considered to be a major executioner of apoptosis (175). Elevated frequencies of Fas expressing NK cells following IL-10R blockade were accompanied by increased frequencies of pulmonary NK cells positive for intracellular active caspase-3 (Fig. 3.20A and B). Collectively, these data suggest that impaired NK cell responses in the absence of IL-10R signalling were a consequence of increased apoptosis.

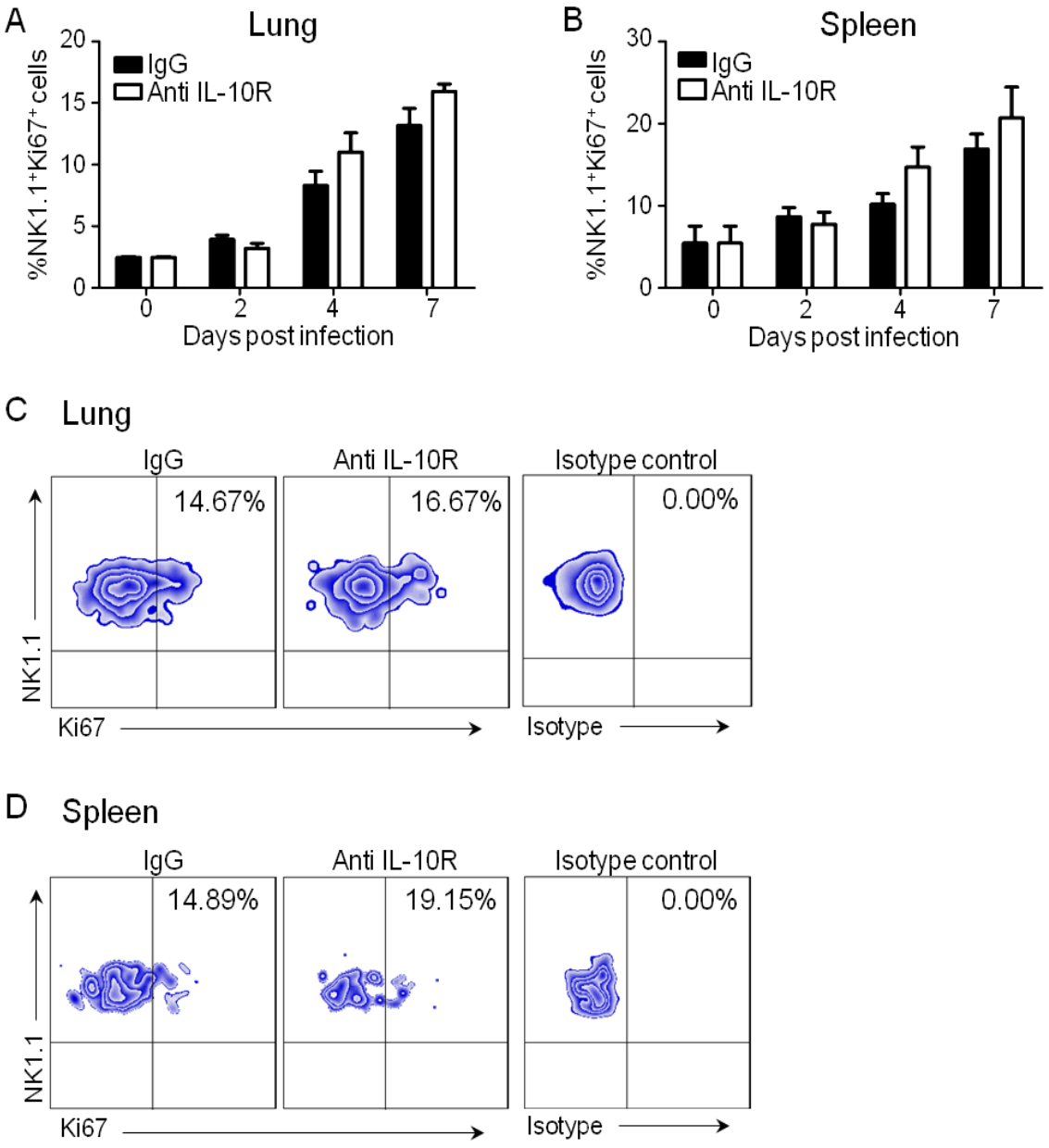

Figure 3.17. Anti-IL-10R treatment does not influence NK cell proliferation
Mice were infected with MCMV and treated with IgG or anti-IL-10R. Proliferation of pulmonary (A and C) and splenic (B and D) NK cells assessed by detection of intracellular Ki67 expression directly *ex vivo*. (A and B) NK cell proliferation in the lung and spleen (B) of mice treated with IgG (closed bars) or anti-IL-10R (open bars). Results represent the mean ± SEM of 4-6 mice per group (C and D) Representative zebra flow cytometry plots showing direct *ex vivo* Ki67 expression by NK^+CD3^- cells in lungs (C) and spleens (D) of IgG (left panel) and anti-IL-10R (middle panel) treated mice, 4 days p.i. Isotype staining controls are also shown (right panel). Data represent 2 independent experiments.

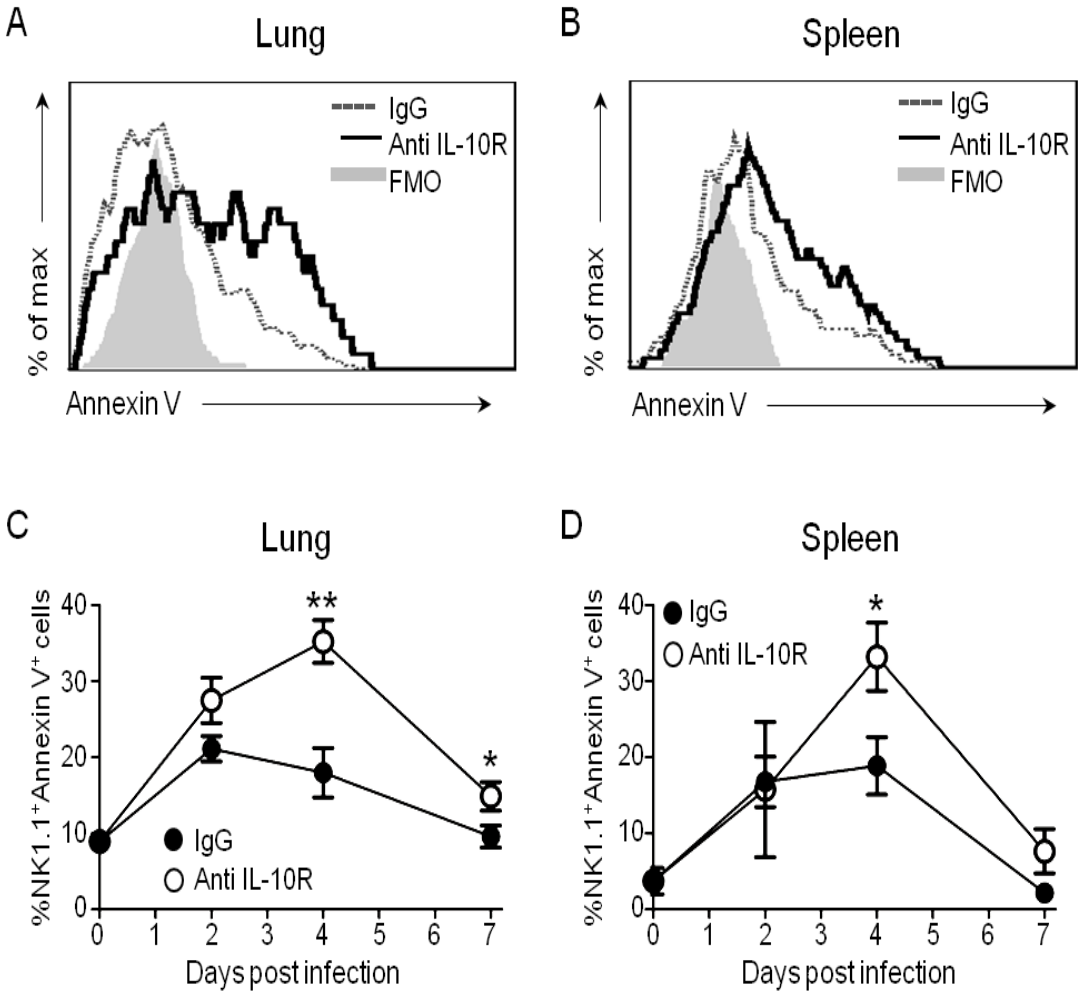

Figure 3.18. IL-10R blockade enhances NK cell apoptosis during acute MCMV infection

Mice were infected with MCMV and treated with IgG or anti-IL-10R and apoptosis of NK cells was assessed by Annexin V binding. (A and B) Representative overlay histograms of Annexin V binding of NK cells in the lungs (A) and spleens (B) of mice following treatment with anti-IL-10R (solid line) or IgG (dashed line) 4 days p.i (shaded histogram = FMO control). (C and D) Annexin V binding by NK cells in the lungs (C) and spleens (D) of mice treated with IgG (closed circles) or anti-IL-10R (open circles) shown as percentage of NK^+CD3^- cells over a 7 day time course. Results are expressed as the mean ± SEM of 4-6 mice per group and represent 2-3 independent experiments. *p<0.05, **p<0.01

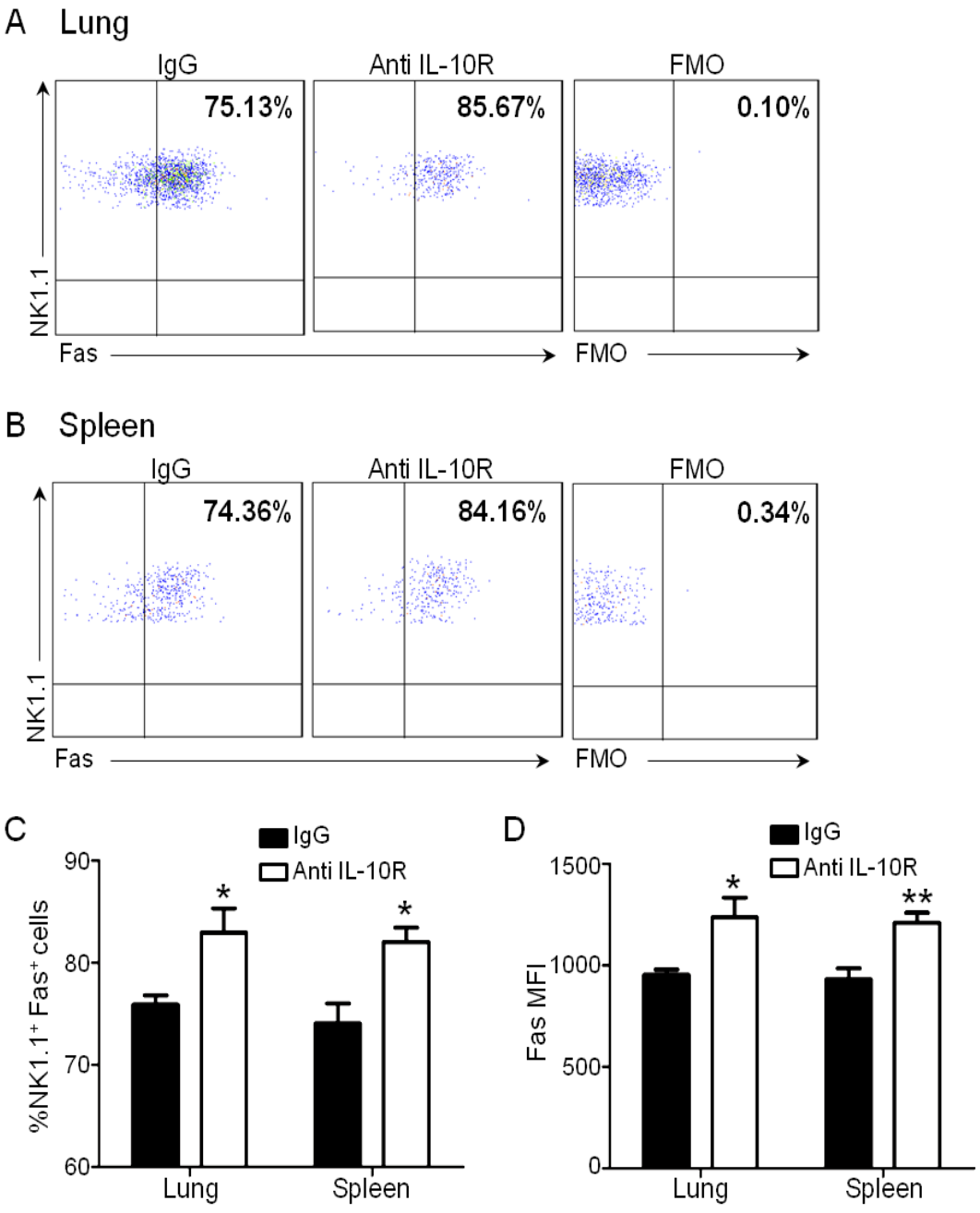

Figure 3.19. IL-10R blockade leads to increased expression of Fas by NK cells
MCMV-infected mice were treated with IgG or anti-IL-10R on day 0 and Fas expression analysed 4 days p.i. (A and B) Representative bivariate flow cytometry plots showing Fas expression by NK cells from the lungs (A) and spleens (B) of IgG (left panel) and anti-IL-10R (middle panel) treated mice. FMO negative staining controls are also shown (right panel). (C) Proportion of NK^+CD3^- cells expressing Fas in the lungs and spleens of mice treated with IgG (closed bars) or anti-IL-10R (open bars). (D) MFI of Fas expression by pulmonary and splenic NK cells from IgG (closed bars) and anti-IL-10R (open bars). Results are expressed as the mean ± SEM of 5 mice per group and represent 3 independent experiments. *p<0.05, **p<0.01

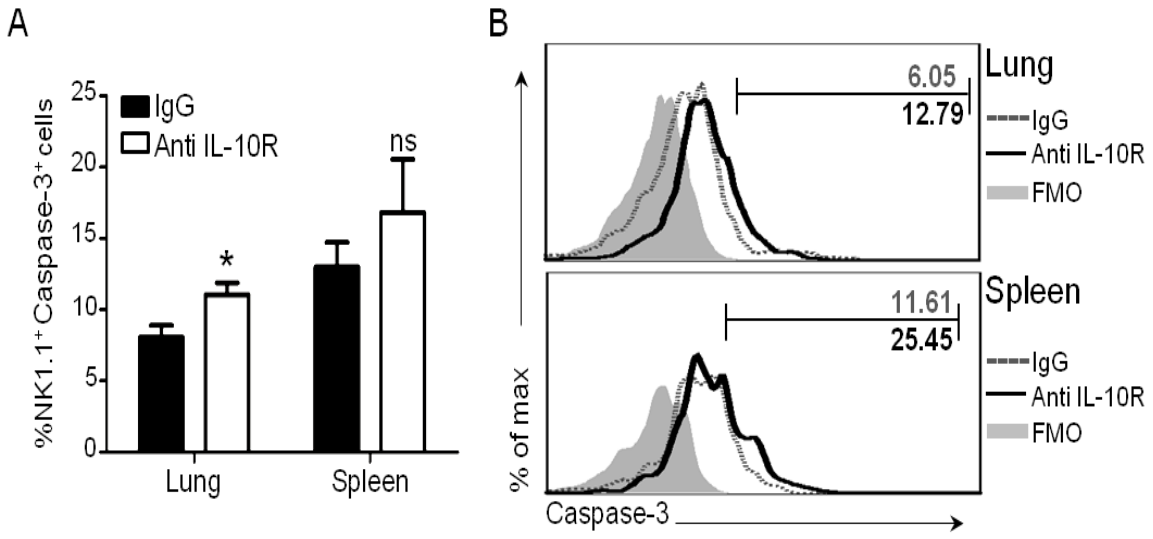

Figure 3.20. Enhanced NK cell apoptosis following IL-10R blockade is associated with increased expression of intracellular caspase-3

(A) Proportion of NK^+CD3^- cells expressing intracellular caspase-3 (active form) in the lungs and spleens of mice 4 days p.i, treated with IgG (closed bars) or anti-IL-10R (open bars) directly *ex vivo*. Results are expressed as the mean ± SEM of 4 mice per group. (B) Representative overlay histograms of caspase-3 expression by NK cells in the lungs (top) and spleens (bottom) of mice following treatment with anti-IL-10R (solid line) or IgG (dashed line) 4 days p.i (shaded histogram = FMO control). Data represent 3 independent experiments. *p<0.05, ns=not significant.

3.2.15. Anti-IL-10R treatment increases the frequency of apoptosis in multiple NK cell subsets

As NK cell function was affected by IL-10R blockade, I hypothesised that the phenotype of NK cells would also be modulated in the absence of IL-10R signalling. Therefore, phenotypic analysis comparing NK cells from anti-IL-10R and IgG treated mice was performed. Expression of CD11b and CD27 defines the maturation status of murine NK cells, as well as CD27 expression being associated with cytotoxic effector functions (176, 177). The proportion of NK cells in both the lung (Fig. 3.21A) and spleen (Fig. 3.21B) that resided in each defined subset of maturation was comparable between anti-IL-10R and IgG treated mice (for antibody specificity and staining controls, refer to Fig. 3.22A-D). These individual subsets were then assessed for levels of apoptosis. Splenic $CD11b^{high}CD27^{high}$ NK cells were the predominant NK cell subset that bound Annexin V (Fig. 3.21D); whereas high frequencies of apoptosis were observed in $CD27^{high}$ and $CD27^{low}$ pulmonary NK cell populations (Fig. 3.21C). However, anti-IL-10R blockade further increased the frequency of apoptotic pulmonary and splenic $CD11b^{high}CD27^{high}$ mature NK cells, as well as the less mature $CD11b^{low}CD27^{high}$ NK cells (Fig. 3.21C and D), which is in accordance with the increased levels of apoptosis observed at 4 days p.i in the absence of IL-10R signalling (Fig. 3.18).

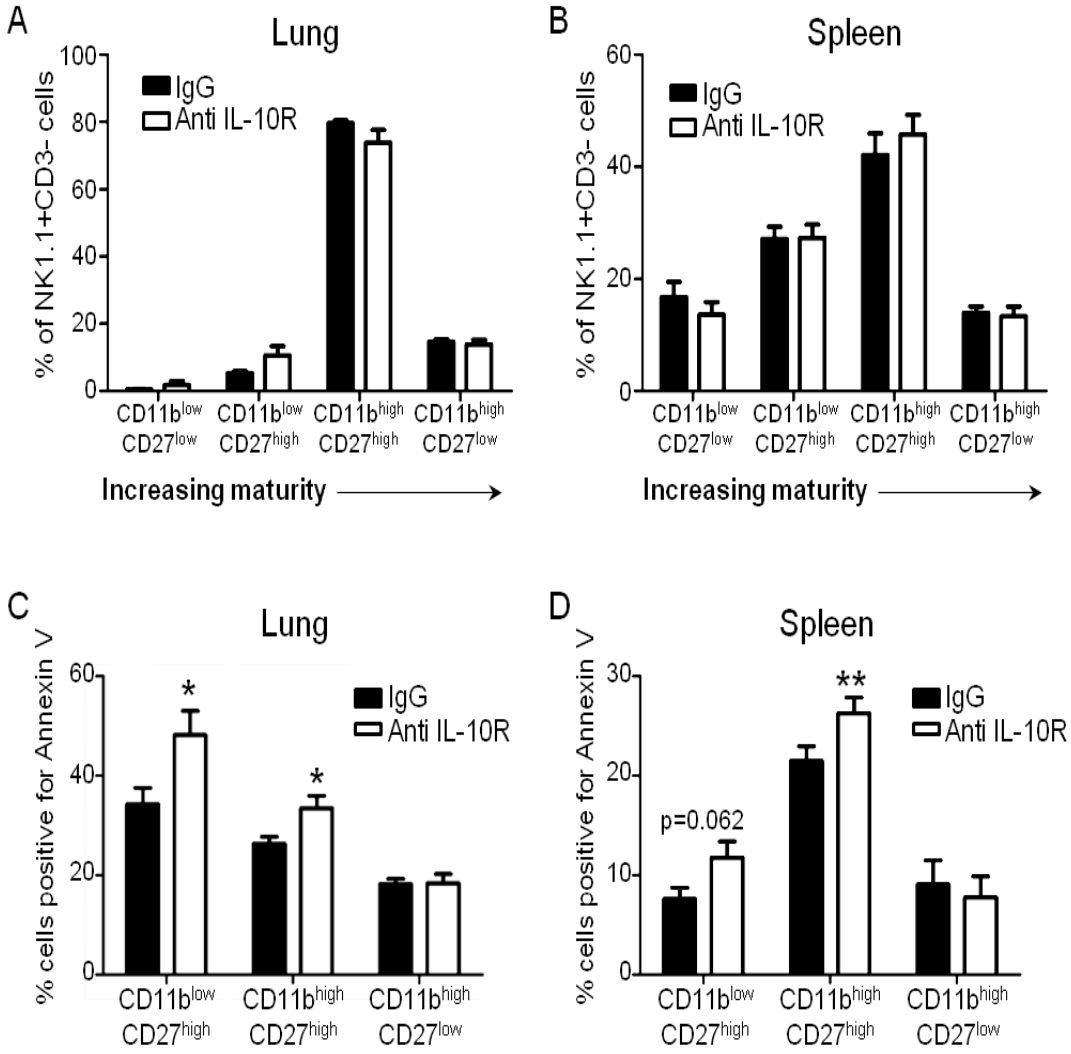

Figure 3.21. Anti-IL-10R blockade increases the frequency of apoptosis in both mature and less mature NK cell subsets

MCMV-infected mice were treated with IgG (closed bars) or anti-IL-10R (open bars). After 4 days, NK cell subsets in the lung (A) and spleen (B) were defined based on CD11b and CD27 co-expression (FMOs were used to define gating as shown in Fig. 3.22). Proportion of Annexin V binding NK cells in each subset was then assessed (C and D) Annexin V binding by NK cell subsets in the lungs (C) and spleens (D) of mice treated with IgG or anti-IL-10R. Results are expressed as the mean ± SEM of 8 mice per group and represent 2 independent experiments. *p<0.05, **p<0.01

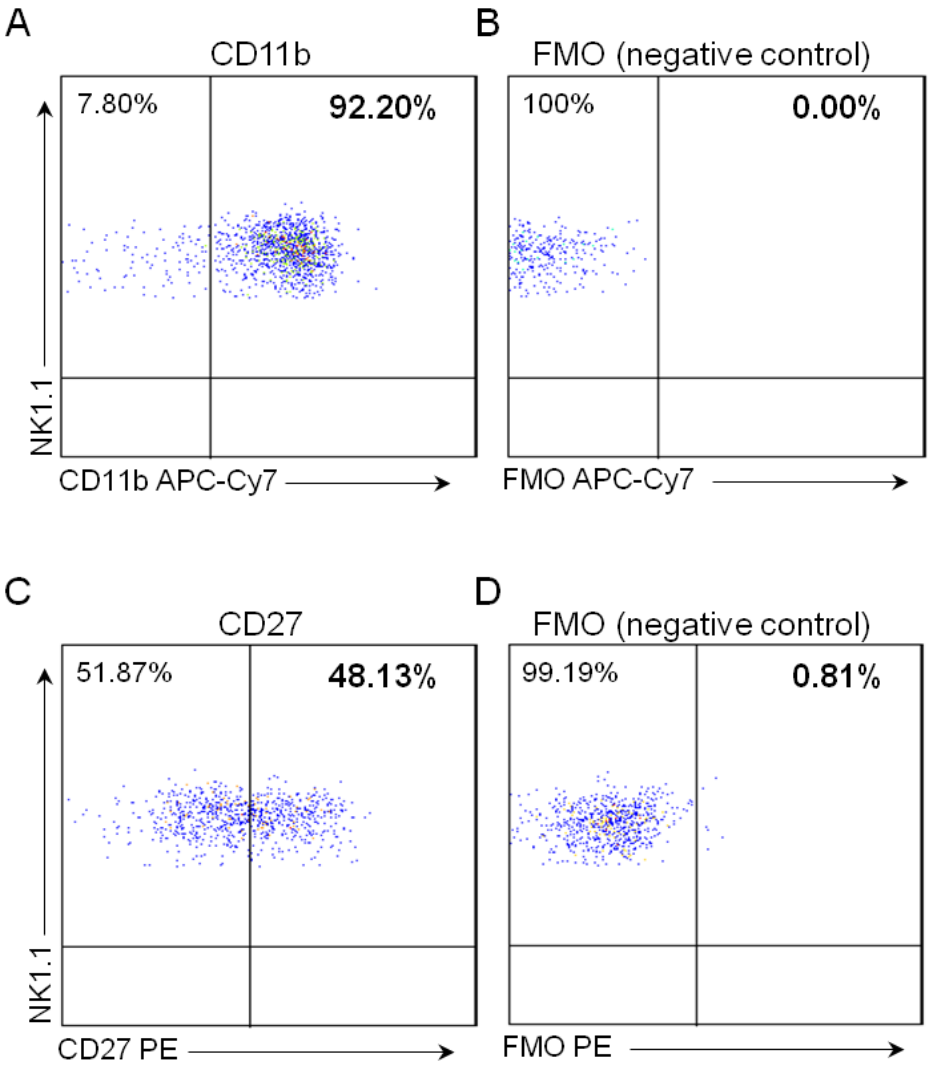

Figure 3.22. Analysis of CD11b and CD27 antibody staining by flow cytometry
Representative bivariate flow cytometry plots showing surface CD11b and CD27 expression by pulmonary NK cells from MCMV-infected mice 4 days p.i. Cells were incubated with Live/Dead Fixable Aqua and then surface stained with CD11b-APC-Cy7 (A) or CD27-PE (C). FMO staining panels were used as negative controls (B and D).

3.2.16. IL-10R blockade enhances NK cell activation-induced cell death

To establish why IL-10R blockade preferentially induced NK cell apoptosis, the activation status of NK cells was first assessed. Strikingly, NK cell expression of activation markers CD25 (lung and spleen) and CD69 (lung only) was associated with increased Annexin V binding (Fig. 3.23A and B) at day 4 p.i, suggesting that NK cells exhibiting a heightened activation status were preferentially undergoing apoptosis.

Importantly, when CD25 and CD69 expression by NK cells was compared in mice treated with anti-IL-10R and control IgG, a marked increase in the proportion of NK cells that were positive for CD25 (lung and spleen, Fig. 3.24A) and CD69 (lung only, Fig. 3.24B) was observed at 4 days p.i. This elevation in activation marker expression was also evident on a per cell basis as shown by MFI, with the exception of splenic CD69 expression (Fig. 3.24C and D). These data, taken with enhanced IFNγ expression by NK cells from anti-IL-10R treated mice (Fig. 3.15A and B); imply that IL-10R blockade enhanced NK cell activation. Critically, anti-IL-10R treatment significantly enhanced the proportion of NK cells that co-expressed activation markers (CD25, lung and spleen; CD69, lung only) and active caspase-3 in the lung (Fig. 3.25A) and the spleen (Fig. 3.25B). Thus, these data demonstrate that impaired NK cell accumulation following IL-10R blockade was the consequence of enhanced activation-induced death of NK cells.

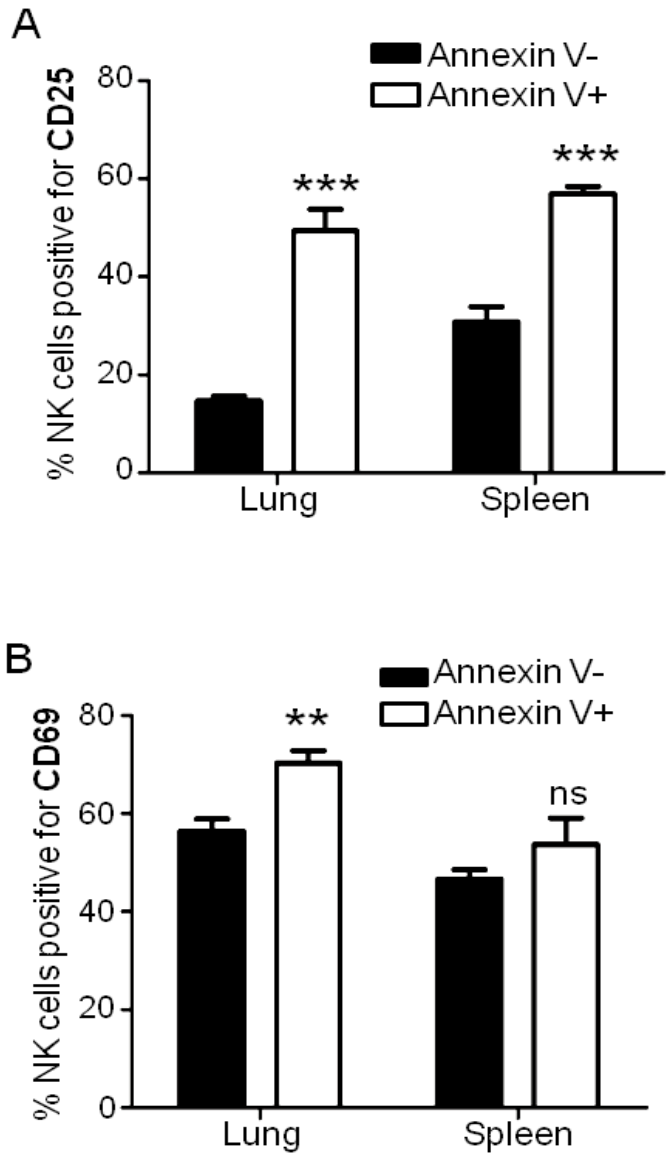

Figure 3.23. Increased apoptosis is associated with expression of activation markers CD25 and CD69

Expression of CD25 (A) and CD69 (B) by Annexin V^- (closed bars) and Annexin V^+ (open bars) NK cells in the lungs and spleens 4 days p.i. Results are expressed as the mean ± SEM of 6 mice per group and represent 2 independent experiments. **p<0.01, ***p<0.001, ns=not significant.

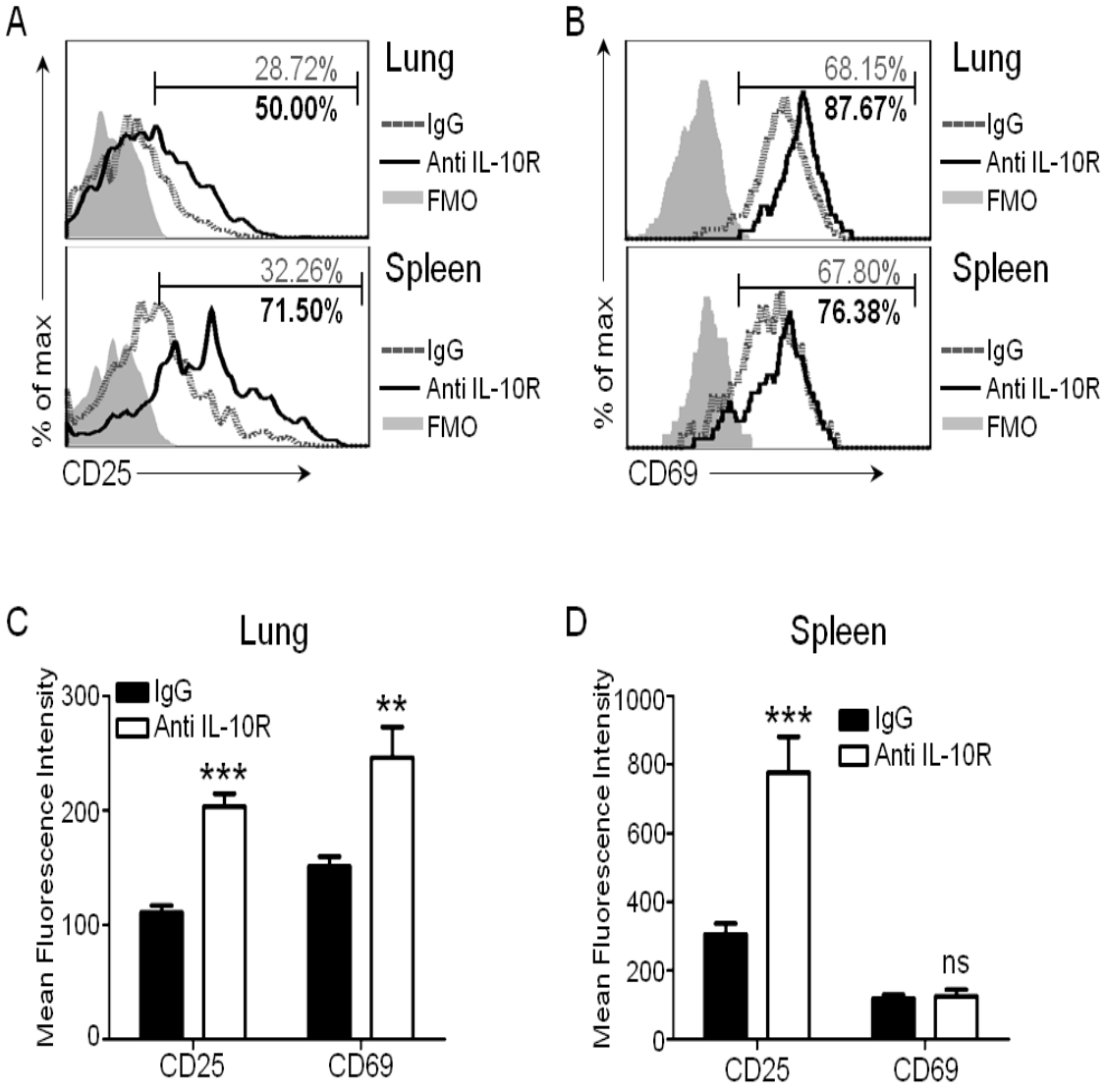

Figure 3.24. Anti-IL-10R blockade increases the expression of activation markers CD25 and CD69 on NK cells

(A and B) Representative histograms of CD25 (A) and CD69 (B) expression by pulmonary (top) and splenic (bottom) NK cells from IgG (dashed line) and anti-IL-10R (solid line) treated mice, 4 days p.i with MCMV. Results are representative of 2 independent experiments, each constituting of 6 mice per group. (C and D) MFI of CD25 and CD69 expression by pulmonary (C) and splenic (D) NK cells from IgG (closed bars) and anti-IL-10R (open bars) treated mice 4 days after infection. Results are expressed as mean ± SEM of 4-6 mice per group and represent 3 independent experiments. **p<0.01, ***p<0.001, ns=not significant.

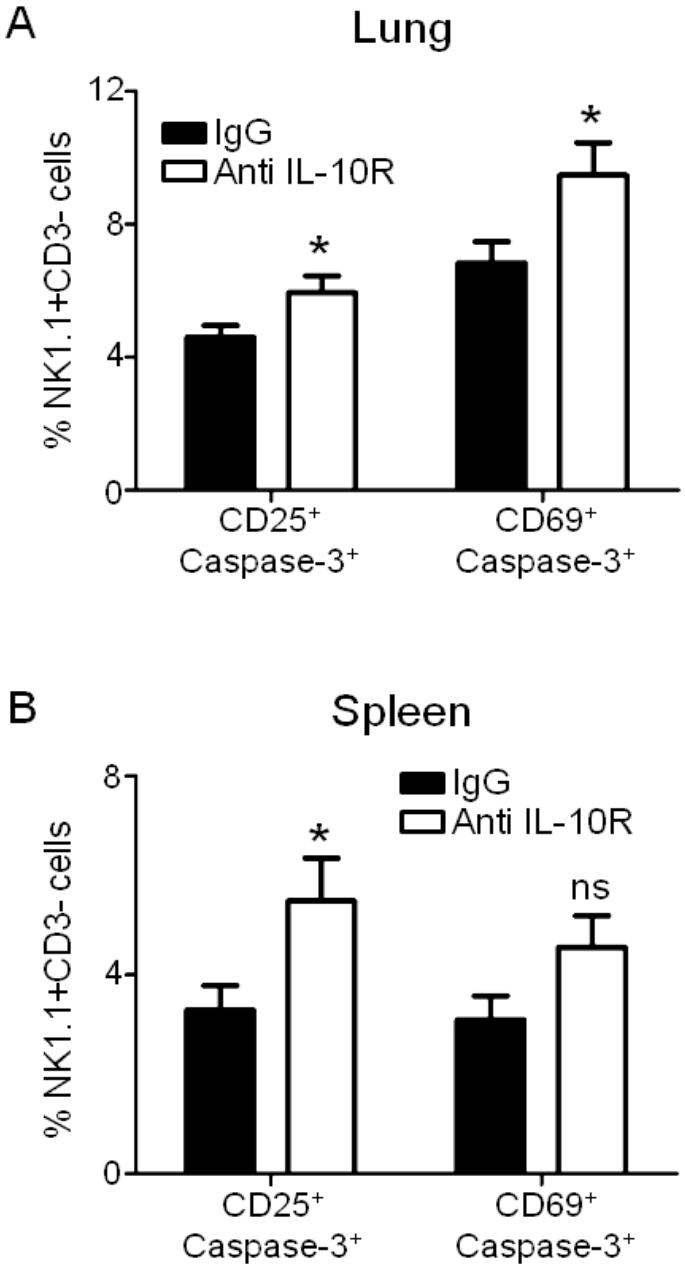

Figure 3.25. Anti-IL-10R blockade increases co-expression of activation markers and active caspase-3 by NK cells

Percentages of NK cells in the lung (A) and spleen (B) co-expressing intracellular active caspase-3 and CD25 or CD69, 4 days p.i. Results are expressed as mean ± SEM of 8 mice per group and represent 2 independent experiments. *p<0.05, ns=not significant.

3.2.17. IL-10 does not directly inhibit activation-induced NK cell death

The mechanism(s) by which NK cells from anti-IL-10R treated mice were undergoing activation-induced cell death was unclear. To determine whether IL-10 directly acted on NK cells to regulate this process, IL-10R expression on NK cells was first examined. NK cells from the lung (Fig. 3.26A and C) and the spleen (Fig. 3.26B and C) expressed low levels of IL-10R constitutively and up-regulated expression upon infection. The anti-IL-10R antibody clone used for IL-10R detection by flow cytometry was the same used for *in vivo* IL-10R blockade. Subsequently, I observed low staining of IL-10R in treated mice (Fig. 3.26A and B) thus demonstrating the blocking anti-IL-10R antibody remained bound to IL-10R expressing NK cells during the 4-day experiment.

Because IL-10R was expressed on NK cells during MCMV infection, I investigated whether IL-10 was directly influencing their survival. Splenocytes and pulmonary leukocytes were isolated 4 days after MCMV infection and incubated in the presence or absence of recombinant IL-10. Importantly, IL-10 did not reduce *ex vivo* NK cell apoptosis as compared to NK cells incubated without IL-10 (Fig. 3.27A). Furthermore, a trend of increased IFNγ expression by pulmonary and splenic NK cells was observed following incubation with IL-10 *in vitro* (Fig. 3.27B). In accordance with published data (159, 161, 162), these observations suggest that IL-10 has a stimulatory role in direct NK cell regulation, and imply that IL-10 inhibits activation-induced NK cell death during acute MCMV infection via an indirect mechanism.

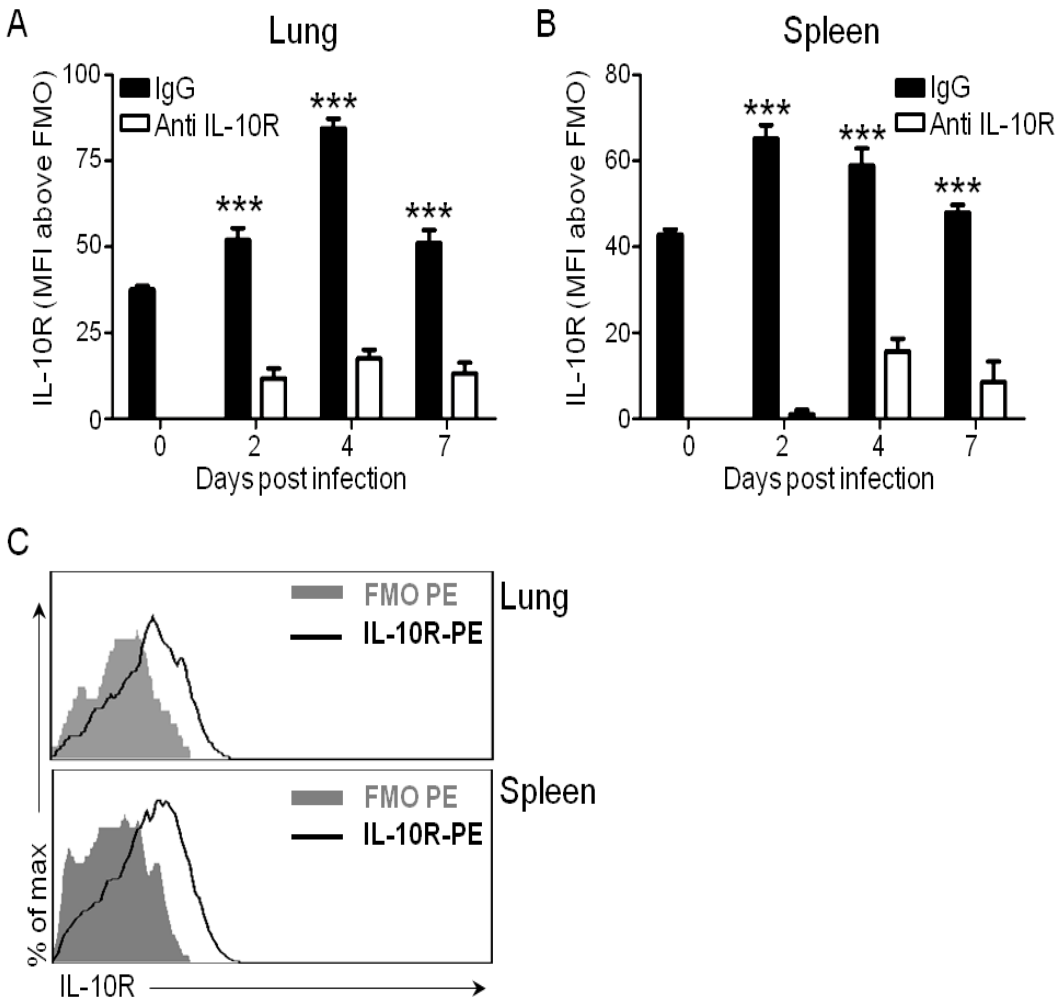

Figure 3.26. IL-10R expression by pulmonary and splenic NK cells
(A and B) Expression of IL-10R on $NK^{+}CD3^{-}$ cells in the lungs (A) and spleens (B) of naïve mice and MCMV-infected mice treated with IgG (closed bars) or anti-IL-10R (open bars) over a 7 day time course. Results are expressed as the mean ± SEM of 4-6 mice per group. (C) Representative overlay histograms showing surface IL-10R expression (open histograms) and FMO staining controls (shaded histograms) by pulmonary (top panel) and splenic (bottom panel) NK cells from MCMV-infected mice 4 days p.i. ***p<0.001

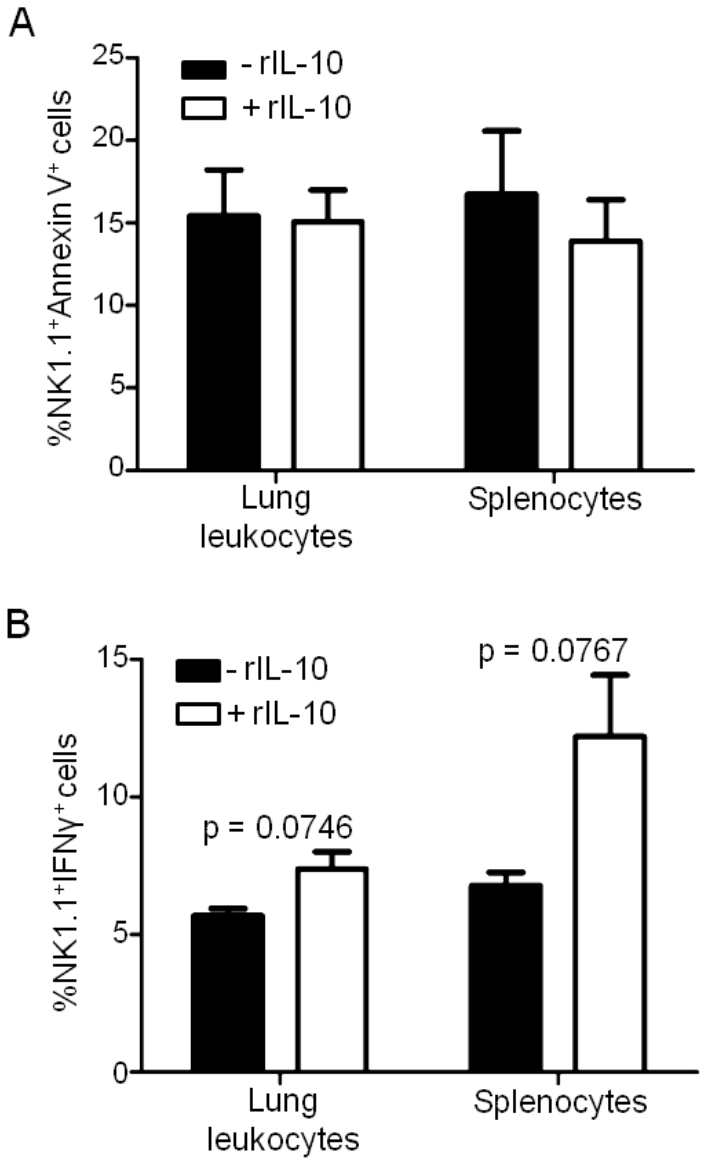

Figure 3.27. IL-10 does not directly inhibit NK cell apoptosis during MCMV infection
(A and B) Lung leukocytes and splenocytes were isolated 4 days p.i. Cells were cultured in a 96-well plate for 18 hours in the presence (open bars) or absence (closed bars) of 50ng/ml of recombinant murine IL-10. (A) Proportion of NK cells from the lungs (left) and spleens (right) of MCMV-infected mice that bound Annexin V. (B) To assess IFNγ production, 2µg/ml brefeldin A was added to some of the wells for the last 8 hours of culture. Proportion of IFNγ producing NK cells isolated from the lungs (left) and spleens (right) of MCMV-infected mice are shown. Results are expressed as the mean ± SEM of 3 mice per group and represent 2 independent experiments.

3.3. Discussion

It has been previously shown that MCMV is a potent inducer of IL-10 production (167, 178). The visceral organs are significant sites targeted by the virus during the acute-phase of infection, therefore it was important to establish if MCMV infection up-regulated IL-10 expression in these organs. As seen during persistent infection, virus induced IL-10 was detected in the spleen within the first 4 days of infection. Acute MCMV infection also induced IL-10 production in the lung, and both organs showed significantly higher IL-10 levels than seen in uninfected controls. Previous work using IL-10-GFP reporter mice showed B cells to be a significant source of IL-10 during MCMV infection (179). My analysis of different cell types after *ex vivo* polyclonal stimulation 4 days p.i was in agreement with this data, with B cells representing one of the predominant cell types capable of expressing IL-10. Inflammatory macrophages from the lung and dendritic cells from the spleen were other populations of cells expressing high levels of IL-10. As shown previously, MCMV-infected macrophages secrete IL-10 *in vitro* (178). Whether or not IL-10 producing APCs observed during *in vivo* infection were infected or not remains to be determined in experiments utilising GFP-expressing MCMV. There is some evidence, albeit limited, suggesting that HCMV and MCMV can infect B cells (180, 181). Again, it is not possible to say if the B cells producing the IL-10 in my experiments were infected or not. However, in numerous non-infectious models, B cells are an important source of IL-10 (179, 182, 183), thus demonstrating that viral infections of B cells is not a necessity for the induction of IL-10 expression by this lymphocyte subset.

An antagonistic antibody was used to block IL-10R signalling during acute MCMV infection. Surprisingly, the absence of IL-10R signalling led to a transient, but statistically significant increase in viral DNA load, suggesting IL-10 affords protection from acute MCMV infection. Interestingly however, this increase in virus load did not reach a statistically significant level when measured by plaque assay to detect replicating virus, implying that some caution must be taken when interpreting these results. It is however

important to note that the levels of detectable replicating virus, especially in the lung, are extremely low. This is due in part to the crude methodology used to homogenise infected tissues that results in a large loss of infectious virions. Therefore, measurement of viral DNA load affords a more representative insight into the degree of virus burden *in vivo*. Using this method of virus load measurement, a substantial increase of 2-3 logs was observed when mice were depleted of NK cells. The huge increase in virus load shows that NK cells are critical for controlling early MCMV infection. This finding is in agreement with previous studies that have shown the importance of NK cells in MCMV infection by a number of different methods including adoptive transfer of NK cells into suckling mice (87), utilising NK cell deficient mice (169), or depletion of NK cells by administering a NK specific antibody (89, 170). Crucially, a further increase in virus load in NK cell deficient mice following IL-10R blockade was not observed, strongly implying that anti-IL-10R treatment was having a negative effect on NK cells and their ability to control the virus at this early time point.

No differences in virus load were observed in anti-IL-10R treated and IgG treated mice at day 7 p.i. At this time, I concurrently observed elevated virus-specific $CD4^+$ T cell responses. Different cellular immune mechanisms can compensate for each other during MCMV infection (184, 185). I therefore hypothesise that the absence of a significant increase in virus burden 7 days p.i in anti-IL-10R treated mice was due to enhanced T cell control of the elevated virus load.

MCMV infection induced a decline in NK cell numbers in the lung and spleen. This has been previously observed in the spleen when NK cell numbers were tracked during MCMV infection (171-173), although this initial NK cell contraction was overlooked in these studies. I investigated the mechanisms driving this contraction and observed a high frequency of NK cell apoptosis at this time point in both organs, suggesting that cell death is a likely explanation for NK cell contraction. Expansion of the NK cell compartment from

2 days p.i was accompanied by a decrease in apoptosis over time, in conjunction with an increase in NK cell proliferation. The increase in NK cell numbers was due largely to a rapid expansion of the Ly49H$^+$ population between days 4 and 7, as previously shown in acute infection of C57BL/6 mice (171, 186). To ascertain whether IL-10 influenced this process, NK cell accumulation was assessed in the absence of IL-10R signalling. Blockade of IL-10R did not influence initial NK cell contraction but reduced later expansion of NK cell numbers. Importantly, it was not the preferential expansion of the Ly49H$^+$ NK cells that was inhibited by anti-IL-10R treatment, rather apoptosis of the NK cell population as a whole was substantially enhanced and prolonged, as demonstrated by enhanced levels of Annexin V binding accompanied by increased expression of Fas and intracellular caspase-3 (pulmonary NK cells only).

As previously discussed, two major antiviral functions of NK cells during viral infection are the production of IFNγ and direct lysis of infected cells. As NK cell accumulation was impaired in the absence of IL-10R signalling, NK cell IFNγ production and cytotoxicity were assessed in order to ascertain if functionality was also impaired. Interestingly, cytotoxic NK cell numbers were reduced following IL-10R blockade whereas the frequency of IFNγ producing cells was comparable in both groups. Indeed on a per cell basis, more IFNγ was produced in the absence of IL-10R signalling. Therefore, the data suggest that IL-10 preferentially limits apoptosis of cytotoxic NK cells subsequently promoting their accumulation. NK cells have been shown to exhibit dual functionality of IFNγ expression and degranulation (187), therefore I cannot rule out the differential regulation of the dual-functioning NK cells by IL-10. This could be addressed by co-staining for IFNγ and CD107a. Irrespective, my data clearly demonstrates that by limiting apoptosis of the cytotoxic NK cells capable of killing virally infected cells, IL-10 promotes antiviral responses early in MCMV infection.

Maturation of murine NK cells has been defined as a four-stage process, each stage being characterised by the expression of CD11b and CD27 (176), with higher expression of CD27 being synonymous with greater effector/cytotoxic functions. The proportion of NK cells that fell into each defined subset of maturation was not influenced by IL-10R blockade, but critically, the $CD27^{high}$ NK cells were the ones exhibiting increased levels of apoptosis in the absence of IL-10R signalling. This observation, in concordance with the CD107a data, further strengthens the argument that IL-10 promotes antiviral responses by limiting apoptosis of those NK cells capable of mediating effector/cytotoxic functions.

Phenotypic analysis of the Annexin V positive versus negative cells revealed that those NK cells undergoing apoptosis were more activated (as characterised by CD69 and CD25 expression). By comparing the expression of CD69 and CD25 on NK cells from control mice and anti-IL-10R treated mice, it transpired that in the absence of IL-10R signalling, a higher frequency of NK cells were activated and expressed significantly higher levels of the activation markers on a per cell basis. In conjunction with amplified IFNγ expression, these data imply that IL-10R blockade enhanced NK cell activation. Taken with my data demonstrating that IL-10R blockade results in increased NK cell apoptosis, I therefore conclude that IL-10 reduces activation-induced cell death of NK cells during acute MCMV infection.

NK cells in the lung and spleen were found to constitutively express low levels of IL-10R, and expression was slightly up-regulated upon infection. Therefore, IL-10 could exert protective effects directly on the NK cells by signalling through the IL-10R. However, incubation with recombinant IL-10 *in vitro* did not reduce NK cell apoptosis or IFNγ expression. In fact, a trend towards increased IFNγ was observed, implying that, in accordance with published work (159, 162) incubation of NK cells with IL-10 increases IFNγ expression. These data therefore suggest that IL-10 does not directly inhibit NK cell activation induced death *in vivo*.

Previous studies have demonstrated the importance of MCMV-induced IL-12 and TNFα in early NK cell IFNγ production and viral control (24, 92, 174). Although these cytokines are important for optimal NK cell responses to MCMV, it has also been shown that over-expression of IFNγ actually reduces NK cell development (188) and, intriguingly, that TNFα and IL-12 enhance apoptosis of IL-2 stimulated human NK cells (189). Interestingly, elevated levels of NK cell apoptosis and reduced NK cell accumulation following IL-10R blockade was accompanied by significantly elevated expression of IFNγ, IL-12 (lung and spleen) and TNFα (lung only). The finding that pro-inflammatory cytokines are found in greater amounts in the absence of IL-10R signalling is in itself not surprising. However, these heightened levels of pro-inflammatory cytokines after IL-10R blockade may contribute to increased NK cell apoptosis. The data therefore implies that IL-10 indirectly regulates NK cell survival by limiting the expression of pro-inflammatory cytokines.

The liver is another site targeted by MCMV during acute infection. However, unlike the lung and spleen NK cell responses in this organ were unaffected by IL-10R blockade and, importantly, nor was virus load. Thus, these data imply that the mechanisms regulating hepatic NK cell responses to MCMV differ from those in splenic and pulmonary infection. Indeed, previous studies have shown that splenic NK cells provide antiviral immunity in a perforin-dependent manner whereas in the liver, the production of IFNγ by NK cells is critical for antiviral protection (170, 190). Furthermore, during acute infection, the NK cell population in the liver does not undergo the same initial contraction as that observed in the lung and spleen (171, 172). Also, Vα14 iNKT cells are found in high numbers in the liver and participate in protective immunity to MCMV (191, 192). Although the numbers of Vα14 iNKT cells were not assessed in the liver during acute MCMV infection, based on hepatic virus load, I hypothesise that hepatic iNKT cell responses are unlikely to be regulated by IL-10.

In a separate study, Oakley *et al* (165) utilised IL-10-deficient mice to demonstrate that, in agreement with my findings, the absence of IL-10R signalling during MCMV infection led to more weight loss and severe disease. However, contrary to my experiments, they found that virus replication in the spleen in the IL-10 gene deficient mice was actually reduced in comparison to wt controls. Unfortunately, the absence of NK cell characterisation in this study precludes direct comparison with my own experiments. Furthermore, their analysis of virus load in the spleens of wt mice over 12 days of infection revealed comparable levels of replicating virus at days 3 and 12 p.i. This finding has never been observed in my model of infection where Ly49H$^+$ NK cell expansion rapidly controls the virus, thus levels of replicating virus in the spleen at day 12 are undetectable. Therefore, direct comparisons between the two studies are not possible. A separate study by Tang-Feldman *et al* (193) found that repletion of IL-10 into IL-10 knockout mice did not influence splenic or hepatic viral DNA load despite suppressing the exaggerated pro-inflammatory cytokine response observed in these mice. However, a comparison of virus load between wt and IL-10 knockout mice was not performed which would have allowed a more direct evaluation with my results. Despite the inability to directly compare the results of these two studies with my current findings, it is clear that subtle differences exist between the two systems of using either IL-10 gene deficient mice or antibody blockade of IL-10R. Importantly, however, my experimental approach of inhibiting IL-10R signalling prevents the possibility of developmental factors or compensatory mechanisms associated with gene-deficient mice that may influence results obtained from these experiments.

In summary, I have uncovered a surprising antiviral role for IL-10 during acute MCMV infection through the limitation of activation-induced NK cell death. These experiments highlight the importance of the balance between pro-inflammatory and inhibitory signals during acute viral infection and demonstrate that without sufficient regulation, an NK cell response can be driven to apoptosis, leading to impaired control of acute virus infection.

Chapter 4 - Generating HCMV virus constructs with modifications to cmvIL-10

4.1. Introduction

4.1.1. Functions of cmvIL-10

The long co-evolution of HCMV with its mammalian host has resulted in the virus developing an array of mechanisms to modulate host immune responses, as discussed in section 1.7.3. One such HCMV-encoded immune-modulatory protein is cmvIL-10, a homologue of human IL-10. The cmvIL-10 protein is encoded by an ORF (UL111A) composed of five exons and has two introns within the cmvIL-10 gene which match the position of the first and third introns of the IL-10 gene, suggesting that these genes are related (130). However it is unclear whether HCMV captured the partially spliced IL-10mRNA sequence from infected cells or captured the IL-10 gene, which subsequently evolved into the cmvIL-10 gene. Despite limited homology to human IL-10 (27%) it binds to IL-10R1 with essentially the same affinity as IL-10, and is capable of inducing signal transduction events characteristic of IL-10 signalling (130, 194).

One of the first studies demonstrating the biological activity of cmvIL-10 used recombinant protein expressed in either human cells or bacteria. Protein expressed in human cells profoundly inhibited proliferation of PBMCs, decreased production of pro-inflammatory cytokines from PBMC and monocyte cultures, and down-regulated monocyte surface expression of MHC class I and class II proteins. Bacterium-expressed cmvIL-10 reduced mitogen-stimulated proliferation of PBMCs comparable to that of human IL-10 (195). In addition, cmvIL-10 also decreased production of pro-inflammatory cytokines by PBMCs and monocytes, and decreased cell surface expression of both MHC class I and class II molecules (195).

Given the role for IL-10 in suppressing maturation and cytokine production of DCs (section 1.9.1), it was hypothesised that cmvIL-10 would also antagonise DC function. This was tested by incubating DCs with supernatants from cells infected with HCMV (AD169 strain) or infected with a UL111A-deletion variant of AD169. In the absence of cmvIL-10 containing supernatant, LPS-stimulated DCs progressed to maturity. In contrast, LPS-stimulated DCs cultured with AD169-conditioned media exhibited reduced maturation, decreased migration in response to the lymph node homing chemokine CCL19, and significantly impaired pro-inflammatory cytokine production (196). This inability to secrete cytokines, IL-12 in particular, is in part potentiated by the induction of endogenous cellular IL-10 expression by the DCs themselves (196). Moreover, cmvIL-10 inhibits inflammatory cytokine transcription, in particular TNFα and IL-1β, by blocking NFκB transcriptional activity in human monocytes (197).

Additional investigation into the effects of cmvIL-10 on DCs revealed that incubation with recombinant protein enhanced the density of the molecule DC-SIGN, which is a lectin expressed on the cell surface of immature DCs and functions as a receptor for several viruses including HCMV, thus enhancing HCMV-infection and possibly increasing dissemination (198). Furthermore, in the presence of recombinant cmvIL-10, LPS-induced up-regulation of both MHC class I and class II molecules was partially blocked, as was the enhancement of the co-stimulatory molecules CD40, CD80, CD86, B7-H1 and B7-DC, hence impairing DC function (198). CmvIL-10 also increases apoptosis associated with DC maturation by blocking up-regulation of anti-apoptotic molecules (198).

In addition to the potent anti-inflammatory functions that IL-10 exerts, it also plays a role in promoting the growth and differentiation of B cells (section 1.9.1). In accordance, incubation of human B cells with recombinant cmvIL-10 stimulated B cell proliferation and autocrine production of cellular IL-10 in a dose-dependent manner (199).

Intriguingly, UL111A expression is also detected in natural and experimental latent infection (200). This latency-associated cmvIL-10 transcript (LAcmvIL-10) was identified from the alternate splicing of the cmvIL-10 transcript and contains only the first of the two introns contained in the full length transcript of UL111A (131, 200). Subsequently, LAcmvIL-10 retains only some of the functional characteristics of the full length cmvIL-10. Unlike cmvIL-10, LAcmvIL-10 does not stimulate B cell proliferation (199), trigger phosphorylation of STAT3 or inhibit expression of co-stimulatory molecules or maturation markers on DCs (131). LAcmvIL-10 has the ability however to down-regulate MHC class II molecules on the surface of monocytes (131), and as monocytes support latent infection, HCMV may express LAcmvIL-10 to avoid immune recognition during this phase of infection. An AD169 virus with a deleted UL111A gene was used to demonstrate that MHC class II levels were increased significantly on latently infected myeloid progenitor cells, which was associated with an increase in PBMC and $CD4^+$ T cell responses against these cells as compared to wt-infected cells, suggesting that this gene provides an immune evasion strategy during latency (201). However, the conclusions of this study should be treated with caution due to the use of a highly mutated strain of HCMV (AD169) and also that the full length UL111A gene was deleted, therefore cmvIL-10 as well as LAcmvIL-10 would be deleted, thus the phenotype observed may not be dependent on the absence of LAcmvIL-10 alone.

Importantly, using a rhesus CMV (RhCMV) model of infection, which unlike other experimental models encodes a functional IL-10 homologue (rhcmvIL-10), Barry and colleagues demonstrated that infection with a rhcmvIL-10 deleted virus results in a greater macrophage infiltrate to the site of infection, increased DC accumulation in the draining lymph nodes, and enhanced both humoral responses and virus-specific T cell responses compared to infection with a wt virus (202). Furthermore, vaccination of rhesus macaques with a virus containing a mutated rhcmvIL-10 gene that could not bind to the IL-10R1 resulted in production of antibodies against wt rhcmvIL-10 that neutralised its biological

activity but did not cross-react with rhesus cellular IL-10 (203, 204). Thus, these studies demonstrated that targeting cmvIL-10 could aid in the design of vaccines or therapeutic strategies against HCMV infection, therefore an understanding of the functions of cmvIL-10 in a biologically relevant system is critical.

4.1.2. The role of the UL128-UL131A genes in HCMV infection

In early studies, MD-DCs were reported to be susceptible to infection with HCMV strains that had been propagated in endothelial cell cultures with an infection rate of ~80-90%, whereas the rate of infection with fibroblast-adapted HCMV strains was negligible (205). Based on experimental evidence from loss-of-function phenotypes in knockout mutants and natural variants, and the gain-of-function phenotypes by trans-complementation with individual genes, the UL128 gene locus of HCMV, which contains the UL128, UL130 and UL131A genes, was identified as being indispensible for both productive infection of endothelial cells and transmission to leukocytes (57). It was then documented that the same genetic determinants were also required for HCMV to productively infect DCs (206). Furthermore, the UL128-131A gene products are also essential for infection of monocytes, and that the UL128 protein in particular can block chemokine-driven migration and chemokine receptor internalisation (207).

Interestingly, two independent studies examining the coding sequences of the UL131A, UL130 and UL128 genes of HCMV among field isolates and low passage clinical isolates found them to be highly conserved, suggesting that all were essential for growth in endothelial cells and virus transfer to leukocytes (208, 209). Entry of HCMV into biologically relevant epithelial and endothelial cells involves endocytosis followed by low-pH-dependent fusion facilitated by the UL128, UL130 and UL131 gene products. These form complexes with the virion envelope glycoprotein gH/gL. Utilising knockout mutants lacking UL128, UL130 and UL131 proteins revealed that all three proteins must bind simultaneously to gH/gL for the production of complexes that can function to allow entry

into epithelial and endothelial cells (210). Therefore, a mutation in any one of the ORFs can abolish endothelial cell tropism. Hence, a single nucleotide insertion in UL131A exon 1 encoded by the highly passaged laboratory HCMV strain AD169 results in the inability of this virus to efficiently infect endothelial cells (57). Repair of this mutated gene restores the ability of AD169 to infect both epithelial and endothelial cells (211).

The broad cell tropism shown by clinical isolates of HCMV is lost during adaptation of the virus during propagation in fibroblasts *in vitro*; a result strongly associated with mutations in the UL128 locus. The gene products of UL128-131A have no apparent role for replication in fibroblasts. Indeed, there appears to be a selective advantage for HCMV to lose or inactivate these genes during replication and spread in this cell type (210). Furthermore, viruses with a mutation in the UL128 locus produced greater yields of infectious progeny than those with intact genes (56). Due to the genetically unstable nature of clinical isolates cultured in fibroblasts, it is therefore necessary to use caution when choosing and monitoring HCMV strains for experimental studies of vulnerable functions, particularly those involved in cell tropism (56).

4.1.3. Hypothesis

Studies of the function of cmvIL-10 have so far utilised either recombinant protein or strains of HCMV that contained mutations due to propagation in the laboratory. To date, our lab has been unable to reliably detect cmvIL-10 during productive infection using monoclonal antibodies, and at the time of starting these investigations, no good evidence showing that the protein is expressed by the virus had been published. Therefore I aimed to test the following hypothesis;

“CmvIL-10 protein is expressed during acute HCMV infection”

Furthermore, in chapter 3, I identified an important role for mammalian IL-10 during acute MCMV infection, and consequently, wanted to investigate if virally expressed IL-10 homologues may also have the potential to influence pathogenesis. However, MCMV does not express a viral IL-10 homologue and therefore this cannot be tested in the MCMV infection model. If cmvIL-10 protein is expressed during acute HCMV infection, the functions of cmvIL-10 during infection in biologically relevant cells can be tested. Therefore, utilising the Merlin BAC containing the almost fully intact HCMV genome, I also aimed to test the following hypothesis;

“CmvIL-10 suppresses anti-viral immune responses during acute HCMV infection”.

4.2. Results

4.2.1. Insertion of a selectable cassette at the end of the UL111A gene

In order to first visualise the expression of cmvIL-10 protein during infection, a gene encoding GFP was to be inserted at the C-terminus end of the UL111A gene. Further, to assess the immune suppressive effects of cmvIL-10, a UL111A knockout mutant would be generated. To assess expression and function of UL111A during infection of biologically relevant cells, modified viruses would require an intact UL128 locus to enable infection of endothelial and epithelial cells, and MD-DCs. Thus, a BAC containing almost the full-length genome of the low passage HCMV strain Merlin was utilised (58). This BAC (pAL1120) is a self-exercising Merlin BAC containing a gene encoding Cre recombinase. This version of Cre has a synthetic intron to prevent expression in *E. Coli*, but upon transfection into mammalian cells, Cre recombinase is expressed and mediates removal of the BAC vector by recombination between *loxP* sites engineered at the junctions with the virus genome (58) (see Fig 4.1A for visual representation). pAL1120 also has a fully intact UL128-131A region and contains only one mutation as compared to the Merlin clinical isolate, which is a frameshift in RL13. RL13 encodes a highly glycosylated protein located in the virion envelope and expression of this gene severely impairs HCMV replication in fibroblasts and epithelial cell cultures (58). Thus pAL1120 represents the best possible construct for the generation of modified viruses.

To create the modified viruses, the technique of recombineering was utilised. In the first round of recombineering, a selectable cassette was inserted at the C-terminus end of the UL111A gene of pAL1120 (see Fig 4.1B for visual representation). The selectable cassette encodes a gene for ampicillin resistance (positive selection), a sacB gene which confers susceptibility to sucrose (negative selection), and a lacZ gene encoding β-galactosidase which causes bacteria to appear blue when grown in the presence of X-gal (colourogenic selection). The cassette was amplified with primers containing overlapping homology to both the cassette and the target site of insertion, i.e. the end of the UL111A

gene (section 2.16.1). The SW102 bacteria containing the HCMV genome have a defective phage expressing the lambda red genes which mediate homologous recombination between stretches of DNA. The bacteria were made competent and the amplified cassette was inserted by electroporation (section 2.16.2). The bacteria were grown on plates containing ampicillin, IPTG (an inducer of the lacZ gene and necessary for galactosidase production) and X-gal (a modified galactose sugar). Correct insertion of the cassette resulted in the bacteria becoming resistant to ampicillin as well as appearing blue in colour after ~24 hours (Fig. 4.2A). In the second round of recombineering, the sacB gene would be selected against, consequently it was important to check that the sacB was functional, as PCR errors that prevent it from working properly occur in ~25% of colonies. Therefore, 4 blue colonies were streaked onto plates containing ampicillin and onto plates containing sucrose (Fig. 4.2B). Three of the 4 colonies picked were inhibited on the sucrose plates, thus representing bacteria containing a fully functional sacB gene (colonies A-C were inhibited but D was only partially inhibited, see Fig. 4.2B). DNA from these 3 colonies was then extracted and restriction digest was performed with the restriction endonucleases *Bam*HI and *Hind*-III (section 2.16.3). Recognisable restriction endonuclease cleavage patterns for the Merlin BAC were observed (Fig. 4.2C). To test that recombination had occurred in the correct place with no errors, a sequencing PCR reaction was performed and the subsequent PCR product was sequenced (section 2.16.3). The 80 base pairs at either end of the cassette were checked to ensure no errors had been introduced during recombination. This new BAC containing the sacB cassette at the end of UL111A was designated the number pAL1307.

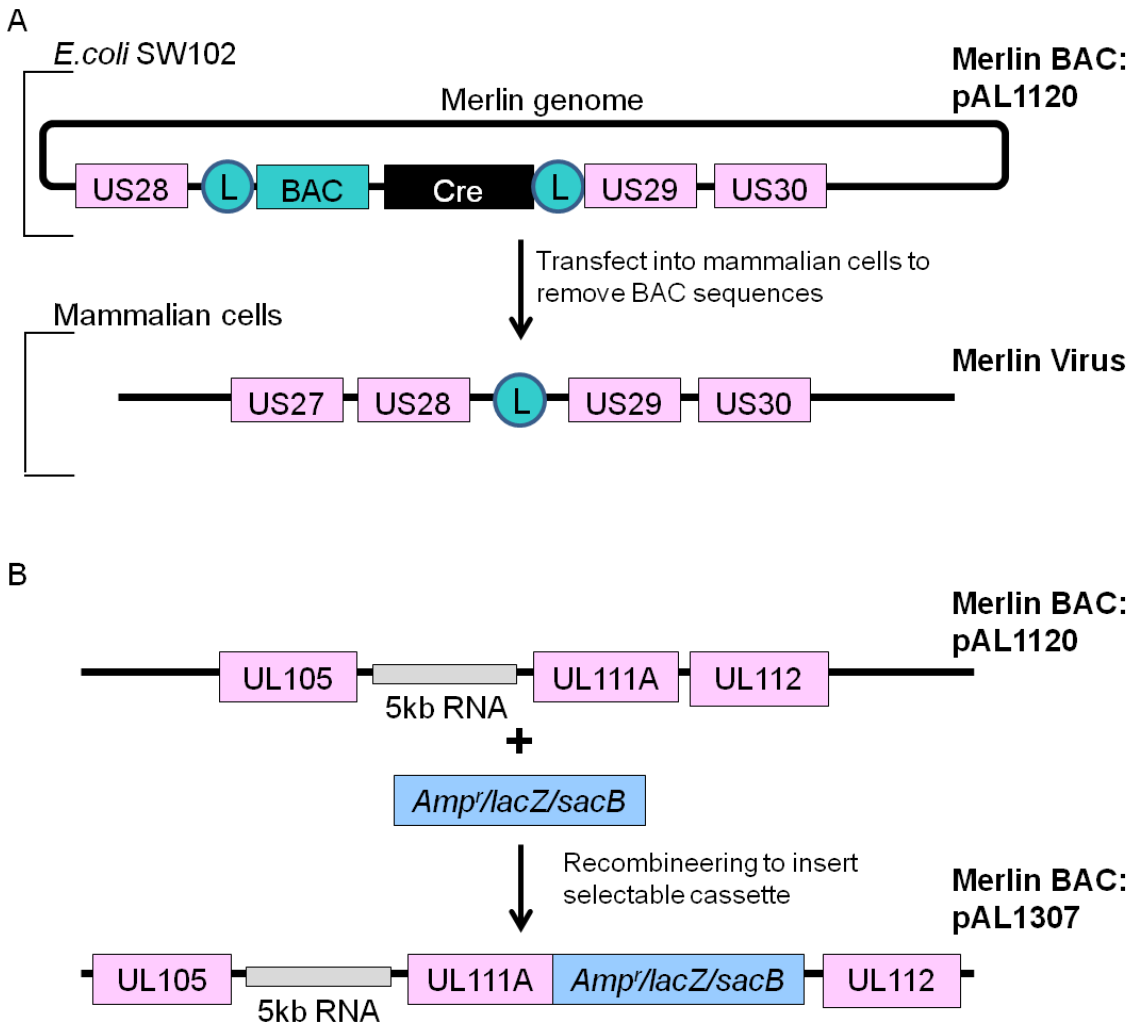

Figure 4.1. Diagramatic representation of the HCMV Merlin BAC and insertion of a selectable cassette through recombineering
(A) Diagram of the Merlin BAC (pAL1120) showing approximate insertion site of the BAC vector. Pink boxes indicate protein-coding regions, blue circles denote *loxP* sites, the blue BAC box represents pBeloBAC11 (see section 2.16, Fig. 2.1), and the black Cre box represents a Cre recombinase gene containing a synthetic intron. (B) Diagram of the selectable cassette containing genes for ampicillin resistance, lacZ and SacB inserted at the C-terminus of the UL111A via recombineering.

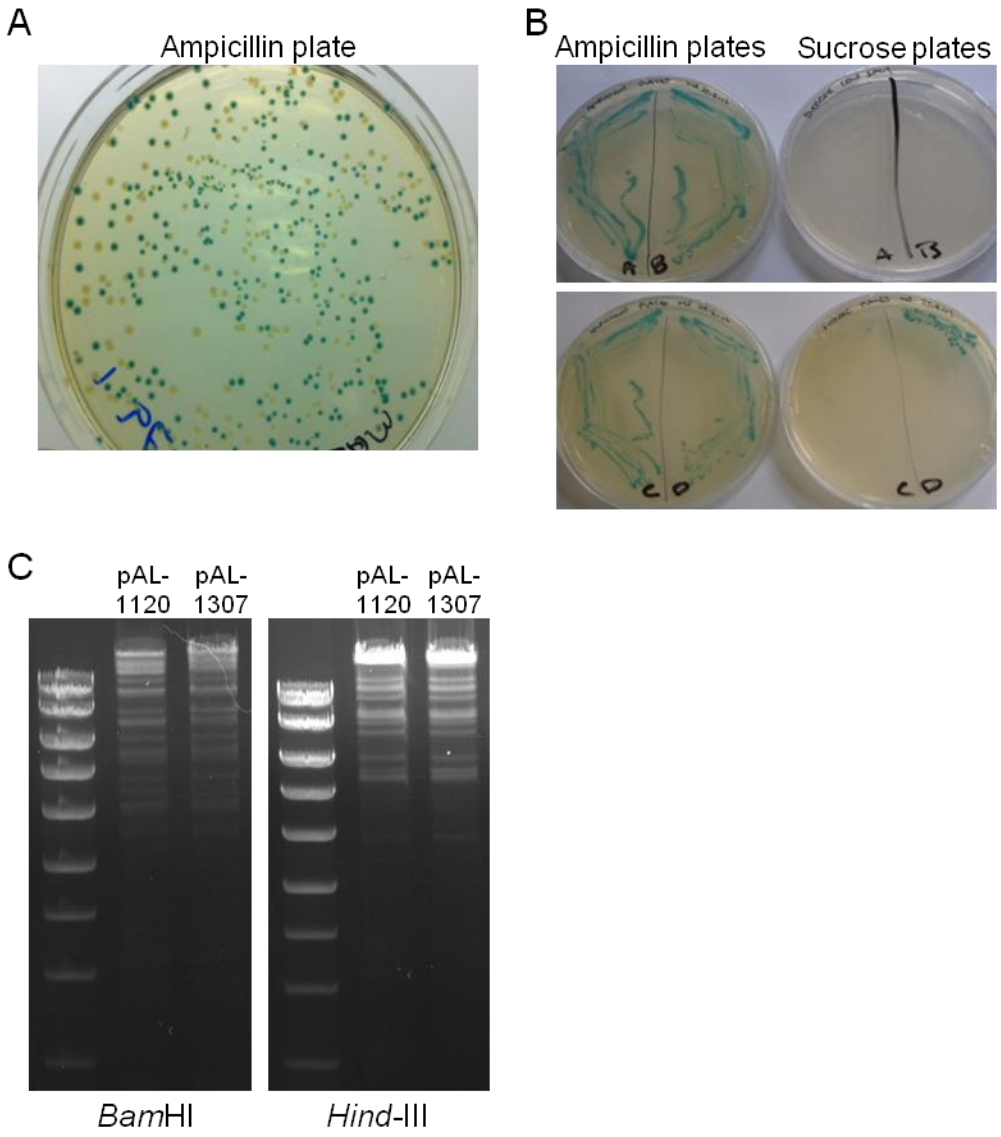

Figure 4.2. Recombineering of a Merlin BAC
(A and B) Positive, negative and colourogenic selection. Recombineering was used to insert a selectable cassette encoding genes for ampicillin resistance, sucrose susceptibility and lacZ at the end of the UL111A gene of the Merlin BAC, pAL1120. (A) Recombineered SW102 bacteria were grown on plates containing ampicillin for 24 hours. (B) To check for correct insertion of the cassette by inhibition of growth by sucrose, 4 blue colonies were picked and grown on 2 separate plates containing either ampicillin (left-hand plates) or sucrose (right-hand plates). (C) Restriction endonuclease profiles of DNA from pAL1120 and pAL1307 (Merlin UL111A_selection cassette).

4.2.2. Generation of new viruses with modifications in the UL111A gene

A second round of recombineering was performed to create 3 new viruses from pAL1307 with modifications to the UL111A gene: a UL111A knockout virus (MerlinΔUL111A), a virus encoding GFP at the end of the UL111A gene (Merlin UL111A_GFP) to enable visualisation of cmvIL-10 expression, and a virus construct in which the UL111A gene was replaced with a gene encoding GFP (MerlinΔUL111A/GFP), thus representing a control for GFP expression and the absence of UL111A. These modified constructs are visually represented in Fig 4.3A.

To delete UL111A, an oligonucleotide with regions of homology flanking UL111A and the sacB cassette was electroporated into pAL1307, thus removing both the UL111A gene and the sacB cassette. To insert GFP into the place of UL111A for generation of the MerlinΔUL111A/GFP construct, GFP-encoding DNA amplified with arms of homology flanking both UL111A and the sacB cassette was electroporated into pAL1307, thus removing both UL111A and the sacB cassette, leaving GFP in this region. To insert GFP at the C-terminus end of UL111A (for generation of Merlin UL111A_GFP), GFP-encoding DNA amplified with arms of homology flanking the sacB cassette was electroporated into pAL1307, thus replacing the cassette with GFP.

After electroporation and recovery, bacteria were grown on sucrose plates. If the selectable cassette had been removed and/or replaced, bacteria would no longer be sensitive to sucrose and would appear white instead of blue. DNA from 4 of these white colonies was then extracted, restriction endonuclease digests performed (Fig. 4.3B), and the deleted/inserted sequences were PCR-amplified, sequenced and analysed to make sure no errors had been introduced. These new Merlin BACs were designated the numbers pAL1308 (MerlinΔUL111A), pAL1309 (MerlinΔUL111A/GFP) and pAL1310 (Merlin UL111A_GFP).

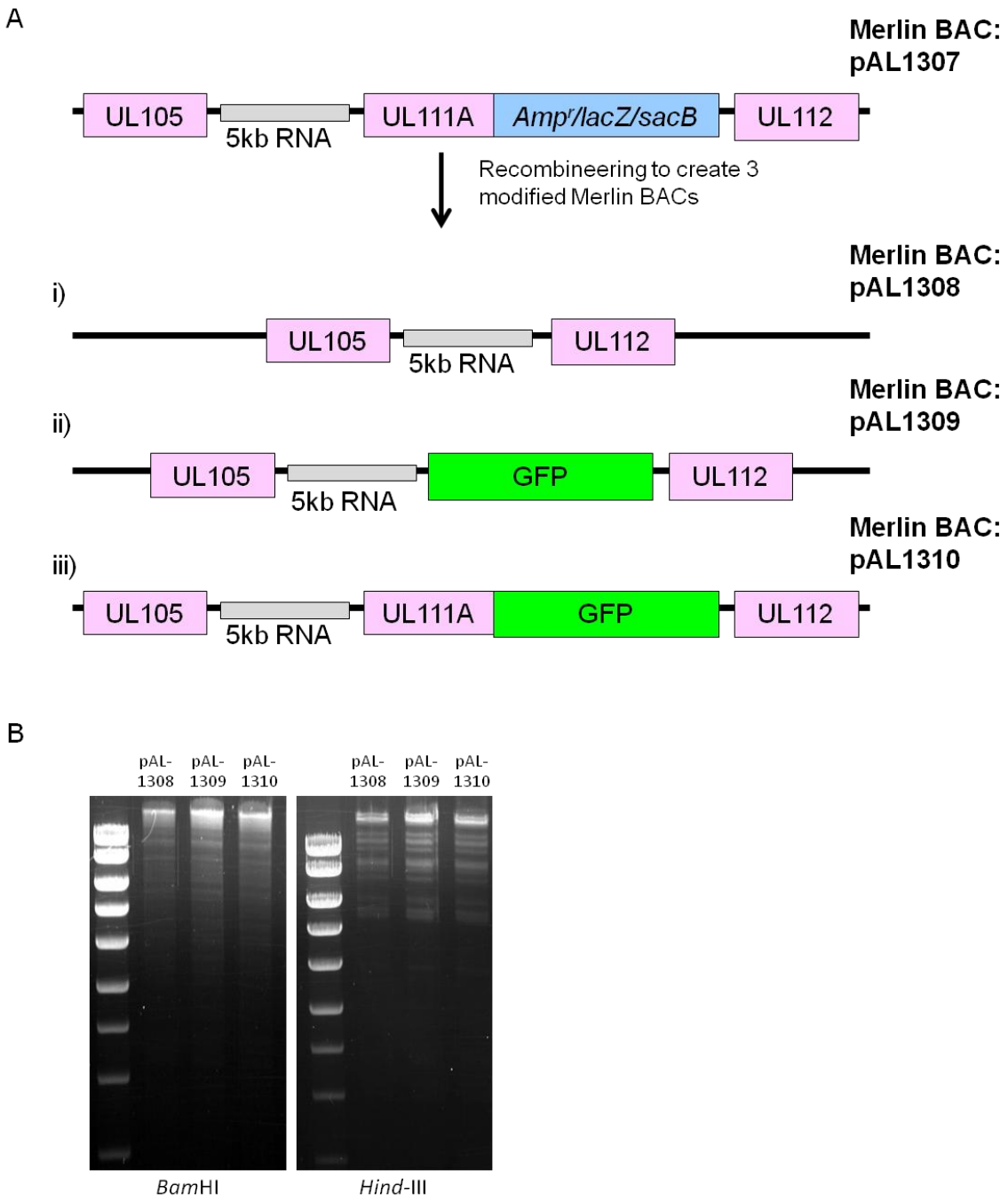

Figure 4.3. Generation of modified Merlin BACs through recombineering
(A) Diagramatic representation of the Merlin BAC pAL1120 before recombineering and the 3 new modified Merlin BACs after recombineering (pAL1308 (MerlinΔUL111A), pAL1309 (MerlinΔUL111A/GFP) and pAL1310 (Merlin UL111A_GFP)). (B) Restriction endonuclease profiles of DNA from pAL1308, pAL1309 and pAL1310.

4.2.3. Transfection of viruses into ARPE-19 cells

As previously discussed, the UL128 locus of HCMV mutates relatively rapidly when propagated in fibroblasts but remains intact when cultured in epithelial or endothelial cells. Therefore, DNA derived from the newly generated Merlin BACs was transfected into the human retinal pigment epithelial cell line ARPE-19 in order to preserve the intact HCMV genome. Once plaques appeared, cells were trypsinised and re-propagated in order to increase virus spread via cell-to-cell contact. After re-propagation, infected cells were analysed for GFP expression (Fig. 4.4). GFP was observed in the cells transfected with Merlin UL111A_GFP (Merlin 1310) (Fig. 4.4E and F). Interestingly, under the same magnification and exposure time, GFP expression could hardly be detected in cells transfected with MerlinΔUL111A/GFP (Merlin 1309) under x10 magnification (Fig. 4.4C) and expression was only detected very weakly under x40 magnification (Fig. 4.4D). No GFP was seen in cells transfected with MerlinΔUL111A (Merlin 1308) (Fig. 4.4A and B) as the GFP gene was not inserted into this virus, and this therefore served as a negative control. In cells infected with both Merlin 1309 and Merlin 1310, the GFP expression appeared to be diffused throughout the cells.

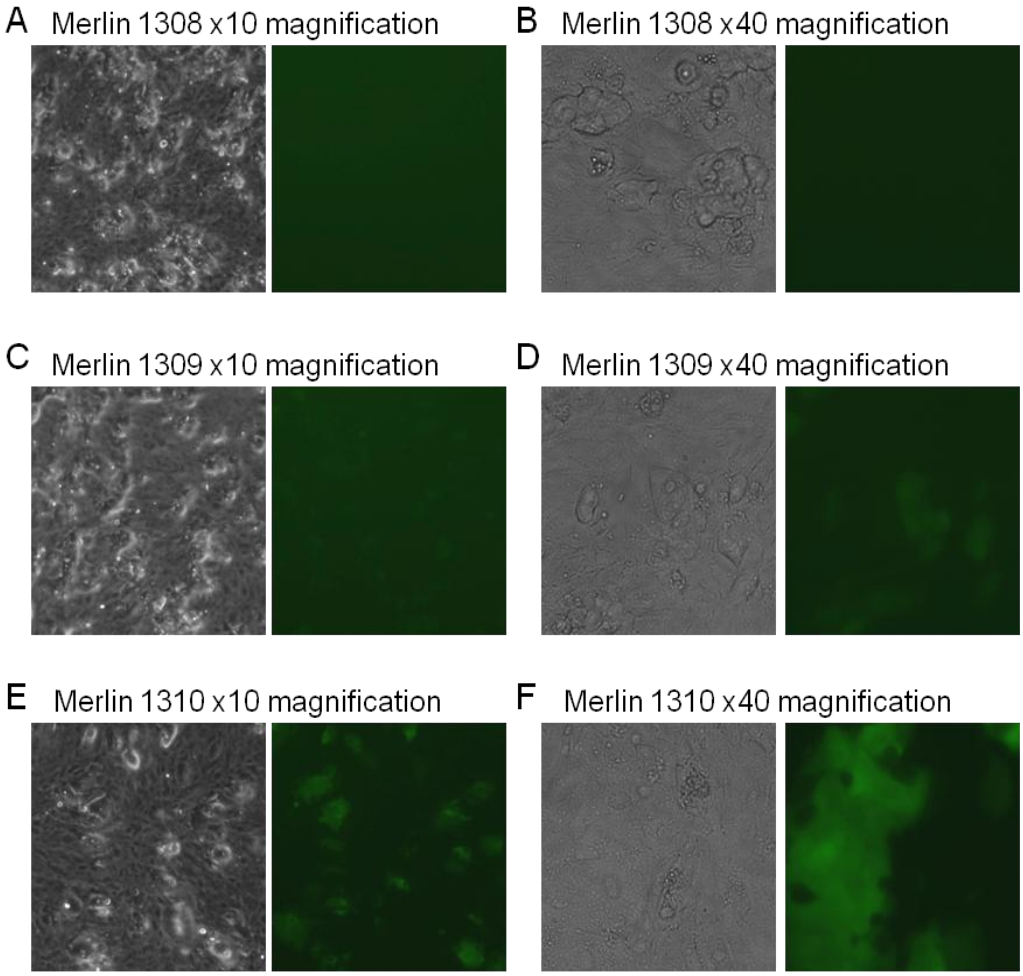

Figure 4.4. Growth of BAC-derived viruses in ARPE-19 cells
DNA from pAL1308 (A and B), pAL1309 (C and D) and pAL1310 (E and F) Merlin BACs was transfected into ARPE-19 cells. After the appearance of plaques, cells were trypsinised and re-propagated to enhance virus spread via cell-to-cell contact. Images show infected cells under light microscopy (left-hand images) and under fluorescence microscopy (right-hand images) to analyse GFP expression. Infected cells were analysed under x10 magnification (A, C and E) and x40 magnification (B, D and F).

4.2.4. Utilising GFP to visualise cmvIL-10 expression during infection

The production of each virus was initially scaled up by propagation in HFFs grown in 6 x T175 flasks. To minimise the chance of mutations occurring in the UL128, UL130 or UL131A genes due to growth in fibroblasts, virus propagation in HFFs was kept to just two passages in order to keep the number of rounds of replications to a minimum. Since the intact UL128 locus in these viruses limits cell-to-cell transmission in fibroblasts, growth was very slow and yields were extremely low (for example, from 6 x T175 flasks, titres varied from as low as 2 x 10^5 PFU/ml to maximum titres of 1.2 x 10^6 PFU/ml of highly concentrated stock of no more than 3mls total volume). Once a virus stock was generated, a time course of infection was performed to determine growth kinetics and temporal control of expression from the UL111A promoter. HFFs were mock-infected, or infected with Merlin 1120, Merlin 1308, Merlin 1309 and Merlin 1310 at an MOI of 3.

At 24 hours, infected cells (Fig. 4.5B-E) began to look rounded as compared to mock infected control (Fig. 4.5A), but expression of GFP could not be detected at this early time point in cells infected with Merlin 1309 (Fig. 4.5D) and Merlin 1310 (Fig. 4.5E). At 72 hours p.i (Fig. 4.6), GFP expression could be seen, with more robust expression in cells infected with Merlin 1310 (Fig. 4.6E) than Merlin 1309 (Fig. 4.6D). The reason for Merlin 1310 showing far greater intensity of GFP expression than Merlin 1309 is unclear although this differential was also observed in ARPE-19 cells (Fig. 4.4). By 144 hours p.i (Fig. 4.7), intensity of GFP expression was even further enhanced in cells infected with Merlin 1310 (Fig. 4.7E), therefore these data provide evidence that cmvIL-10 is expressed during productive infection. GFP expression was again diffuse throughout the cells, the same expression pattern that was observed in the ARPE-19 infections (Fig. 4.4). There is a chance that proteases could have cleaved and released GFP and therefore it was important to establish by western blot if the observed GFP expression was a reliable representation of cmvIL-10 protein expression and intracellular localisation.

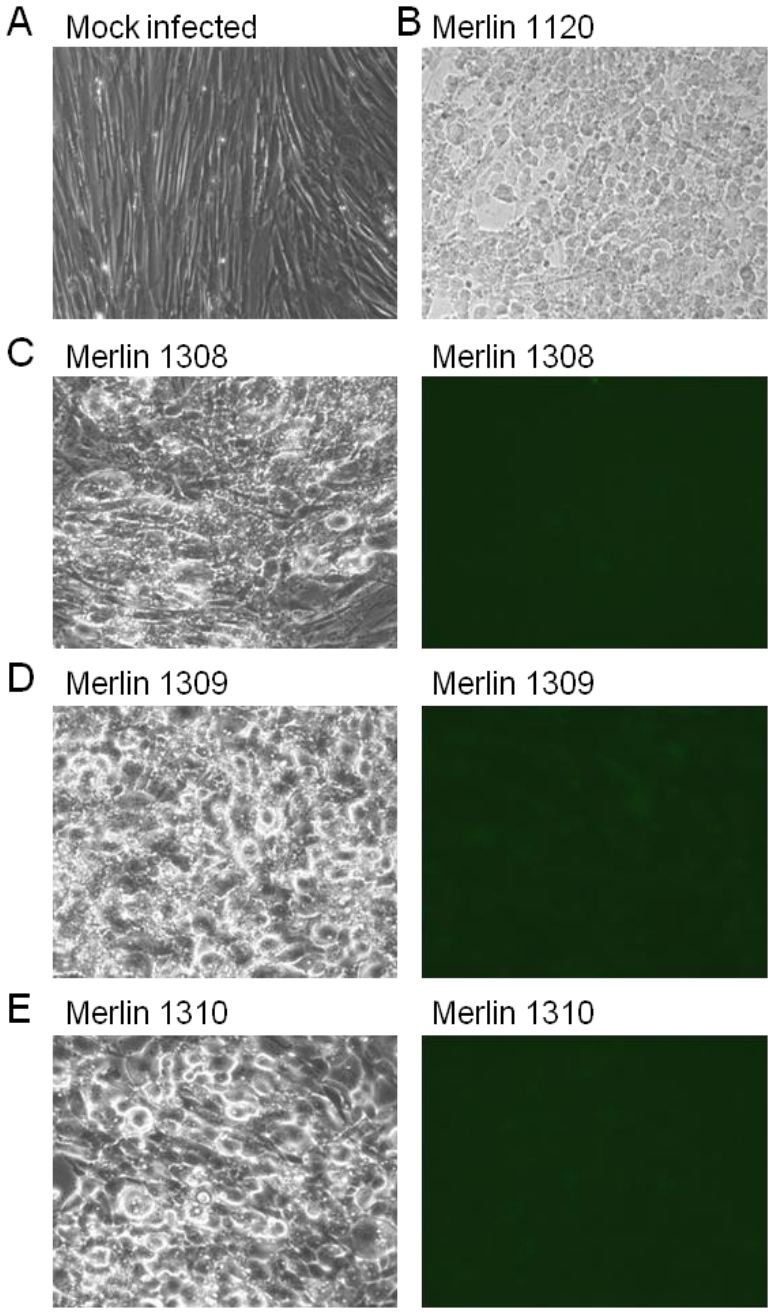

Figure 4.5. HFF cells 24 hours post-infection with Merlin BAC-derived viruses
HFF cells were infected with BAC-derived viruses at an MOI of 3 and examined for infection and GFP expression after 24 hours. (A and B) Light microscopy images of mock-infected cells (A) and cells infected with Merlin 1120 (B). (C-E) Light microscopy images (left-hand pictures) and fluorescence images (right-hand pictures) of cells infected with Merlin1308 (C), Merlin 1309 (D) and Merlin 1310 (E) under x25 magnification.

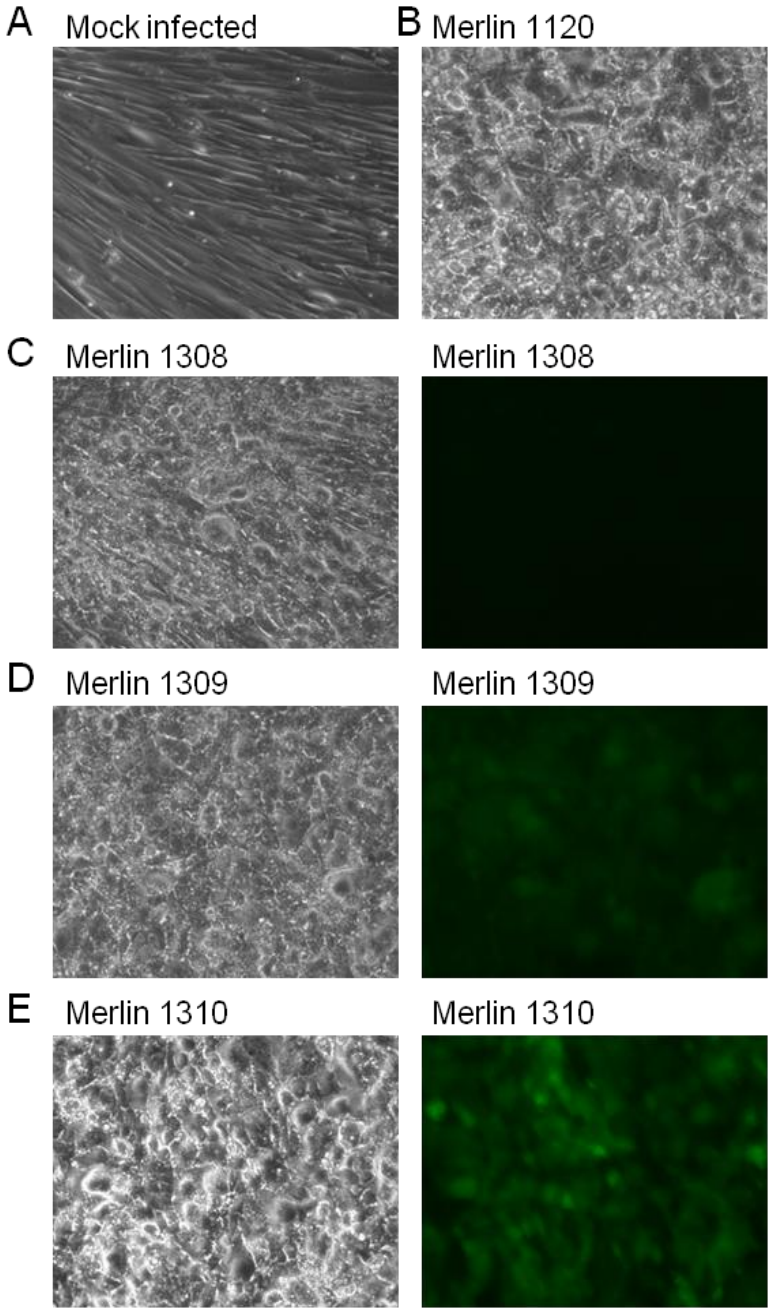

Figure 4.6. HFF cells 72 hours post-infection with Merlin BAC-derived viruses
HFF cells were infected with BAC-derived viruses at an MOI of 3 and examined for infection and GFP expression after 72 hours. (A and B) Light microscopy images of mock-infected cells (A) and cells infected with Merlin 1120 (B). (C-E) Light microscopy images (left-hand pictures) and fluorescence images (right-hand pictures) of cells infected with Merlin1308 (C), Merlin 1309 (D) and Merlin 1310 (E) under x25 magnification.

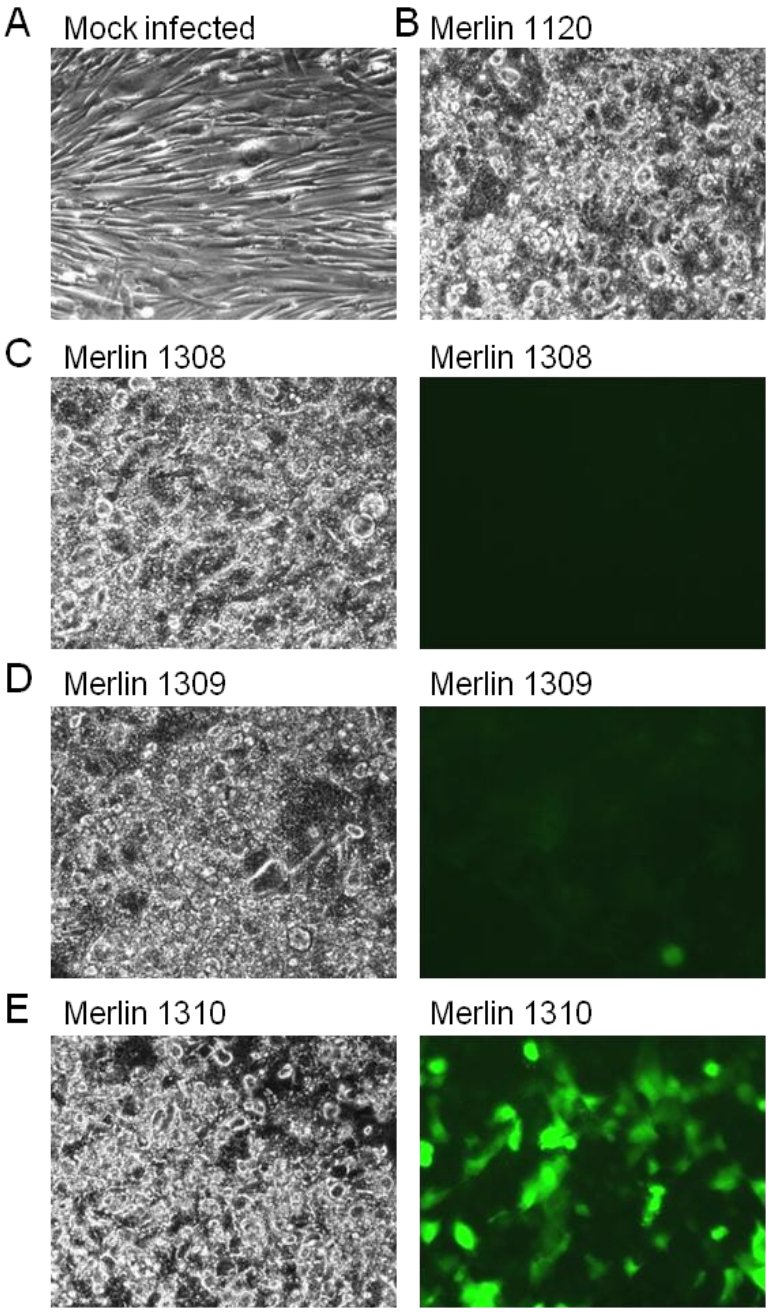

Figure 4.7. HFF cells 144 hours post-infection with Merlin BAC-derived viruses
HFF cells were infected with BAC-derived viruses at an MOI of 3 and examined for infection and GFP expression after 144 hours. (A and B) Light microscopy images of mock-infected cells (A) and cells infected with Merlin 1120 (B). (C-E) Light microscopy images (left-hand pictures) and fluorescence images (right-hand pictures) of cells infected with Merlin1308 (C), Merlin 1309 (D) and Merlin 1310 (E) under x25 magnification.

4.2.5. Detection of cmvIL-10 protein and GFP during infection

The result obtained with the GFP construct provided both confidence that the IL-10 promoter was functional and evidence that a cmvIL-10 fusion construct was being expressed. The generation of deletion mutants also made it possible to test for the expression of cmvIL-10 from the virus with a relevant control that would distinguish non-specific binding. In western blot experiments, cmvIL-10 protein was not detected at the early time point of 24 hours p.i, but was present in lysates from cells infected with the wt Merlin 1120 at 72 hours and 144 hours p.i (Fig. 4.8A). In agreement with the lack of GFP expression observed in cells infected with Merlin 1309 and Merlin 1310 at 24 hours p.i (Fig. 4.5), GFP was not detected by western blot at this time point (Fig. 4.8B). Also in agreement with the expression of GFP shown in Fig. 4.6 and Fig. 4.7, GFP was detected in lysates from cells infected with Merlin 1309 and Merlin 1310 at 72 hours and 144 hours p.i, with intensity of GFP expression greatest 144 hours p.i (Fig. 4.8B). Intriguingly, cmvIL-10 protein could not be detected at any time point in the lysates from cells infected with Merlin 1310, either in isolation or as a fusion protein with GFP (the fusion protein having a predicted size of 42-45k Daltons) (Fig. 4.8A and B).

These initial experiments revealed that the cmvIL-10_GFP virus Merlin 1310 expressed GFP during infection but as the cmvIL-10_GFP fusion protein could not be detected, GFP expression in this virus could not be used as a reliable read out for cmvIL-10 protein, as was initially planned. Due to the large amounts of time taken to grow enough virus to perform assays with, it was not feasible to repeat this finding or resolve this issue in the available time.

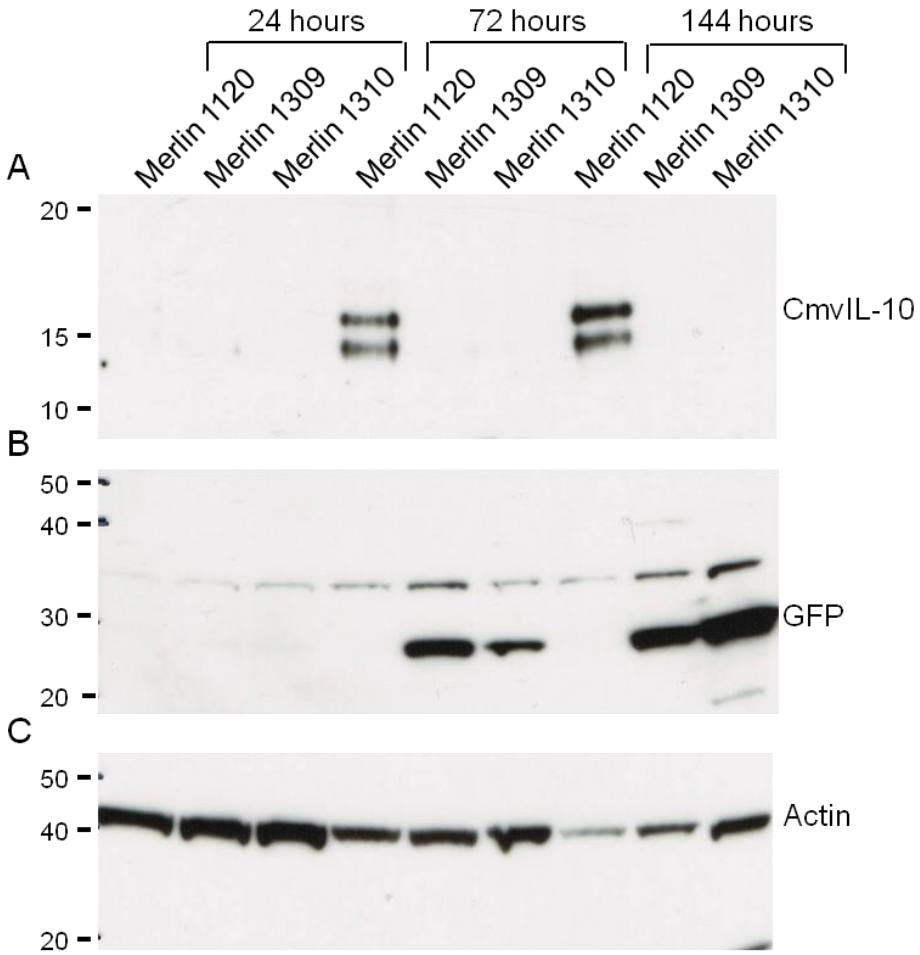

Figure 4.8. Detection of cmvIL-10 protein and GFP during infection with modified Merlin viruses

HFF cells were infected with BAC-derived viruses at an MOI of 3 and cells collected at 24 hours, 72 hours and 144 hours p.i. Lysates were prepared and examined for cmvIL-10 protein expression (A), GFP expression (B) and actin expression (C).

4.2.6. Infection of DCs with a modified Merlin strain of HCMV

To enable utilisation of the UL111A knockout virus to elucidate the functions of cmvIL-10 in infections, the issue of very low virus yields needed to be addressed. The strains of HCMV TB40/E and FIX are remarkable in apparently being relatively stable endothelial and epithelial cell tropic. While the Merlin 1308, 1309 and 1310 viruses were being generated and characterised in the above experiments, Dr Richard Stanton developed two new Merlin-BAC vectors in which the complete endogenous UL128 locus was replaced with the equivalent region from TB40/E-BAC4 (pAL1477-2) or strain FIX (pAL1477-3). I hypothesised that viruses derived from these modified BACs may resolve the issue of low virus yields from virus propagation in fibroblasts, yet still enable infection of different cell types, including DCs. It was necessary to first establish whether Merlin 1477-2 and Merlin 1477-3 were capable of infecting DCs.

MD-DCs were generated according to the protocol described in section 2.21. MD-DCs were then infected at an MOI of 30 with Merlin 1477-2, Merlin 1477-3 and a TB40/E positive control virus. All 3 viruses contained an IRES-GFP at the end of the IE2 gene and therefore GFP expression was utilised to differentiate between infected and non-infected cells. After 3 days, MD-DCs were harvested and analysed for GFP expression by flow cytometry. To assess the efficiency of infection, gates were drawn around the GFP positive cells. Infection with the TB40/E virus resulted in ~66% of the MD-DCs becoming infected, Merlin 1477-2 infected ~19% of DCs and Merlin 1477-3 infected ~56% of cells (Fig. 4.9). This experiment demonstrated that MD-DCs could indeed be infected with these modified Merlin viruses.

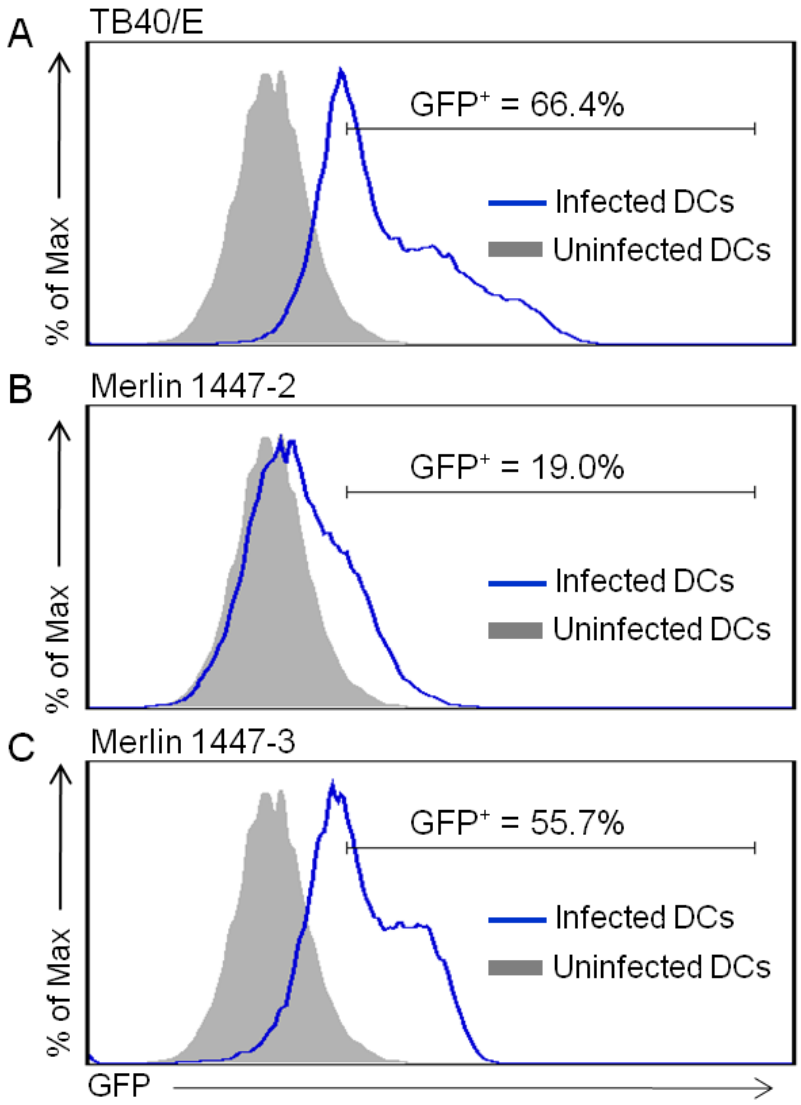

Figure 4.9. Infection of monocyte-derived DCs with TB40/E and modified Merlin strains of HCMV

Representative overlay histograms of GFP expression (blue solid line) within MD-DCs infected at an MOI of 30 with TB40/E (A), Merlin 1477-2 (B) or Merlin 1477-3 (C) at 3 days p.i. Shaded histograms represent uninfected MD-DCs.

4.3. Discussion

The aims of the experiments in this chapter were to visualise cmvIL-10 protein during productive HCMV infection as well as to elucidate a possible role for viral IL-10 during infection of biologically relevant cells. This would enable comparisons to be made between the roles of mammalian IL-10 in acute MCMV infection which were uncovered in chapter 3, with the role of cmvIL-10 in HCMV infection.

To address the first aim, a Merlin virus that encoded GFP at the end of the UL1111A gene, which would be expressed as a fusion protein with cmvIL-10, was constructed in order to track expression of this protein during infection of biologically relevant cells. This virus was successfully created and GFP expression was observed during productive infection of both ARPE-19 and HFF cells. Further analysis by western blot of these infected cells revealed that although GFP expression could be detected throughout a 144 hour period of infection, the GFP_cmvIL-10 fusion protein could not. However, during infection of cells with the wt virus, cmvIL-10 protein was detected. It is likely that the fusion protein is being expressed but cmvIL-10 does not survive, and possible explanations for this are that the GFP was being cleaved from the fusion protein, or that cmvIL-10 is subject to post-transcriptional regulation and the presence of a large protein at the C-terminus of the UL111A gene might alter the mechanisms for this regulation, or that the GFP is being picked up from an endogenous promoter, hence the high expression observed. If this was the case, the fusion protein should also be expressed, but I did not find evidence of this in the lysates of infected cells. However, there is also a strong possibility that the protein is secreted and therefore it would not be detected in cell lysates. The supernatants from these infections were analysed for protein expression by western blot but no protein was detected. This was only attempted once and it is possible that by repeating this experiment and improving the supernatant concentrating process, that the cmvIL-10_GFP fusion protein may be detected from supernatants. Unfortunately, due to the limitation of low virus yields, detailed investigation may be problematical.

A second aim of this chapter was to create a UL111A knockout virus that otherwise contained the full length HCMV genome (other than the mutated RL13), including the fully intact UL128 locus to allow infection of biologically relevant cells including epithelial and endothelial cells as well as DCs, with the aim to further elucidate the functions of cmvIL-10 and compare this to the roles found for mammalian IL-10 during acute MCMV infection. This virus was also successfully created, however the issue of low virus yields again caused significant limitations. It had been previously demonstrated in initial studies that the Merlin virus with no mutations in the UL128 gene locus produced much smaller plaques, had restricted cell-to-cell transmission and resulted in clear reductions in the levels of infectious virus released into the supernatant as compared to the Merlin virus containing mutations in this gene region (58). However, from these initial studies the extent to which virus yields were reduced were not apparent and consequently the large time scales needed to generate enough usable virus were overlooked. Therefore, due to the time constraints of my studies, it was decided that the time and effort required to obtain usable titres of these viruses was no longer feasible; therefore the investigations with this virus were halted.

To prevent a similar problem in future investigations, a slightly modified approach is proposed. This would involve using modified Merlin viruses containing the UL128 locus from either a TB40/E virus or an HCMV clinical isolate VR1814 as described in section 4.2.6, thus making these viruses permissive to DCs and epithelial and endothelial cells (212, 213). These viruses could then be modified by recombineering to make a UL111A knockout virus. A knockout virus from the TB40/E strain was not created due to the possibility that more than one virus was involved in the derivation of TB40/E, and therefore caution against its use as a general laboratory strain, especially when making correlations between phenotypes is essential (55). Before knocking out UL111A from either of these viruses, it was critical to establish that they were capable of infecting MD-DCs; therefore both were tested alongside the TB40/E virus. Incubation with the

TB40/E virus resulted in approximately two thirds of the DCs becoming infected. Merlin 1477-2 and Merlin 1477-3 viruses were also successful at infecting DCs, however Merlin 1477-3 reached a much higher percentage of infected cells than Merlin 1477-2. By optimising the infection technique by increasing the MOI and/or by using centrifugation to aid virus entry, it is likely that this infection rate could be increased further. However, time constraints unfortunately meant that I could not explore this possibility further. Nevertheless, for future studies to elucidate HCMV gene functions that might require a deletion mutant, such as a UL111A knockout virus, the above approach appears to provide a virus which is both permissive to DCs and other biologically relevant cell types, and also contains a near complete wt HCMV genome which is far more clinically relevant than any other laboratory strains used to date.

Determining the functions of cmvIL-10 during acute and latent infection still represents an important area of research, as exploitation of immune inhibitory receptors such as the IL-10R are important targets for herpesviruses in dampening down antiviral immune responses and establishing latency within the host. Consequently, virus-encoded proteins that manipulate these receptors, such as cmvIL-10, represent possible therapeutic targets by promoting antiviral responses. As discussed in section 4.1.1, studies demonstrating rhcmvIL-10 as a viable vaccine candidate because of its high immunogenicity during natural infection combined with the lack of cross-reactivity with rhesus cellular IL-10 (203, 204) reveal the possible usefulness of targeting UL111A to improve immune responses to HCMV. Importantly, the relatively low sequence homology between human IL-10 and cmvIL-10 is also critical in offering the potential of targeting UL111A in a vaccine setting without affecting endogenous IL-10. Enhancing our current understanding of not only the initial effects cmvIL-10 has in dampening antiviral immune responses during acute infection but also how it shapes the long-term virus-host balance will be critical in facilitating the development of both prophylactic and therapeutic strategies.

Chapter 5 - Investigating the immune protective role of IL-22 during acute MCMV infection

5.1. Introduction

5.1.1. The role of IL-22 in viral infections

IL-22 plays an important role in host defence, inflammation and tissue repair, as discussed in chapter 1.10.1 and reviewed by Sonnerburg *et al* (135). However, the importance of IL-22 in viral infections has been less well explored. One of the first studies that linked IL-22 with viral infections showed that repeatedly HIV-1 exposed, uninfected individuals had up-regulated levels of T cell-derived IL-22 in their serum and cell supernatants, suggesting IL-22 and the subsequent acute-phase protein pathway it induces is associated with host resistance to HIV infection (214). Furthermore, Indian patients infected with HIV-1 subtype C were found to have high levels of systemic IL-22, along with IL-10 and C-reactive protein, and this was associated with low viral replication *in vitro* (215). In mice, IL-22 exerts a protective function in LCMV infection; IL-7 driven induction of IL-22 provides cytoprotection in the liver as shown by enhanced hepatitis following IL-22 neutralisation (216). Conversely, a study analysing the role of IL-22 in human HCV infection found that despite an up-regulation of hepatic IL-22 during infection, IL-22 did not directly regulate antiviral proteins and had no effect on HCV replication (217). A similar finding was observed in hepatitis B virus (HBV) infection. In HBV transgenic mice, IL-22 increased the expression of pro-inflammatory genes and reduced the severity of liver damage, but did not directly inhibit virus replication (218). In humans, patients with acute and chronic HBV infection have a significant increase in the concentration of serum IL-22, and the authors speculated that the increase in IL-22 levels provides protection against liver inflammation and fibrosis during HBV infection (218, 219). The role of IL-22 during primary influenza infection in mice has also been investigated. Anti-IL-22 neutralisation *in vivo* did not dramatically affect weight loss and survival and surprisingly, mice treated with anti-IL-22 actually showed a moderate

reduction in viral titres in the lung and trachea (220). Furthermore, IL-22 protects influenza infected airway epithelial cells from death *in vitro*, but has no effect on viral replication (221). Collectively, these data demonstrate that the effect of IL-22 during viral infections is unclear and appears to be pathogen-dependent, especially when assessing the effects that IL-22 has on control of virus replication. However, the majority of studies to date suggest IL-22 provides varying degrees of protection against virus-driven immune pathology, especially by those pathogens that cause liver damage.

5.1.2 Hypothesis

The IL-10 family of cytokines are critical in host defence against various pathogens. Type III IFNs (IL-28A, IL-28B and IL-29) preferentially promote antiviral responses and co-operate with type I IFNs to aid viral clearance, and the IL-20 subfamily of cytokines, including IL-22, provide critical protection against bacterial and yeast infections (reviewed in (100)). However, a clearer understanding of the role that IL-22 plays in virus infections *in vivo* is required. Thus, I utilised a neutralising anti-IL-22 antibody during acute MCMV infection to test the following hypothesis:

"IL-22 may provide protective immunity during acute MCMV infection".

5.2. Results

5.2.1. IL-22 is expressed in tissues of both naïve and MCMV-infected mice

To investigate the hypothesis that IL-22 plays a protective role in acute MCMV infection, I first analysed IL-22 expression during the first 4 days of infection. Homogenates from organs targeted by MCMV during early infection were taken at 2 and 4 days p.i, analysed for IL-22 protein expression and compared to levels found in homogenates from naïve control mice. IL-22 protein was detected in the lungs, livers and spleens of both naïve and infected mice (Fig. 5.1), with a significant increase in all three organs at day 4 p.i compared to uninfected mice.

In order to identify the source of IL-22 during MCMV infection, IL-22 staining for flow cytometry was first optimised. Lymphocytes were incubated with or without PMA, ionomycin and IL-23 for 4 hours. Cells were then stained for intracellular IL-22 (Fig. 5.2). Gates were set according to the FMO control (Fig. 5.2A). IL-22 positive cells increased approximately two fold when polyclonally stimulated compared to unstimulated cells (Fig. 5.2B and C); therefore this *ex vivo* stimulation technique was used to identify which cell populations were capable of expressing IL-22.

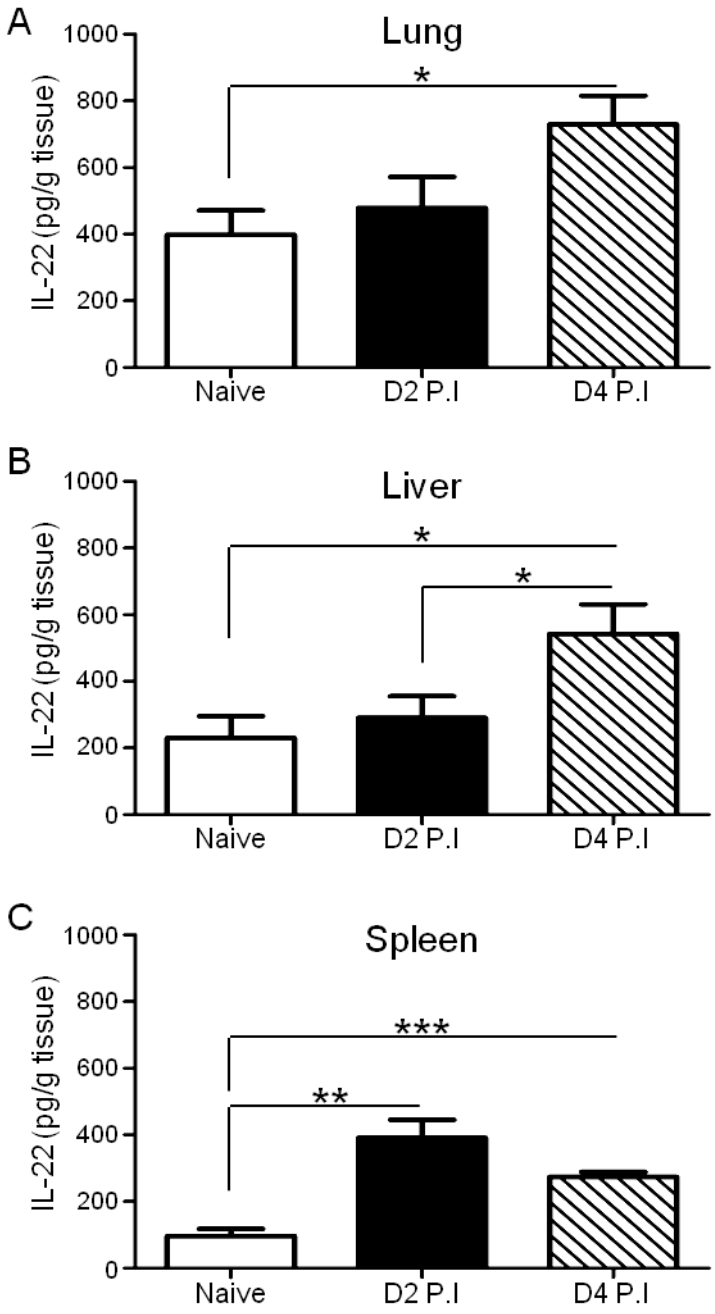

Figure 5.1. IL-22 expression in the lung, liver and spleen of naïve and MCMV-infected mice

IL-22 protein concentrations in lung, liver and spleen homogenates from naïve mice (open bars), MCMV-infected mice 2 days p.i (closed bars) and MCMV-infected mice infected 4 days p.i (cross hatched bars). Results show the mean ± SEM of 4-6 mice per group and represent 2 independent experiments. *p<0.05, **p<0.01, ***p<0.001

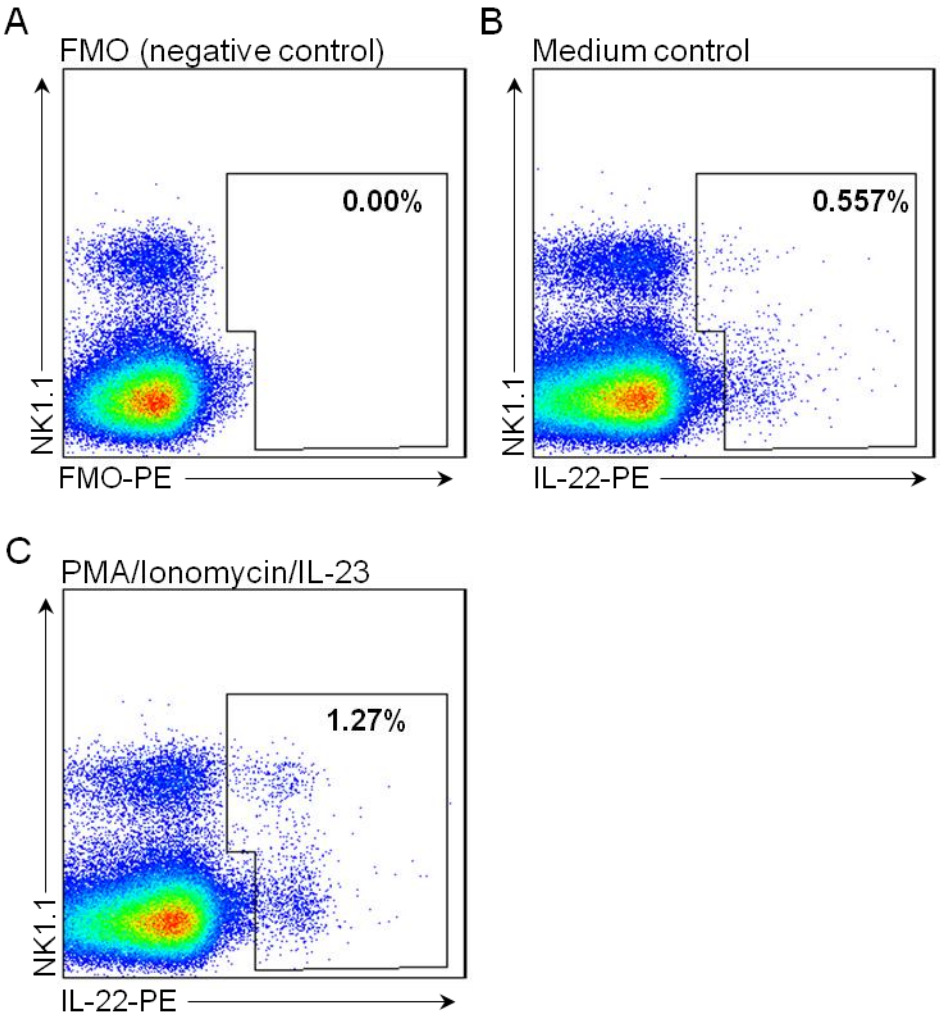

Figure 5.2. Analysis of intracellular IL-22 antibody staining by flow cytometry
Bivariate flow cytometry plots showing IL-22 expression by pulmonary lymphocytes from MCMV-infected mice 4 days p.i. Cells were incubated for 4 hours with medium alone or with PMA/Ionomycin and IL-23 in the presence of brefeldin A. Following surface staining, cells were stained for intracellular IL-22 production with anti-IL-22-PE. (A) FMO negative staining control was used to draw the IL-22 positive gate. (B) IL-22 expression with no *ex vivo* stimulation. (C) IL-22 expression following *ex vivo* stimulation.

Lymphocytes from the lung, liver and spleen from day 4 infected mice, as well as naïve controls, were stimulated *ex vivo* as described above, and IL-22 production by different cell types was examined. In naïve mice, IL-22 production was seen in NK cells, γδ T cells, and $CD4^+$ and $CD8^+$ T cells in all three organs (Fig. 5.3). At day 4 p.i, IL-22 expression was again seen in all 4 cell types (Fig. 5.4A-C). Gates were drawn based on the FMO staining controls (Fig. 5.4D). In some instances, the proportion of IL-22 expressing cells was higher than naïve controls, for example the NK cell populations had a higher proportion of cells expressing IL-22 at day 4 p.i compared to naïve controls (Fig. 5.5). However, when calculated back to total numbers, it was only the liver where a significant increase in total numbers of $IL\text{-}22^+$ cells was observed (Fig. 5.6B). The lung and the spleen showed comparable numbers between naïve and day 4 MCMV-infected mice (Fig. 5.6A and C).

5.2.2. NK cells are a significant source of IL-22 and exhibit a similar phenotype to non-IL-22 producing NK cells

Given that NK cells appeared to be an important source of IL-22 in at least two organs of infected mice (Fig. 5.6A and B), IL-22 protein expression was analysed at day 4 p.i in mice that were depleted of NK cells during MCMV infection. In NK cell-depleted mice, there was a highly significant reduction in IL-22 protein in both the lung and the liver as compared to non-depleted mice (Fig. 5.7A and B), but this was not observed in the spleen (Fig. 5.7C) where NK cells appear to be a less significant population of cells contributing to IL-22 production (Fig. 5.6C). These data suggest that NK cells are an important source of IL-22 during MCMV infection in the lung and the liver. A slight caveat of the NK cell depletion experiment is that NK cell-depleted mice have a significantly higher virus load compared to the non-depleted ones, which may have an effect on IL-22 production. However, this will be addressed later on in the chapter (section 5.2.12).

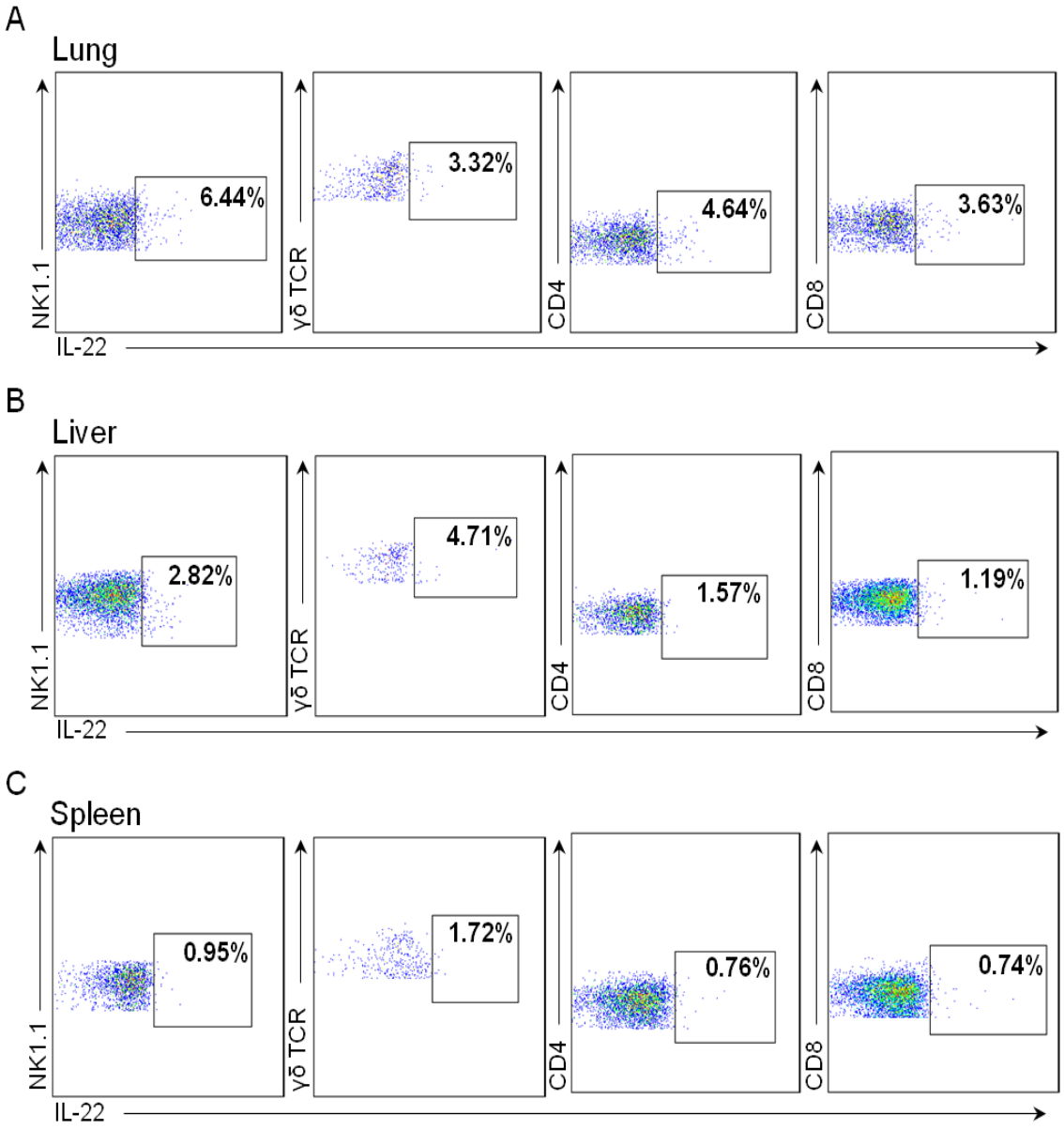

Figure 5.3. Expression of IL-22 by lymphocytes of the lung, liver and spleen in naïve mice

Representative bivariate flow cytometry plots showing IL-22 expression by NK cells, γδ T cells, $CD4^+$ and $CD8^+$ T cells from the lung (A), liver (B) and spleen (C) of naïve mice. Results are representative of 4 individual experiments with 3-4 mice per group.

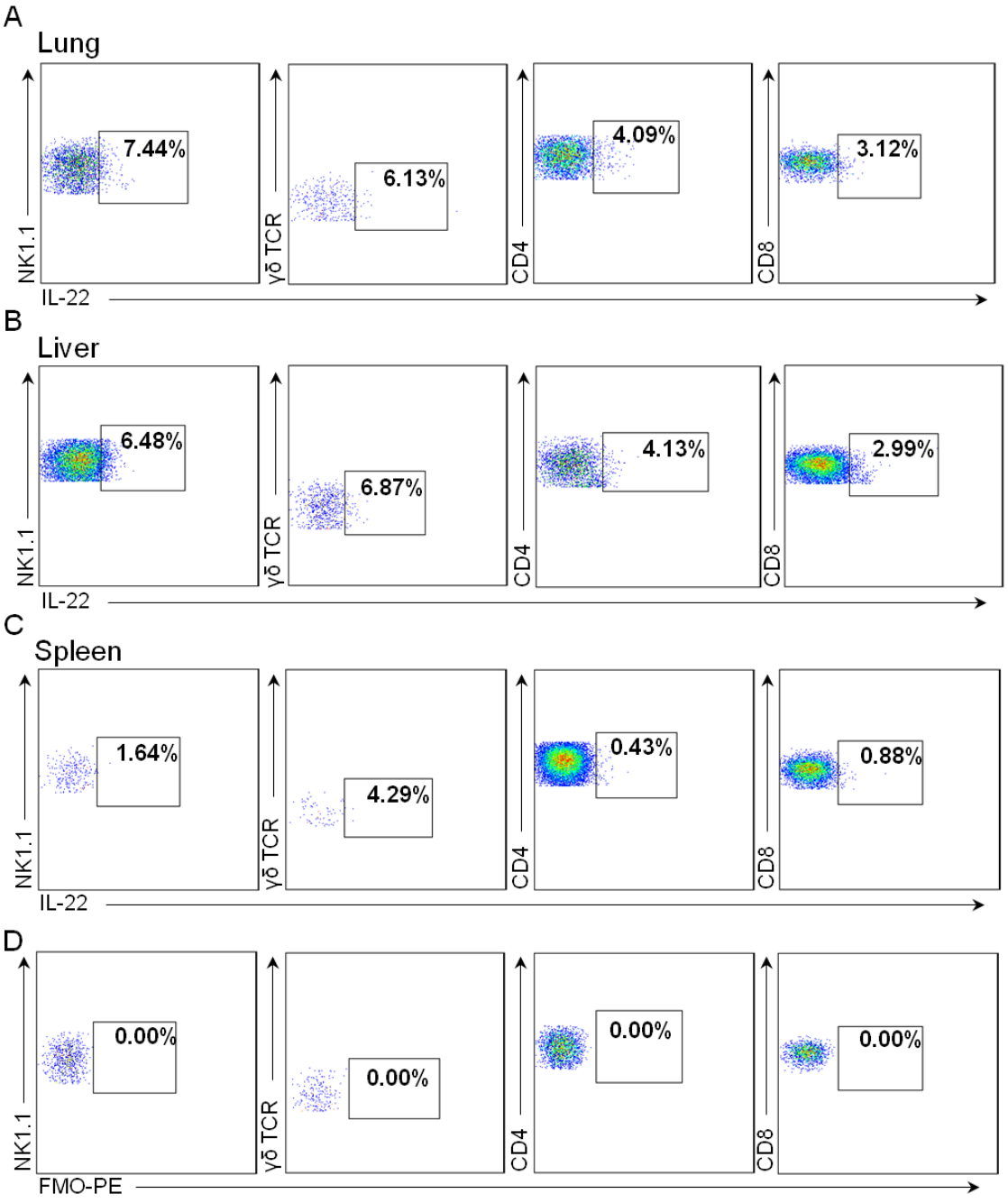

Figure 5.4. Expression of IL-22 by lymphocytes of the lung, liver and spleen in MCMV-infected mice

Representative bivariate flow cytometry plots showing IL-22 expression by NK cells, γδ T cells, $CD4^+$ and $CD8^+$ T cells from the lung (A), liver (B) and spleen (C) of day 4 MCMV-infected mice. (D) FMO staining controls. Results are representative of 4 individual experiments with 3-4 mice per group.

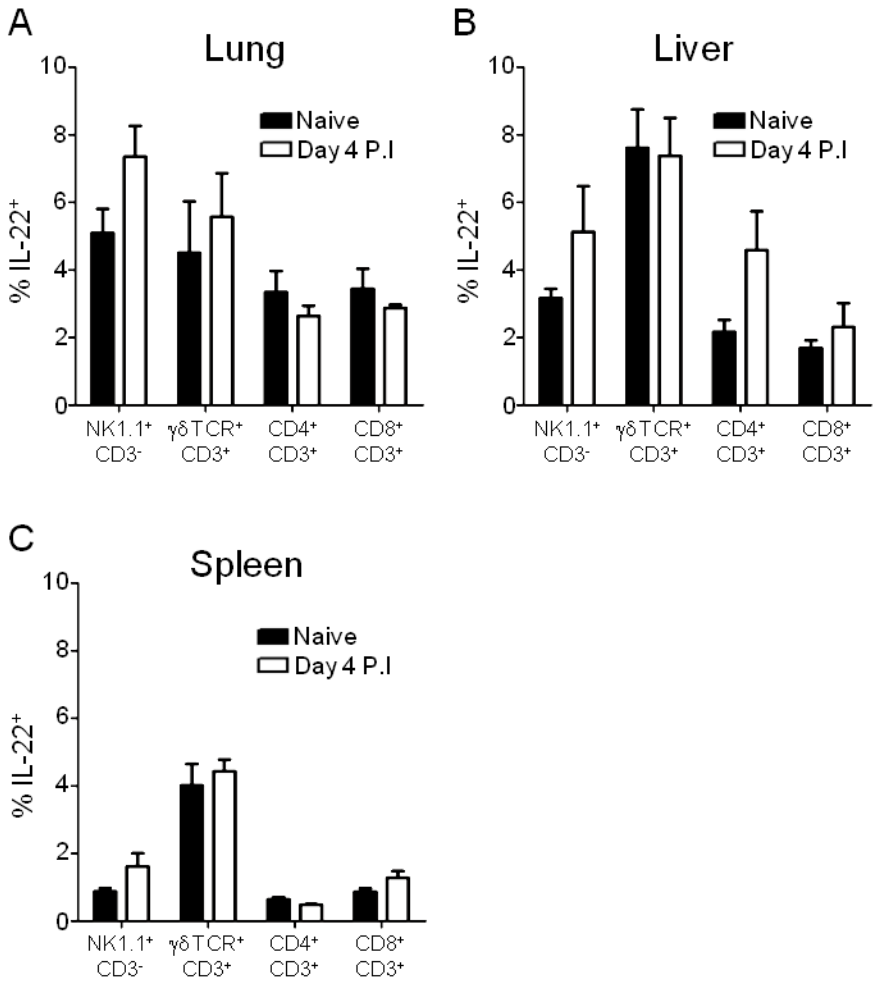

Figure 5.5. Proportion of IL-22 positive lymphocytes from the lung, liver and spleen in naïve and MCMV-infected mice

Proportion of IL-22 positive NK cells, γδ T cells, $CD4^+$ and $CD8^+$ T cells from the lung (A), liver (B) and spleen (C) of naïve (closed bars) and day 4 infected (open bars) mice. Results show the mean ± SEM of 3-4 mice per group and represent 4 individual experiments. *$p<0.05$

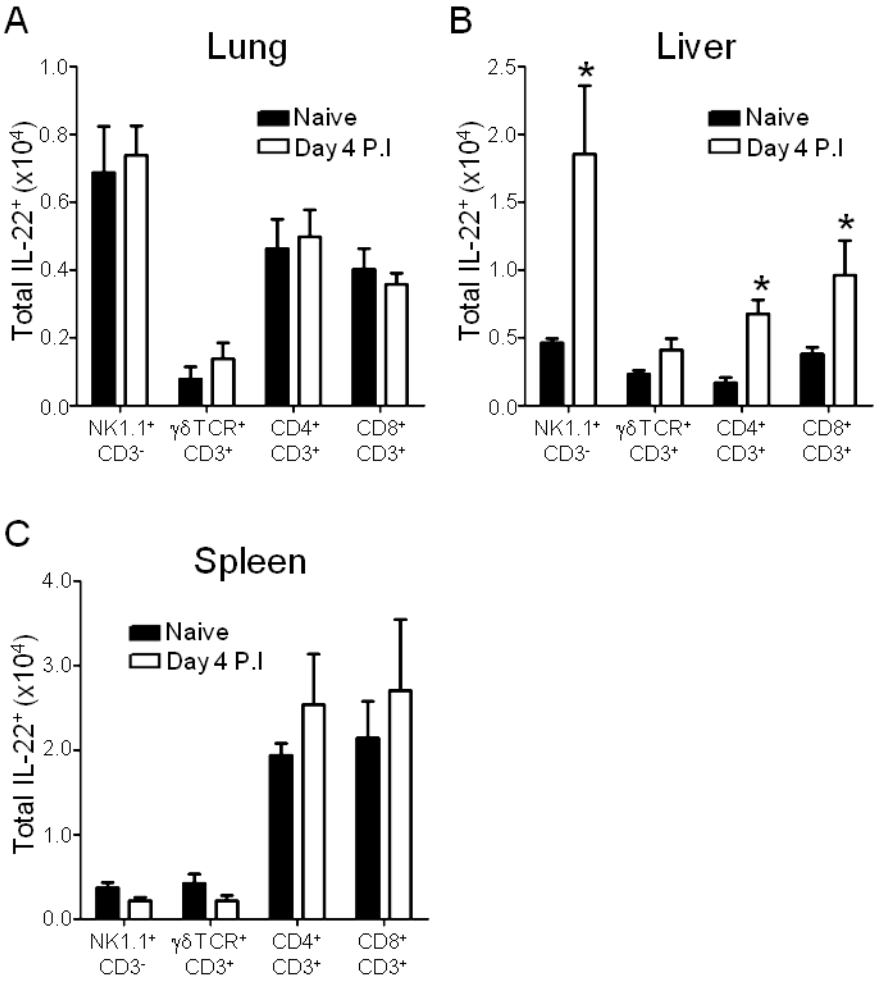

Figure 5.6. Total numbers of IL-22 positive lymphocytes from the lung, liver and spleen in naïve and MCMV-infected mice

Total numbers of IL-22 positive NK cells, γδ T cells, $CD4^+$ and $CD8^+$ T cells from the lung (A), liver (B) and spleen (C) of naïve (closed bars) and day 4 infected (open bars) mice. Results show the mean ± SEM of 3-4 mice per group and represent 4 individual experiments. *$p<0.05$

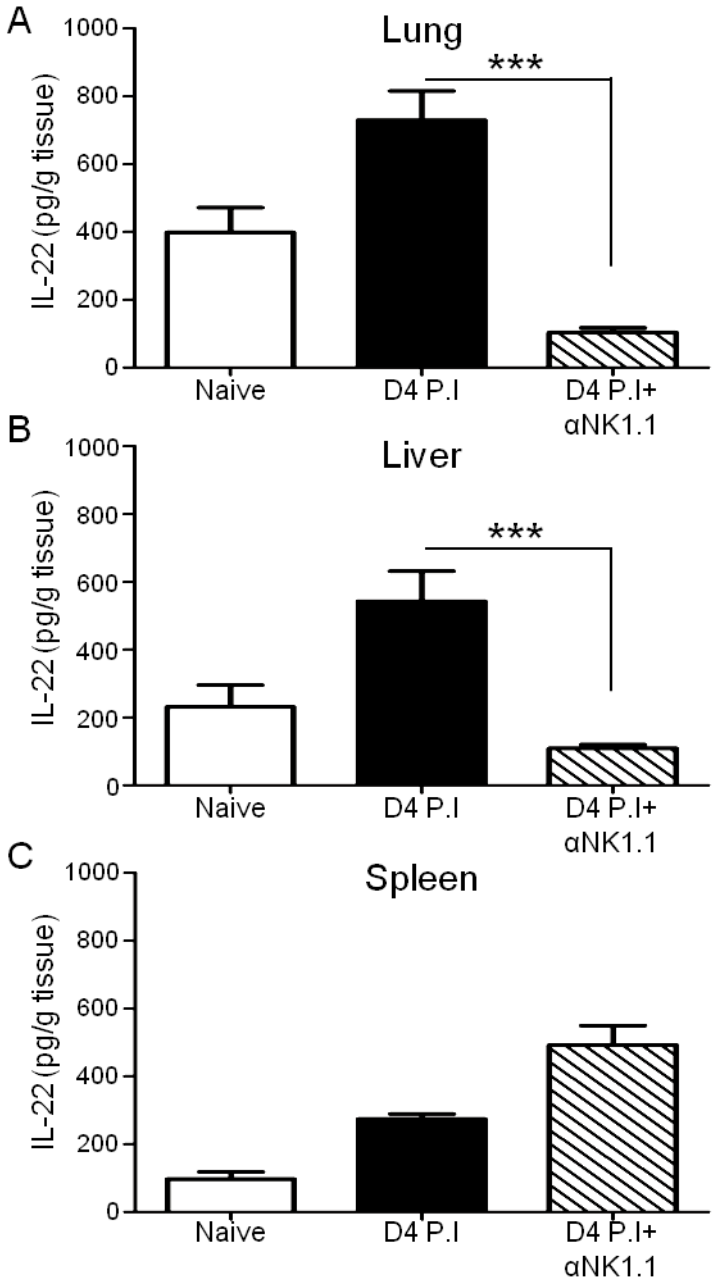

Figure 5.7. IL-22 expression in the lung and liver of MCMV-infected mice is significantly decreased in the absence of NK cells

IL-22 protein concentrations in lung, liver and spleen homogenates from naïve mice (open bars), day 4 MCMV-infected mice (closed bars) and day 4 MCMV-infected mice treated with an anti-NK1.1 antibody to deplete NK cells (cross hatched bars). Results show the mean ± SEM of 4-7 mice per group and represent 2 independent experiments. ***p<0.001

Next, I investigated whether IL-22 positive NK cells were of a different phenotype to the IL-22 negative NK cells. Therefore a number of cell surface markers were examined at both time points (Fig. 5.8A and B). Expression of Ly49H, an activating receptor which specifically recognises the MCMV protein m157; KLRG-1, an inhibitory receptor expressed in a subset of mature NK cells (and T cells); and CD127, which is the IL-7 receptor and is critical in the development of many lymphocytes, and is expressed at intermediate levels by a subset of IL-22 producing RORγt^{+} ILCs (222). Expression of all of these markers was comparable between the IL-22 positive and negative NK cells, and at both time points. Expression of CD69, a marker of cell activation, was as expected, up-regulated at 4 days p.i compared to NK cells from naïve mice. CD11b expression was higher in the IL-22 negative NK cells, whereas CD122 expression was higher in the IL-22 positive NK cells at both time points. CD11b is important for NK cell survival (223) and is also a marker of NK cell maturity when used in conjunction with CD27 (176). Signalling via CD122 is important for NK cell development and peripheral survival (224). Despite the slight differences in expression of these two markers, overall it appears that both IL-22 positive and IL-22 negative NK cells have a mature NK cell phenotype and are activated upon infection to similar levels.

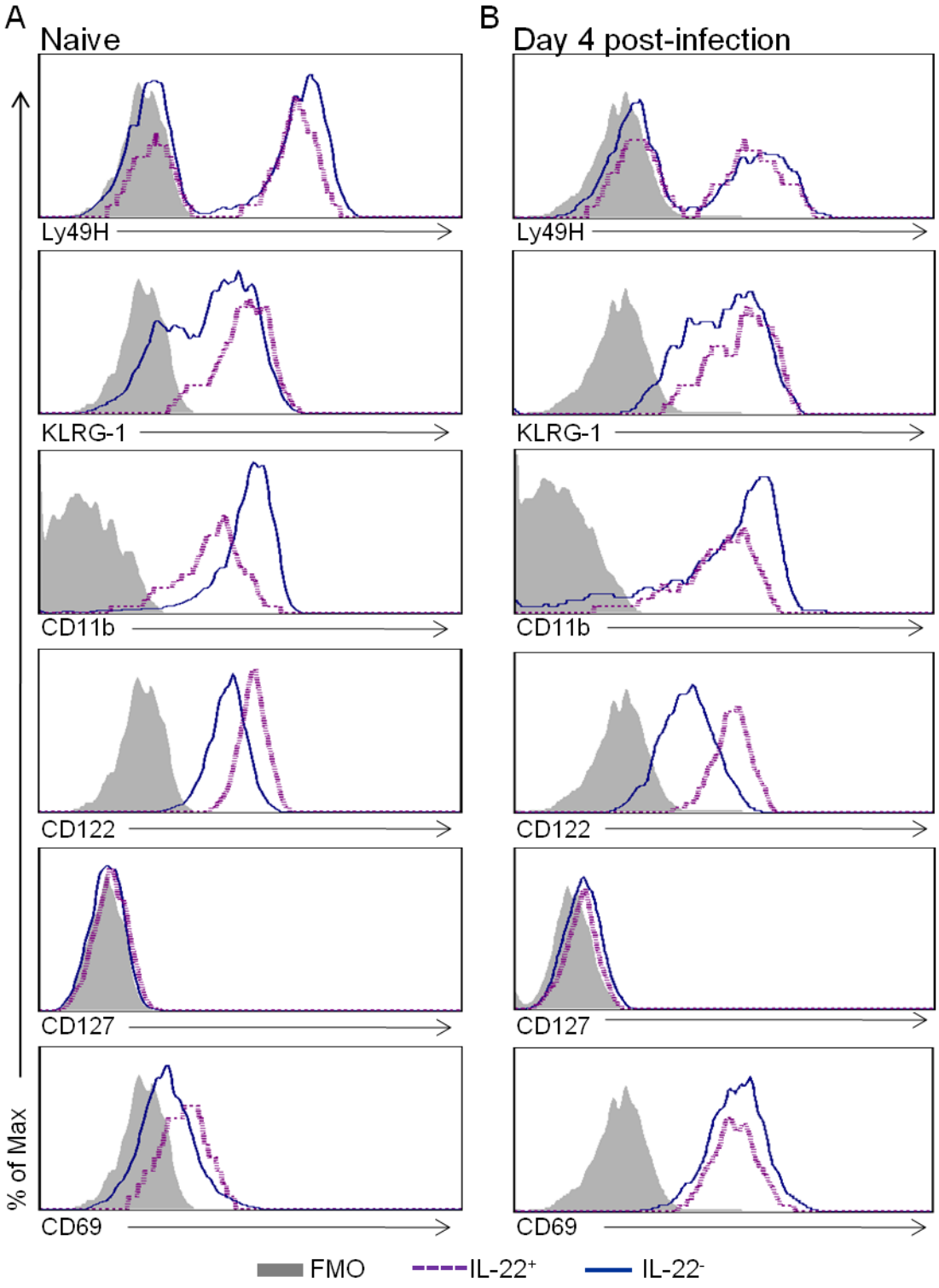

Figure 5.8. Expression of surface markers on pulmonary NK1.1^{+}IL-22^{+} and NK1.1^{+}IL-22^{-} cells in naïve and MCMV-infected mice
Representative overlay histograms of pulmonary NK1.1^{+}IL-22^{+} (dashed purple line) and NK1.1^{+}IL-22^{-} (solid blue line) from naïve (A) and day 4 infected mice (B) (shaded histogram = FMO control). Results represent 4 mice per group.

5.2.3. Neutralising IL-22 in the lung increases virus load during acute MCMV infection

Having established that IL-22 protein expression is increased during acute MCMV infection, I hypothesised that IL-22 provided protective immunity during early infection. Due to the importance of IL-22 in modulating immune responses in mucosal surfaces (140, 141), I first focused on a mucosal site of acute infection, the lung. To achieve this, mice were intra-nasally administered an anti-IL-22 antibody on the day of infection. Virus load was then assessed at 4 days p.i by measuring MCMV DNA in the lungs and spleens of mice treated with anti-IL-22 or an IgG control, as detected using MCMV gB-specific primers. In accordance with my hypothesis, viral DNA loads were significantly increased in the lungs at 4 days p.i in mice treated with anti-IL-22 as compared to IgG controls (Fig. 5.9A), but not in the spleens (Fig. 5.9B), implying that IL-22 has an antiviral role in the lung during acute MCMV infection. However, intra-nasal neutralisation of IL-22 did not affect virus-induced weight loss over the first 4 days of infection (Fig. 5.9B), demonstrating that localised administration of anti-IL-22 did not influence clinical signs of disease.

To determine whether elevated viral DNA load after anti-IL-22 administration was associated with an alteration in the MCMV-induced cellular immune response, accumulation of different cell populations was examined at 4 days p.i. No significant difference was seen in T cells ($CD3^+$), NK cells ($NK1.1^+CD3^-$), alveolar macrophages ($CD11c^{hi}CD11b^{hi}$), inflammatory macrophages ($CD11b^+7/4^{hi}F4/80^+$) or non-inflammatory monocytes/macrophages ($CD11b^+7/4^{lo}F4/80^+$), either by proportion of cells (Fig. 5.10A) or by total numbers (Fig. 5.10B). However there was a trend towards a decrease in both the proportion and total numbers of neutrophils ($Ly6G^+CD11b^{hi}$) in the lungs of mice given the anti-IL-22 antibody as compared to IgG treated mice (Fig. 5.10A and B).

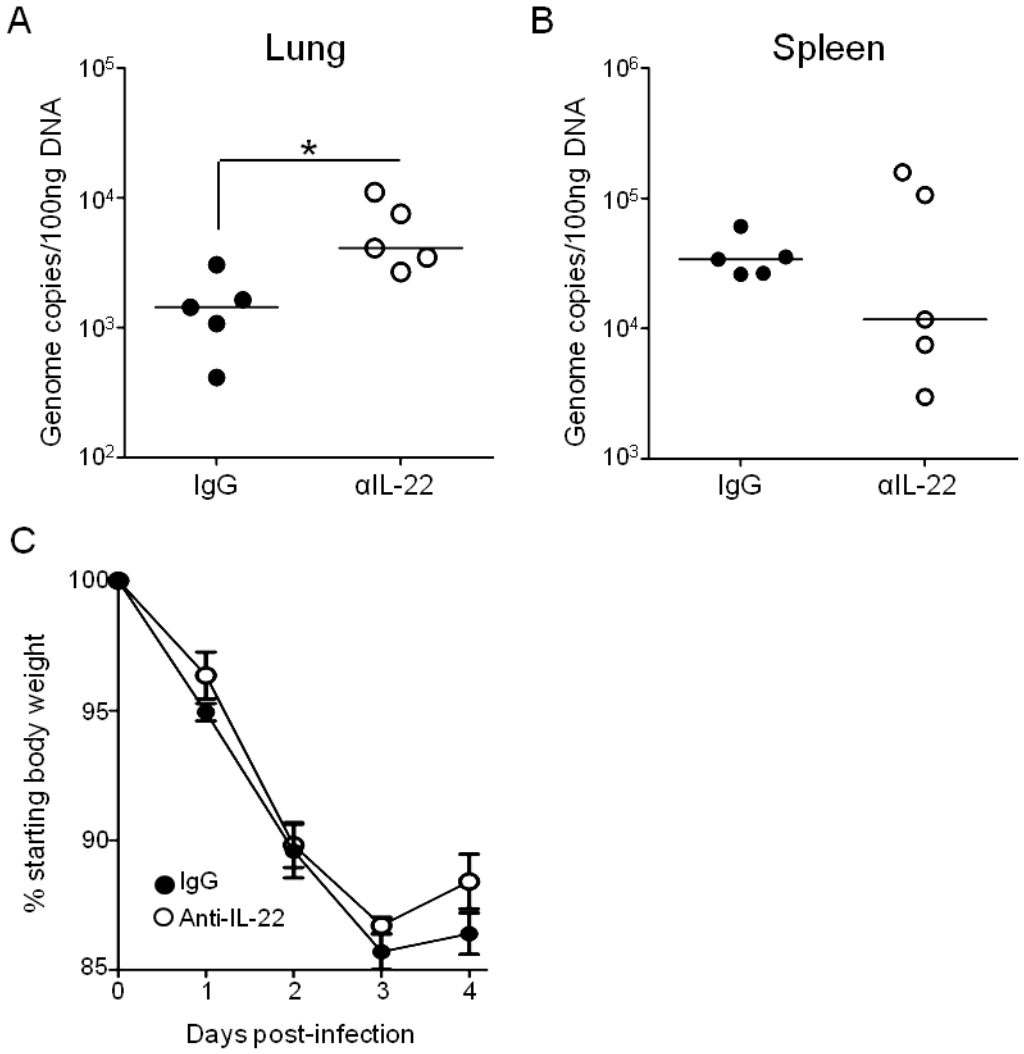

Figure 5.9. Intranasal neutralisation of IL-22 during acute MCMV infection leads to an increase in virus load in the lung but is not associated with enhanced weight loss

Mice were infected with MCMV and intra-nasally administered an IgG control (closed circles) or an anti-IL-22 neutralising antibody (open circles). (A and B) Genomic DNA was isolated from the lungs and spleens of infected mice at 4 days p.i and MCMV gB was detected by qPCR. Data was normalized to β-actin and is expressed as genome copy number per 100ng genomic DNA. Horizontal bars represent the median value. (C) Weight loss shown as percent of starting weight. Results are expressed as mean ± SEM of 5 mice per group. These data are representative of 2 independent experiments. *$p<0.05$

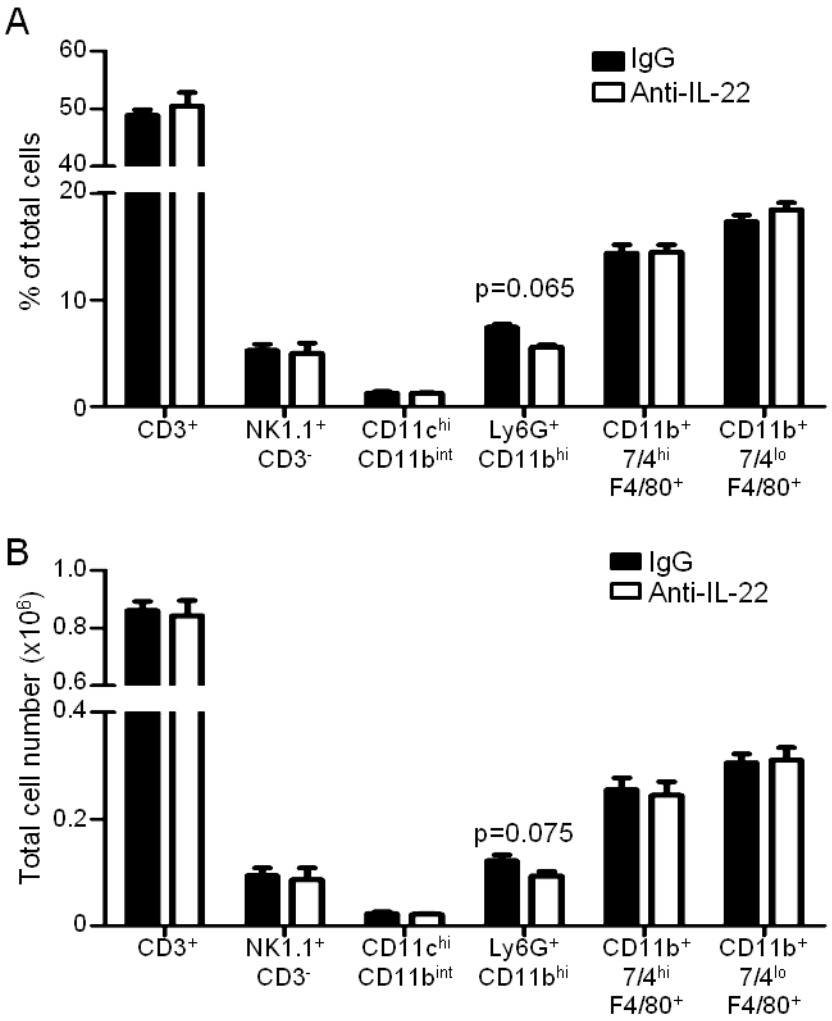

Figure 5.10. Intranasal neutralisation of IL-22 does not affect cellular accumulation during acute MCMV infection

Mice were infected with MCMV and intra-nasally administered an IgG control (closed bars) or an anti-IL-22 neutralising antibody (open bars). Leukocytes from the lung were isolated 4 days p.i and the proportion (A) and total numbers (B) of different cellular populations were analysed by flow cytometry. Results are expressed as the mean ± SEM of 5 mice per group. These data are representative of 2 independent experiments. *p<0.05

5.2.4. Systemic neutralisation of IL-22 increases virus load in the lung and liver during acute MCMV infection

To further explore the hypothesis that IL-22 has a broad antiviral role during acute MCMV infection, the model of intra-nasal administration of anti-IL-22 was altered in order to neutralise IL-22 systemically. This was achieved by administering the antibody intravenously on the day of infection and, in 4 day experiments, also at 2 days p.i. Virus load was then assessed by plaque assay at days 2 and 4 p.i in the lungs, livers and spleens. Interestingly, levels of replicating virus were significantly higher as early as 2 days p.i in the lungs and livers of mice treated with the anti-IL-22 antibody as compared to IgG treated controls, and remained significantly higher at day 4 p.i (Fig. 5.11A and B). However, in the spleen, no significant differences in virus load were observed between the two groups at either time point (Fig. 5.11C). In the lung, replicating virus is usually difficult to detect as early as 2 days p.i, as seen in the IgG treated control mice, where replicating virus was detected in only 4 out of 10 mice (Fig. 5.11A). Conversely, in the absence of IL-22, replicating virus could be detected in 8 of 10 mice, 7 of which to a higher level than those observed in the control group. At day 4 p.i, replicating virus could be detected in the lungs of all mice, however the anti-IL-22 treated group had on average over 3-fold higher virus loads than the controls. In the livers of IL-22 neutralised mice, this increase in virus load was even more striking, where levels of replicating virus were on average 7- and 9-fold higher at days 2 and 4 p.i respectively, as compared to IgG controls (Fig. 5.11B).

Virus-induced weight loss was also assessed following systemic IL-22 neutralisation. Unlike the intra-nasal model, the systemic absence of IL-22 led to exacerbated weight loss over the first 4 days of infection, which is an indicator of enhanced clinical disease (Fig. 5.11D). This observation taken in conjunction with the virus load data demonstrates that IL-22 provides protective immunity during acute MCMV infection in a tissue-dependent manner that influences the clinical outcome of infection.

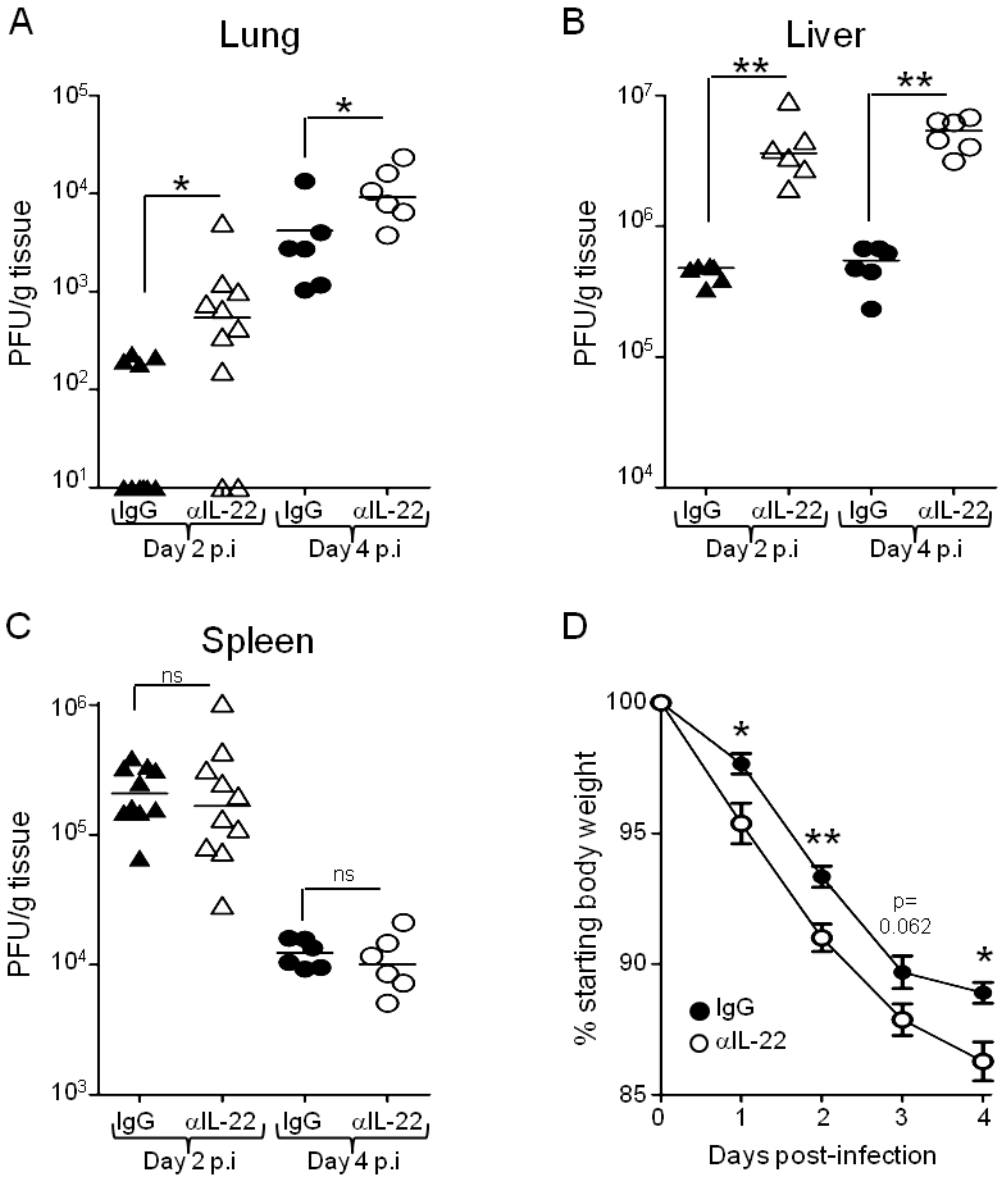

Figure 5.11. Systemic neutralisation of IL-22 leads to an organ specific increase in virus load and enhanced virus-induced weight loss

Mice were infected with MCMV and intravenously administered an IgG control (closed symbols) or an anti-IL-22 neutralising antibody (open symbols). (A-C) Homogenates from the lungs (A), livers (B) and spleens (C) of mice infected for 2 and 4 days were prepared for high sensitivity plaque assays to detect replicating virus. Data is expressed as PFU per gram of tissue. Horizontal bars show median values. (D) Weight loss shown as percent of starting weight. Results are expressed as mean ± SEM of 6 mice per group. Data represent 3 independent experiments. *p<0.05, **p<0.01, ns=not significant

3.2.5. Increased virus load in the absence of IL-22 during acute MCMV infection is not associated with decreased levels of pro-inflammatory cytokines

Early response to MCMV infection is characterised by a rapid up-regulation of pro-inflammatory cytokines (193, 225, 226). I hypothesised that the increase in virus load observed in the lung and liver in the absence of IL-22 would be associated with reduced levels of pro-inflammatory cytokines, as IL-22 induces pro-inflammatory responses such as the production of cytokines, chemokines and acute-phase proteins from many cell types (227). To test this hypothesis, MCMV-infected mice were treated with either anti-IL-22 or an IgG control, and at 2 days p.i, homogenates from the lung and liver were analysed for levels of pro-inflammatory cytokines. Homogenates from the spleen, where increased virus loads were not observed following IL-22 neutralisation were also analysed. Following IL-22 neutralisation, no significant differences in production of any cytokines tested were observed in any of the organs analysed (Fig. 5.12A-C). Levels of the T_h1 and T_h2 associated pro-inflammatory cytokines IFNγ, TNFα, IL-5 and IL-6 were comparable between anti-IL-22 treated and IgG treated mice. Levels of the anti-inflammatory cytokine IL-10 were also analysed, and again, no significant differences were observed between the two treatments in any organs examined. Therefore, altered expression levels of pro-inflammatory cytokines were not associated with increases in virus load following IL-22 neutralisation.

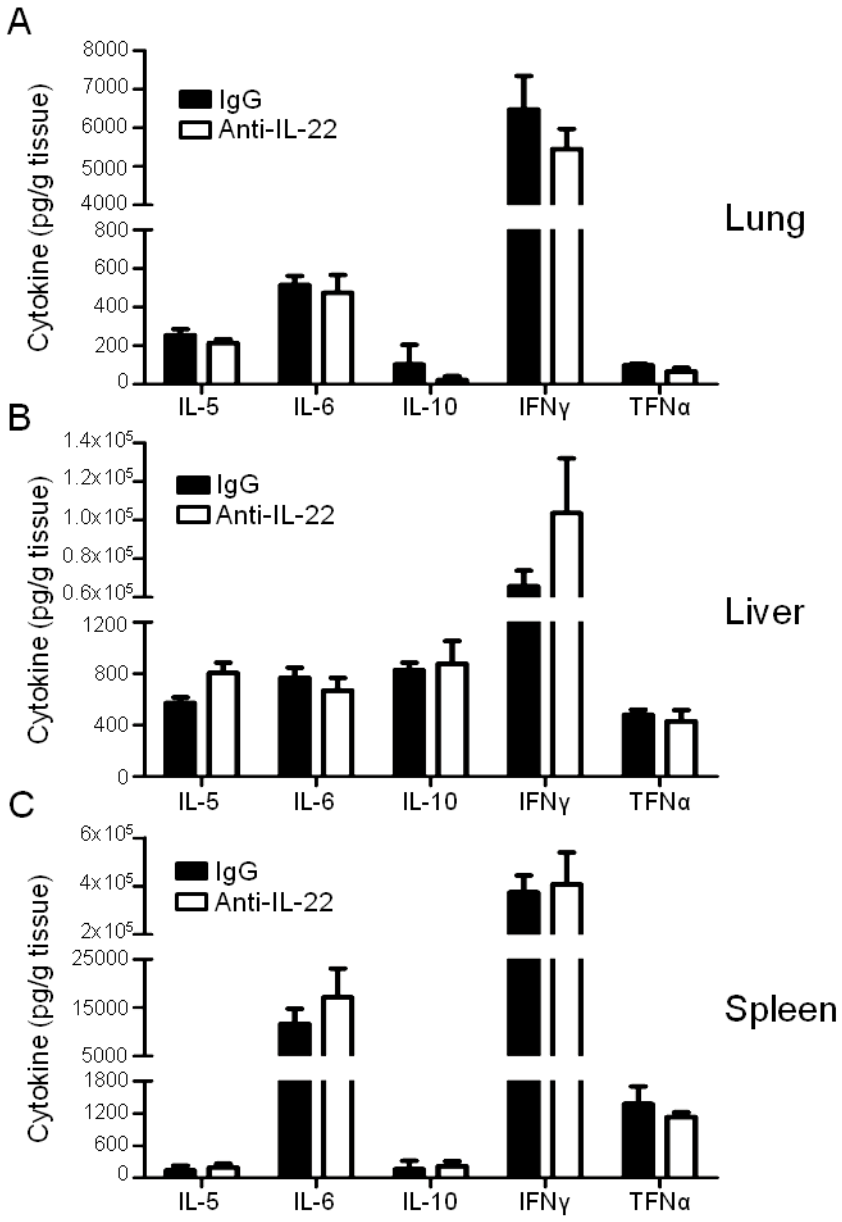

Figure 5.12. Anti-IL-22 administration does not influence Th1 and Th2 associated cytokine production in MCMV-infected mice

Mice were infected with MCMV and treated with IgG (closed bars) or anti-IL-22 (open bars). Levels of cytokines were assessed at 2 days p.i. Cytokine protein concentrations in lung (A), liver (B) and spleen (C) homogenates were measured by cytometric bead array. Results represent the mean ± SEM of 6 mice per group.

5.2.6. IL-22 neutralisation is associated with an impairment of Ly6G$^+$ neutrophil infiltration

Following administration of anti-IL-22 via the intra-nasal route, a trend towards a reduced accumulation of neutrophils was observed (Fig. 5.10). To see if this was repeated following systemic neutralisation of IL-22, leukocytes from the lung, liver and spleen were isolated from day 2 MCMV-infected mice, and neutrophils along with various APC populations were analysed. In the lung and the liver, neutrophils represent a substantial population of the total infiltrating immune cells at 2 days p.i, but interestingly, mice treated with anti-IL-22 showed a reduction in the percentage of neutrophils that accumulated in these two organs as compared to control treated mice (Fig. 5.13A and B). This reduction in neutrophil infiltration can also been seen when calculated as total cell numbers (Fig. 5.13D and E). APC populations were unaffected by IL-22 neutralisation (Fig. 5.13D and E). In the spleen, neutrophils account for only a very small proportion of the entire cellular infiltrate and the absence of IL-22 does not alter the proportion or total numbers of neutrophils accumulating in the spleen (Fig. 5.13C and F).

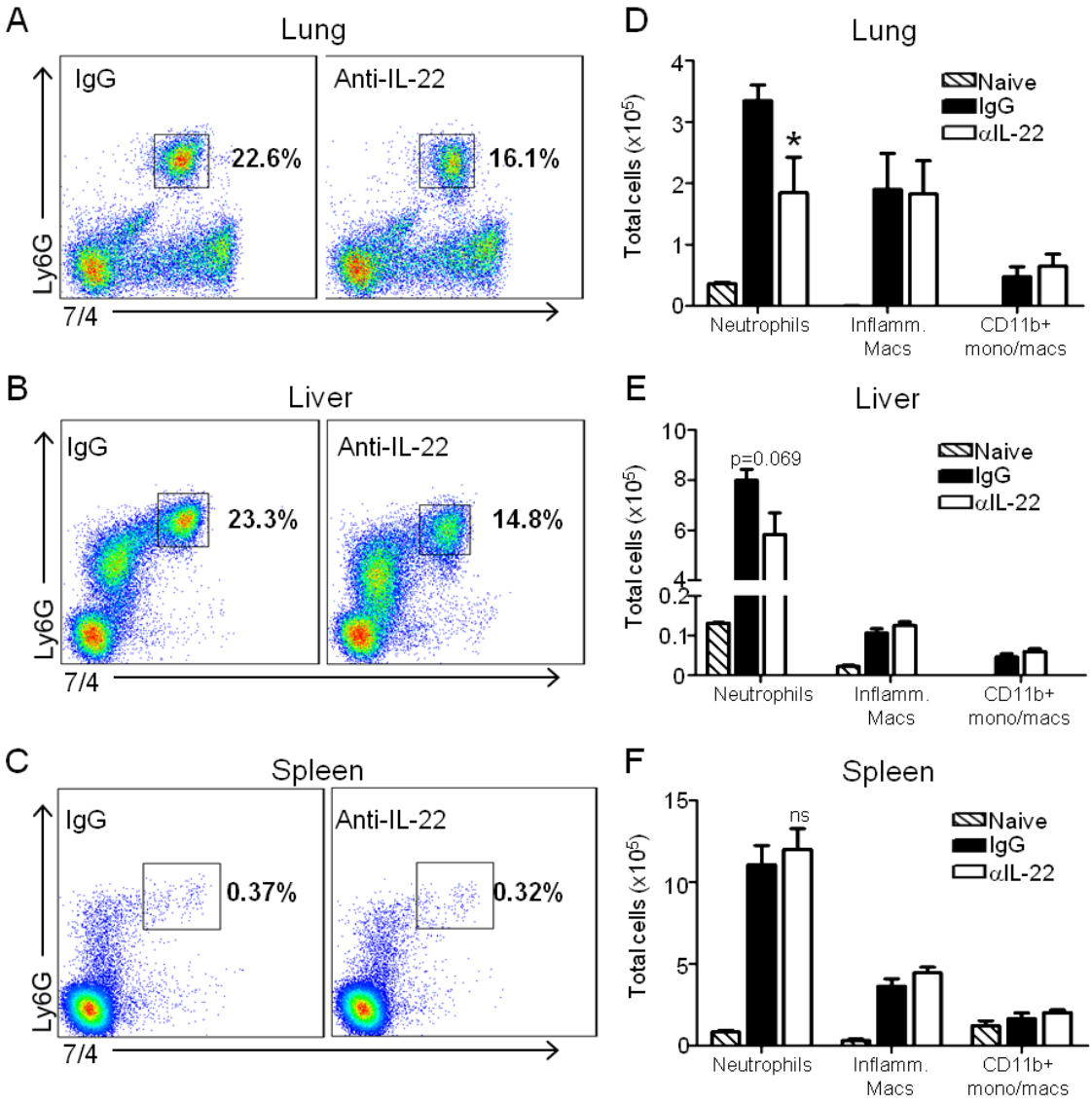

Figure 5.13. IL-22 neutralisation during acute MCMV infection is associated with impaired neutrophil accumulation in the lung and liver

MCMV-infected mice were administered IgG or anti-IL-22 by IV injection and leukocytes isolated from lungs, livers and spleens at 2 days p.i. (A-C) Representative bivariate flow cytometry plots showing neutrophil accumulation following IgG administration (left-hand plots) and anti-IL-22 administration (right-hand plots). (D-F) Total numbers of neutrophils, inflammatory macrophages and $CD11b^+$ monocytes/macrophages in naïve (cross hatched bars), and day 2 infected mice treated with IgG (black bars) or anti-IL-22 (white bars). Results show mean ± SEM of 6 mice per group and represent 3 independent experiments.

5.2.7. Chemokines associated with neutrophil recruitment are not down-regulated following IL-22 neutralisation

A possible mechanism for the reduction in neutrophil accumulation in the lung and liver following anti-IL-22 treatment could be impaired recruitment. Neutrophils express the chemokine receptor CXCR2 which binds to the chemokine CXCL1; therefore a reduction in this chemokine could prevent efficient recruitment of neutrophils into infected lungs and livers. Homogenates from these organs as well as spleens from naïve mice and MCMV-infected mice treated with IgG or anti-IL-22 at 2 days p.i were analysed for CXCL1 protein expression. Infected mice showed significant upregulation of CXCL1 compared to naïve controls. However, no significant differences were observed between IgG and anti-IL-22 treated mice although a trend towards an decrease in CXCL1 expression was seen in the liver of anti-IL-22 treated mice (Fig. 5.14A-C). It was possible that looking even earlier during infection may yield significant differences in CXCL1 expression between the IgG and anti-IL-22 treated mice, therefore homogenates from day 1 infected mice were also examined for CXCL1 protein expression. However, no significant differences were observed (Fig. 5.14D-F).

As well as CXCL1, other chemokines are also important in recruitment of neutrophils. To assess if IL-22 neutralisation inhibited mRNA expression of CXCL2 and CXCL5, RNA was extracted from livers of day 1 MCMV-infected mice and mRNA expression of these chemokines, along with CXCL1, was analysed by qPCR (Fig. 5.15A-C). However, expression of these genes between IgG treated mice and anti-IL-22 treated mice was comparable, as was the expression of G-CSF (Fig. 5.15D) which is important for stimulating survival, proliferation, and differentiation of neutrophils.

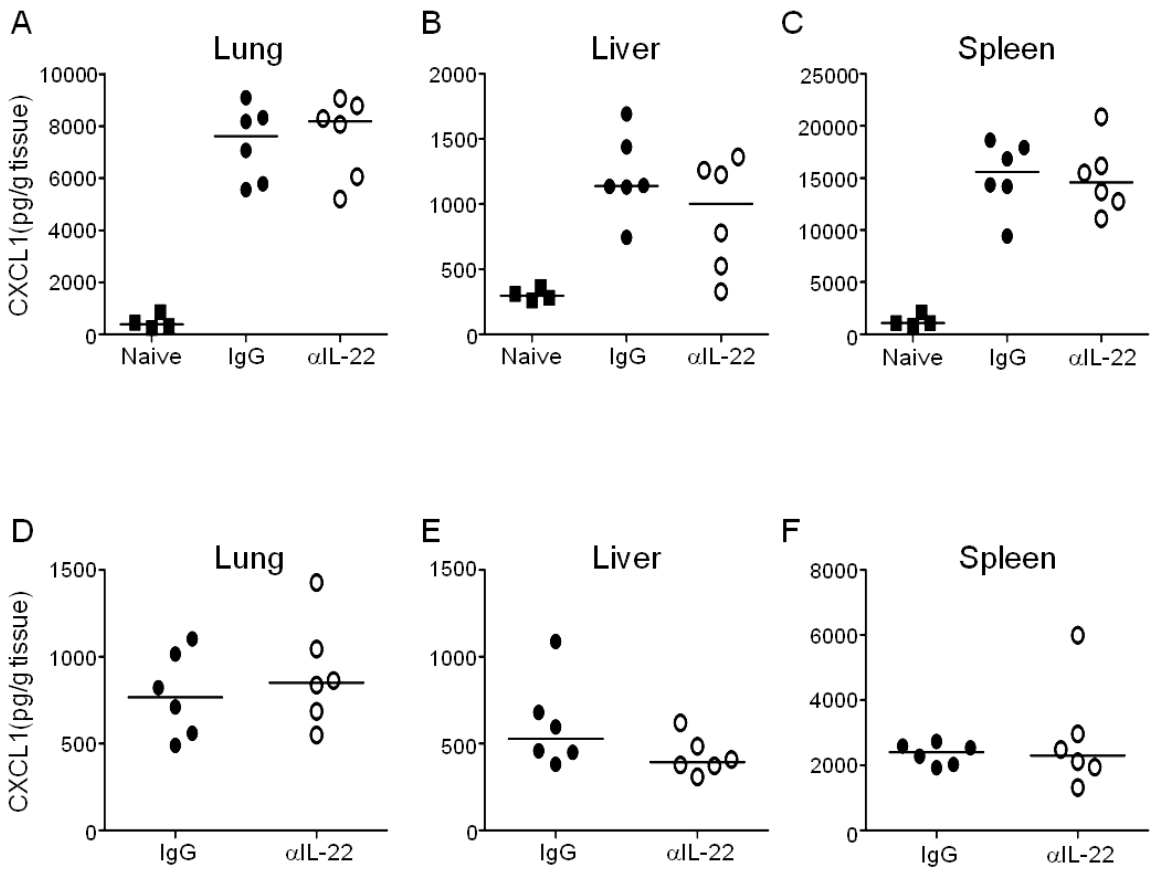

Figure 5.14. Anti-IL-22 treatment does not lead to a reduction in CXCL1
(A-C) CXCL1 protein concentrations in lung, liver and spleen homogenates from naïve mice (squares) or 2 day MCMV-infected mice treated with IgG (closed circles) or anti-IL-22 (open circles). (D-F) CXCL1 protein concentrations in lung, liver and spleen homogenates from 1 day MCMV-infected mice treated with IgG (closed circles) or anti-IL-22 (open circles). Horizontal bars represent the median value. Data are representative of 2 independent experiments.

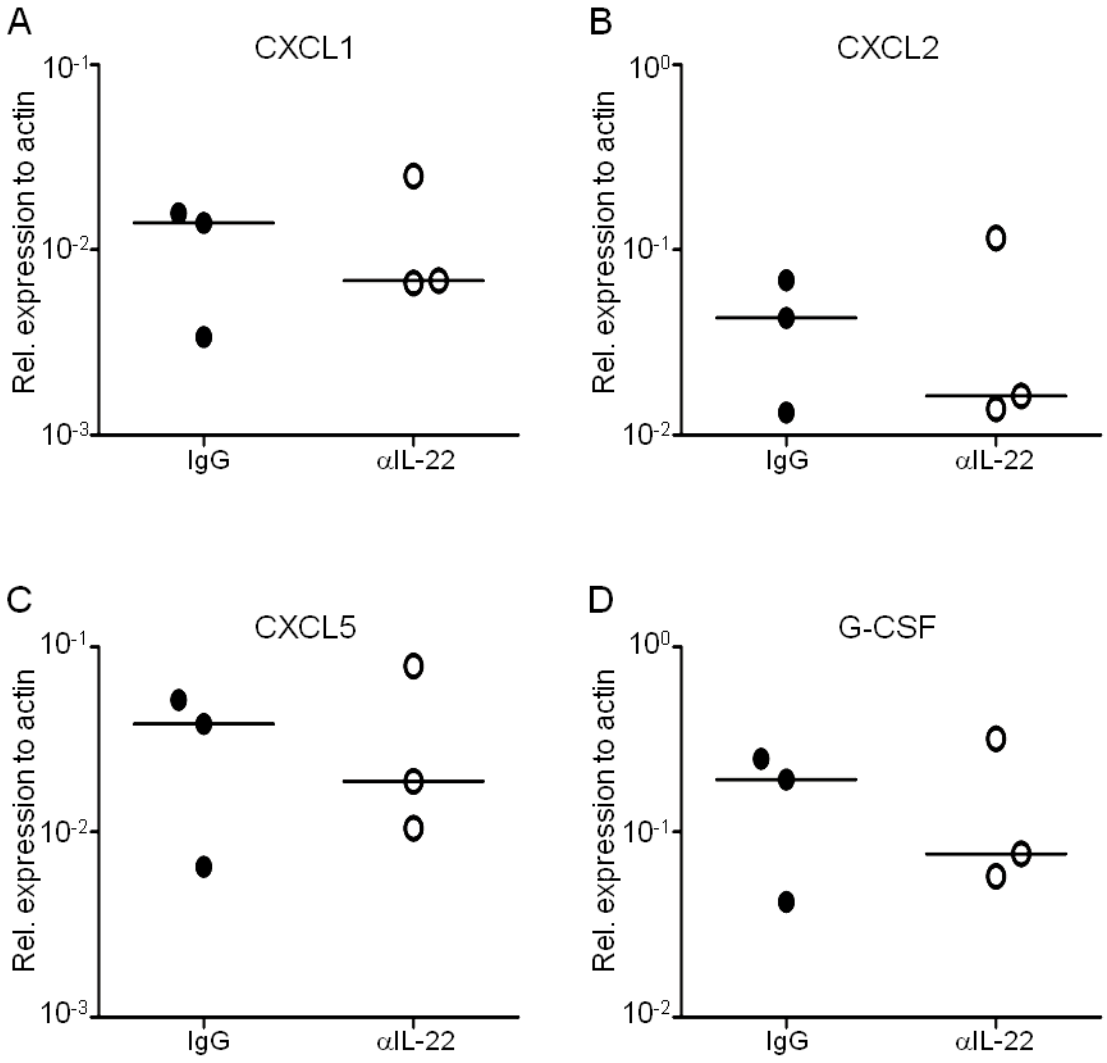

Figure 5.15. Neutralisation of IL-22 does not cause a reduction in expression of chemokines associated with neutrophil accumulation and survival
MCMV-infected mice were treated with IgG (closed circles) or anti-IL-22 (open circles). At day 1 p.i, livers were excised and RNA was extracted and converted to cDNA. Expression of genes associated with neutrophil chemotaxis and survival was analysed by qPCR. Data is shown as gene expression relative to β-actin expression. Horizontal bars represent the median value. Data represent 2 experiments.

5.2.8. CD11b expression on neutrophils is up-regulated upon MCMV infection

CD11b is a component in the CD11b/CD18 adhesion protein complex, and when rolling adherent neutrophils are stimulated, they rapidly immobilise through activation of this complex, allowing them to migrate from the blood circulation into target tissue (228, 229). Therefore the up-regulation of CD11b expression is a sign of neutrophil activation (229). To investigate if MCMV infection led to neutrophil activation, neutrophils were isolated from naïve and day 2 MCMV-infected mice and CD11b expression was analysed. In order to minimise the possibility of the neutrophils becoming activated during isolation, each step was performed on ice. Due to a more involved process of isolating leukocytes from the liver, and consequently increasing the chances of *ex vivo* activation, only neutrophils from the lung and spleen were analysed. In naïve mice, neutrophils in both the lung and the spleen expressed intermediate levels of CD11b (Fig. 5.16A and B; dashed lines). Interestingly, splenic neutrophils isolated from 2 day MCMV-infected mice showed enhanced CD11b expression compared to naïve mice, with the MFI of CD11b increasing from 323 to 986 (Fig. 5.16B; solid line). This increased expression was even more enhanced in neutrophils isolated from the lung of MCMV-infected mice, with the MFI of CD11b reaching 1136 compared to 365 in naïve mice (Fig. 5.16A; solid line). Therefore this data suggests that neutrophils become activated upon MCMV infection.

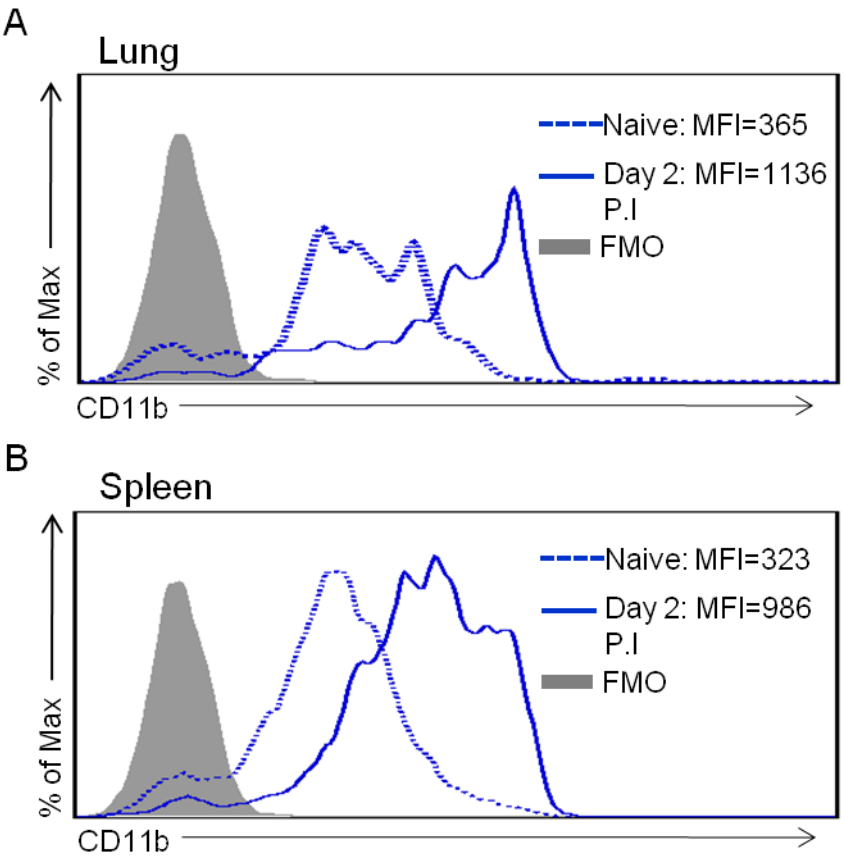

Figure 5.16. MCMV infection is associated with an up-regulation of CD11b expression on neutrophils

Representative overlay histograms of CD11b expression on neutrophils isolated from the lung (A) and spleen (B) of naïve mice (dashed line) and day 2 MCMV-infected mice (solid line) (shaded histogram = FMO control). Results represent 3 mice per group.

5.2.9 Administration of 1A8 antibody leads to specific loss of neutrophils

To test the hypothesis that neutrophils are important in controlling MCMV infection, mice were administered a Ly6G-specific monoclonal antibody, clone 1A8, to deplete neutrophils, during infection. This antibody has been shown to specifically deplete neutrophils without depleting Gr-1^{+} (Ly6C^{+}) monocytes (230). To ensure neutrophils were being depleted without affecting other monocyte populations in my model, mice were administered either anti-Ly6G (1A8) or an IgG control and infected with MCMV. Organs were taken at 4 days p.i and neutrophils and APC populations in each organ were analysed by flow cytometry. Mice treated with anti-Ly6G (Fig. 5.17, right-hand panels) showed specific loss of neutrophils in the lung, liver and spleen as compared IgG treated controls (Fig. 5.17, left-hand panels).

5.2.10. MCMV-infected mice show exacerbated weight loss following neutrophil depletion

Having established that mice administered with anti-Ly6G were selectively depleted of neutrophils during MCMV infection, virus-induced weight loss was measured in mice with or without neutrophils. In the absence of neutrophils during early infection, mice exhibited exacerbated weight loss compared to non-depleted mice (Fig. 5.18, open circles and closed circles respectively), suggesting that neutrophils protected the mice against the clinical signs of disease. To rule out the possibility that the absence of neutrophils in uninfected mice would also lead to enhanced weight loss, naïve controls were treated with either anti-Ly6G or IgG and their weights also measured over 4 days (Fig. 5.18, open triangles and closed triangles respectively). No significant weight loss was observed in either group. Therefore, this data shows that during acute MCMV infection, neutrophils are required to protect the mice from more severe virus-induced weight loss.

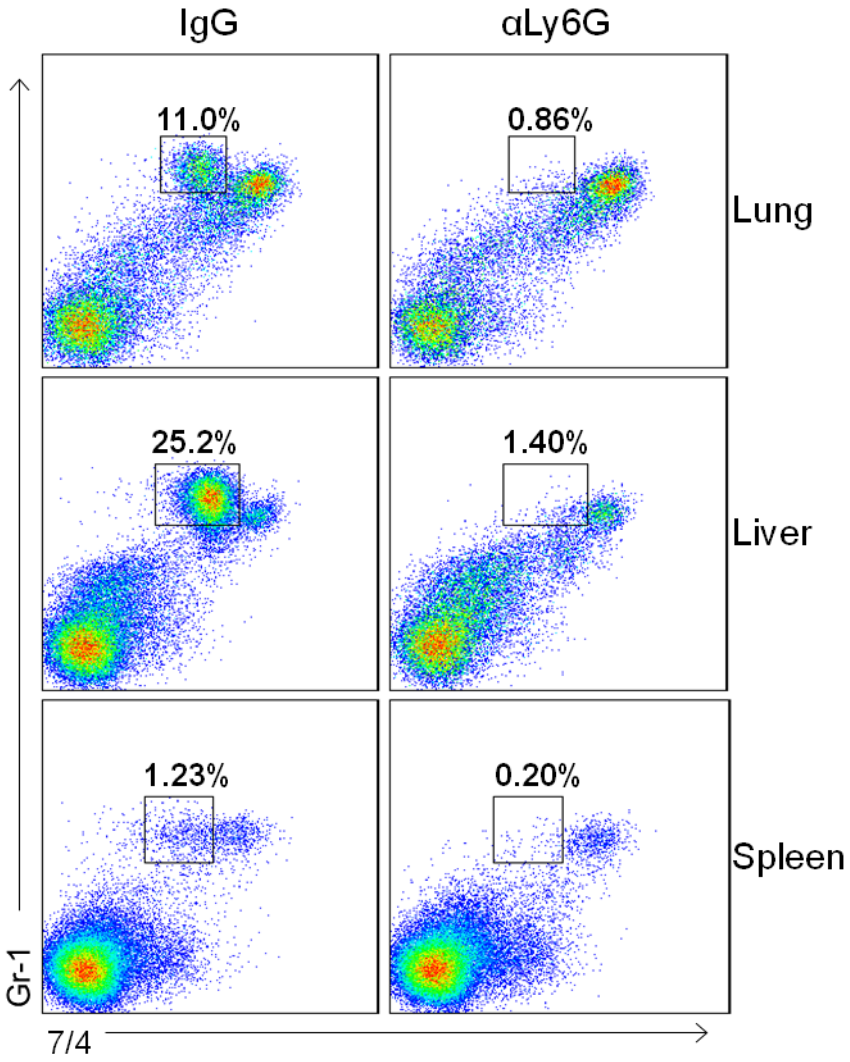

Figure 5.17. Administration of an anti-Ly6G antibody (1A8) specifically depletes neutrophils during MCMV infection
MCMV-infected mice were administered an anti-Ly6G depleting antibody (right-hand panels) or an IgG control (left-hand panels) on the day of infection and at day 2 p.i. Representative bivariate flow cytometry plots showing leukocytes isolated from the lung, liver and spleen of 4 day infected mice. Neutrophils are gated on Gr-1^{hi}7/4^{int} cells. Results represent 6 mice per group.

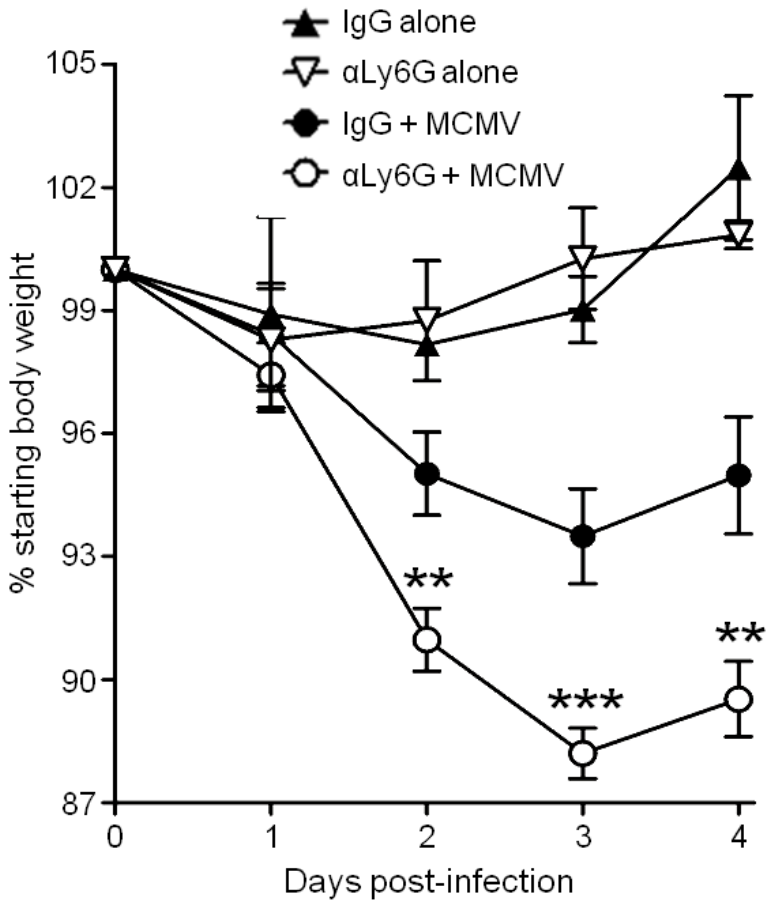

Figure 5.18. The absence of neutrophils during acute MCMV infection leads to enhanced virus-induced weight loss

Naïve mice (triangles) and MCMV-infected mice (circles) were treated with either an anti-Ly6G antibody (open symbols) or an IgG control (closed symbols) on day 0 and day 2 p.i. Weight loss is shown as percent of starting weight. Results are expressed as mean ± SEM of 6 mice per group. Data represent 3 independent experiments. **p<0.01, ***p<0.001

5.2.11. The absence of neutrophils in MCMV-infected mice leads to increased virus load in the lung and liver at day 4 post-infection

Increased virus-induced weight loss observed in mice following neutrophil depletion supported my hypothesis that these cells have a protective role during acute MCMV infection. To investigate this further, virus load was then assessed by plaque assay at 4 days p.i in the lungs, liver and spleens. In accordance with my hypothesis, the lungs and livers of mice treated with anti-Ly6G had significantly higher virus loads than IgG control treated mice (Fig. 5.19A and B). Interestingly, virus loads in the spleen were comparable between mice with and without neutrophils (Fig. 5.19C). Thus, these data show that neutrophils have an antiviral function in the lung and the liver during acute MCMV infection.

5.2.12. Increased virus load does not lead to a significant reduction in IL-22

As discussed in section 5.2.2, IL-22 protein expression was markedly reduced in the lung and liver following NK cell depletion during acute MCMV infection, suggesting NK cells were an important source of IL-22. However, NK cell depletion during infection leads to a significant increase in virus load. To investigate whether increased virus load contributes to the reduction in IL-22 levels, perhaps via induction (directly or indirectly) of death of IL-22 producing cells, I examined homogenates from neutrophil depleted mice for IL-22 protein expression, as these mice also exhibited increased virus loads as compared to IgG controls. However, unlike the NK cell depleted mice (Fig. 5.20A and C), the neutrophil depleted mice did not show a significant reduction in IL-22 expression levels (Fig. 5.20B and D). This suggests that it was in fact the lack of NK cells that led to the observed reduction in IL-22 and not the increase in virus load, and highlights that neutrophils are not a significant source of IL-22 in MCMV infection.

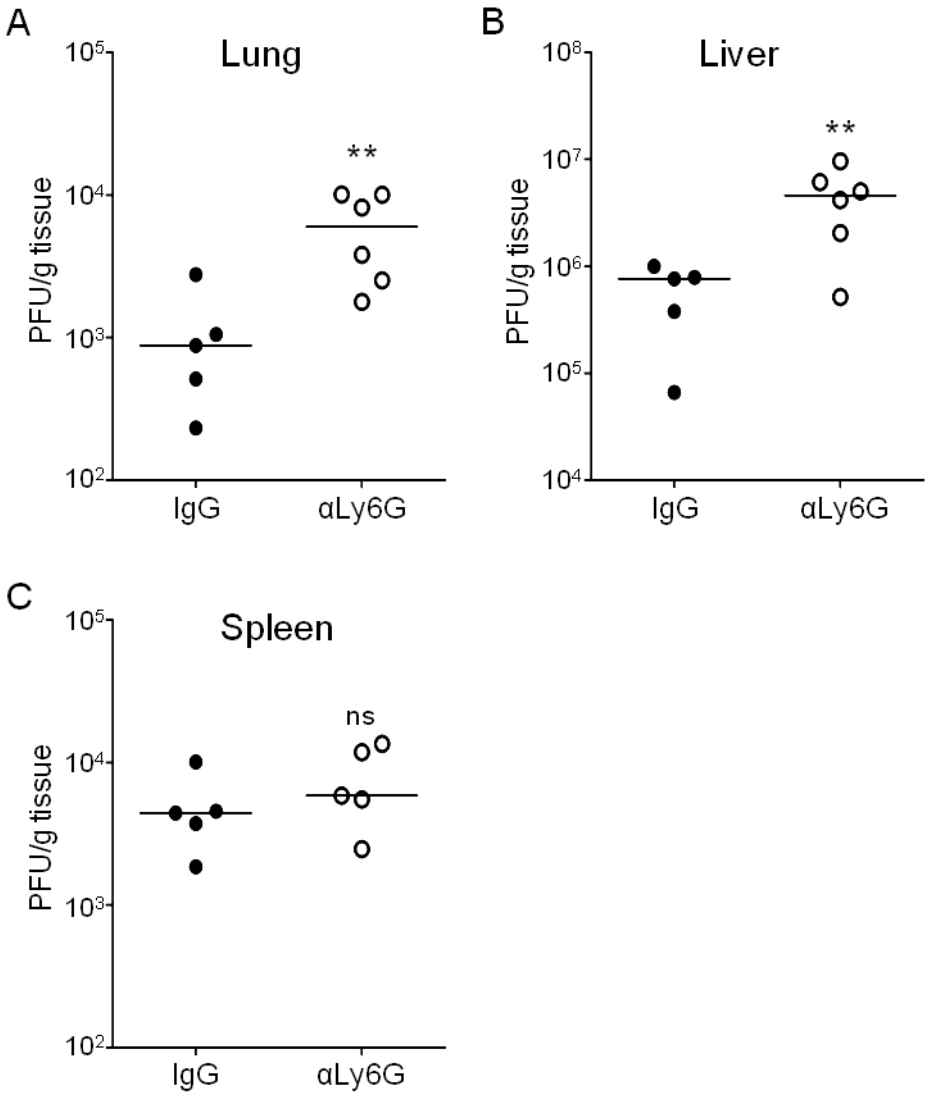

Figure 5.19. The absence of neutrophils during acute MCMV infection leads to increased virus load in the lung and liver at 4 days post-infection
Mice were infected with MCMV and administered an IgG control (closed symbols) or an anti-Ly6G antibody (open symbols). Homogenates from the lungs (A), livers (B) and spleens (C) of mice infected for 4 days were prepared for high sensitivity plaque assays to detect replicating virus. Data is expressed as PFU per gram of tissue. Horizontal bars show median values. Data is representative of 3 independent experiments. **p<0.01, ns=not significant.

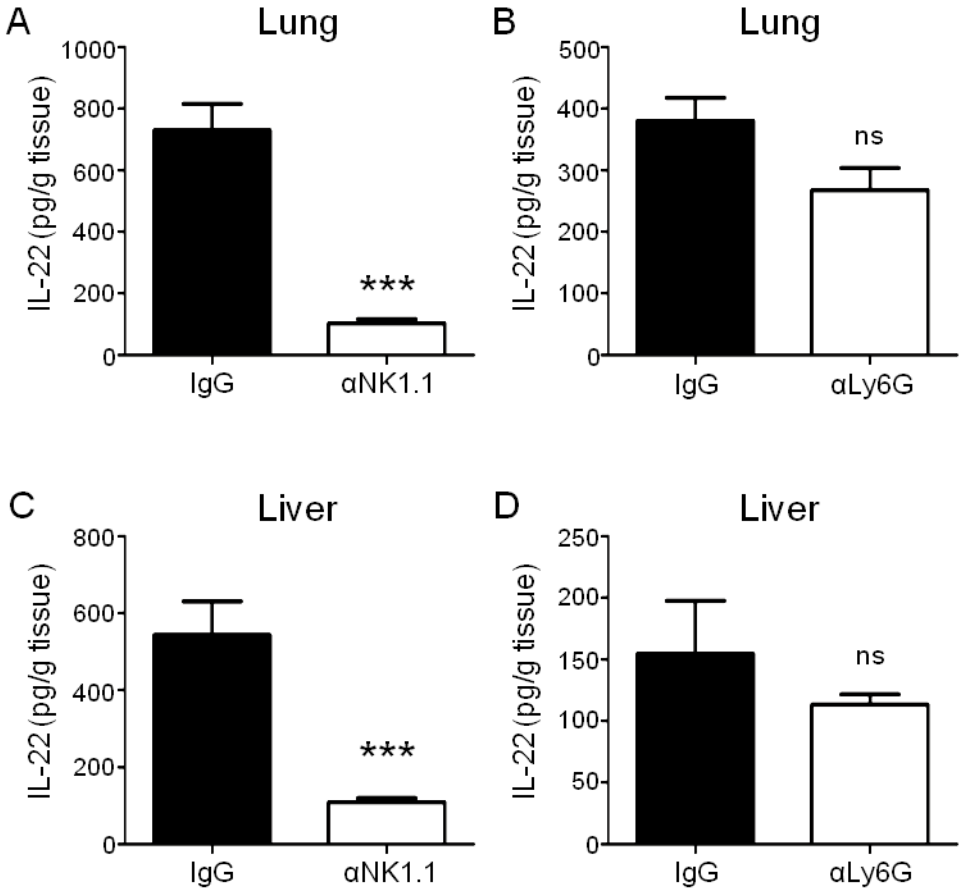

Figure 5.20. Increased virus load does not lead to a significant reduction in IL-22 expression

IL-22 protein concentrations in lung (A and B) and liver (C and D) from homogenates from day 4 MCMV-infected mice treated with IgG (open bars), anti-NK1.1 (A and C, closed bars) or anti-Ly6G (B and D, closed bars). Results show the mean ± SEM of 4-7 mice per group. ***p<0.001, ns=not significant.

5.2.13. The absence of neutrophils in MCMV-infected mice does not lead to increased virus load at day 2 post-infection

Increased virus load at day 4 p.i in the lung and the liver was observed in mice following neutrophil depletion (Fig. 5.19). However, to see if this antiviral protection afforded by neutrophils also occurred earlier in infection, virus load was assessed by plaque assay after 2 days of infection in mice treated with IgG or anti-Ly6G. Interestingly, no significant differences in virus load were observed in the lungs, livers or spleens of mice depleted of neutrophils as compared to non-depleted controls at this time point (Fig. 5.21).

5.2.14. NK cell function is not enhanced by the presence of neutrophils during acute MCMV infection

It has recently been demonstrated that neutrophils are required for NK cell development during normal homeostasis (231) and are also critical for NK cell activation during *Legionella pneumophila* infection (231, 232). I therefore hypothesised that neutrophil-NK cell crosstalk could be important in limiting virus load during the acute-phase of infection. To explore this hypothesis further, mice were administered either anti-Ly6G or an IgG control and infected with MCMV. At 4 days p.i, hepatic lymphocytes were isolated from livers and NK cell function was analysed under different *ex vivo* stimulating conditions. However, the absence of neutrophils in mice treated with anti-Ly6G did not inhibit either CD107a mobilisation or IFNγ expression by NK cells either directly *ex vivo* or after stimulation with plate-bound anti-NKp46 or by PMA/Ionomycin stimulation (Fig. 5.22A and B). In fact, mice treated with anti-Ly6G actually showed increased expression of CD107a on NK cells directly *ex vivo* and following PMA/Ionomycin stimulation as compared to IgG treated controls (Fig. 5.22A). This suggests that neutrophils do not enhance NK cell function during acute MCMV infection. However, to further confirm this, MCMV-infected mice were administered either an IgG control, anti-Ly6G, anti-NK1.1 or both anti-Ly6G and anti-NK1.1. At 4 days p.i, livers were taken and homogenates were analysed for replicating virus levels by high-sensitivity plaque assay. Both anti-Ly6G and anti-NK1.1

treatment led to a significant increase in virus load compared to control treated mice, but a further significant increase in virus load was observed in mice given both depleting antibodies (Fig. 5.22C). This suggests that both cell types play a protective role in early MCMV infection and the absence of both has an additive effect on levels of replicating virus.

5.2.15. Neutrophils from MCMV-infected mice express a distinct gene transcription profile

Having ruled out the possibility that activation of NK cells was enhanced by neutrophils during acute MCMV infection, the question of how neutrophils were providing antiviral immunity was still to be answered. In an attempt to elucidate the mechanism(s) through which neutrophils protect against MCMV, leukocytes from 2 day infected mice were isolated from the liver. MACs separation was then performed in order to purify $Ly6G^+$ neutrophils from the remaining $Ly6G^-$ leukocyte population. The two populations were then analysed by flow cytometry to assess purity levels. The Ly6G positive population had a purity of approximately 80% (Fig. 5.23A) and the Ly6G negative population contained less than 2% of neutrophils (Fig. 5.23B).

RNA was then extracted from the $Ly6G^+$ and $Ly6G^-$ populations and mRNA expression levels of pro-inflammatory and neutrophil-associated genes were analysed by qPCR (Fig. 5.24). Viperin was originally identified as being induced in fibroblasts upon HCMV infection (233). Viperin is rapidly induced upon IFN stimulation or infection with various viruses, including acute and chronic LCMV, where viperin has been shown to contribute to the antimicrobial activity of neutrophils (234). Expression of inducible nitric oxide synthase (iNOS) produces large amounts of nitric oxide which has been reported to be important in the elimination of various viruses including CMV. iNOS knockout mice develop significantly higher titres of infectious virus in the lung (235) and are more susceptible to lethal infection with MCMV than wt mice (236). The expression of both

viperin and iNOS at the mRNA level was significantly higher in the $Ly6G^+$ population than the $Ly6G^-$ population, suggesting that neutrophils are a significant source of viperin and iNOS during acute MCMV infection. Cathepsin C activates a number of serine proteins including granzymes A and B. Cathepsin C knockout mice have organ specific defects in the ability to control MCMV replication and is therefore important in limiting viral replication (237). The interferon-induced Mx1 protein confers resistance to influenza virus by inhibiting viral mRNA synthesis in the nucleus of virally infected cells (238). Both of these genes are expressed at significantly higher levels in the $Ly6G^-$ population, suggesting that these proteins do not contribute to the antiviral activity of neutrophils.

Acute MCMV infection induces production of type I interferons which are potent activators of antiviral pathways. There are two known waves of IFNα/β production during early infection, the first occurring as early as 8 hours p.i which is driven by the engagement of the LTβ receptor with a membrane-bound heterodimer of LTα and LTβ (239). Interestingly, the second wave of IFNαβ expression correlates with the kinetics of neutrophil accumulation, at least in MCMV-infected livers (240). IFNα/β knockout mice and mice deficient in LTβ signalling are highly susceptible to MCMV infection (241) therefore these are important molecules for resistance to MCMV. However, when the mRNA expression of these was analysed, levels of IFNα/β and LTα/β were all significantly higher in the $Ly6G^-$ population as compared to the $Ly6G^+$ population, therefore suggesting that neutrophils are not a major source of these antiviral molecules. Expression levels of IFNγ and TNFα were also analysed as positive and negative controls respectively, based on known low and high expression of these molecules in neutrophils. As expected, neutrophils expressed significantly higher levels of TNFα but significantly less IFNγ than the $Ly6G^-$ cell population.

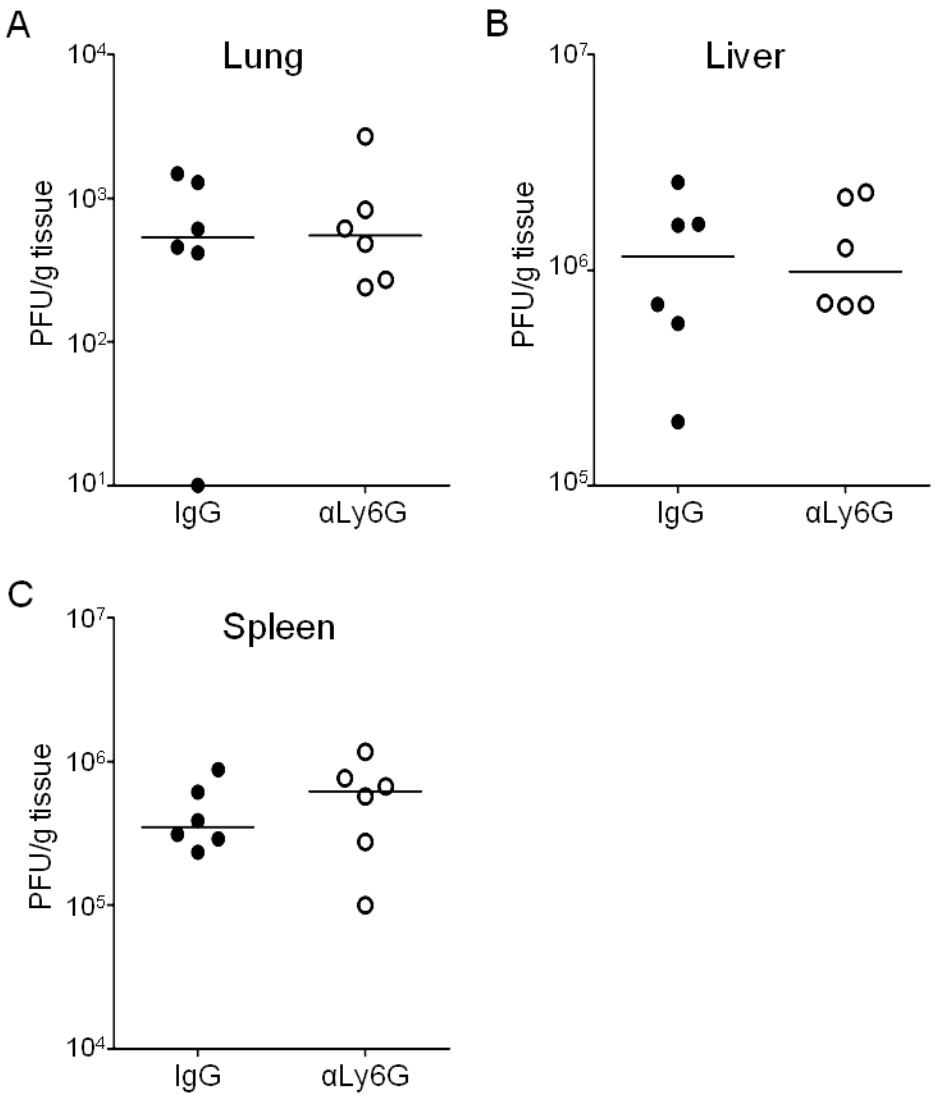

Figure 5.21. The absence of neutrophils during acute MCMV infection does not lead to increased virus at day 2 post-infection

Mice were infected with MCMV and administered an IgG control (closed symbols) or an anti-Ly6G antibody (open symbols). Homogenates from the lungs (A), livers (B) and spleens (C) of mice infected for 2 days were prepared for high sensitivity plaque assays to detect replicating virus. Data is expressed as PFU per gram of tissue. Horizontal bars show median values. Data is representative of 2 independent experiments.

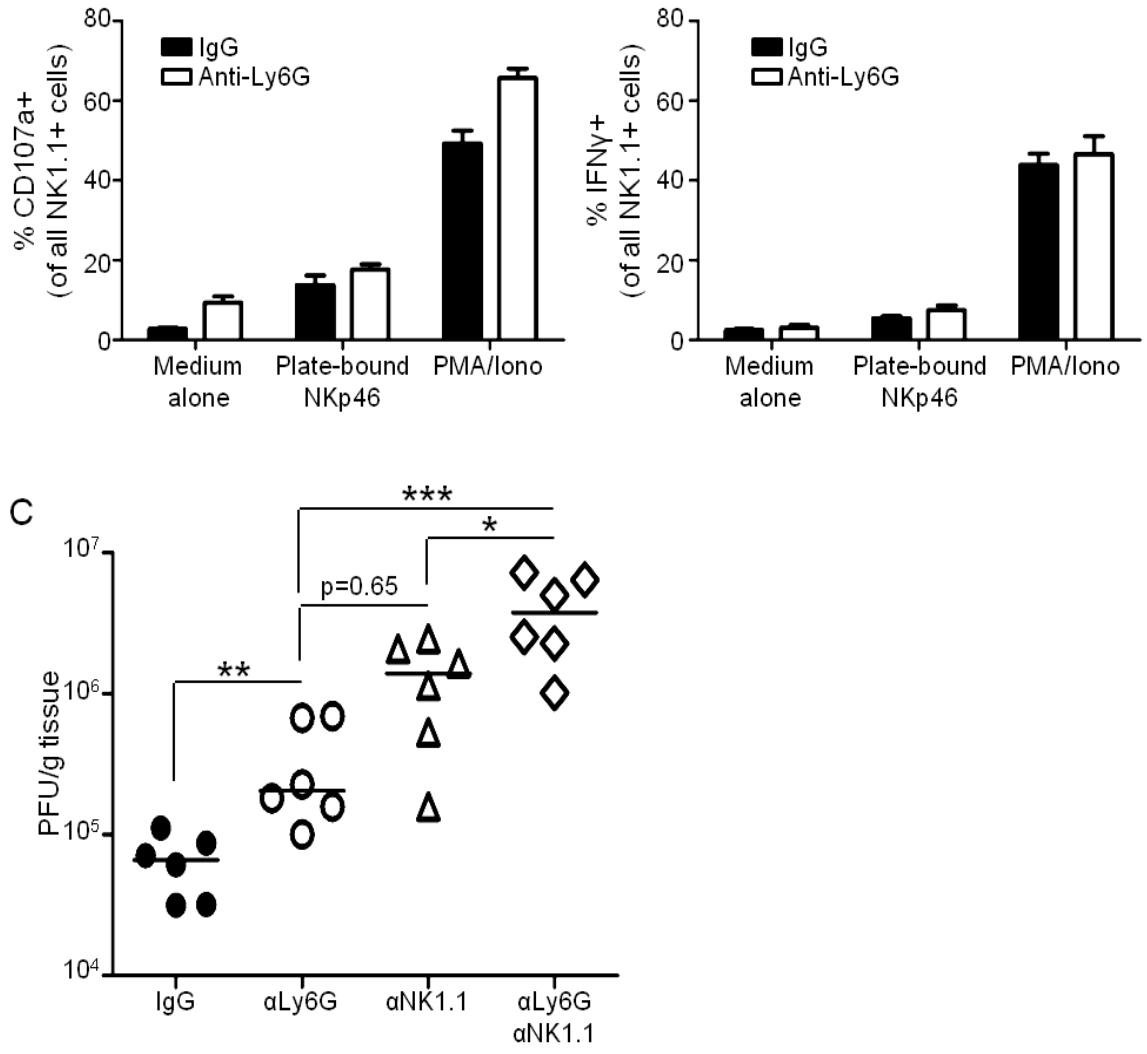

Figure 5.22. Neutrophils do not enhance NK cell function during acute MCMV infection

(A-B) Mice were infected with MCMV and administered an IgG control (closed bars) or an anti-Ly6G antibody (open bars). Lymphocytes were isolated from the livers at 4 days p.i and incubated for 4 hours with medium alone, plate-bound NKp46 or PMA/Ionomycin and analysed for expression of CD107a at the cell surface as well as intracellular IFNγ. Results show mean ± SEM of 6 mice per group. (C) Mice were infected with MCMV and administered an IgG control (closed circles), anti-Ly6G (open circles), anti-NK1.1 (open triangles) or anti-Ly6G and anti-NK1.1 (open diamonds). Homogenates from the livers of 4 day infected mice were prepared for high sensitivity plaque assays to detect replicating virus. Data is expressed as PFU per gram of tissue. Horizontal bars show median values. *p<0.05, **p<0.01, ns=not significant.

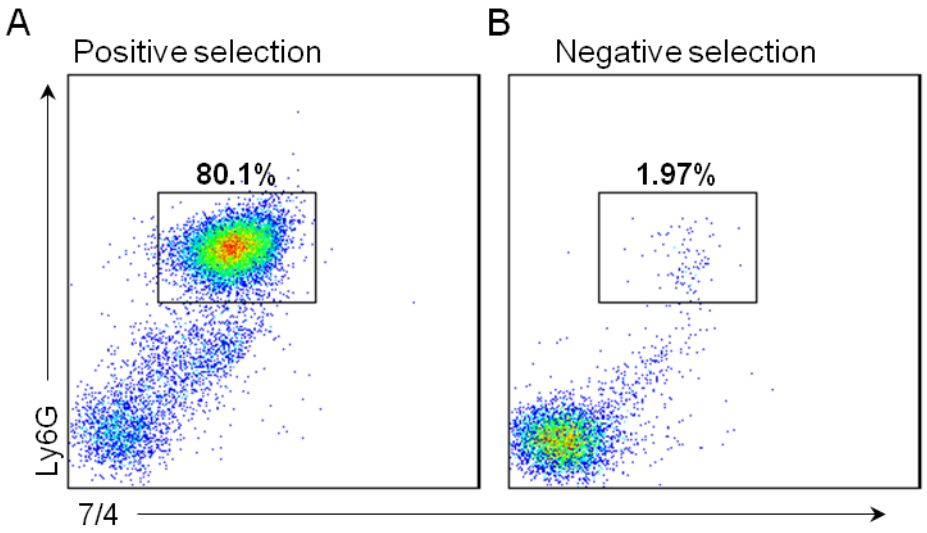

Figure 5.23. Analysis of Ly6G$^+$ cells following MACS separation
Leukocytes were isolated from the livers of day 2 MCMV-infected mice. Ly6G positive cells were separated from the Ly6G negative cells by MACS separation. The positive fraction (A) and negative fraction (B) were then analysed by flow cytometry for the proportion of Ly6G positive cells. Results represent 3 mice per group.

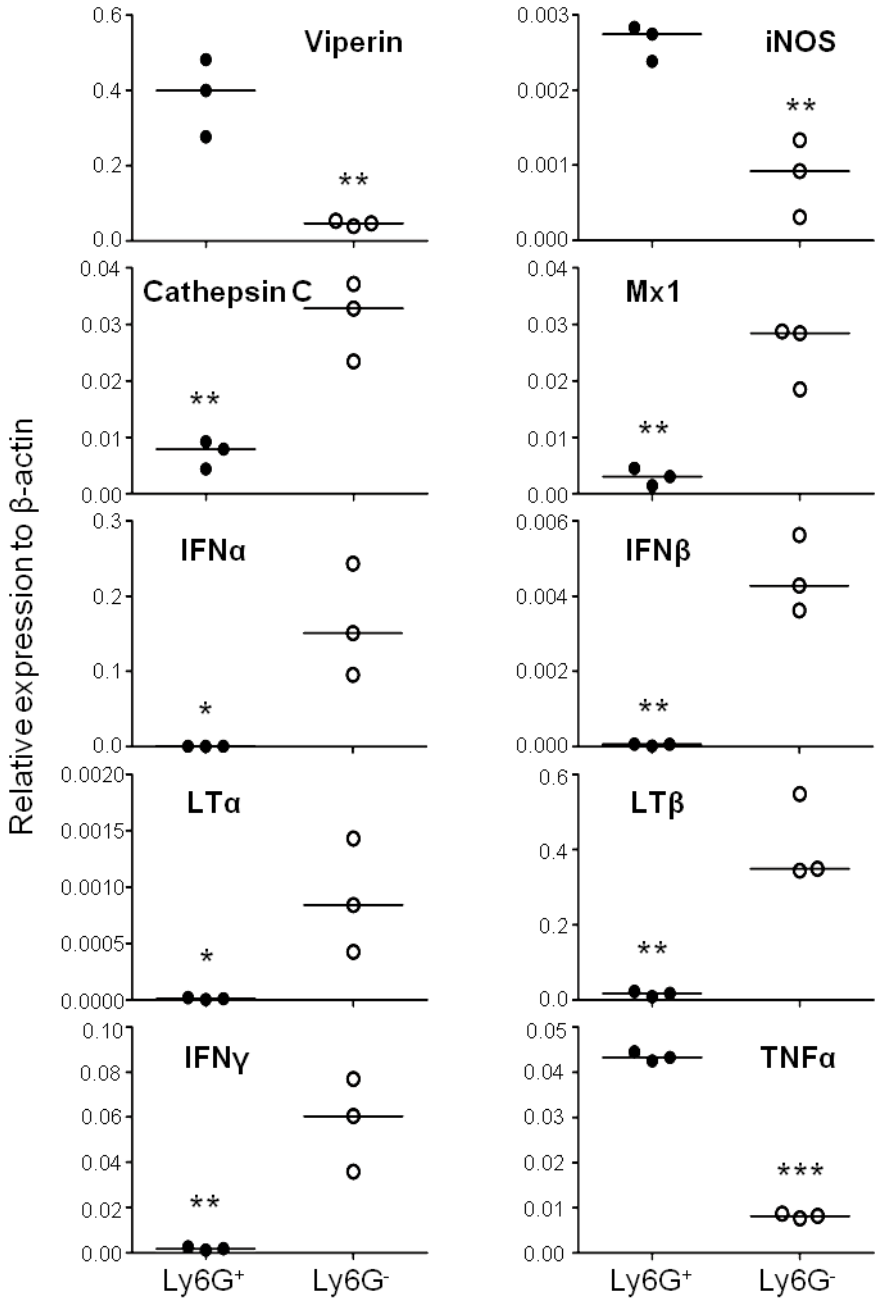

Figure 5.24. Neutrophils from MCMV-infected mice express a distinct gene transcription profile

Leukocytes were isolated from the livers of day 2 MCMV-infected mice. Ly6G positive cells (closed circles) were separated from the Ly6G negative cells (open circles) by MACS separation. RNA was then extracted from both populations of cells and converted to cDNA. Expression of different genes was detected by qPCR. Data is shown as gene expression relative to β-actin expression. Horizontal bars represent the median value. *p<0.05, **p<0.01, ***p<0.001

5.2.16. MCMV-infected livers from neutrophil depleted mice show a similar gene transcription profile as non-depleted mice

Neutrophils from MCMV-infected mice show a different pro-inflammatory transcription profile compared to non-neutrophils, and express significantly higher levels of viperin, iNOS and TNFα (Fig. 5.24). Therefore, to assess if the production of any of these molecules contributed to the protective immunity that neutrophils provide during early *in vivo* MCMV infection, livers from day 2 infected mice that were depleted of neutrophils were analysed for the same pro-inflammatory genes and compared to livers from non-depleted mice. However, livers from neutrophil depleted mice showed a very similar level of expression in all of the genes analysed (Fig. 5.25).

5.2.17 Nitric oxide expression in neutrophils increases in the presence of MCMV

As gene expression analysis of livers from IgG and anti-Ly6G MCMV-infected mice did not reveal any differences in the antiviral genes tested, other possible mechanisms for how neutrophils provide antiviral immunity were explored. Reactive oxygen species (ROS) and nitric oxide (NO) are known products of neutrophils which act as broad spectrum inhibitors of pathogens. To assess if neutrophils could be directly activated by MCMV, neutrophils were purified from naïve mice. High levels of purity (>90%) were reached by using sequential negative followed by positive selection (Fig. 5.26A) (section 2.13.2). These neutrophils were then incubated overnight in the presence or absence of MCMV and analysed for APF fluorescence, which is an indicator of ROS, and DAF-FM diacetate fluorescence, which is a read out for NO production. Neutrophils incubated with MCMV did not show an up-regulation in APF fluorescence compared to those without virus (Fig. 5.26B) in either percentage (6.68% vs. 5.67%) or MFI (217 vs. 194), but interestingly NO expression was significantly increased (Fig. 5.26C) both by percentage (89.5% vs. 58.4%) and MFI (15900 vs. 2703), suggesting that neutrophils are directly activated by MCMV and up-regulate NO expression in response to the virus.

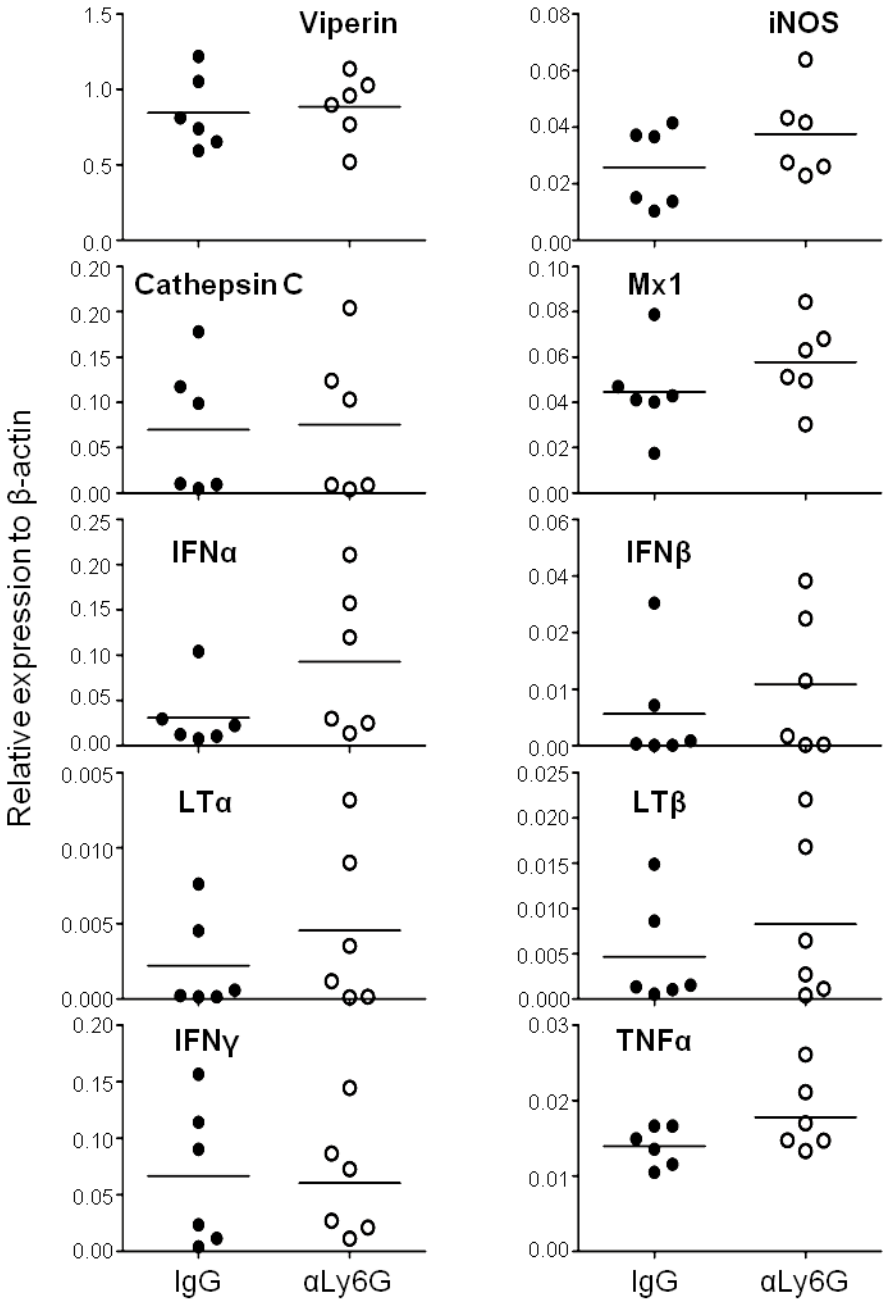

Figure 5.25. MCMV-infected livers from neutrophil depleted mice show a similar gene transcription profile as non-depleted mice
MCMV-infected mice were treated with IgG (closed circles) or anti-Ly6G (open circles). At day 2 p.i, livers were excised and RNA was extracted and converted to cDNA. Expression of different genes was detected by qPCR. Data is shown as gene expression relative to β-actin expression. Horizontal bars represent the median value.

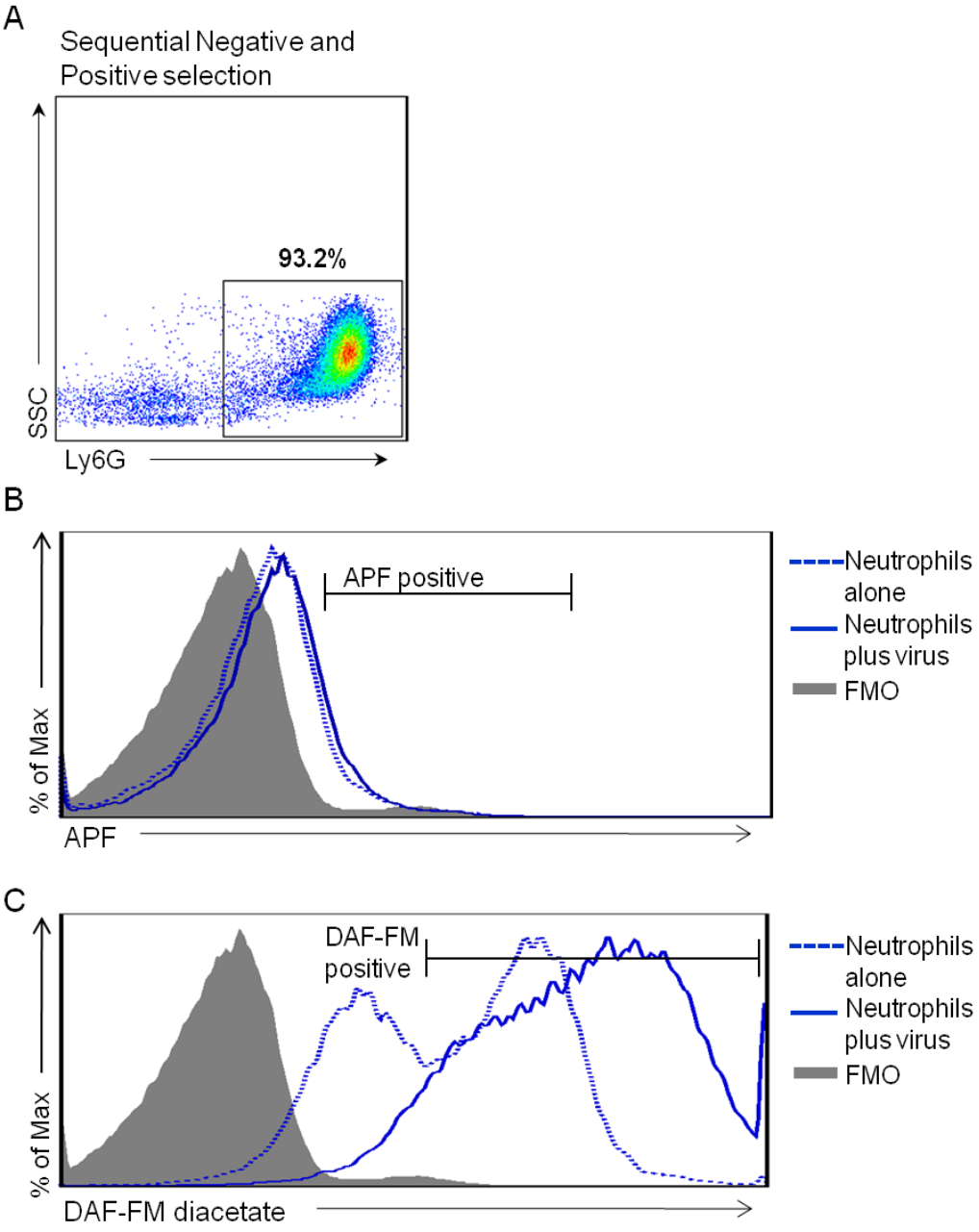

Figure 5.26. Increased release of nitric oxide by neutrophils in the presence of MCMV

(A) Representative facs plot showing purified neutrophils isolated from spleens of naïve mice following sequential negative and positive selection. (B and C) Representative overlay histograms of APF (B) and DAF-FM diacetate (C) fluorescence in purified neutrophils incubated overnight in the presence (solid blue line) or absence (dashed blue line) of MCMV (shaded histogram = FMO control). Results represent 3 independent experiments.

5.2.18. Neutrophils directly inhibit MCMV replication *in vitro*

To determine if neutrophils could directly inhibit MCMV replication, purified neutrophils from naïve mice were incubated with MCMV-infected 3T3 cells at varying effector to target ratios for 7 days. Supernatants were then taken and analysed for levels of replicating virus by standard plaque assay. Interestingly, the levels of replicating virus in the supernatants decreased proportionately as the ratio of neutrophils to targets increased (Fig. 5.27). The levels of replicating virus decreased significantly from an average of 405 PFU/ml when no neutrophils were present (ration of 0:1) to an average of 50 PFU/ml when the ratio of neutrophils to 3T3s was 1:1, thus demonstrating that neutrophils can directly inhibit MCMV replication *in vitro*. A freeze/thawed control was also included to demonstrate that it an the inhibition of MCMV replication was not an artefact of dying neutrophils.

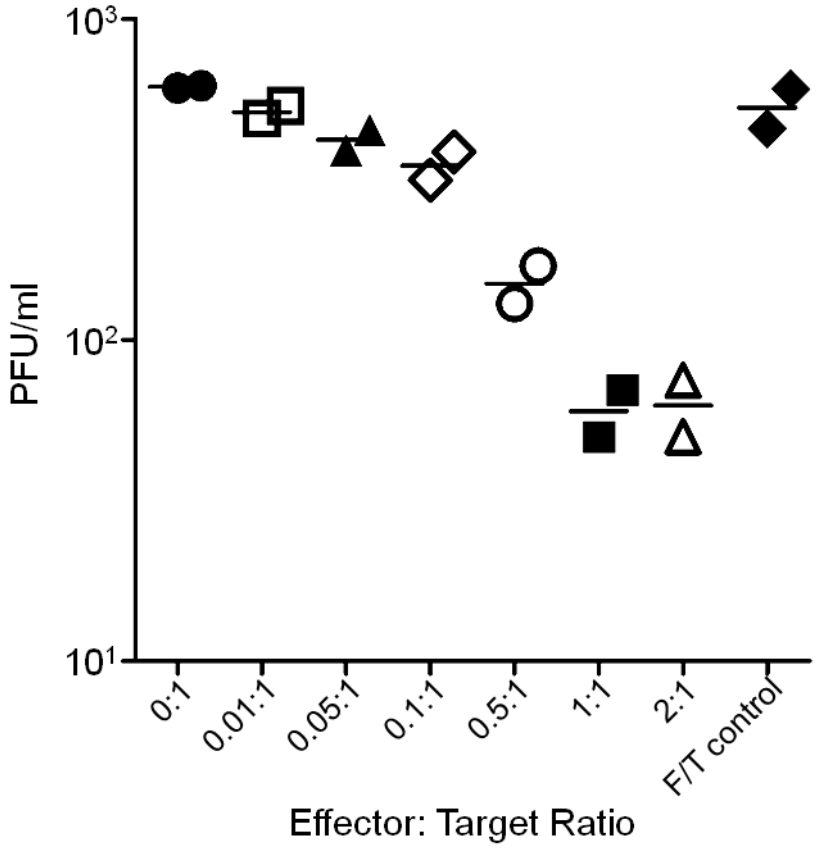

Figure 5.27. Neutrophils directly inhibit MCMV replication *in vitro*
Purified neutrophils were incubated with MCMV-infected 3T3 cells (MOI of 0.02) for 7 days at varying effector:target (neutrophil:3T3) ratios. Supernatants were then taken for plaque assays and amounts of replicating virus were measured. Data is expressed as PFU/ml and results are representative of 2 independent experiments. F/T = freeze thawed control.

5.3 Discussion

It has been previously shown that IL-22 mRNA expression is increased in the livers of mice with MCMV-induced hepatitis as compared to uninfected controls (242). During acute MCMV infection, the virus targets not only the liver, but other visceral organs including the lung and the spleen. Analysis of IL-22 at the protein level revealed that IL-22 is expressed in the visceral organs of naïve mice as well as in infected mice, where a significant increase in IL-22 expression was observed. This observation supports and expands on the findings of Brand *et al* who showed an increase in IL-22 mRNA in the liver (242).

The ability of many different cell types to express IL-22 has been extensively reviewed (100, 135, 136, 227, 243). Unsurprisingly, $CD4^+$ and $CD8^+$ T cells were found to express IL-22 in both naïve and infected mice. IL-22 derived from γδ T cells was shown to protect against lung fibrosis in a mouse model of hypersensitivity pneumonitis (148), therefore this cell type was also analysed for IL-22 expression in my MCMV model. Although IL-22 was found to be expressed by a small proportion of the γδ T cells, when calculated back to total numbers, they were found to be a relatively minor population contributing to overall IL-22. As well as the widely discussed sub-population of $ROR\gamma t^+$ mucosal NK cells (244), conventional $NK1.1^+$ cells capable of producing IFNγ, have also been shown to produce IL-22 in influenza infected mice (220). Similar to the findings of Guo and Topham (220), IL-22 producing $NK1.1^+$ $CD3^-$ cells were also detected in MCMV infection, and were actually the dominant population of cells in the lung and the liver of MCMV-infected mice that produced IL-22. The phenotype of these IL-22 producing NK cells was then analysed further. They were found to express conventional NK cell surface markers including Ly49H, KLRG-1, CD11b and CD122, as well as CD69 upon MCMV infection, suggesting that these were mature, conventional $NK1.1^+$ NK cells, distinct from the more immature-like $ROR\gamma t^+$ mucosal NK cells. This conclusion is supported by the previously published observation that lung NK cells capable of producing IL-22 during influenza infection are

also of a mature phenotype, similar to that found in splenic NK cells, and are likely to be distinct from the gut innate lymphoid-like NK-IL-22 cells previously described (220). ILCs that lack expression of most linage markers have also been shown to be important producers of IL-22 (reviewed in (135)). $NKp46^+$ ILCs express IL-22 but are found predominantly in the skin and small intestine, and $CD4^+$ ILCs are a dominant source of IL-22 in the large intestine and are therefore likely to be an irrelevant source of IL-22 in the organs of interest in this MCMV model. Interestingly, in humans, a subset of IL-22 producing ILCs can be detected in the adult lung and gut but these express CD127 (245), so are again likely to be distinct from mature, conventional NK cells capable of producing IL-22.

Analysis of IL-22 expression by flow cytometry revealed that NK cells were the dominant source of IL-22 in the lung and liver at 4 days p.i, which was confirmed by NK cell depletion experiments. In the absence of NK cells during acute MCMV infection, IL-22 protein levels were markedly reduced, although not completely abolished, again suggesting NK cells are the predominant source of lung and liver IL-22, however, other cell populations also contribute. Depletion of NK cells during influenza infection also leads to a reduction in total IL-22 protein in the lung, although this reduction was not as great as was observed in my MCMV model (220). Associated with a lack of NK cells during acute MCMV infection is a significant increase in virus load, therefore to rule out that the increase in virus load wasn't the cause of reduced IL-22, levels of IL-22 protein were measured following depletion of neutrophils which also leads to an increase in virus load. As no significant reduction was seen, this validates the conclusion that NK cells significantly contribute to IL-22 production in the lung and liver of MCMV-infected mice.

A neutralising anti-IL-22 antibody was administered intravenously on the day of infection to explore the hypothesis that IL-22 has an antiviral role during acute MCMV infection. As early as 2 days p.i, a significant increase in virus load was observed in mice given the neutralising antibody in both the lung and liver and this persisted until day 4 p.i. Interestingly, IL-22 neutralisation did not influence virus load in the spleen. This is not that surprising, given what is so far known about the expression of the IL-22R. IL-22Rα is expressed exclusively on non-haematopoietic cells and its expression is predominantly found in epithelial cells of barrier surfaces including the oral/gastrointestinal tract, skin and lung, and is also found to be strongly expressed in the liver (246, 247). Therefore, if there is limited IL-22Rα expression in cells of the spleen, IL-22 is unlikely to play an important role in this organ and thus, neutralisation of IL-22 would have limited, if any, effects.

As well as the increase in virus load in the lung and liver following IL-22 neutralisation, interestingly, a reduction in neutrophil accumulation was also observed in these two IL-22 responsive organs. IL-22Rα is not usually expressed on leukocytes, but in anaplastic lymphoma kinase-positive (ALK^+) anaplastic large cell lymphoma (ALCL) patients, this receptor is expressed on T cells. In an investigation to examine the consequences of aberrant expression of this receptor, a mouse model of ALK^+ALCL was set up by generating transgenic mice expressing IL-22Rα on lymphocytes (248). The IL-22Rα transgenic mice developed severe neutrophilia in association with increased serum IL-22, IL-17 and G-CSF. However, no other direct link with IL-22 and neutrophil recruitment has been reported. In humans, patients with ulcerative colitis and Crohn's disease have increased levels of IL-22 in the inflamed mucosa, and IL-22 was shown to promote pro-inflammatory gene expression in epithelial cells, including IL-8 (CXCL8), a chemo-attractant for human neutrophils (249, 250). Mice do not have an IL-8 homologue but other known neutrophil attractants include CXCL1, CXCL2 and CXCL5. G-CSF is also important in stimulating survival, proliferation, differentiation and function of neutrophils (251).

To investigate if IL-22 neutralisation during MCMV infection resulted in a reduction in chemokines associated with neutrophil chemotaxis, expression of these at both the mRNA and protein level was measured and compared to expression in IgG treated mice. However, no significant effect on these chemokines was seen following anti-IL-22 treatment, although a slight trend towards reduced CXCL1 was observed in the livers of anti-IL-22 treated mice. Interestingly, neutralisation of IL-22 during *Klebsiella pneumoniae* infection is not associated with diminished G-CSF or CXCL1 levels (143). Lower amounts of CXCL1 and G-CSF in the lungs during infection were only seen when IL-22 was neutralised in IL-17 knockout mice, suggesting IL-17 and IL-22 work in conjunction to induce expression of these chemokines. Furthermore, CXCL1 and CXCL5 expression were induced in human bronchial endothelial cells when stimulated with both IL-17 and IL-22 (143). However, treatment with recombinant IL-22 during infection resulted in an increase in CXCL1 and CXCL2 transcripts in the bronchial epithelium (143). Interestingly, a single IP injection of recombinant IL-22 into wt mice resulted in increased neutrophil counts in the blood as well as increased levels of CXCL1 at 1 hour post-injection but was not observed 24 hours post-injection (142). These data suggest that IL-22 has the potential of inducing neutrophil-associated chemokines and hence lead to an increase in neutrophil accumulation, possibly in conjunction with IL-17, depending on the model system used. It is possible that in my MCMV model, looking 24 hours p.i for differences in chemokine expression was actually too late. Therefore, I cannot rule out the possibility that the reduction in neutrophils observed following anti-IL-22 treatment in MCMV-infected mice was a consequence of reduced neutrophil-associated chemokines. Also, it is conceivable that IL-22 may act to enhance neutrophil mobilisation from the bone marrow. Further analysis at different time points, as well as looking in different compartments including the blood, would be needed to answer this question more definitively.

To date, the majority of studies investigating the relationship between CMV and neutrophils have been *in vitro* experiments with HCMV. Infection of fibroblasts with HCMV results in increased expression of the neutrophil chemo-attractant IL-8 at the mRNA and protein level (252) and infection of endothelial cells by HCMV also resulted in increased levels of both IL-8 and GROα (now known as CXCL1) (253). Both studies showed that release of these chemokines enhanced neutrophil migration in a transendothelial migration assay. Further work on HCMV-induced chemokines revealed that the HCMV genes, UL146 and UL147, encode the viral homologues of CXCL1 and CXCL2 (vCXCL1 and vCXCL2). As yet, there is no evidence to suggest that vCXCL2 is a functional chemokine, however, vCXCL1 has been shown to act as an agonist on both CXCR1 and CXCR2; further adding to the premise that HCMV infection enhances neutrophil migration (254, 255). The consensus by the authors of all these studies for why HCMV would induce neutrophil recruitment is that neutrophils can be infected directly by HCMV or acquire infectious virus particles during transmigration and therefore aid virus dissemination.

Crucially however, no direct *in vivo* evidence regarding the role that neutrophils play in herpesvirus infections exists. Two early studies demonstrated that *in vitro*, MCMV infection reduced chemotactic activity of neutrophils (256) and that during acute infection *in vivo*, migration of neutrophils out of the blood was impaired (257). The authors suggest that direct viral infection of neutrophils may contribute to altered function. This reduction in chemotactic activity was also observed in a guinea pig model of CMV (258). Interestingly, a study into the antiviral effects of leukotrine B4 (LTB4) on CMV infection revealed that stimulation with LTB4 could activate neutrophils via the LTB4 receptor which led to a reduction in virus titres in CMV-infected human leukocytes (259). This was further supported by *ex vivo* experiments using LTB4 treated neutrophils from mice which also displayed antiviral activity towards CMV via release of antimicrobial peptides (259).

Given the results of the studies described above in conjunction with my observations that a reduction in neutrophil accumulation was associated with an increase in virus load following anti-IL-22 administration, the hypothesis that neutrophils perform an antiviral role during acute MCMV infection was tested. Neutrophils were depleted using an anti-Ly6G specific antibody (1A8), which was shown to be neutrophil specific and did not cause depletion of any other cell subset. Enhanced virus-induced weight loss was observed in mice depleted of neutrophils, suggesting the mice were suffering from more severe clinical symptoms of disease, but importantly, virus load was significantly increased in the lung and the liver at 4 days p.i. Interestingly, neutrophil depletion did not influence virus load in the spleen. An explanation for why neutrophil depletion does not have an effect on virus load in the spleen is that at 4 days p.i, neutrophils only account for a very small proportion of the total cells (approximately 1%) and therefore deleting these is likely to have far less of an impact than in other organs where neutrophils make up a much more significant cell population, such as in the lung and liver. None the less, this data supports the hypothesis that neutrophils do have an antiviral role but in an organ specific manner.

The novel finding that neutrophils have a protective role against acute MCMV led me to investigate if they provided this antiviral immunity as early as 2 days p.i. Interestingly, no difference in virus load following neutrophil depletion was seen in the lung or liver at this earlier time point, despite neutrophils making up a significant population of cells in both organs. The long held view of neutrophils as short-lived effector cells of an acute inflammatory response whose primary role is to clear extracellular pathogens is no longer considered accurate. This is due to recent evidence showing their importance in the regulation of innate and adaptive immunity in response to various infections and inflammatory disorders (reviewed in (8, 260)). Neutrophils have been shown to engage in complex bidirectional interactions with macrophages, DCs, NK cells and T and B cells (8). The delayed kinetics of antiviral immunity provided by neutrophils in this model of acute MCMV infection suggested at first a non-direct mechanism for how neutrophils are

providing protection. Given the capability of neutrophils for crosstalk and the known importance of NK cells during early MCMV infection, NK cell function was examined in the presence or absence of neutrophils at 4 days p.i. Interestingly, levels of IFNγ production by NK cells were comparable between both groups and in fact, in the absence of neutrophils, CD107a expression was slightly enhanced when neutrophils were depleted, suggesting that neutrophils play no role in NK cell function during acute MCMV infection. It is also worthwhile to note that depletion of both NK cells and neutrophils during MCMV infection resulted in a significant increase in virus load compared to virus loads seen when just one cell type was depleted, suggesting that both populations are important in providing antiviral immunity during acute MCMV infection.

Following on from the lack of evidence in support of the hypothesis that neutrophil-NK cell crosstalk led to protection from MCMV, the possibility that neutrophils were exerting their antiviral activities directly was next explored. When first comparing mRNA expression of a range of pro-inflammatory and neutrophil associated genes from hepatic $Ly6G^{+}$ neutrophils with $Ly6G^{-}$ cells from the liver, viperin, iNOS and TNFα were expressed at significantly higher levels in the neutrophil population as compared to the non-neutrophil cell population. Therefore, if expression of one or more of these was significantly lower in livers from neutrophil depleted mice, this could provide an insight into a possible mechanism for how neutrophils were providing antiviral immunity. However, no differences were seen at the mRNA level of any of the genes analysed. On the other hand, this is not that surprising given that it is not exclusively neutrophils that express these molecules, but a whole range of immune cells and therefore depleting just one of the populations of cells that produce these is unlikely to have an effect on expression when analysing the tissue as a whole. Furthermore, my analysis only addressed a very small proportion of neutrophil associated genes, whereas neutrophils have been shown to express numerous cytokines, chemokines and angiogenic factors either spontaneously or under stimulation (8), and therefore, more in depth analysis would need to be done in

order to address exactly which of these genes were up-regulated in neutrophils upon infection with MCMV.

To further explore the question of how neutrophils provided antiviral protection, *in vitro* assays were set up to investigate if neutrophils inhibited MCMV replication directly. Interestingly, when highly purified neutrophils from naïve mice were incubated with MCMV overnight, a significant up-regulation in fluorescence of DAF-FM diacetate was seen. This increase in fluorescence is caused when DAF-FM diacetate reacts with NO, suggesting NO production within the neutrophils was enhanced in the presence of MCMV. NO has been shown to be important for antiviral inflammatory and immune defences in the human lung (261). It has also been demonstrated that NO has antiviral effects during Japanese encephalitis virus infection (262, 263), as well as having important anti-inflammatory and antiviral roles during human rhinovirus infections (264). It is possible therefore that an increase in NO production by neutrophils may also have antiviral effects against MCMV.

To attempt to elucidate further if MCMV replication could be directly inhibited by neutrophils, 3T3 cells were infected with MCMV and then incubated with highly purified neutrophils in varying ratios of effector cells to target cells. Remarkably, as the ratio of neutrophils to targets was titrated upwards, a significant decrease in replicating virus was observed, demonstrating that neutrophils could directly inhibit MCMV replication. Future studies could be performed by repeating this *in vitro* assay but also encompassing the presence of a range of different neutralising antibodies and inhibitors such as anti-TNFα, anti-IFNα/β, anti-IFNγ as well as more specific neutrophil inhibitors such as iNOS inhibitors, protease inhibitors, DPI to prevent superoxide release and cytochalasin B or D to scramble actin and impact on phagocytosis and degranulation, in order to elucidate the mechanism for this antiviral activity.

Finally, it is important to note that neutralising IL-22 during acute MCMV infection led to the observation of impaired neutrophil accumulation, which consequently uncovered a novel role for neutrophils during early infection. However, as discussed, depletion of neutrophils caused a significant increase in virus load in the lung and liver at 4 days p.i, but not at 2 days p.i. Crucially, neutralisation of IL-22 caused significant increase in virus load in these two organs at both time points. This suggests that IL-22 is playing an antiviral role via additional mechanisms other than just in the recruitment of neutrophils. To date, mechanisms by which IL-22 provides protection through regulating host defence and inflammation include the induction of pro-inflammatory cytokines and chemokines to recruit various leukocytes to control invading pathogens, the production and secretion of antimicrobial peptides and defensins, the secretion on mucins from goblet cells, and finally the activation of STAT3 in epithelial cells to enhance wound healing (100, 135, 149, 227). One or more of these mechanisms may also contribute to the control of early MCMV infection, such as IL-22-induced production of beta-defensins from epithelial cells, which could potentially provide antimicrobial activity against MCMV. However, further investigation into these possible mechanisms is required. This could be achieved by using a mucosal challenge model of MCMV infection to assess the role that IL-22 may play in infections via mucosal surfaces, which may be considered more physiologically relevant.

In summary, I have revealed a tissue-specific antiviral role for IL-22 during acute MCMV infection. Interestingly, via the observation that neutralisation of IL-22 was associated with a reduction in neutrophil numbers, I have also demonstrated that neutrophils can directly inhibit MCMV replication. A summary of these findings is shown in Fig. 5.28. These experiments not only uncover a novel role for IL-22 in host defence against viral pathogens, but also provide a new insight into the importance of neutrophils in limiting MCMV infection. These data therefore challenge the widely held view that comes from *in vitro* experiments which suggests that the only role for neutrophils in HCMV infection is to aid viral dissemination.

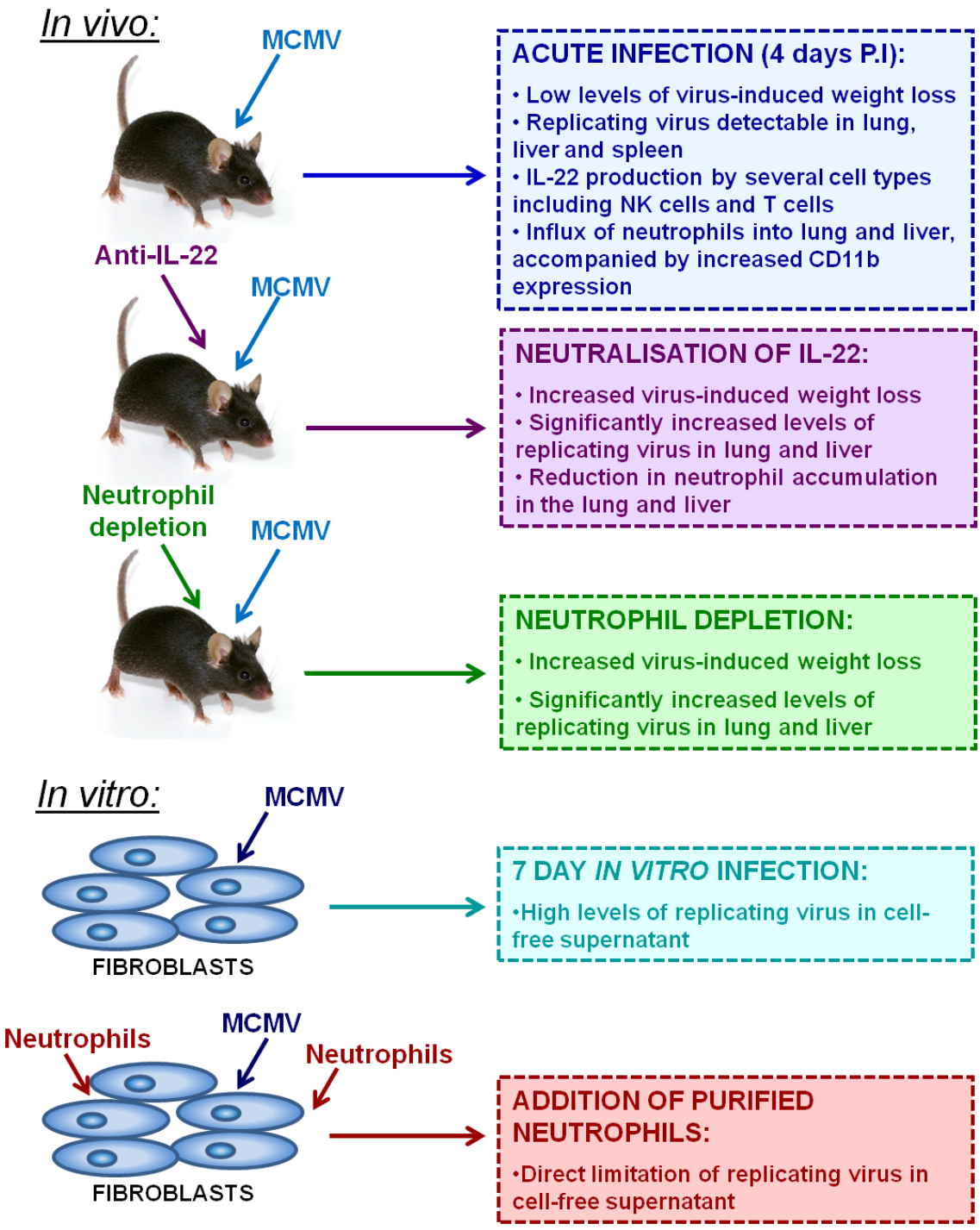

Figure 5.28. Summary of *in vivo* and *in vitro* findings on the role of IL-22 and neutrophils during acute MCMV infection
In vivo experiments revealed a tissue-specific antiviral role for IL-22 during acute MCMV infection which was associated with a reduction in neutrophil accumulation. Neutrophil depletion experiments also revealed an antiviral role for neutrophils during acute MCMV infection and *in vitro* experiments demonstrated that neutrophils can directly inhibit MCMV replication

Chapter 6 - General discussion

In this thesis, I set out to elucidate the role of mammalian IL-10 during acute MCMV infection, and also the role that the IL-10 family member IL-22 has during infection. These studies afforded novel insights into the *in vivo* functions of these cytokines. Firstly, a surprising antiviral role for IL-10 during acute MCMV infection was revealed, which was achieved via limitation of activation-induced death of NK cells, thus leading to a reduction in virus load. Secondly, a tissue-specific antiviral role for IL-22 during acute MCMV infection was also discovered; and further investigation into this led to the unpredicted finding that neutrophils play a protective role during infection by directly inhibiting MCMV replication.

MCMV is the best-characterised and most widely used animal model for cytomegalovirus infection and is a powerful tool for defining the host immune response to infection due to the availability of extensive immunological reagents as well as transgenic mice with specific immune defects. In conjunction with the MCMV infection model, I utilised both blocking and neutralising antibodies to demonstrate previously unknown protective functions of the related cytokines IL-10 and IL-22 against acute herpesvirus infections *in vivo*. However, the ultimate reason for carrying out research in MCMV is to enhance our understanding of host-virus interactions which can be translated into the context of HCMV interactions with human hosts. From this research, we could potentially achieve better therapeutic strategies to treat HCMV infection or an HCMV vaccine to significantly reduce morbidity and mortality associated with HCMV infection and disease and consequently realise substantial savings in the health care costs associated with HCMV disease. Therefore I will discuss the findings made in this thesis in relation to this more extensive, long-term goal.

Firstly, I will address the question of whether IL-10 could be used as a therapeutic target for HCMV. Due to the broad anti-inflammatory effects of IL-10, a variety of clinical studies have been undertaken using systemic administration of recombinant IL-10 to treat patients with immune-mediated inflammatory diseases such as psoriasis, Crohn's disease and rheumatoid arthritis. Early phase I and phase II studies showed promising results in psoriasis and Crohn's disease, although results were less promising in rheumatoid arthritis patients. However, larger psoriasis studies showed only modest therapeutic benefits, whilst the most favourable clinical responses in Crohn's disease patients were observed at an intermediate dose of IL-10 (reviewed in (265)).

Experimental evidence suggests that exogenous IL-10 administration to HIV-infected monocyte-derived macrophages results in a dose-related inhibition of HIV reverse transcription activity and HIV proliferation. Furthermore, exogenous IL-10 may inhibit viral assembly in HIV-infected macrophages. Taken together, these findings strongly suggest that IL-10 administration to HIV-infected individuals may be beneficial (reviewed in (266)). To date, three phase I trials of treatment with recombinant human IL-10 in HIV infection have been reported. One study described a transient reduction in HIV replication; however the other two studies showed no significant reduction in HIV levels or changes in $CD4^+$ T cell counts. Thus, IL-10 may be useful in arresting detrimental inflammatory responses caused by HIV, but may be ineffective when viral replication is ongoing (reviewed in (266)). Experiments using human PBMCs from individuals who were infected with a variety of pathogens demonstrated that immune responsiveness to these pathogens was improved in the presence of anti-IL-10 monoclonal antibodies. These specific pathogens included leishmaniasis, schistosomiasis, leprosy and tuberculosis (reviewed in (102, 265)).

Could administration of recombinant IL-10, or conversely treatment with anti-IL-10 antibodies promote immune responses against HCMV infection? I demonstrated in chapter 3 of this thesis that IL-10 is expressed by numerous haematopoietic cells during acute MCMV infection and that virus-induced IL-10 promotes the accumulation of NK cells by limiting NK cell activation-induced death, which leads to enhanced viral clearance. Interestingly, an earlier study using an model of MCMV infection with uncontrolled virus replication in mice lacking perforin, demonstrated that NK cell-derived IL-10 suppressed pathogenic $CD8^+$ T cell responses and limited MCMV replication (186). From the results of my investigations in conjunction with results from this study, it can be inferred that via its suppressive properties of limiting self-destructive immune responses, endogenous IL-10 functions to protect the host during acute herpesvirus infection. Therefore it could be suggested that increasing host IL-10 levels through the administration of recombinant IL-10 during primary infection may further enhance antiviral immunity against HCMV. However, it would be critical to ensure that the host immune response was not so severely suppressed by IL-10 that it could not mount any kind of attack against viral invasion, as the balance between pro-inflammatory and inhibitory signals during acute infection is an extremely important and finely tuned one, and if tipped too far in favour of immune inhibition, may lead to severe consequences. Furthermore, primary HCMV infection in immune-competent hosts is generally asymptomatic and therefore therapeutic treatment at this stage is very unlikely. Moreover, the predominant conclusion from the collective clinical studies described above was that therapeutic administration of IL-10 is unlikely to be beneficial in situations where pathogens have not yet been eradicated/are still undergoing replication.

Additionally, the complex nature of herpesvirus infections makes potential treatment of HCMV infection with IL-10 even more problematic. After acute infection, herpesviruses establish persistency or latency within the host. It has been demonstrated in MCMV that during the chronic replicating or chronic latent stages of infection, endogenous IL-10

antagonizes antiviral immunity, thus contributing to viral dissemination and the development of latency within the host (167, 168). Therefore, inhibiting the IL-10 signalling pathway with anti-IL-10 antibodies to promote immune responses during these stages may be a more beneficial pathway to explore, as this could lead to a reduction in chronic HCMV infections, dissemination and reactivation, thus limiting the harmful consequences associated with this, such as congenital infections. Indeed, targeting the cmvIL-10 gene, UL111A, to improve immune responses to HCMV is a real possibility, as demonstrated by the work of Barry and colleagues showing rhcmvIL-10 to be a viable vaccine candidate because of its high immunogenicity during natural infection combined with the lack of cross-reactivity with rhesus cellular IL-10 (203, 204). Therefore I attempted to elucidate the functions of cmvIL-10 in a biologically relevant system by generating a cmvIL-10 deficient Merlin strain of HCMV. However, despite successfully creating this virus, the issue of low virus yields caused significant limitations to this research. Resolutions to this issue have nonetheless been discussed thoroughly in section 4.3.

The second major discussion point that arises from the results of my thesis is whether IL-22 could be used as a therapeutic target for HCMV. Studies of mouse model systems and observations of human diseases including IBD, psoriasis, rheumatoid arthritis and cystic fibrosis where elevated levels of IL-22 are observed (reviewed in (135, 136)) indicate that targeting the IL-22-IL-22R pathway with functional agonists and antagonists such as recombinant cytokine or even via gene therapy delivery may provide new therapies for the treatment of infection, chronic inflammatory disorders and wound healing. However, the dual pro-inflammatory and anti-inflammatory functions of IL-22 are the biggest obstacle for developing therapeutics based on this cytokine.

The overriding message from previous studies investigating the role of IL-22 in viral infections was that the effects of this cytokine were pathogen-dependent. I demonstrated in chapter 5 that IL-22 is expressed by NK cells and $CD4^+$, $CD8^+$ and γδ T cells during acute MCMV infection, and that IL-22 provides tissue-specific protection by limiting MCMV replication. This is the first study to unequivocally demonstrate an antiviral role for IL-22 during herpesvirus infections. This would suggest that increasing IL-22 levels within the host during CMV infection could potentially enhance antiviral immunity. One advantage that administering IL-22 to HCMV infected individuals would have over that of IL-10 is that unlike the IL-10R1 which is expressed by most haematopoietic cells, the IL-22R1 is exclusively expressed on non-haematopoietic cells. The IL-22R1 is found extensively on epithelial cells, suggesting an important role in mucosal immunity, and is found on hepatocytes and has previously been shown to be important in limiting liver damage. My data showed that in the absence of IL-22 during acute MCMV infection, both the lung and liver had increased virus loads. Importantly, CMV remains the most important pathogen following lung transplantation (267) and is the most common cause of death after liver transplantation (268), thus enhancing IL-22 production after organ transplants may be beneficial by reducing virus load and subsequent CMV related disease of these organs. Furthermore, epithelial cells expressing the IL-22R are also found in the salivary gland. As one transmission route of HCMV is via saliva, treatment of IL-22 in HCMV infected individuals could potentially reduce levels of virus replication during the chronic replicating or chronic latent stages of infection or decrease the occurrences and severity of virus reactivation, thus reducing dissemination and spread of the virus. Therefore a major research focus of the laboratory is to establish a mucosal MCMV challenge model to enable the assessment of the role that IL-22 may play in infections via mucosal surface(s) using inoculum representative of “natural” infection.

Whilst investigating the effects of the cytokines IL-10 and IL-22 during acute MCMV infection, a somewhat unexpected finding was revealed. In chapter 5, I demonstrated that neutrophils have an antiviral role that had not been previously shown in relation to herpesvirus infections. *In vivo*, neutrophils protect against virus-induced weight loss and contribute to controlling viral replication in a tissue-dependent manner and *in vitro,* I established that neutrophils could directly inhibit MCMV replication. This finding could potentially be of great importance if it is proved that neutrophils also promote antiviral immunity against HCMV infection. Not only would it challenge the broadly held view that neutrophils are only important for aiding viral dissemination during infection, but may also have consequences for HCMV treatment.

HCMV infection is currently treated with a range of antiviral drugs including ganciclovir which is used in the treatment of CMV retinitis, CMV colitis and CMV disease in bone marrow and solid organ recipients; valganciclovir which is used in treatment of HIV patients and transplant recipients; foscarnet which is used against drug resistant CMV and for CMV retinitis; and cidofovir which is used to treat CMV retinitis in AIDS patients (269). However, one of the side effects of these antiviral drugs is that patients develop neutropenia. For example, both the pre-emptive treatment and the prophylactic treatment of CMV disease in haematopoietic cell transplant recipients with ganciclovir results in neutropenia (270). The treatment of congenital CMV infection in neonates results in transient neutropenia and post-natal treatment can result in absolute neutropenia (271). Neutropenia is also associated with cidofovir treatment of CMV retinitis (269). Currently, foscarnet is the preferred drug for patients who cannot be treated with ganciclovir due to dose-limiting neutropenia (272), although it is still considered only a second-line choice of therapy. If the finding in the mouse model of CMV infection that neutrophils actually protect against CMV infection holds true in human infection, then using drugs that cause neutropenia would be detrimental in fighting CMV disease. Thus, in the absence of neutropenia with foscarnet treatment, research into how this could be used more

extensively in the treatment of CMV disease would be beneficial. Given the associated toxicity of this (and other) antiviral treatments, these data clearly highlight a critical need for new refined antiviral treatment approaches.

The results from my investigations suggest three obvious routes of further exploration. Firstly, as discussed above, more research needs to be done in order to elucidate the mechanism for how neutrophils directly inhibit MCMV replication, and more importantly, ascertain if this is relevant to HCMV. Secondly, my results on the antiviral activity of IL-22 in chapter 5 open up a second avenue of further investigation which includes 1) deciphering the additional mechanisms for how IL-22 provides antiviral protection against acute MCMV infection from as early as 2 days p.i; 2) set up a mucosal MCMV challenge model to enable the assessment of the role that IL-22 may play in infections via mucosal surfaces; 3) establishing if this cytokine also has antiviral properties during the chronic replicating and chronic latent phases of infection, especially as T cells play an important role in controlling infection during these phases, and therefore if it is possible to induce expression of IL-22 by T cells under the right polarizing conditions, this method could be exploited to enhance IL-22 expression to provide antiviral protection; and 4) determining if IL-22 enhances immunity against HCMV infection.

Finally, a more generalised question could be asked, based on what has been revealed in this thesis about the roles of both IL-10 and IL-22 during acute MCMV infection: do other cytokines of the IL-10 family provide antiviral protection against herpesvirus infections? IL-22 belongs to the IL-20 subfamily whose roles to date include protecting against extracellular pathogens. Could IL-19, IL-20, IL-24 or IL-26 also provide protection from viral pathogens? The third subfamily of IL-10 family members are the type III IFNs; IL-28A, IL-28B and IL-29. These are expressed in response to most viruses and interestingly, administration of type III IFNs during a murine model of HSV-2 led to a reduction in hepatic viral titres and furthermore, in a localised model of HSV-2 infection,

type III IFN treatment totally prevented development of disease (273). If investigation into administration of these cytokines during MCMV infection also yields promising antiviral results, these could potentially be other targets for effective therapeutic treatment against HCMV infections.

6.1 Conclusion

I have shown that two members of the IL-10 family of cytokines, IL-10 and IL-22, provide antiviral protection against acute MCMV infection. IL-10 achieves this by sustaining the balance between pro-inflammatory and inhibitory signals received by NK cells to guard from activation-induced cell death. The mechanisms through which IL-22 exerts its antiviral functions are still to be fully elucidated; however, one way in which it accomplishes this is through enhancing neutrophil accumulation into specific tissues, wherein the neutrophils inhibit virus replication. These novel findings have enhanced our understanding of cytokine biology in the context of viral infections *in vivo* and highlight important considerations for future research into herpesvirus infections.

References

1. Beisel, C. E. 2000. Cytomegalovirus Vaccine Development. Division of Microbiology and Infectious Diseases, National Institute of Allergy and Infectious Diseases, National Institutes of Health, The Jordan Report. 105-110.
2. Boeckh, M., and A. P. Geballe. 2011. Cytomegalovirus: pathogen, paradigm, and puzzle. *J Clin Invest* 121: 1673-1680.
3. Amin, K. 2012. The role of mast cells in allergic inflammation. *Respir Med* 106: 9-14.
4. Bhargava, P., and C. H. Lee. 2012. Role and function of macrophages in the metabolic syndrome. *Biochem J* 442: 253-262.
5. Karp, C. L., and P. J. Murray. 2012. Non-canonical alternatives: what a macrophage is 4. *J Exp Med* 209: 427-431.
6. Adema, G. J. 2009. Dendritic cells from bench to bedside and back. *Immunol Lett* 122: 128-130.
7. Fukaya, T., H. Takagi, H. Taya, and K. Sato. 2011. DCs in immune tolerance in steady-state conditions. *Methods Mol Biol* 677: 113-126.
8. Mantovani, A., M. A. Cassatella, C. Costantini, and S. Jaillon. 2011. Neutrophils in the activation and regulation of innate and adaptive immunity. *Nat Rev Immunol* 11: 519-531.
9. Brinkmann, V., U. Reichard, C. Goosmann, B. Fauler, Y. Uhlemann, D. S. Weiss, Y. Weinrauch, and A. Zychlinsky. 2004. Neutrophil extracellular traps kill bacteria. *Science* 303: 1532-1535.
10. Stone, K. D., C. Prussin, and D. D. Metcalfe. 2010. IgE, mast cells, basophils, and eosinophils. *J Allergy Clin Immunol* 125: S73-80.
11. Sun, J. C., and L. L. Lanier. 2011. NK cell development, homeostasis and function: parallels with $CD8^+$ T cells. *Nat Rev Immunol* 11: 645-657.
12. Pancer, Z., and M. D. Cooper. 2006. The evolution of adaptive immunity. *Annu Rev Immunol* 24: 497-518.
13. LeBien, T. W., and T. F. Tedder. 2008. B lymphocytes: how they develop and function. *Blood* 112: 1570-1580.
14. Delves, P., S. Martin, D. Burton, and I. Roitt. *Essential Immunology*. Blackwell Publishing Ltd.
15. Marshall, N. B., and S. L. Swain. 2011. Cytotoxic CD4 T cells in antiviral immunity. *J Biomed Biotechnol* 2011: 954602.
16. Balasubramani, A., R. Mukasa, R. D. Hatton, and C. T. Weaver. 2010. Regulation of the Ifng locus in the context of T-lineage specification and plasticity. *Immunol Rev* 238: 216-232.
17. Zhu, J., H. Yamane, and W. E. Paul. 2010. Differentiation of effector CD4 T cell populations (*). *Annu Rev Immunol* 28: 445-489.
18. Schnare, M., G. M. Barton, A. C. Holt, K. Takeda, S. Akira, and R. Medzhitov. 2001. Toll-like receptors control activation of adaptive immune responses. *Nat Immunol* 2: 947-950.
19. Vivier, E., D. H. Raulet, A. Moretta, M. A. Caligiuri, L. Zitvogel, L. L. Lanier, W. M. Yokoyama, and S. Ugolini. 2011. Innate or adaptive immunity? The example of natural killer cells. *Science* 331: 44-49.
20. Biron, C. A., K. B. Nguyen, G. C. Pien, L. P. Cousens, and T. P. Salazar-Mather. 1999. Natural killer cells in antiviral defense: function and regulation by innate cytokines. *Annu Rev Immunol* 17: 189-220.

21. Biron, C. A., H. C. Su, and J. S. Orange. 1996. Function and Regulation of Natural Killer (NK) Cells during Viral Infections: Characterization of Responses in Vivo. *Methods* 9: 379-393.
22. Welsh, R. M., J. O. Brubaker, M. Vargas-Cortes, and C. L. O'Donnell. 1991. Natural killer (NK) cell response to virus infections in mice with severe combined immunodeficiency. The stimulation of NK cells and the NK cell-dependent control of virus infections occur independently of T and B cell function. *J Exp Med* 173: 1053-1063.
23. Welsh, R. M., C. L. O'Donnell, and L. D. Shultz. 1994. Antiviral activity of NK 1.1+ natural killer cells in C57BL/6 scid mice infected with murine cytomegalovirus. *Nat Immun* 13: 239-245.
24. Orange, J. S., and C. A. Biron. 1996. An absolute and restricted requirement for IL-12 in natural killer cell IFN-gamma production and antiviral defense. Studies of natural killer and T cell responses in contrasting viral infections. *J Immunol* 156: 1138-1142.
25. Orange, J. S., and C. A. Biron. 1996. Characterization of early IL-12, IFN-alphabeta, and TNF effects on antiviral state and NK cell responses during murine cytomegalovirus infection. *J Immunol* 156: 4746-4756.
26. Orange, J. S., B. Wang, C. Terhorst, and C. A. Biron. 1995. Requirement for natural killer cell-produced interferon gamma in defense against murine cytomegalovirus infection and enhancement of this defense pathway by interleukin 12 administration. *J Exp Med* 182: 1045-1056.
27. Gazit, R., R. Gruda, M. Elboim, T. I. Arnon, G. Katz, H. Achdout, J. Hanna, U. Qimron, G. Landau, E. Greenbaum, Z. Zakay-Rones, A. Porgador, and O. Mandelboim. 2006. Lethal influenza infection in the absence of the natural killer cell receptor gene Ncr1. *Nat Immunol* 7: 517-523.
28. Orange, J. S. 2002. Human natural killer cell deficiencies and susceptibility to infection. *Microbes Infect* 4: 1545-1558.
29. Waldhauer, I., and A. Steinle. 2008. NK cells and cancer immunosurveillance. *Oncogene* 27: 5932-5943.
30. Cooper, M. A., J. E. Bush, T. A. Fehniger, J. B. VanDeusen, R. E. Waite, Y. Liu, H. L. Aguila, and M. A. Caligiuri. 2002. In vivo evidence for a dependence on interleukin 15 for survival of natural killer cells. *Blood* 100: 3633-3638.
31. McVicar, D. W., and D. N. Burshtyn. 2001. Intracellular signaling by the killer immunoglobulin-like receptors and Ly49. *Sci STKE* 2001: re1.
32. Ma, L. L., C. L. Wang, G. G. Neely, S. Epelman, A. M. Krensky, and C. H. Mody. 2004. NK cells use perforin rather than granulysin for anticryptococcal activity. *J Immunol* 173: 3357-3365.
33. Smyth, M. J., E. Cretney, J. M. Kelly, J. A. Westwood, S. E. Street, H. Yagita, K. Takeda, S. L. van Dommelen, M. A. Degli-Esposti, and Y. Hayakawa. 2005. Activation of NK cell cytotoxicity. *Mol Immunol* 42: 501-510.
34. Strowig, T., F. Brilot, and C. Münz. 2008. Noncytotoxic functions of NK cells: direct pathogen restriction and assistance to adaptive immunity. *J Immunol* 180: 7785-7791.
35. Gonzales, C. M., C. B. Williams, V. E. Calderon, M. B. Huante, S. T. Moen, V. L. Popov, W. B. Baze, J. W. Peterson, and J. J. Endsley. 2012. Antibacterial role for natural killer cells in host defense to Bacillus anthracis. *Infect Immun* 80: 234-242.
36. Yun, C. H., A. Lundgren, J. Azem, A. Sjöling, J. Holmgren, A. M. Svennerholm, and B. S. Lundin. 2005. Natural killer cells and Helicobacter pylori infection: bacterial antigens and interleukin-12 act synergistically to induce gamma interferon

production. *Infect Immun* 73: 1482-1490.
37. Boehm, U., T. Klamp, M. Groot, and J. C. Howard. 1997. Cellular responses to interferon-gamma. *Annu Rev Immunol* 15: 749-795.
38. Cooper, M. A., and W. M. Yokoyama. 2010. Memory-like responses of natural killer cells. *Immunol Rev* 235: 297-305.
39. O'Leary, J. G., M. Goodarzi, D. L. Drayton, and U. H. von Andrian. 2006. T cell- and B cell-independent adaptive immunity mediated by natural killer cells. *Nat Immunol* 7: 507-516.
40. Cooper, M. A., J. M. Elliott, P. A. Keyel, L. Yang, J. A. Carrero, and W. M. Yokoyama. 2009. Cytokine-induced memory-like natural killer cells. *Proc Natl Acad Sci U S A* 106: 1915-1919.
41. Sun, J. C., J. N. Beilke, and L. L. Lanier. 2009. Adaptive immune features of natural killer cells. *Nature* 457: 557-561.
42. Paust, S., H. S. Gill, B. Z. Wang, M. P. Flynn, E. A. Moseman, B. Senman, M. Szczepanik, A. Telenti, P. W. Askenase, R. W. Compans, and U. H. von Andrian. 2010. Critical role for the chemokine receptor CXCR6 in NK cell-mediated antigen-specific memory of haptens and viruses. *Nat Immunol* 11: 1127-1135.
43. Sun, J. C., S. Lopez-Verges, C. C. Kim, J. L. DeRisi, and L. L. Lanier. 2011. NK cells and immune "memory". *J Immunol* 186: 1891-1897.
44. Bego, M. G., and S. St Jeor. 2006. Human cytomegalovirus infection of cells of hematopoietic origin: HCMV-induced immunosuppression, immune evasion, and latency. *Exp Hematol* 34: 555-570.
45. Wang, D., Q. C. Yu, J. Schröer, E. Murphy, and T. Shenk. 2007. Human cytomegalovirus uses two distinct pathways to enter retinal pigmented epithelial cells. *Proc Natl Acad Sci U S A* 104: 20037-20042.
46. Cannon, M. J., D. S. Schmid, and T. B. Hyde. 2010. Review of cytomegalovirus seroprevalence and demographic characteristics associated with infection. *Rev Med Virol* 20: 202-213.
47. Crough, T., and R. Khanna. 2009. Immunobiology of human cytomegalovirus: from bench to bedside. *Clin Microbiol Rev* 22: 76-98, Table of Contents.
48. Gandhi, M. K., and R. Khanna. 2004. Human cytomegalovirus: clinical aspects, immune regulation, and emerging treatments. *Lancet Infect Dis* 4: 725-738.
49. De Keyzer, K., S. Van Laecke, P. Peeters, and R. Vanholder. 2011. Human cytomegalovirus and kidney transplantation: a clinician's update. *Am J Kidney Dis* 58: 118-126.
50. Scholz, M., H. W. Doerr, and J. Cinatl. 2003. Human cytomegalovirus retinitis: pathogenicity, immune evasion and persistence. *Trends Microbiol* 11: 171-178.
51. Sylwester, A. W., B. L. Mitchell, J. B. Edgar, C. Taormina, C. Pelte, F. Ruchti, P. R. Sleath, K. H. Grabstein, N. A. Hosken, F. Kern, J. A. Nelson, and L. J. Picker. 2005. Broadly targeted human cytomegalovirus-specific CD4+ and CD8+ T cells dominate the memory compartments of exposed subjects. *J Exp Med* 202: 673-685.
52. Hadrup, S. R., J. Strindhall, T. Køllgaard, T. Seremet, B. Johansson, G. Pawelec, P. thor Straten, and A. Wikby. 2006. Longitudinal studies of clonally expanded CD8 T cells reveal a repertoire shrinkage predicting mortality and an increased number of dysfunctional cytomegalovirus-specific T cells in the very elderly. *J Immunol* 176: 2645-2653.
53. Limaye, A. P., K. A. Kirby, G. D. Rubenfeld, W. M. Leisenring, E. M. Bulger, M. J. Neff, N. S. Gibran, M. L. Huang, T. K. Santo Hayes, L. Corey, and M. Boeckh. 2008. Cytomegalovirus reactivation in critically ill immunocompetent patients. *JAMA* 300: 413-422.

54. Arvin, A. M., P. Fast, M. Myers, S. Plotkin, R. Rabinovich, and N. V. A. Committee. 2004. Vaccine development to prevent cytomegalovirus disease: report from the National Vaccine Advisory Committee. *Clin Infect Dis* 39: 233-239.
55. Dolan, A., C. Cunningham, R. D. Hector, A. F. Hassan-Walker, L. Lee, C. Addison, D. J. Dargan, D. J. McGeoch, D. Gatherer, V. C. Emery, P. D. Griffiths, C. Sinzger, B. P. McSharry, G. W. Wilkinson, and A. J. Davison. 2004. Genetic content of wild-type human cytomegalovirus. *J Gen Virol* 85: 1301-1312.
56. Dargan, D. J., E. Douglas, C. Cunningham, F. Jamieson, R. J. Stanton, K. Baluchova, B. P. McSharry, P. Tomasec, V. C. Emery, E. Percivalle, A. Sarasini, G. Gerna, G. W. Wilkinson, and A. J. Davison. 2010. Sequential mutations associated with adaptation of human cytomegalovirus to growth in cell culture. *J Gen Virol* 91: 1535-1546.
57. Hahn, G., M. G. Revello, M. Patrone, E. Percivalle, G. Campanini, A. Sarasini, M. Wagner, A. Gallina, G. Milanesi, U. Koszinowski, F. Baldanti, and G. Gerna. 2004. Human cytomegalovirus UL131-128 genes are indispensable for virus growth in endothelial cells and virus transfer to leukocytes. *J Virol* 78: 10023-10033.
58. Stanton, R. J., K. Baluchova, D. J. Dargan, C. Cunningham, O. Sheehy, S. Seirafian, B. P. McSharry, M. L. Neale, J. A. Davies, P. Tomasec, A. J. Davison, and G. W. Wilkinson. 2010. Reconstruction of the complete human cytomegalovirus genome in a BAC reveals RL13 to be a potent inhibitor of replication. *J Clin Invest* 120: 3191-3208.
59. Loenen, W. A., C. A. Bruggeman, and E. J. Wiertz. 2001. Immune evasion by human cytomegalovirus: lessons in immunology and cell biology. *Semin Immunol* 13: 41-49.
60. Alcami, A. 2003. Viral mimicry of cytokines, chemokines and their receptors. *Nat Rev Immunol* 3: 36-50.
61. Poole, E., C. A. King, J. H. Sinclair, and A. Alcami. 2006. The UL144 gene product of human cytomegalovirus activates NFkappaB via a TRAF6-dependent mechanism. *EMBO J* 25: 4390-4399.
62. Cheung, T. C., I. R. Humphreys, K. G. Potter, P. S. Norris, H. M. Shumway, B. R. Tran, G. Patterson, R. Jean-Jacques, M. Yoon, P. G. Spear, K. M. Murphy, N. S. Lurain, C. A. Benedict, and C. F. Ware. 2005. Evolutionarily divergent herpesviruses modulate T cell activation by targeting the herpesvirus entry mediator cosignaling pathway. *Proc Natl Acad Sci U S A* 102: 13218-13223.
63. Miller-Kittrell, M., and T. E. Sparer. 2009. Feeling manipulated: cytomegalovirus immune manipulation. *Virol J* 6: 4.
64. Mocarski, E. S. 2002. Immunomodulation by cytomegaloviruses: manipulative strategies beyond evasion. *Trends Microbiol* 10: 332-339.
65. Reeves, M. B., A. A. Davies, B. P. McSharry, G. W. Wilkinson, and J. H. Sinclair. 2007. Complex I binding by a virally encoded RNA regulates mitochondria-induced cell death. *Science* 316: 1345-1348.
66. Atalay, R., A. Zimmermann, M. Wagner, E. Borst, C. Benz, M. Messerle, and H. Hengel. 2002. Identification and expression of human cytomegalovirus transcription units coding for two distinct Fcgamma receptor homologs. *J Virol* 76: 8596-8608.
67. Biron, C. A., K. S. Byron, and J. L. Sullivan. 1989. Severe herpesvirus infections in an adolescent without natural killer cells. *N Engl J Med* 320: 1731-1735.
68. Gazit, R., B. Z. Garty, Y. Monselise, V. Hoffer, Y. Finkelstein, G. Markel, G. Katz, J. Hanna, H. Achdout, R. Gruda, T. Gonen-Gross, and O. Mandelboim. 2004.

Expression of KIR2DL1 on the entire NK cell population: a possible novel immunodeficiency syndrome. *Blood* 103: 1965-1966.
69. Venema, H., A. P. van den Berg, C. van Zanten, W. J. van Son, M. van der Giessen, and T. H. The. 1994. Natural killer cell responses in renal transplant patients with cytomegalovirus infection. *J Med Virol* 42: 188-192.
70. Quinnan, G. V., N. Kirmani, A. H. Rook, J. F. Manischewitz, L. Jackson, G. Moreschi, G. W. Santos, R. Saral, and W. H. Burns. 1982. Cytotoxic t cells in cytomegalovirus infection: HLA-restricted T-lymphocyte and non-T-lymphocyte cytotoxic responses correlate with recovery from cytomegalovirus infection in bone-marrow-transplant recipients. *N Engl J Med* 307: 7-13.
71. Jackson, S. E., G. M. Mason, and M. R. Wills. 2011. Human cytomegalovirus immunity and immune evasion. *Virus Res* 157: 151-160.
72. Beck, S., and B. G. Barrell. 1988. Human cytomegalovirus encodes a glycoprotein homologous to MHC class-I antigens. *Nature* 331: 269-272.
73. Wilkinson, G. W., P. Tomasec, R. J. Stanton, M. Armstrong, V. Prod'homme, R. Aicheler, B. P. McSharry, C. R. Rickards, D. Cochrane, S. Llewellyn-Lacey, E. C. Wang, C. A. Griffin, and A. J. Davison. 2008. Modulation of natural killer cells by human cytomegalovirus. *J Clin Virol* 41: 206-212.
74. Tomasec, P., V. M. Braud, C. Rickards, M. B. Powell, B. P. McSharry, S. Gadola, V. Cerundolo, L. K. Borysiewicz, A. J. McMichael, and G. W. Wilkinson. 2000. Surface expression of HLA-E, an inhibitor of natural killer cells, enhanced by human cytomegalovirus gpUL40. *Science* 287: 1031.
75. Arnon, T. I., H. Achdout, O. Levi, G. Markel, N. Saleh, G. Katz, R. Gazit, T. Gonen-Gross, J. Hanna, E. Nahari, A. Porgador, A. Honigman, B. Plachter, D. Mevorach, D. G. Wolf, and O. Mandelboim. 2005. Inhibition of the NKp30 activating receptor by pp65 of human cytomegalovirus. *Nat Immunol* 6: 515-523.
76. Tomasec, P., E. C. Wang, A. J. Davison, B. Vojtesek, M. Armstrong, C. Griffin, B. P. McSharry, R. J. Morris, S. Llewellyn-Lacey, C. Rickards, A. Nomoto, C. Sinzger, and G. W. Wilkinson. 2005. Downregulation of natural killer cell-activating ligand CD155 by human cytomegalovirus UL141. *Nat Immunol* 6: 181-188.
77. Iversen, A. C., P. S. Norris, C. F. Ware, and C. A. Benedict. 2005. Human NK cells inhibit cytomegalovirus replication through a noncytolytic mechanism involving lymphotoxin-dependent induction of IFN-beta. *J Immunol* 175: 7568-7574.
78. Lopez-Vergès, S., J. M. Milush, B. S. Schwartz, M. J. Pando, J. Jarjoura, V. A. York, J. P. Houchins, S. Miller, S. M. Kang, P. J. Norris, D. F. Nixon, and L. L. Lanier. 2011. Expansion of a unique CD57^{+}NKG2Chi natural killer cell subset during acute human cytomegalovirus infection. *Proc Natl Acad Sci U S A* 108: 14725-14732.
79. Kavanagh, D. G., and A. B. Hill. 2001. Evasion of cytotoxic T lymphocytes by murine cytomegalovirus. *Semin Immunol* 13: 19-26.
80. Krmpotic, A., I. Bubic, B. Polic, P. Lucin, and S. Jonjic. 2003. Pathogenesis of murine cytomegalovirus infection. *Microbes Infect* 5: 1263-1277.
81. Kucić, N., H. Mahmutefendić, and P. Lucin. 2005. Inhibition of protein kinases C prevents murine cytomegalovirus replication. *J Gen Virol* 86: 2153-2161.
82. Doom, C. M., and A. B. Hill. 2008. MHC class I immune evasion in MCMV infection. *Med Microbiol Immunol* 197: 191-204.
83. Webb, J. R., S. H. Lee, and S. M. Vidal. 2002. Genetic control of innate immune responses against cytomegalovirus: MCMV meets its match. *Genes Immun* 3: 250-262.

84. Fleming, P., N. Davis-Poynter, M. Degli-Esposti, E. Densley, J. Papadimitriou, G. Shellam, and H. Farrell. 1999. The murine cytomegalovirus chemokine homolog, m131/129, is a determinant of viral pathogenicity. *J Virol* 73: 6800-6809.
85. Noda, S., S. A. Aguirre, A. Bitmansour, J. M. Brown, T. E. Sparer, J. Huang, and E. S. Mocarski. 2006. Cytomegalovirus MCK-2 controls mobilization and recruitment of myeloid progenitor cells to facilitate dissemination. *Blood* 107: 30-38.
86. Brune, W., C. Ménard, J. Heesemann, and U. H. Koszinowski. 2001. A ribonucleotide reductase homolog of cytomegalovirus and endothelial cell tropism. *Science* 291: 303-305.
87. Bukowski, J. F., J. F. Warner, G. Dennert, and R. M. Welsh. 1985. Adoptive transfer studies demonstrating the antiviral effect of natural killer cells in vivo. *J Exp Med* 161: 40-52.
88. Shellam, G. R., J. E. Allan, J. M. Papadimitriou, and G. J. Bancroft. 1981. Increased susceptibility to cytomegalovirus infection in beige mutant mice. *Proc Natl Acad Sci U S A* 78: 5104-5108.
89. Bukowski, J. F., B. A. Woda, and R. M. Welsh. 1984. Pathogenesis of murine cytomegalovirus infection in natural killer cell-depleted mice. *J Virol* 52: 119-128.
90. Welsh, R. M., P. L. Dundon, E. E. Eynon, J. O. Brubaker, G. C. Koo, and C. L. O'Donnell. 1990. Demonstration of the antiviral role of natural killer cells in vivo with a natural killer cell-specific monoclonal antibody (NK 1.1). *Nat Immun Cell Growth Regul* 9: 112-120.
91. Shanley, J. D. 1990. In vivo administration of monoclonal antibody to the NK 1.1 antigen of natural killer cells: effect on acute murine cytomegalovirus infection. *J Med Virol* 30: 58-60.
92. Orange, J. S., and C. A. Biron. 1996. Characterization of early IL-12, IFN-alphabeta, and TNF effects on antiviral state and NK cell responses during murine cytomegalovirus infection. *J Immunol* 156: 4746-4756.
93. Revilleza, M. J., R. Wang, J. Mans, M. Hong, K. Natarajan, and D. H. Margulies. 2011. How the virus outsmarts the host: function and structure of cytomegalovirus MHC-I-like molecules in the evasion of natural killer cell surveillance. *J Biomed Biotechnol* 2011: 724607.
94. Babić, M., A. Krmpotić, and S. Jonjić. 2011. All is fair in virus-host interactions: NK cells and cytomegalovirus. *Trends Mol Med* 17: 677-685.
95. Pyzik, M., E. M. Gendron-Pontbriand, and S. M. Vidal. 2011. The impact of Ly49-NK cell-dependent recognition of MCMV infection on innate and adaptive immune responses. *J Biomed Biotechnol* 2011: 641702.
96. Sun, J. C., and L. L. Lanier. 2009. The Natural Selection of Herpesviruses and Virus-Specific NK Cell Receptors. *Viruses* 1: 362.
97. Fiorentino, D. F., M. W. Bond, and T. R. Mosmann. 1989. Two types of mouse T helper cell. IV. Th2 clones secrete a factor that inhibits cytokine production by Th1 clones. *J Exp Med* 170: 2081-2095.
98. Moore, K. W., A. O'Garra, R. de Waal Malefyt, P. Vieira, and T. R. Mosmann. 1993. Interleukin-10. *Annu Rev Immunol* 11: 165-190.
99. Mege, J. L., S. Meghari, A. Honstettre, C. Capo, and D. Raoult. 2006. The two faces of interleukin 10 in human infectious diseases. *Lancet Infect Dis* 6: 557-569.
100. Ouyang, W., S. Rutz, N. K. Crellin, P. A. Valdez, and S. G. Hymowitz. 2011. Regulation and functions of the IL-10 family of cytokines in inflammation and disease. *Annu Rev Immunol* 29: 71-109.
101. Saraiva, M., and A. O'Garra. 2010. The regulation of IL-10 production by immune

cells. *Nat Rev Immunol* 10: 170-181.
102. Moore, K. W., R. de Waal Malefyt, R. L. Coffman, and A. O'Garra. 2001. Interleukin-10 and the interleukin-10 receptor. *Annu Rev Immunol* 19: 683-765.
103. Koppelman, B., J. J. Neefjes, J. E. de Vries, and R. de Waal Malefyt. 1997. Interleukin-10 down-regulates MHC class II alphabeta peptide complexes at the plasma membrane of monocytes by affecting arrival and recycling. *Immunity* 7: 861-871.
104. Bazzoni, F., N. Tamassia, M. Rossato, and M. A. Cassatella. 2010. Understanding the molecular mechanisms of the multifaceted IL-10-mediated anti-inflammatory response: lessons from neutrophils. *Eur J Immunol* 40: 2360-2368.
105. Groux, H., M. Bigler, J. E. de Vries, and M. G. Roncarolo. 1998. Inhibitory and stimulatory effects of IL-10 on human CD8+ T cells. *J Immunol* 160: 3188-3193.
106. Itoh, K., and S. Hirohata. 1995. The role of IL-10 in human B cell activation, proliferation, and differentiation. *J Immunol* 154: 4341-4350.
107. Couper, K. N., D. G. Blount, and E. M. Riley. 2008. IL-10: the master regulator of immunity to infection. *J Immunol* 180: 5771-5777.
108. Gazzinelli, R. T., M. Wysocka, S. Hieny, T. Scharton-Kersten, A. Cheever, R. Kühn, W. Müller, G. Trinchieri, and A. Sher. 1996. In the absence of endogenous IL-10, mice acutely infected with Toxoplasma gondii succumb to a lethal immune response dependent on CD4+ T cells and accompanied by overproduction of IL-12, IFN-gamma and TNF-alpha. *J Immunol* 157: 798-805.
109. Li, C., L. A. Sanni, F. Omer, E. Riley, and J. Langhorne. 2003. Pathology of Plasmodium chabaudi chabaudi infection and mortality in interleukin-10-deficient mice are ameliorated by anti-tumor necrosis factor alpha and exacerbated by anti-transforming growth factor beta antibodies. *Infect Immun* 71: 4850-4856.
110. Louis, H., J. L. Van Laethem, W. Wu, E. Quertinmont, C. Degraef, K. Van den Berg, A. Demols, M. Goldman, O. Le Moine, A. Geerts, and J. Devière. 1998. Interleukin-10 controls neutrophilic infiltration, hepatocyte proliferation, and liver fibrosis induced by carbon tetrachloride in mice. *Hepatology* 28: 1607-1615.
111. Arai, T., K. Abe, H. Matsuoka, M. Yoshida, M. Mori, S. Goya, H. Kida, K. Nishino, T. Osaki, I. Tachibana, Y. Kaneda, and S. Hayashi. 2000. Introduction of the interleukin-10 gene into mice inhibited bleomycin-induced lung injury in vivo. *Am J Physiol Lung Cell Mol Physiol* 278: L914-922.
112. Demols, A., J. L. Van Laethem, E. Quertinmont, C. Degraef, M. Delhaye, A. Geerts, and J. Deviere. 2002. Endogenous interleukin-10 modulates fibrosis and regeneration in experimental chronic pancreatitis. *Am J Physiol Gastrointest Liver Physiol* 282: G1105-1112.
113. Nelson, D. R., G. Y. Lauwers, J. Y. Lau, and G. L. Davis. 2000. Interleukin 10 treatment reduces fibrosis in patients with chronic hepatitis C: a pilot trial of interferon nonresponders. *Gastroenterology* 118: 655-660.
114. Sun, J., A. Cardani, A. K. Sharma, V. E. Laubach, R. S. Jack, W. Müller, and T. J. Braciale. 2011. Autocrine regulation of pulmonary inflammation by effector T-cell derived IL-10 during infection with respiratory syncytial virus. *PLoS Pathog* 7: e1002173.
115. Sun, J., R. Madan, C. L. Karp, and T. J. Braciale. 2009. Effector T cells control lung inflammation during acute influenza virus infection by producing IL-10. *Nat Med* 15: 277-284.
116. McKinstry, K. K., T. M. Strutt, A. Buck, J. D. Curtis, J. P. Dibble, G. Huston, M. Tighe, H. Hamada, S. Sell, R. W. Dutton, and S. L. Swain. 2009. IL-10 deficiency unleashes an influenza-specific Th17 response and enhances survival against high-

dose challenge. *J Immunol* 182: 7353-7363.
117. Brooks, D. G., M. J. Trifilo, K. H. Edelmann, L. Teyton, D. B. McGavern, and M. B. Oldstone. 2006. Interleukin-10 determines viral clearance or persistence in vivo. *Nat Med* 12: 1301-1309.
118. Ejrnaes, M., C. M. Filippi, M. M. Martinic, E. M. Ling, L. M. Togher, S. Crotty, and M. G. von Herrath. 2006. Resolution of a chronic viral infection after interleukin-10 receptor blockade. *J Exp Med* 203: 2461-2472.
119. Filippi, C. M., and M. G. von Herrath. 2008. IL-10 and the resolution of infections. *J Pathol* 214: 224-230.
120. Slobedman, B., P. A. Barry, J. V. Spencer, S. Avdic, and A. Abendroth. 2009. Virus-encoded homologs of cellular interleukin-10 and their control of host immune function. *J Virol* 83: 9618-9629.
121. Taus, N. S., D. R. Herndon, D. L. Traul, J. P. Stewart, M. Ackermann, H. Li, D. P. Knowles, G. S. Lewis, and K. A. Brayton. 2007. Comparison of ovine herpesvirus 2 genomes isolated from domestic sheep (Ovis aries) and a clinically affected cow (Bos bovis). *J Gen Virol* 88: 40-45.
122. Fleming, S. B., C. A. McCaughan, A. E. Andrews, A. D. Nash, and A. A. Mercer. 1997. A homolog of interleukin-10 is encoded by the poxvirus orf virus. *J Virol* 71: 4857-4861.
123. Hsu, D. H., R. de Waal Malefyt, D. F. Fiorentino, M. N. Dang, P. Vieira, J. de Vries, H. Spits, T. R. Mosmann, and K. W. Moore. 1990. Expression of interleukin-10 activity by Epstein-Barr virus protein BCRF1. *Science* 250: 830-832.
124. Stewart, J. P., F. G. Behm, J. R. Arrand, and C. M. Rooney. 1994. Differential expression of viral and human interleukin-10 (IL-10) by primary B cell tumors and B cell lines. *Virology* 200: 724-732.
125. de Waal Malefyt, R., J. Haanen, H. Spits, M. G. Roncarolo, A. te Velde, C. Figdor, K. Johnson, R. Kastelein, H. Yssel, and J. E. de Vries. 1991. Interleukin 10 (IL-10) and viral IL-10 strongly reduce antigen-specific human T cell proliferation by diminishing the antigen-presenting capacity of monocytes via downregulation of class II major histocompatibility complex expression. *J Exp Med* 174: 915-924.
126. Salek-Ardakani, S., J. R. Arrand, and M. Mackett. 2002. Epstein-Barr virus encoded interleukin-10 inhibits HLA-class I, ICAM-1, and B7 expression on human monocytes: implications for immune evasion by EBV. *Virology* 304: 342-351.
127. Zeidler, R., G. Eissner, P. Meissner, S. Uebel, R. Tampé, S. Lazis, and W. Hammerschmidt. 1997. Downregulation of TAP1 in B lymphocytes by cellular and Epstein-Barr virus-encoded interleukin-10. *Blood* 90: 2390-2397.
128. Go, N. F., B. E. Castle, R. Barrett, R. Kastelein, W. Dang, T. R. Mosmann, K. W. Moore, and M. Howard. 1990. Interleukin 10, a novel B cell stimulatory factor: unresponsiveness of X chromosome-linked immunodeficiency B cells. *J Exp Med* 172: 1625-1631.
129. Rousset, F., E. Garcia, T. Defrance, C. Péronne, N. Vezzio, D. H. Hsu, R. Kastelein, K. W. Moore, and J. Banchereau. 1992. Interleukin 10 is a potent growth and differentiation factor for activated human B lymphocytes. *Proc Natl Acad Sci U S A* 89: 1890-1893.
130. Kotenko, S. V., S. Saccani, L. S. Izotova, O. V. Mirochnitchenko, and S. Pestka. 2000. Human cytomegalovirus harbors its own unique IL-10 homolog (cmvIL-10). *Proc Natl Acad Sci U S A* 97: 1695-1700.
131. Jenkins, C., W. Garcia, M. J. Godwin, J. V. Spencer, J. L. Stern, A. Abendroth, and

B. Slobedman. 2008. Immunomodulatory properties of a viral homolog of human interleukin-10 expressed by human cytomegalovirus during the latent phase of infection. *J Virol* 82: 3736-3750.
132. Dumoutier, L., J. Louahed, and J. C. Renauld. 2000. Cloning and characterization of IL-10-related T cell-derived inducible factor (IL-TIF), a novel cytokine structurally related to IL-10 and inducible by IL-9. *J Immunol* 164: 1814-1819.
133. Xie, M. H., S. Aggarwal, W. H. Ho, J. Foster, Z. Zhang, J. Stinson, W. I. Wood, A. D. Goddard, and A. L. Gurney. 2000. Interleukin (IL)-22, a novel human cytokine that signals through the interferon receptor-related proteins CRF2-4 and IL-22R. *J Biol Chem* 275: 31335-31339.
134. Wolk, K., and R. Sabat. 2006. Interleukin-22: a novel T- and NK-cell derived cytokine that regulates the biology of tissue cells. *Cytokine Growth Factor Rev* 17: 367-380.
135. Sonnenberg, G. F., L. A. Fouser, and D. Artis. 2011. Border patrol: regulation of immunity, inflammation and tissue homeostasis at barrier surfaces by IL-22. *Nat Immunol* 12: 383-390.
136. Zenewicz, L. A., and R. A. Flavell. 2008. IL-22 and inflammation: leukin' through a glass onion. *Eur J Immunol* 38: 3265-3268.
137. Dumoutier, L., D. Lejeune, D. Colau, and J. C. Renauld. 2001. Cloning and characterization of IL-22 binding protein, a natural antagonist of IL-10-related T cell-derived inducible factor/IL-22. *J Immunol* 166: 7090-7095.
138. Liang, S. C., X. Y. Tan, D. P. Luxenberg, R. Karim, K. Dunussi-Joannopoulos, M. Collins, and L. A. Fouser. 2006. Interleukin (IL)-22 and IL-17 are coexpressed by Th17 cells and cooperatively enhance expression of antimicrobial peptides. *J Exp Med* 203: 2271-2279.
139. Kolls, J. K., P. B. McCray, and Y. R. Chan. 2008. Cytokine-mediated regulation of antimicrobial proteins. *Nat Rev Immunol* 8: 829-835.
140. Sanos, S. L., V. L. Bui, A. Mortha, K. Oberle, C. Heners, C. Johner, and A. Diefenbach. 2009. RORgammat and commensal microflora are required for the differentiation of mucosal interleukin 22-producing NKp46+ cells. *Nat Immunol* 10: 83-91.
141. Cella, M., A. Fuchs, W. Vermi, F. Facchetti, K. Otero, J. K. Lennerz, J. M. Doherty, J. C. Mills, and M. Colonna. 2009. A human natural killer cell subset provides an innate source of IL-22 for mucosal immunity. *Nature* 457: 722-725.
142. Liang, S. C., C. Nickerson-Nutter, D. D. Pittman, Y. Carrier, D. G. Goodwin, K. M. Shields, A. J. Lambert, S. H. Schelling, Q. G. Medley, H. L. Ma, M. Collins, K. Dunussi-Joannopoulos, and L. A. Fouser. 2010. IL-22 induces an acute-phase response. *J Immunol* 185: 5531-5538.
143. Aujla, S. J., Y. R. Chan, M. Zheng, M. Fei, D. J. Askew, D. A. Pociask, T. A. Reinhart, F. McAllister, J. Edeal, K. Gaus, S. Husain, J. L. Kreindler, P. J. Dubin, J. M. Pilewski, M. M. Myerburg, C. A. Mason, Y. Iwakura, and J. K. Kolls. 2008. IL-22 mediates mucosal host defense against Gram-negative bacterial pneumonia. *Nat Med* 14: 275-281.
144. Ma, H. L., S. Liang, J. Li, L. Napierata, T. Brown, S. Benoit, M. Senices, D. Gill, K. Dunussi-Joannopoulos, M. Collins, C. Nickerson-Nutter, L. A. Fouser, and D. A. Young. 2008. IL-22 is required for Th17 cell-mediated pathology in a mouse model of psoriasis-like skin inflammation. *J Clin Invest* 118: 597-607.
145. Muñoz, M., M. M. Heimesaat, K. Danker, D. Struck, U. Lohmann, R. Plickert, S. Bereswill, A. Fischer, I. R. Dunay, K. Wolk, C. Loddenkemper, H. W. Krell, C. Libert, L. R. Lund, O. Frey, C. Hölscher, Y. Iwakura, N. Ghilardi, W. Ouyang, T.

Kamradt, R. Sabat, and O. Liesenfeld. 2009. Interleukin (IL)-23 mediates Toxoplasma gondii-induced immunopathology in the gut via matrixmetalloproteinase-2 and IL-22 but independent of IL-17. *J Exp Med* 206: 3047-3059.

146. Geboes, L., L. Dumoutier, H. Kelchtermans, E. Schurgers, T. Mitera, J. C. Renauld, and P. Matthys. 2009. Proinflammatory role of the Th17 cytokine interleukin-22 in collagen-induced arthritis in C57BL/6 mice. *Arthritis Rheum* 60: 390-395.
147. Takahashi, K., K. Hirose, S. Kawashima, Y. Niwa, H. Wakashin, A. Iwata, K. Tokoyoda, J. C. Renauld, I. Iwamoto, T. Nakayama, and H. Nakajima. 2011. IL-22 attenuates IL-25 production by lung epithelial cells and inhibits antigen-induced eosinophilic airway inflammation. *J Allergy Clin Immunol* 128: 1067-1076.e1061-1066.
148. Simonian, P. L., F. Wehrmann, C. L. Roark, W. K. Born, R. L. O'Brien, and A. P. Fontenot. 2010. γδ T cells protect against lung fibrosis via IL-22. *J Exp Med* 207: 2239-2253.
149. Zenewicz, L. A., G. D. Yancopoulos, D. M. Valenzuela, A. J. Murphy, M. Karow, and R. A. Flavell. 2007. Interleukin-22 but not interleukin-17 provides protection to hepatocytes during acute liver inflammation. *Immunity* 27: 647-659.
150. Radaeva, S., R. Sun, H. N. Pan, F. Hong, and B. Gao. 2004. Interleukin 22 (IL-22) plays a protective role in T cell-mediated murine hepatitis: IL-22 is a survival factor for hepatocytes via STAT3 activation. *Hepatology* 39: 1332-1342.
151. Zenewicz, L. A., G. D. Yancopoulos, D. M. Valenzuela, A. J. Murphy, S. Stevens, and R. A. Flavell. 2008. Innate and adaptive interleukin-22 protects mice from inflammatory bowel disease. *Immunity* 29: 947-957.
152. Kamanaka, M., S. Huber, L. A. Zenewicz, N. Gagliani, C. Rathinam, W. O'Connor, Y. Y. Wan, S. Nakae, Y. Iwakura, L. Hao, and R. A. Flavell. 2011. Memory/effector (CD45RB(lo)) CD4 T cells are controlled directly by IL-10 and cause IL-22-dependent intestinal pathology. *J Exp Med* 208: 1027-1040.
153. Zheng, Y., P. A. Valdez, D. M. Danilenko, Y. Hu, S. M. Sa, Q. Gong, A. R. Abbas, Z. Modrusan, N. Ghilardi, F. J. de Sauvage, and W. Ouyang. 2008. Interleukin-22 mediates early host defense against attaching and effacing bacterial pathogens. *Nat Med* 14: 282-289.
154. Dhiman, R., M. Indramohan, P. F. Barnes, R. C. Nayak, P. Paidipally, L. V. Rao, and R. Vankayalapati. 2009. IL-22 produced by human NK cells inhibits growth of Mycobacterium tuberculosis by enhancing phagolysosomal fusion. *J Immunol* 183: 6639-6645.
155. Copeland, N. G., N. A. Jenkins, and D. L. Court. 2001. Recombineering: a powerful new tool for mouse functional genomics. *Nat Rev Genet* 2: 769-779.
156. Stanton, R. J., B. P. McSharry, M. Armstrong, P. Tomasec, and G. W. Wilkinson. 2008. Re-engineering adenovirus vector systems to enable high-throughput analyses of gene function. *Biotechniques* 45: 659-662, 664-658.
157. Liu, Y., S. H. Wei, A. S. Ho, R. de Waal Malefyt, and K. W. Moore. 1994. Expression cloning and characterization of a human IL-10 receptor. *J Immunol* 152: 1821-1829.
158. Carson, W. E., M. J. Lindemann, R. Baiocchi, M. Linett, J. C. Tan, C. C. Chou, S. Narula, and M. A. Caligiuri. 1995. The functional characterization of interleukin-10 receptor expression on human natural killer cells. *Blood* 85: 3577-3585.
159. Cai, G., R. A. Kastelein, and C. A. Hunter. 1999. IL-10 enhances NK cell proliferation, cytotoxicity and production of IFN-gamma when combined with IL-

18. *Eur J Immunol* 29: 2658-2665.
160. Qian, C., X. Jiang, H. An, Y. Yu, Z. Guo, S. Liu, H. Xu, and X. Cao. 2006. TLR agonists promote ERK-mediated preferential IL-10 production of regulatory dendritic cells (diffDCs), leading to NK-cell activation. *Blood* 108: 2307-2315.
161. Mocellin, S., M. Panelli, E. Wang, C. R. Rossi, P. Pilati, D. Nitti, M. Lise, and F. M. Marincola. 2004. IL-10 stimulatory effects on human NK cells explored by gene profile analysis. *Genes Immun* 5: 621-630.
162. Shibata, Y., L. A. Foster, M. Kurimoto, H. Okamura, R. M. Nakamura, K. Kawajiri, J. P. Justice, M. R. Van Scott, Q. N. Myrvik, and W. J. Metzger. 1998. Immunoregulatory roles of IL-10 in innate immunity: IL-10 inhibits macrophage production of IFN-gamma-inducing factors but enhances NK cell production of IFN-gamma. *J Immunol* 161: 4283-4288.
163. Scott, M. J., J. J. Hoth, M. Turina, D. R. Woods, and W. G. Cheadle. 2006. Interleukin-10 suppresses natural killer cell but not natural killer T cell activation during bacterial infection. *Cytokine* 33: 79-86.
164. Chiu, B. C., V. R. Stolberg, and S. W. Chensue. 2008. Mononuclear phagocyte-derived IL-10 suppresses the innate IL-12/IFN-gamma axis in lung-challenged aged mice. *J Immunol* 181: 3156-3166.
165. Oakley, O. R., B. A. Garvy, S. Humphreys, M. H. Qureshi, and C. Pomeroy. 2008. Increased weight loss with reduced viral replication in interleukin-10 knock-out mice infected with murine cytomegalovirus. *Clin Exp Immunol* 151: 155-164.
166. Cheeran, M. C., S. Hu, J. M. Palmquist, T. Bakken, G. Gekker, and J. R. Lokensgard. 2007. Dysregulated interferon-gamma responses during lethal cytomegalovirus brain infection of IL-10-deficient mice. *Virus Res* 130: 96-102.
167. Jones, M., K. Ladell, K. K. Wynn, M. A. Stacey, M. F. Quigley, E. Gostick, D. A. Price, and I. R. Humphreys. 2010. IL-10 restricts memory T cell inflation during cytomegalovirus infection. *J Immunol* 185: 3583-3592.
168. Humphreys, I. R., C. de Trez, A. Kinkade, C. A. Benedict, M. Croft, and C. F. Ware. 2007. Cytomegalovirus exploits IL-10-mediated immune regulation in the salivary glands. *J Exp Med* 204: 1217-1225.
169. Loh, J., D. T. Chu, A. K. O'Guin, W. M. Yokoyama, and H. W. Virgin. 2005. Natural killer cells utilize both perforin and gamma interferon to regulate murine cytomegalovirus infection in the spleen and liver. *J Virol* 79: 661-667.
170. Tay, C. H., and R. M. Welsh. 1997. Distinct organ-dependent mechanisms for the control of murine cytomegalovirus infection by natural killer cells. *J Virol* 71: 267-275.
171. Dokun, A. O., S. Kim, H. R. Smith, H. S. Kang, D. T. Chu, and W. M. Yokoyama. 2001. Specific and nonspecific NK cell activation during virus infection. *Nat Immunol* 2: 951-956.
172. Robbins, S. H., M. S. Tessmer, T. Mikayama, and L. Brossay. 2004. Expansion and contraction of the NK cell compartment in response to murine cytomegalovirus infection. *J Immunol* 173: 259-266.
173. Dokun, A. O., D. T. Chu, L. Yang, A. S. Bendelac, and W. M. Yokoyama. 2001. Analysis of in situ NK cell responses during viral infection. *J Immunol* 167: 5286-5293.
174. Nguyen, K. B., T. P. Salazar-Mather, M. Y. Dalod, J. B. Van Deusen, X. Q. Wei, F. Y. Liew, M. A. Caligiuri, J. E. Durbin, and C. A. Biron. 2002. Coordinated and distinct roles for IFN-alpha beta, IL-12, and IL-15 regulation of NK cell responses to viral infection. *J Immunol* 169: 4279-4287.
175. Maher, S., D. Toomey, C. Condron, and D. Bouchier-Hayes. 2002. Activation-

induced cell death: the controversial role of Fas and Fas ligand in immune privilege and tumour counterattack. *Immunol Cell Biol* 80: 131-137.
176. Chiossone, L., J. Chaix, N. Fuseri, C. Roth, E. Vivier, and T. Walzer. 2009. Maturation of mouse NK cells is a 4-stage developmental program. *Blood* 113: 5488-5496.
177. Hayakawa, Y., and M. J. Smyth. 2006. CD27 dissects mature NK cells into two subsets with distinct responsiveness and migratory capacity. *J Immunol* 176: 1517-1524.
178. Redpath, S., A. Angulo, N. R. Gascoigne, and P. Ghazal. 1999. Murine cytomegalovirus infection down-regulates MHC class II expression on macrophages by induction of IL-10. *J Immunol* 162: 6701-6707.
179. Madan, R., F. Demircik, S. Surianarayanan, J. L. Allen, S. Divanovic, A. Trompette, N. Yogev, Y. Gu, M. Khodoun, D. Hildeman, N. Boespflug, M. B. Fogolin, L. Gröbe, M. Greweling, F. D. Finkelman, R. Cardin, M. Mohrs, W. Müller, A. Waisman, A. Roers, and C. L. Karp. 2009. Nonredundant roles for B cell-derived IL-10 in immune counter-regulation. *J Immunol* 183: 2312-2320.
180. Rice, G. P., R. D. Schrier, and M. B. Oldstone. 1984. Cytomegalovirus infects human lymphocytes and monocytes: virus expression is restricted to immediate-early gene products. *Proc Natl Acad Sci U S A* 81: 6134-6138.
181. Olding, L. B., F. C. Jensen, and M. B. Oldstone. 1975. Pathogenesis of of cytomegalovirus infection. I. Activation of virus from bone marrow-derived lymphocytes by in vitro allogenic reaction. *J Exp Med* 141: 561-572.
182. Matsushita, T., K. Yanaba, J. D. Bouaziz, M. Fujimoto, and T. F. Tedder. 2008. Regulatory B cells inhibit EAE initiation in mice while other B cells promote disease progression. *J Clin Invest* 118: 3420-3430.
183. Rieger, A., and A. Bar-Or. 2008. B-cell-derived interleukin-10 in autoimmune disease: regulating the regulators. *Nat Rev Immunol* 8: 486-487.
184. Polić, B., H. Hengel, A. Krmpotić, J. Trgovcich, I. Pavić, P. Luccaronin, S. Jonjić, and U. H. Koszinowski. 1998. Hierarchical and redundant lymphocyte subset control precludes cytomegalovirus replication during latent infection. *J Exp Med* 188: 1047-1054.
185. Jonjić, S., W. Mutter, F. Weiland, M. J. Reddehase, and U. H. Koszinowski. 1989. Site-restricted persistent cytomegalovirus infection after selective long-term depletion of CD4+ T lymphocytes. *J Exp Med* 169: 1199-1212.
186. Lee, S. H., K. S. Kim, N. Fodil-Cornu, S. M. Vidal, and C. A. Biron. 2009. Activating receptors promote NK cell expansion for maintenance, IL-10 production, and CD8 T cell regulation during viral infection. *J Exp Med* 206: 2235-2251.
187. Walzer, T., M. Bléry, J. Chaix, N. Fuseri, L. Chasson, S. H. Robbins, S. Jaeger, P. André, L. Gauthier, L. Daniel, K. Chemin, Y. Morel, M. Dalod, J. Imbert, M. Pierres, A. Moretta, F. Romagné, and E. Vivier. 2007. Identification, activation, and selective in vivo ablation of mouse NK cells via NKp46. *Proc Natl Acad Sci U S A* 104: 3384-3389.
188. Shimozato, O., J. R. Ortaldo, K. L. Komschlies, and H. A. Young. 2002. Impaired NK cell development in an IFN-gamma transgenic mouse: aberrantly expressed IFN-gamma enhances hematopoietic stem cell apoptosis and affects NK cell differentiation. *J Immunol* 168: 1746-1752.
189. Ross, M. E., and M. A. Caligiuri. 1997. Cytokine-induced apoptosis of human natural killer cells identifies a novel mechanism to regulate the innate immune response. *Blood* 89: 910-918.

190. Pien, G. C., A. R. Satoskar, K. Takeda, S. Akira, and C. A. Biron. 2000. Cutting edge: selective IL-18 requirements for induction of compartmental IFN-gamma responses during viral infection. *J Immunol* 165: 4787-4791.
191. Wesley, J. D., M. S. Tessmer, D. Chaukos, and L. Brossay. 2008. NK cell-like behavior of Valpha14i NK T cells during MCMV infection. *PLoS Pathog* 4: e1000106.
192. van Dommelen, S. L., H. A. Tabarias, M. J. Smyth, and M. A. Degli-Esposti. 2003. Activation of natural killer (NK) T cells during murine cytomegalovirus infection enhances the antiviral response mediated by NK cells. *J Virol* 77: 1877-1884.
193. Tang-Feldman, Y. J., G. R. Lochhead, S. R. Lochhead, C. Yu, and C. Pomeroy. 2011. Interleukin-10 repletion suppresses pro-inflammatory cytokines and decreases liver pathology without altering viral replication in murine cytomegalovirus (MCMV)-infected IL-10 knockout mice. *Inflamm Res* 60: 233-243.
194. Jones, B. C., N. J. Logsdon, K. Josephson, J. Cook, P. A. Barry, and M. R. Walter. 2002. Crystal structure of human cytomegalovirus IL-10 bound to soluble human IL-10R1. *Proc Natl Acad Sci U S A* 99: 9404-9409.
195. Spencer, J. V., K. M. Lockridge, P. A. Barry, G. Lin, M. Tsang, M. E. Penfold, and T. J. Schall. 2002. Potent immunosuppressive activities of cytomegalovirus-encoded interleukin-10. *J Virol* 76: 1285-1292.
196. Chang, W. L., N. Baumgarth, D. Yu, and P. A. Barry. 2004. Human cytomegalovirus-encoded interleukin-10 homolog inhibits maturation of dendritic cells and alters their functionality. *J Virol* 78: 8720-8731.
197. Nachtwey, J., and J. V. Spencer. 2008. HCMV IL-10 suppresses cytokine expression in monocytes through inhibition of nuclear factor-kappaB. *Viral Immunol* 21: 477-482.
198. Raftery, M. J., D. Wieland, S. Gronewald, A. A. Kraus, T. Giese, and G. Schönrich. 2004. Shaping phenotype, function, and survival of dendritic cells by cytomegalovirus-encoded IL-10. *J Immunol* 173: 3383-3391.
199. Spencer, J. V., J. Cadaoas, P. R. Castillo, V. Saini, and B. Slobedman. 2008. Stimulation of B lymphocytes by cmvIL-10 but not LAcmvIL-10. *Virology* 374: 164-169.
200. Jenkins, C., W. Garcia, A. Abendroth, and B. Slobedman. 2008. Expression of a human cytomegalovirus latency-associated homolog of interleukin-10 during the productive phase of infection. *Virology* 370: 285-294.
201. Cheung, A. K., D. J. Gottlieb, B. Plachter, S. Pepperl-Klindworth, S. Avdic, A. L. Cunningham, A. Abendroth, and B. Slobedman. 2009. The role of the human cytomegalovirus UL111A gene in down-regulating CD4+ T-cell recognition of latently infected cells: implications for virus elimination during latency. *Blood* 114: 4128-4137.
202. Chang, W. L., and P. A. Barry. 2010. Attenuation of innate immunity by cytomegalovirus IL-10 establishes a long-term deficit of adaptive antiviral immunity. *Proc Natl Acad Sci U S A* 107: 22647-22652.
203. Logsdon, N. J., M. K. Eberhardt, C. E. Allen, P. A. Barry, and M. R. Walter. 2011. Design and analysis of rhesus cytomegalovirus IL-10 mutants as a model for novel vaccines against human cytomegalovirus. *PLoS One* 6: e28127.
204. Eberhardt, M. K., W. L. Chang, N. J. Logsdon, Y. Yue, M. R. Walter, and P. A. Barry. 2012. Host immune responses to a viral immune modulating protein: immunogenicity of viral interleukin-10 in rhesus cytomegalovirus-infected rhesus macaques. *PLoS One* 7: e37931.

205. Riegler, S., H. Hebart, H. Einsele, P. Brossart, G. Jahn, and C. Sinzger. 2000. Monocyte-derived dendritic cells are permissive to the complete replicative cycle of human cytomegalovirus. *J Gen Virol* 81: 393-399.
206. Gerna, G., E. Percivalle, D. Lilleri, L. Lozza, C. Fornara, G. Hahn, F. Baldanti, and M. G. Revello. 2005. Dendritic-cell infection by human cytomegalovirus is restricted to strains carrying functional UL131-128 genes and mediates efficient viral antigen presentation to CD8+ T cells. *J Gen Virol* 86: 275-284.
207. Straschewski, S., M. Patrone, P. Walther, A. Gallina, T. Mertens, and G. Frascaroli. 2011. Protein pUL128 of human cytomegalovirus is necessary for monocyte infection and blocking of migration. *J Virol* 85: 5150-5158.
208. Baldanti, F., S. Paolucci, G. Campanini, A. Sarasini, E. Percivalle, M. G. Revello, and G. Gerna. 2006. Human cytomegalovirus UL131A, UL130 and UL128 genes are highly conserved among field isolates. *Arch Virol* 151: 1225-1233.
209. Sun, Z. R., Y. H. Ji, Q. Ruan, R. He, Y. P. Ma, Y. Qi, Z. Q. Mao, and Y. J. Huang. 2009. Structure characterization of human cytomegalovirus UL131A, UL130 and UL128 genes in clinical strains in China. *Genet Mol Res* 8: 1191-1201.
210. Ryckman, B. J., B. L. Rainish, M. C. Chase, J. A. Borton, J. A. Nelson, M. A. Jarvis, and D. C. Johnson. 2008. Characterization of the human cytomegalovirus gH/gL/UL128-131 complex that mediates entry into epithelial and endothelial cells. *J Virol* 82: 60-70.
211. Wang, D., and T. Shenk. 2005. Human cytomegalovirus UL131 open reading frame is required for epithelial cell tropism. *J Virol* 79: 10330-10338.
212. Sinzger, C., G. Hahn, M. Digel, R. Katona, K. L. Sampaio, M. Messerle, H. Hengel, U. Koszinowski, W. Brune, and B. Adler. 2008. Cloning and sequencing of a highly productive, endotheliotropic virus strain derived from human cytomegalovirus TB40/E. *J Gen Virol* 89: 359-368.
213. Lozza, L., D. Lilleri, E. Percivalle, C. Fornara, G. Comolli, M. G. Revello, and G. Gerna. 2005. Simultaneous quantification of human cytomegalovirus (HCMV)-specific CD4+ and CD8+ T cells by a novel method using monocyte-derived HCMV-infected immature dendritic cells. *Eur J Immunol* 35: 1795-1804.
214. Missé, D., H. Yssel, D. Trabattoni, C. Oblet, S. Lo Caputo, F. Mazzotta, J. Pène, J. P. Gonzalez, M. Clerici, and F. Veas. 2007. IL-22 participates in an innate anti-HIV-1 host-resistance network through acute-phase protein induction. *J Immunol* 178: 407-415.
215. Arias, J. F., R. Nishihara, M. Bala, and K. Ikuta. 2010. High systemic levels of interleukin-10, interleukin-22 and C-reactive protein in Indian patients are associated with low in vitro replication of HIV-1 subtype C viruses. *Retrovirology* 7: 15.
216. Pellegrini, M., T. Calzascia, J. G. Toe, S. P. Preston, A. E. Lin, A. R. Elford, A. Shahinian, P. A. Lang, K. S. Lang, M. Morre, B. Assouline, K. Lahl, T. Sparwasser, T. F. Tedder, J. H. Paik, R. A. DePinho, S. Basta, P. S. Ohashi, and T. W. Mak. 2011. IL-7 engages multiple mechanisms to overcome chronic viral infection and limit organ pathology. *Cell* 144: 601-613.
217. Dambacher, J., F. Beigel, K. Zitzmann, M. H. Heeg, B. Göke, H. M. Diepolder, C. J. Auernhammer, and S. Brand. 2008. The role of interleukin-22 in hepatitis C virus infection. *Cytokine* 41: 209-216.
218. Zhang, Y., M. A. Cobleigh, J. Q. Lian, C. X. Huang, C. J. Booth, X. F. Bai, and M. D. Robek. 2011. A proinflammatory role for interleukin-22 in the immune response to hepatitis B virus. *Gastroenterology* 141: 1897-1906.
219. Xiang, X., H. Gui, N. J. King, L. Cole, H. Wang, Q. Xie, and S. Bao. 2011. IL-22

and non-ELR-CXC chemokine expression in chronic hepatitis B virus-infected liver. *Immunol Cell Biol*.
220. Guo, H., and D. J. Topham. 2010. Interleukin-22 (IL-22) production by pulmonary Natural Killer cells and the potential role of IL-22 during primary influenza virus infection. *J Virol* 84: 7750-7759.
221. Paget, C., S. Ivanov, J. Fontaine, J. Renneson, F. Blanc, M. Pichavant, L. Dumoutier, B. Ryffel, J. C. Renauld, P. Gosset, M. Si-Tahar, C. Faveeuw, and F. Trottein. 2012. Interleukin-22 is produced by invariant natural killer T lymphocytes during influenza A virus infection: potential role in protection against lung epithelial damages. *J Biol Chem* 287: 8816-8829.
222. Eberl, G. 2012. Development and evolution of RORγt+ cells in a microbe's world. *Immunol Rev* 245: 177-188.
223. Zhang, T., S. Liu, P. Yang, C. Han, J. Wang, J. Liu, Y. Han, Y. Yu, and X. Cao. 2009. Fibronectin maintains survival of mouse natural killer (NK) cells via CD11b/Src/beta-catenin pathway. *Blood* 114: 4081-4088.
224. Ohno, S., T. Sato, K. Kohu, K. Takeda, K. Okumura, M. Satake, and S. Habu. 2008. Runx proteins are involved in regulation of CD122, Ly49 family and IFN-gamma expression during NK cell differentiation. *Int Immunol* 20: 71-79.
225. Pomeroy, C., D. Delong, C. Clabots, P. Riciputi, and G. A. Filice. 1998. Role of interferon-gamma in murine cytomegalovirus infection. *J Lab Clin Med* 132: 124-133.
226. Cheng, J., Q. Ke, Z. Jin, H. Wang, O. Kocher, J. P. Morgan, J. Zhang, and C. S. Crumpacker. 2009. Cytomegalovirus infection causes an increase of arterial blood pressure. *PLoS Pathog* 5: e1000427.
227. Ouyang, W., J. K. Kolls, and Y. Zheng. 2008. The biological functions of T helper 17 cell effector cytokines in inflammation. *Immunity* 28: 454-467.
228. Anderson, S. I., N. A. Hotchin, and G. B. Nash. 2000. Role of the cytoskeleton in rapid activation of CD11b/CD18 function and its subsequent downregulation in neutrophils. *J Cell Sci* 113 (Pt 15): 2737-2745.
229. Chen, Y., S. Mendoza, G. Davis-Gorman, Z. Cohen, R. Gonzales, H. Tuttle, P. F. McDonagh, and R. R. Watson. 2003. Neutrophil activation by murine retroviral infection during chronic ethanol consumption. *Alcohol Alcohol* 38: 109-114.
230. Daley, J. M., A. A. Thomay, M. D. Connolly, J. S. Reichner, and J. E. Albina. 2008. Use of Ly6G-specific monoclonal antibody to deplete neutrophils in mice. *J Leukoc Biol* 83: 64-70.
231. Jaeger, B. N., J. Donadieu, C. Cognet, C. Bernat, D. Ordoñez-Rueda, V. Barlogis, N. Mahlaoui, A. Fenis, E. Narni-Mancinelli, B. Beaupain, C. Bellanné-Chantelot, M. Bajénoff, B. Malissen, M. Malissen, E. Vivier, and S. Ugolini. 2012. Neutrophil depletion impairs natural killer cell maturation, function, and homeostasis. *J Exp Med* 209: 565-580.
232. Spörri, R., N. Joller, H. Hilbi, and A. Oxenius. 2008. A novel role for neutrophils as critical activators of NK cells. *J Immunol* 181: 7121-7130.
233. Chin, K. C., and P. Cresswell. 2001. Viperin (cig5), an IFN-inducible antiviral protein directly induced by human cytomegalovirus. *Proc Natl Acad Sci U S A* 98: 15125-15130.
234. Hinson, E. R., N. S. Joshi, J. H. Chen, C. Rahner, Y. W. Jung, X. Wang, S. M. Kaech, and P. Cresswell. 2010. Viperin is highly induced in neutrophils and macrophages during acute and chronic lymphocytic choriomeningitis virus infection. *J Immunol* 184: 5723-5731.
235. Fernandez, J. A., E. G. Rodrigues, and M. Tsuji. 2000. Multifactorial protective

mechanisms to limit viral replication in the lung of mice during primary murine cytomegalovirus infection. *Viral Immunol* 13: 287-295.
236. Noda, S., K. Tanaka, S. Sawamura, M. Sasaki, T. Matsumoto, K. Mikami, Y. Aiba, H. Hasegawa, N. Kawabe, and Y. Koga. 2001. Role of nitric oxide synthase type 2 in acute infection with murine cytomegalovirus. *J Immunol* 166: 3533-3541.
237. Andoniou, C. E., P. Fleming, V. R. Sutton, J. A. Trapani, and M. A. Degli-Esposti. 2011. Cathepsin C limits acute viral infection independently of NK cell and CD8+ T-cell cytolytic function. *Immunol Cell Biol* 89: 540-548.
238. Zürcher, T., J. Pavlovic, and P. Staeheli. 1992. Nuclear localization of mouse Mx1 protein is necessary for inhibition of influenza virus. *J Virol* 66: 5059-5066.
239. Fodil-Cornu, N., and S. M. Vidal. 2008. Type I interferon response to cytomegalovirus infection: the kick-start. *Cell Host Microbe* 3: 59-61.
240. Schneider, K., A. Loewendorf, C. De Trez, J. Fulton, A. Rhode, H. Shumway, S. Ha, G. Patterson, K. Pfeffer, S. A. Nedospasov, C. F. Ware, and C. A. Benedict. 2008. Lymphotoxin-mediated crosstalk between B cells and splenic stroma promotes the initial type I interferon response to cytomegalovirus. *Cell Host Microbe* 3: 67-76.
241. Banks, T. A., S. Rickert, C. A. Benedict, L. Ma, M. Ko, J. Meier, W. Ha, K. Schneider, S. W. Granger, O. Turovskaya, D. Elewaut, D. Otero, A. R. French, S. C. Henry, J. D. Hamilton, S. Scheu, K. Pfeffer, and C. F. Ware. 2005. A lymphotoxin-IFN-beta axis essential for lymphocyte survival revealed during cytomegalovirus infection. *J Immunol* 174: 7217-7225.
242. Brand, S., J. Dambacher, F. Beigel, K. Zitzmann, M. H. Heeg, T. S. Weiss, T. Prüfer, T. Olszak, C. J. Steib, M. Storr, B. Göke, H. Diepolder, M. Bilzer, W. E. Thasler, and C. J. Auernhammer. 2007. IL-22-mediated liver cell regeneration is abrogated by SOCS-1/3 overexpression in vitro. *Am J Physiol Gastrointest Liver Physiol* 292: G1019-1028.
243. Rutz, S., and W. Ouyang. 2011. Regulation of interleukin-10 and interleukin-22 expression in T helper cells. *Curr Opin Immunol* 23: 605-612.
244. Colonna, M. 2009. Interleukin-22-producing natural killer cells and lymphoid tissue inducer-like cells in mucosal immunity. *Immunity* 31: 15-23.
245. Mjösberg, J. M., S. Trifari, N. K. Crellin, C. P. Peters, C. M. van Drunen, B. Piet, W. J. Fokkens, T. Cupedo, and H. Spits. 2011. Human IL-25- and IL-33-responsive type 2 innate lymphoid cells are defined by expression of CRTH2 and CD161. *Nat Immunol* 12: 1055-1062.
246. Tachiiri, A., R. Imamura, Y. Wang, M. Fukui, M. Umemura, and T. Suda. 2003. Genomic structure and inducible expression of the IL-22 receptor alpha chain in mice. *Genes Immun* 4: 153-159.
247. Wolk, K., S. Kunz, E. Witte, M. Friedrich, K. Asadullah, and R. Sabat. 2004. IL-22 increases the innate immunity of tissues. *Immunity* 21: 241-254.
248. Savan, R., A. P. McFarland, D. A. Reynolds, L. Feigenbaum, K. Ramakrishnan, M. Karwan, H. Shirota, D. M. Klinman, K. Dunleavy, S. Pittaluga, S. K. Anderson, R. P. Donnelly, W. H. Wilson, and H. A. Young. 2011. A novel role for IL-22R1 as a driver of inflammation. *Blood* 117: 575-584.
249. Andoh, A., Z. Zhang, O. Inatomi, S. Fujino, Y. Deguchi, Y. Araki, T. Tsujikawa, K. Kitoh, S. Kim-Mitsuyama, A. Takayanagi, N. Shimizu, and Y. Fujiyama. 2005. Interleukin-22, a member of the IL-10 subfamily, induces inflammatory responses in colonic subepithelial myofibroblasts. *Gastroenterology* 129: 969-984.
250. Brand, S., F. Beigel, T. Olszak, K. Zitzmann, S. T. Eichhorst, J. M. Otte, H. Diepolder, A. Marquardt, W. Jagla, A. Popp, S. Leclair, K. Herrmann, J. Seiderer,

T. Ochsenkühn, B. Göke, C. J. Auernhammer, and J. Dambacher. 2006. IL-22 is increased in active Crohn's disease and promotes proinflammatory gene expression and intestinal epithelial cell migration. *Am J Physiol Gastrointest Liver Physiol* 290: G827-838.

251. Basu, S., G. Hodgson, M. Katz, and A. R. Dunn. 2002. Evaluation of role of G-CSF in the production, survival, and release of neutrophils from bone marrow into circulation. *Blood* 100: 854-861.
252. Craigen, J. L., K. L. Yong, N. J. Jordan, L. P. MacCormac, J. Westwick, A. N. Akbar, and J. E. Grundy. 1997. Human cytomegalovirus infection up-regulates interleukin-8 gene expression and stimulates neutrophil transendothelial migration. *Immunology* 92: 138-145.
253. Grundy, J. E., K. M. Lawson, L. P. MacCormac, J. M. Fletcher, and K. L. Yong. 1998. Cytomegalovirus-infected endothelial cells recruit neutrophils by the secretion of C-X-C chemokines and transmit virus by direct neutrophil-endothelial cell contact and during neutrophil transendothelial migration. *J Infect Dis* 177: 1465-1474.
254. Penfold, M. E., D. J. Dairaghi, G. M. Duke, N. Saederup, E. S. Mocarski, G. W. Kemble, and T. J. Schall. 1999. Cytomegalovirus encodes a potent alpha chemokine. *Proc Natl Acad Sci U S A* 96: 9839-9844.
255. Lüttichau, H. R. 2010. The cytomegalovirus UL146 gene product vCXCL1 targets both CXCR1 and CXCR2 as an agonist. *J Biol Chem* 285: 9137-9146.
256. Bale, J. F., M. E. O'Neil, and T. Greiner. 1985. The interaction of murine cytomegalovirus with murine neutrophils: effect on migratory and phagocytic activities. *J Leukoc Biol* 38: 723-734.
257. Bale, J. F., E. R. Kern, J. C. Overall, and J. R. Baringer. 1983. Impaired migratory and chemotactic activity of neutrophils during murine cytomegalovirus infection. *J Infect Dis* 148: 518-525.
258. Tannous, R., and M. G. Myers. 1983. Acquired chemotactic inhibitors during infection with guinea pig cytomegalovirus. *Infect Immun* 41: 88-96.
259. Gaudreault, E., and J. Gosselin. 2007. Leukotriene B4-mediated release of antimicrobial peptides against cytomegalovirus is BLT1 dependent. *Viral Immunol* 20: 407-420.
260. Kumar, V., and A. Sharma. 2010. Neutrophils: Cinderella of innate immune system. *Int Immunopharmacol* 10: 1325-1334.
261. Xu, W., S. Zheng, R. A. Dweik, and S. C. Erzurum. 2006. Role of epithelial nitric oxide in airway viral infection. *Free Radic Biol Med* 41: 19-28.
262. Lin, Y. L., Y. L. Huang, S. H. Ma, C. T. Yeh, S. Y. Chiou, L. K. Chen, and C. L. Liao. 1997. Inhibition of Japanese encephalitis virus infection by nitric oxide: antiviral effect of nitric oxide on RNA virus replication. *J Virol* 71: 5227-5235.
263. Saxena, S. K., A. Singh, and A. Mathur. 2000. Antiviral effect of nitric oxide during Japanese encephalitis virus infection. *Int J Exp Pathol* 81: 165-172.
264. Sanders, S. P., E. S. Siekierski, J. D. Porter, S. M. Richards, and D. Proud. 1998. Nitric oxide inhibits rhinovirus-induced cytokine production and viral replication in a human respiratory epithelial cell line. *J Virol* 72: 934-942.
265. O'Garra, A., F. J. Barrat, A. G. Castro, A. Vicari, and C. Hawrylowicz. 2008. Strategies for use of IL-10 or its antagonists in human disease. *Immunol Rev* 223: 114-131.
266. Kumar, A., and W. D. Creery. 2000. The therapeutic potential of interleukin 10 in infection and inflammation. *Arch Immunol Ther Exp (Warsz)* 48: 529-538.
267. Zamora, M. R. 2004. Cytomegalovirus and lung transplantation. *Am J Transplant*

4: 1219-1226.
268. Gao, L. H., and S. S. Zheng. 2004. Cytomegalovirus and chronic allograft rejection in liver transplantation. *World J Gastroenterol* 10: 1857-1861.
269. Biron, K. K. 2006. Antiviral drugs for cytomegalovirus diseases. *Antiviral Res* 71: 154-163.
270. Boeckh, M. 2011. Complications, diagnosis, management, and prevention of CMV infections: current and future. *Hematology Am Soc Hematol Educ Program* 2011: 305-309.
271. Adler, S. P., G. Nigro, and L. Pereira. 2007. Recent advances in the prevention and treatment of congenital cytomegalovirus infections. *Semin Perinatol* 31: 10-18.
272. Razonable, R. R., V. C. Emery, and t. A. M. o. t. I. I. H. M. Forum). 2004. Management of CMV infection and disease in transplant patients. 27-29 February 2004. *Herpes* 11: 77-86.
273. Ank, N., H. West, C. Bartholdy, K. Eriksson, A. R. Thomsen, and S. R. Paludan. 2006. Lambda interferon (IFN-lambda), a type III IFN, is induced by viruses and IFNs and displays potent antiviral activity against select virus infections in vivo. *J Virol* 80: 4501-4509.